FACULTY OF ENGINEERING AND APPLIED SCIENCE

INSTITUTE OF SOUND AND VIBRATION RESEARCH

COMBUSTION AS A SOURCE OF DIESEL ENGINE NOISE

by

D. ANDERTON

A Thesis submitted for the

Degree of Doctor of Philosophy

University of Southampton

April 1974

ABSTRACT

FACULTY OF ENGINEERING AND APPLIED SCIENCE

INSTITUTE OF SOUND AND VIBRATION RESEARCH

Doctor of Philosophy

COMBUSTION AS A SOURCE OF DIESEL ENGINE NOISE

by David Anderton

The thesis deals with the study of the exciting propensities of various forms of diesel combustion and the resultant noise radiated by the engine structure.

It is found that the best description of cylinder pressure exciting potential is given by a frequency analysis of the cylinder pressure from a running engine.

A fast Fourier Analysis computational method for the calculation of several thousand harmonics has been developed which enables a fundamental difference, which exists between combustion excitation of four- and two-stroke and turbocharged four-stroke operating cycles, to be shown. At equal firing frequency the excitation of the two-stroke, above 200 Hz, is generally lower than for an equivalent four-stroke. The turbocharged four-stroke approaches nearer to the two-stroke characteristic with an increasing degree of turbocharging. It is also shown that the harmonics of cylinder pressure responsible for transmitting power are the first two harmonics of engine rotational speed. The harmonics controlling noise occur above the 20th.

It was found that the complete form of cylinder pressure development is required to specify the cylinder pressure spectrum. The effects of peak pressure P, rate of pressure rise $\frac{dp}{dt}$, and acceleration of pressure rise $\frac{d^2p}{dt^2}$, on diesel and petrol combustion excitation are found to vary with the fundamental cycle characteristics and the engine speed. This explains why high power output engines provide lower combustion excitation if the B.I.C.E.R.I. variable compression ratio pistons are used.

The results show that the combustion excitation potential of each combustion system can be simply described by a single 'reduced spectrum' which is independent of engine speed and size.

Theoretical considerations of the loading due to combustion, on the assumption of linearity of vibration and acoustic response, have led to the formulation of a combustion noise model. In conjunction with empirically found constants this provides a series of combustion noise prediction formulae based on bore and rated speed and combustion system only. Formulae, based on measured cylinder pressure spectrum values, have also been derived to predict engine combustion noise at any condition of load and speed.

Acknowledgements

The author wishes to express his gratitude to his supervisor, Professor T. Priede, for the encouragement and advice he has given throughout the work.

The author also wishes to thank all his colleagues in the Automotive Group of the I.S.V.R. for their interest and help but particularly Mr. E.C. Grover and Dr. N. Lalor. Also, thanks are due to Mrs. S. Probert for help with computer programming and running.

Special thanks must be given to the Military Vehicles Experimental Establishment who sponsored the work on two stroke cycle diesel engines. Also many firms who helped by supplying test engines and equipment including Fodens Ltd., Rolls Royce Ltd., Detroit Diesel Allison Division, British Leyland Motor Corporation, Weslake, Short and Co. Ltd. and Wade Engineering Ltd.

The author also wishes to express his appreciation of the technical staffs at the Chilworth laboratories under Mr. F. Cummins and Rayleigh laboratories under Mr. D. Stanton for the engine test programme.

Finally, the author would like to thank Mrs. M.Z. Strickland for typing the manuscript and Mr. G. Bazley and Mrs. J. Bull for help in the preparation of the diagrams, and particular thanks to my wife and family for the help and encouragement that they have given me, particularly during the last few weeks.

TABLE OF CONTENTS

LIST OF FIGURES

Chapter 6

6.1 Structure response to one firing of one cylinder in an in line engine.

6.2 Variation of noise and vibration of engine with a force input from a vibrator.

6.3 Mechanism of diesel combustion noise, with particular reference to the speed effect.

6.4 Detail mechanism of diesel combustion noise.

6.5 Comparison of noise spectra for various types of engines.

6.6 Noise of various diesel engines at rated speed.

6.7 Structure attenuation factor for various configurations.

6.8 Mean structure attenuation factor curve.

6.9 Cylinder pressure spectra versus speed for D.I. four stroke

6.10a) Simplified cylinder pressure spectrum
b) Simplified and reduced cylinder pressure spectrum

6.11 Reduced cylinder pressure spectra four stroke D.I. diesel engine at full load.

6.12 Spectrum shape factor Y. As a function of combustion index.

6.13 Spectrum shape factor X. As a function of combustion index.

Chapter 7

7.1 Comparison of Typical 2 and 4 stroke cylinder pressure development.

7.2 Representation of two and four stroke cycles as repetitive functions.

7.3 Half sine wave representation of 2 and 4 stroke cycles.

7.4 Comparison of computed cylinder pressure spectra for 2 and 4 stroke cycle.

7.5 Comparison of measured cylinder pressure spectra for 2 and 4 stroke cycle at same speed.

7.6 Comparison of measured cylinder pressure spectra for 2 and 4 stroke cycle at same firing frequency.

7.7 Comparison of equal bore engines at same speed.

7.8 Comparison of equal bore engines at the same power.

7.9 Harmonic analysis of piston motion for various L/R ratios.

7.10 Relation between noise and power

7.11 Effect of cylinder pressure diagram width on amplitude of fundamental of cylinder pressure spectra.

Chapter 8.

8.1 Comparison of Cylinder pressure developments of conventional D.I., M.A.N. and petrol engines at 1000 rev/min full load.

8.2 Cylinder pressure spectra of a conventional D.I., M.A.N. and petrol engine.

8.3 Comparison of computed cylinder pressure spectra for a fixed piston engine and a variable compression ratio piston engine at high (350) b.m.e.p.

8.4 Effect of smoothing entry to combustion on an extremely high peak pressure diagram giving 350 b.m.e.p.

8.5 General saw tooth waveform.

8.6 Effect of rate of pressure rise on saw tooth waveform spectra.

8.7 Comparison of saw tooth spectra with typical diesel spectra.

8.8 Cylinder pressure development for diesel and petrol combustion with specific changes.

8.9 Cylinder pressure spectra for diesel and petrol combustion with specific changes.

8.10 Cylinder pressure and corresponding noise spectra of 1.5 litre petrol engine at 2000 rev/min full load.

8.11 Frequency range of rate and acceleration of pressure rise effect on cylinder pressure spectrum.

8.12 Modal pressure distribution for the three lowest frequency modes of a cylindrical space in which $\ell < 0.85B$.

Chapter 9.

9.1 Effect of engine parameters on emitted noise - cylinder pressure development basis constant with speed.

9.2 Effect of injection timing on third octave band noise.

9.3 Relation between cylinder pressure level and noise.

9.4 Effect of injection timing on combustion induced noise.

9.5 Cylinder pressure development for D.I. four stroke diesel.

9.6 Combustion excitation and noise at full load for four stroke direct injection diesel.

9.7 Combustion excitation and noise at no load for four stroke direct injection diesel.

9.7A Comparison of various chamber designs.

9.8 Cylinder pressure development for I.D.I. four stroke diesel engine

9.9 Combustion excitation and noise at full load for I.D.I. four stroke diesel engine.

9.10 Combustion excitation and noise at no load for I.D.I. four stroke diesel engine.

9.10A Comparison of two I.D.I. chamber designs.

9.11 Cylinder pressure development for diesel injection two stroke diesel engine.

9.12 Combustion excitation and noise at full load for direct injection two stroke diesel engine.

9.13 Combustion excitation and noise at no load for direct injection two stroke diesel engine.

9.14 Comparison of two and four stroke compression pressures

9.15 Contribution of Rootes blower to two stroke diesel engine noise

9.16 Lysholm blower rig

9.17 Cylinder pressure development of opposed piston two stroke diesel engine.

9.18 Combustion excitation and noise at full load in opposed piston two stroke diesel engine with Rootes blower removed.

9.19 Cylinder pressure development, spectra and noise at full load for turbocharged direct injection four stroke D.I.

9.20 Cylinder pressure development, spectra and noise at no load for turbocharged direct injection four stroke diesel engine.

9.21 Cylinder pressure development of turbocharged two stroke direct injection diesel engine.

9.22 Combustion excitation and noise at full and no load for turbocharged two stroke direct injection diesel engine.

9.23 Cylinder pressure development of fuel injected petrol engine.

9.24 Combustion excitation and noise at full load in fuel injected petrol engine.

9.25 Effect of turbocharging on cylinder pressure spectrum of 4 stroke diesels at rated speed.

Chapter 9 cont'd

9.26 Comparison of 4 and 2 stroke cycle diesel engine cylinder pressure spectra at rated speed.

9.27 Comparison of D.I. and I.D.I. four stroke diesels at rated speed.

9.28 Comparison of petrol and diesel combustion spectra for four stroke engines.

9.29 Noise and cylinder pressure spectra at various injection timings.

9.30 Comparison single nozzle and seven nozzle two stroke diesel combustion.

9.31 Effect of engine parameters on emmitted noise.

Chapter 10

10.1 Reduced cylinder pressure spectra for two indirect injection diesel engines.

10.2 Reduced cylinder pressure spectra for two direct injection normally aspirated diesel engines.

10.3 Reduced cylinder pressure spectra for two Rootes scavenged two stroke diesels.

10.4 Reduced cylinder pressure spectra for two turbocharged direct injection four stroke diesel engines.

10.5 Full load reduced and simplified cylinder pressure spectra for a range of engines.

10.6 Full load reduced and simplified cylinder pressure spectra grouped according to form of combustion.

10.7 Average full load reduced and simplified cylinder pressure spectra for four classes of I.C. engine.

10.8 No load reduced and simplified cylinder pressure spectra for a range of engines.

LIST OF TABLES

NOTATION

a	pressure diagram width
A	piston area
$A(i\omega)$	Fourier Transform
a_k, b_k	Fourier coefficients
a'_k, b'_k	differential values of a_k, b_k.
B	cylinder bore, ins.
c	velocity of sound
C	$\pi/2_a$
Cp	mean piston speed
$C_{AS}(\omega)$	Combined acoustic and structural factor at frequency ω
$C_{A.S.O.}$	Overall combined acoustic and structural factor.
C_n	Complex form of Fourier Coefficients
C_ω	Complex Fourier Transform Coefficient
f	frequency in Hz
f_o	band centre frequency Hz
f_n	basic engine cycle repetition frequency Hz
$I(\omega)$	Noise intensity at frequency ω
I_o	Overall noise intensity
K	percentage bandwidth
k	integer
ℓ	cylinder depth
L	engine stroke
L_{CR}	length of connecting rod
n	average slope of cylinder pressure spectrum dB/decade
N	engine speed, rev/min
$P_{(\omega)}$	pressure amplitude at frequency ω
q	slope of attenuation versus frequency curve dB/decade
v	integer

R_K	modulus value of Fourier Coefficients
R_K'	differential of R_K
R_o	crank radius
S	Structure attenuation factor
S_{trav}	Surface area of measuring sphere
S_{rad}	surface area of engine
S_{1000}	value of structure attenuation factor at 1000 Hz
S_R	Stroke to bore ratio
T	repetition period
$U_o(\omega)$	surface velocity at a point at frequency ω
$<U_o(\omega)>$	area average mean square surface velocity
V_s	cylinder swept volume
W_{ac}	Acoustic power
X	spectrum shape factor excluding engine area effect - dB
Y	spectrum shape factor including engine area effect - dB
Z	number of cylinders
$Z(\omega)$	Mechanical impedance at frequency ω
ω	angular frequency radians/sec
ρ	density of air
ρc	characteristic impedance of air
$\sigma_{rad}\ (\omega)$	acoustic radiation ratio at frequency ω
$(C.P.)_f$	cylinder pressure at frequency f - N/m^2
$(C.P.)_{1000}$	cylinder pressure at frequency 1000 Hz - N/m^2
$C.P._R(1.0)$	cylinder pressure for reduced spectrum at $f/N = 1.0$ - N/m^2
$(C.P.L.)_f$	cylinder pressure level at frequency f - dB re $2 \times 10^{-5} N/m^2$
$(C.P.L.)_{1000}$	cylinder pressure level at frequency 1000 Hz dB --"--
$C.P.L._R(1.0)$	cylinder pressure level for reduced spectrum at $f/N = 1.0$
$(S.P.L.)_{overall}$	overall sound pressure level - dB re $2 \times 10^{-5} N/m^2$
Suffix 2	two stroke cycle operation
Suffix 4	four stroke cycle operation

1.0 INTRODUCTION

Combustion is a controlled explosion. In the case of the Internal Combustion Engine the control is in the form of an iron structure which does not allow the explosion to communicate itself directly with the surrounding air until the pressure is reduced to little above that of a few atmospheres by an expansion and heat loss process. During the controlled explosion, the containing iron structure is forced to expand and deflect slightly causing a pressure wave to be conducted into the surrounding air. The magnitude of this pressure wave is many times less than that of an open explosion and the pressure wave is perceived as noise rather than a destructive pressure blast. The form of the noise perceived depends on the characteristics of the explosion, the containing structure deformation and the containing structure noise radiation characteristics.

It is the purpose of this thesis to explore the characteristics of the explosion as a function of the form of combustion (diesel and petrol operation), the operating cycle (four stroke and two stroke), the combustion system (Direct Injection, Indirect Injection) and combustion system design details (injection and spark timing, nozzle configuration and swirl).

This objective is not a new one. Indeed, it has always been the aim of engine development since the first successful Internal Combustion engines were built in the late 19th Century. It is the means of obtaining the necessary objective measured data which has been lacking in the past. Now, with the development of high class and accurate cylinder pressure transducers, the use of the Fourier analysis approach and the very recent advances in computer technology and electronic instrumentation allowing, for the first time, the computation and measurement of a few thousand Fourier harmonic values, a great deal of this necessary measured information can be obtained.

The literature concerning combustion, vibration and noise is extensive and it is a credit to early workers that they 'guestimated' so accurately on such scant information. What is always confusing in the literature is that so many apparently conflicting results have been obtained on a variety of engines. It is thought that this present work explains to a great extent the reasons for this and lends weight to the validity of the conclusions reached in earlier work.

In diesel engines combustion studies are concerned with general 'rough running' or noise as a result of normal combustion whilst in the petrol engine they are usually concerned with abnormal combustion conditions, such as detonation and rumble. Since in petrol engines these conditions can lead to mechanical failure, they have been studied extensively. Claims that both rate of pressure rise and acceleration of pressure rise are responsible can be substantiated. It is shown that these results are not inconsistent since the controlling feature of the cylinder pressure diagram is found to vary with both frequency range considered and engine speed.

The layout of the thesis is basically in four parts. Firstly, a consideration of the means and accuracy of assessment of the prime variable - the cylinder pressure development. Secondly, a theoretical study of the mechanism of combustion induced noise and the effect of the operating cycle, peak pressure, rate and acceleration of pressure rise on noise and power are presented. Thirdly, the general measured characteristics of a range of engine classes are presented, together with an overall assessment of trends. Finally, the theoretical and measured characteristics are compared and three methods of predicting the combustion induced noise level in diesel engines presented.

2.0 LITERATURE SURVEY OF COMBUSTION AND NOISE IN INTERNAL COMBUSTION ENGINES

2.1 Overall Picture

Throughout the development over the last 98 years of the internal combustion engine the sound produced by combustion has been used to assess the process. Sound due to combustion has been characterised by various onomatopoeic words like Knock, Rumble, Thud, Ping, Wild Ping, Spark Knock and many others depending on the subjective quality of the sound produced. These sounds have from time to time been correlated with various measured quantities of the cylinder pressure development, namely, peak pressure, rate of pressure rise and rate of change of pressure rise. In diesel engines such studies were concerned with normal combustion, whilst in petrol engines they were concerned with abnormal combustion. The study of the relation between cylinder pressure development and noise has always depended on the availability of adequate devices for measuring the cylinder pressure development in running engines and it was not until the 1950's that such adequate transducers were developed. Hence, only since this time have quantitative values been placed on the sounds due to combustion and their interpretation. This is not to imply that earlier results based on a subjective assessment are incorrect. Far from it - ultimately the sounds are judged subjectively - but this process does produce assessments which have blurred edges and are thus open to misinterpretation.

Early workers used the characteristics of a measured cylinder pressure versus time curve to correlate with a subjective sound or vibration level. Sometimes a mechanical single degree of freedom system, which gave a different response to different applied loads, was used. In the 1950's, Pollack (1952) (2.1) and Robinson and Dadson (1956) (2.2), repeating Fletcher and Munson's work of 1933 (2.3), produced "equal loudness" contours which showed that the response of the human ear to sounds at different frequencies varied, and,

moreover, was non-linear with level. This quantified what had been appreciated for many years and was accompanied by a rapid development in instruments capable of measuring the frequency composition of sound and vibration. Sound could now be measured and quantified by a level versus frequency spectrum as well as by subjective assessment. Knock, Rumble, Ping, etc., could also be specified in a similar manner. Austin and Priede (2.4) in 1958 compared the sound spectrum not with the cylinder pressure development but with the frequency spectrum of the cylinder pressure development. Priede (2.5) in 1960 showed that in this way the ability of a particular pressure development to produce sound at a particular frequency could be determined. Priede developed the method whilst working with diesel engines and later, in 1963, Andon and Marks (2.6) applied this method to the assessment of Rumble in petrol engines. In the same year, Craig (2.7) employed a different approach employing the Duhamel Integral technique to calculate the response of a single degree of freedom system to an approximate mathematical expression for cylinder pressure development. It was gradually established that the measured cylinder pressure spectrum specified the combustion noise excitation propensity of an engine and Priede, Grover and Anderton (2.8) in 1968, showed that the cylinder pressure spectrum could be obtained by Fourier analysis using a digital computer. This computational method was used to show that there was a fundamental difference in the shape of the cylinder pressure spectrum caused by the operation cycle; namely, two stroke and four stroke, which had a profound effect on the combustion noise of the two types of engine. This type of analysis was carried further (2.9) in 1969 to show that even in diesel engines, when the rate of pressure rise was not too high, the rate of change of rate of pressure rise (acceleration of pressure rise) controlled high frequency combustion noise, even when peak pressures up to 3,300 psi were employed. In 1970, Anderton, Grover, Lalor and Priede (2.10) extended this approach to include a model for combustion noise in which it was found that, for current production

automotive engines, the engine noise could be predicted from the engine speed and bore. This differs from previous prediction formulae in that it is derived from a consideration of theory and not largely a statistical relationship involving the main engine parameters, as in the case of Zinschenko in 1957 (2.11), Slavin in 1960 (2.12), Pflaum and Hempel in 1966 (2.13) and Cordier and Reyl in 1968 (2.14).

2.2 Early Work (1900-1939)

Ricardo, during the early 1920's realised that the tendency of fuels to detonate in constant volume (petrol) internal combustion engines limited the engine performance. He wrote (2.15), "The phenomenon of detonation as apart from its relation to the nature of the fuel will be dealt with later, but for the present it is sufficient to state that the limit to which the compression ratio can be raised, and therefore the limit of power output and efficiency, is governed by the conditions which control detonation and pre-ignition". Ricardo described Detonation in the following manner: "The phenomenon of detonation appears to be the setting up in the cylinder of an explosion wave. This occurs when the rapidity of combustion of that portion of the working fluid first ignited is such that, by its expansion, it compresses before it the unburnt portion beyond a certain rate. When the rate of temperature rise due to compression by the burning portion of the charge exceeds that at which it can get rid of its heat by conduction, convection, etc., by a certain margin, the remaining portion ignites spontaneously and nearly simultaneously throughout its whole bulk, thus setting up an explosion wave which strikes the walls of the cylinder with a hammer blow and, reacting in its turn, compresses afresh the first portion ignited. This further raises the temperature of that portion and, with it, the temperature of any isolated or partially insulated objects in its vicinity, thus ultimately giving rise to pre-ignition. It would, therefore, appear pretty certain that detonation

depends primarily upon the rate of burning of that portion of the charge first ignited, and it remains to discover what actually controls this rate".

Thus, detonation limited petrol engine performance and mechanically and thermally overloaded an engine structure. These were the reasons for the vast amount of work, still continuing, carried out on various aspects of detonation. Noise and vibration were not at that time of primary concern and were involved largely because, by the noise and vibration produced by a detonating engine, the onset of detonation could be detected - at that time by the human ear.

Ricardo had also at that time identified the three stages of diesel combustion and although not specifically stated, had correlated the severity of the second stage of combustion (uncontrolled burning) with the subjective sound of the running engine. He therefore suggested that the delay period should be shortened for smooth running and mentioned the use of higher compression ratio, and pre-heating of air before entry to the combustion chamber and the degree of pulverisation of the injected fuel as controlling factors in smooth running.

The implication that higher rates of burning in the cylinder are synonomous with engine "rough running" is shared by Heldt (2.16) when, in 1932, he writes of diesel engines: "roughness or harshness of the combustion in diesel engines may be overcome by either increasing the compression pressure or by pre-heating the air entering the cylinder. Both of these expedients have the effect of reducing the ignition lag. Pre-heating the fuel has also been suggested". The slight change of emphasis from Detonation to Roughness shows that roughness (or noise) was of concern to the engine manufacturers very early in diesel engine development.

In 1929, two years earlier than the books of Ricardo and Heldt, Janeway (2.17) examined the problem of detonation from the combustion chamber design aspect. He was concerned with the response of the structure to the combustion

load as well as the chemical aspects, and this was the first investigation to consider if rate of pressure rise or rate of change (acceleration) of pressure rise controlled the shock loading of the engine structure. He wrote, "Since the shock load is produced by the pressure rise of combustion, the source of the trouble is obviously to be found in the characteristic of that pressure rise with respect to time. It is only natural to jump to the conclusion that the maximum rate of pressure rise is the determining factor in shock. However, this is really to superficial to be true, as we found out when we tried to design combustion-chambers around the maximum rate of pressure rise. What happened was that chambers that should have given velvety smoothness, according to this theory, gave a result that was more like sandpaper. After that a new theory had to be found. The next attempt was much closer to the truth. This time we chose the acceleration in the rate of pressure rise as the deciding factor and found that keeping down this acceleration really produced smooth operation.'

'But guesswork, even when attended by good luck, is not a reliable means of progress, so it was necessary to construct a fundamental picture of the problem in order to determine the true relation of the various factors to the result. Since the measure of shock load is the deflection it produces, let us analyse the pressure-time characteristic for its direct effect on deflection of the resisting structure.'

'At any instant during the combustion the deflecting structure resists the impressed force with a restoring force which is proportional to its deflection at that instant, if the action is elastic. Also, since the impressed force is constantly changing, the deflecting structure has a definite velocity. If the rate of increase in the impressed force is built up gradually, so that the rate of deflection can follow it, the restoring force will always exactly balance the impressed force and the maximum rate of pressure rise will in itself determine the maximum rate of deflection and,

consequently, the dynamic load. However, if the acceleration in the rate of increase of the impressed force is appreciable, a force differential must be provided to accelerate the deflecting mass. This required force-differential can come only from an unbalance between the impressed and the restoring forces. As a result, the greater the acceleration in the increase of impressed force, the greater is the instantaneous lag of the deflecting rate behind the rate of force increase. This lag lasts as long as the acceleration continues undiminished. When the acceleration falls off, however, the force differential which has been created between the impressed and restoring forces becomes effective in accelerating the deflecting mass, with the result that a velocity of deflection is built up in excess of that corresponding to the maximum rate of increase in impressed force."

"From this analysis it is evident that no single feature of the pressure-time characteristic can be selected which will give a true quantitative gauge of the shock load. This can be obtained only by an integration involving the entire characteristic."

Janeway used a graphical method to compute the deflection of a given single degree of freedom system, due to an impressed load, given by measured cylinder pressure - time developments. The method used is basically that used subsequently by O'Hara for shock spectrum computation in 1962 when digital computers were sufficiently developed to replace the graphical solution.

In 1932, Le Mesurier and Stansfield (2.18) completed similar investigations on a diesel engine by running with different types of fuel. This produced combustion with varying rates of pressure rise. They showed how the noise and vibration of an engine, as measured by a special instrument, may be correlated with the length of delay period. As delay increased, the rate of pressure rise increased and so did the noise and vibration. Eventually, the conditions where all the fuel was injected during the delay period and

the peak rate of pressure rise and noise and vibration was reached. After this point the rate of rise diminished with increasing delay period, as did the noise and vibration. Those fuels which gave short delay times and smooth running were the ones composed largely of members of the paraffin series, while the long delays were always associated with a large percentage of naphthenes and aromatics.

Pye (2.19) in 1937, described the sound of detonation or "pinking"; "The noise which has given the name of "knocking" to detonation is like that produced by a sharp ringing blow upon the metal of the engine cylinder. Formerly it was supposed to be actually due to some such mechanical cause, which might be derived, it was supposed, from a looseness between moving parts. Experiment soon proved this supposition to be untenable, and in place of a mechanical blow between two solid parts of the engine, we now imagine the noise to be caused by a blow delivered against the cylinder wall, by a wave of high pressure travelling at great speed through the gas which forms the working substance."

Pye also identified diesel combustion as an extension of the same phenomenon where the "knocking" was a constant feature of normal operation. At this time the measurement of the tendency of various fuels and engines to detonate was still the main criterion and Pye listed the following method of detecting its onset: "Apart from the cathode-ray indicator and from simply listening for the characteristic metallic knock, three methods of detecting detonation have been developed. These are the 'bouncing pin', the maximum pressure indicator, and the 'temperature plug'."

"When detonation occurs, pressures may be developed locally far in excess of the normal maximum pressures. These sharp rises of pressures are made use of in the bouncing pin apparatus of Midgeley and Boyd to throw a heavy pin off its seat, so as to make contact at its other end with an easily deflected spring. The duration of contact with this spring is a

rough measure of the original momentum of the pin, and this, in its turn, of the violence of the blow from the detonation wave which gave it the momentum. A record of the number of contacts with the spring, and of the length of their duration, is obtained by the amount of gas produced in an electrolytic circuit which is closed by the contact. The apparatus works very well for comparing the violence and persistence of the detonation with two different fuels; its weakness lies in the fact that it is not satisfactory for detecting incipient detonation, because a certain violence of blow is necessary to displace the bouncing pin. It is very difficult, moreover, to maintain the adjustment of the various parts of the apparatus so that it reacts equally from day to day, to similar degrees of detonation as judged by other methods."

"It is unquestionably important sometimes to have a more positive method of maintaining the same standard between one observer and another, as to what is 'incipient detonation', than is possible when this is left to personal judgement of the noise of the characteristic knock, more especially when high-power and noisy aero-engines are in question. With these, incipient detonation may sometimes be accompanied by no clearly definable noise, and may only be detectable by what may be termed harsh running. A more satisfactory way of getting over the difficulty than by relying on auditory observation is by the use of an adaptation of the Farnborough indicator. If the indicator be connected in the normal way to the engine cylinder, and the balancing pressure is set to one, two or three hundred pounds per square inch above the normal maximum pressure, then the incipient detonation will be marked by an occasional record of an excessive pressure, the frequency depending upon how much the balancing pressure exceeds the normal. A convenient form of this detonation indicator has been worked out in which, as the balancing pressure is gradually raised, its magnitude is indicated on the usual type of 'dial and pointer' pressure gauge. Every

time the cylinder pressure exceeds the balancing pressure a spark passes from the tip of the pressure gauge pointer on to the scale behind it. A standard of detonation is established in terms of a certain number of sparks per minute at some agreed value of the balancing pressure."

"The third, temperature plug, method of detecting detonation depends upon the fact that as soon as detonation begins there is a rise of temperature at the surface of the cylinder head. If a metal plug incorporating a platinum resistance thermometer or a thermocouple element is screwed into a sparking-plug hole, the temperature-rise indicative of incipient detonation can be observed before any knock can be heard."

"Opinions differ as to the convenience and reliability of the various methods, and, indeed, these differ according to circumstances. With the Ricardo E.35 engine, which has been largely used for comparing H.U.C.R. values through its having been first in the field, the bouncing pin cannot be used for reasons of design; and, although the maximum pressure indicator could be used, auditory methods have been found more satisfactory. A skilful observer can repeat observations of H.U.C.R. with fair certainty by auditory methods to 0.05 of a ratio."

"A weakness of all three methods referred to above, and one from which the cathode-ray indicator does not suffer, is that the amount of the effect which is relied upon for indication, whether it is a rise of pressure or of temperature, depends very much upon the position of the indicating point in the cylinder. The sharp rises of pressure and temperature associated with detonation are very local, and, if the indicating point is remote from the centre of disturbance, it may be impossible to get any useful indication at all. The cathode-ray indicator, giving as it does a true record of the pressure wave system which is typical of detonation, travelling to and fro across the cylinder head, should not be subject to the same drawback, and promises to provide a really satisfactory indicator of detonation when

developed for this purpose."

Pye also turned his attention to the roughness of petrol engines. He observed that "Excessive turbulence may produce harsh running, and it has even been found possible, with turbulence of the organised swirl type, to prevent combustion altogether. With normal turbulence in one engine, with ignition at 28^{o} b.t.d.c., the pressure rose steadily at about 17 lb/in^2/ degree of crankshaft rotation. With excessive turbulence, and ignition retarded to 12^{o} b.t.d.c., the rate of rise was over 50 lb/in^2/degree, and a very rough running engine of lower power output was the result. What precisely is meant by a 'rough running' engine is as difficult to define as the meaning of turbulence. It has been stated, when discussing combustion in the diesel engine, that roughness is more easily apprehended from experience of an engine on the test-bed than described in words, and this is equally true of the petrol engine. A rough running engine is noisy without necessarily giving out any of the characteristic knock of detonation; there is also a certain amount of general vibration, unless the engine is very solidly mounted on the test-bed; and if the roughness be allowed to continue for long, both the connecting-rod and main bearings will probably suffer."

"The desired smoothness of running and its relation to turbulence is a point of great importance. Apart from the average rate of pressure rise, smoothness appears to depend particularly, in some designs at any rate, upon the rate of rise at the very beginning of combustion." Pye then illustrated this point with an example showing the same engine with standard and modified combustion to give the same peak pressure and rate of pressure rise, but different entry to combustion.

Turning his attention to the compression ignition diesel engine, Pye wrote that "If the uncontrolled type of combustion with its extreme rate of pressure-rise occurs in an engine after a long delay period, the result is an intolerable roughness of running accompanied by a loud 'kock' somewhat, but

not quite, like the pinking or detonation of a petrol engine. This 'diesel knock' as it has been called, is undoubtedly due to extremely rapid burning, often of a large part of the fuel charge, if the delay before it has been long. There is general agreement that diesel knock is nearly always associated with a long delay period and that, failing its elimination, the shortening of the delay period is of primary importance for the development of a smooth running and reliable engine. Whether or not detonation and diesel knock are identical in their physical nature, they are similar in their effects."

2.3 Later Work (1939-1973)

Hinze in 1949 (2.20) in an excellent paper on the effect of cylinder pressure rise on engine vibrations (with a very good literature survey), states: "In studying these papers the reader is struck by the great divergencies and many controversies between opinions of various authors, in their search for a suitable measure for judging the pressure-time curve, in its effect on the generation of vibrations." Hinze discusses the various methods of analysis used up to that time and then considers the problem of response to a time varying force by assuming:

(a) steady state conditions,

(b) that engine vibration behaves like that of a single harmonic oscillator.

This enabled him to produce dynamic magnification factor curves as a function of the impulse duration due to cylinder firing and the natural period of the harmonic oscillator. He also calculated the maximum kinetic energy in a similar manner, since Fry, Stone and Withrow (2.21) had suggested this as a better criterion.

Hinze used these results to explain the measurements of Le Mesurier and Stansfield (2.22) and Withrow and Fry (2.23), but made no comment upon varying frequency of response.

Hinze concluded,

"(1) In analysing the pressure-time curves of internal combustion engines for their effect on engine vibrations, one has first of all to determine: the ratio between the period of rapid pressure rise and the natural period of the vibratory system; and further, the maximum pressure rise, during the former period, over and above the compression pressure. Only if said ratio exceeds a value of about a quarter, is it worthwhile to analyse the shape of the pressure-time curve more closely for its effect on the response of the vibratory system. It must be kept in mind, though, that the effect of the shape of the pressure-time curve still is a minor one if compared with the duration of the period of rapid pressure rise.

(2) It is fundamentally impossible to express the effect of the particular shape of the pressure time curve on the response of the vibrating system in terms of one single time derivative of the pressure time curve, for the same reason that it is fundamentally impossible to express the particular shape of the pressure-time curve in terms of one single derivation."

This last conclusion is the key to the solution of the varied results obtained over the years, and although Hinze did not consider noise but only vibration, these results are still applicable.

Up until this time, noise of internal combustion engines was a minor design consideration, but as lighter and more powerful engines became available it was obvious that the noise levels were becoming too high for comfort. In recognition of this fact the first Institution papers specifically on diesel engine noise were produced in 1953 - C.H. Bradbury (2.24) in England and J.E. Ancell (2.25) in the U.S.A. Both papers described the complexity and number of noise sources making up a diesel engine and suggested enclosure for noise control. Bradbury investigated and distinguished combustion noise and found that combustion noise was not only dependent on rate of pressure

rise but also on acceleration of pressure rise. Both papers emphasised the importance of the sound pressure level versus the frequency spectrum as opposed to the sound pressure-time variation from the noise assessment standpoint.

In 1958, Austin and Priede (2.4) produced the first paper where modern acoustics technology was applied scientifically to assess the characteristics of diesel engine noise. The work was to "establish fully the mechanisms of the generation and radiation of the various components of the noise, to assess their relative importance and to establish, in principle, means of reducing them." Austin and Priede found that exhaust and air inlet noise were predominant sources of noise. The effect of speed, load, fuel injection equipment, engine covers, flywheel and front pulleys was assessed. The 'basic engine noise' (that radiated by the main engine surfaces) was found to be combustion controlled (i.e., varied as injection timing) and a Fourier Analysis of the cylinder pressure development was obtained by use of electrical analysers. This is the first application of a level-frequency transform being used to compare the noise characteristics of engine combustion. It showed that the main difference between a smooth petrol engine combustion and the more abrupt diesel diagram was largely at the higher frequencies where the level of the spectrum was higher for diesel operation. It was observed that a substantial reduction in the cylinder pressure level at higher (above 300 Hz) frequencies in the petrol engine occurred as load was reduced and that the noise also reduced. The noisiness of different engine structures were compared by means of an attenuation curve (cylinder pressure level in band - sound pressure level in band) and it was observed that the noise radiated by diesel engines was highest in the mid-frequency range (800-2000 Hz). Austin and Priede concluded "The mechanism of the generation and radiation of engine noise is complex, and overwhelming quietening cannot be produced by giving attention to any single factor. Air

intake noise, and valve and timing covers are liable to be strong sources of noise. Reduction in the noise from them may produce a major quietening, and mechanical noise, or in extreme conditions, injection-equipment noise, may then be predominant. In some engines a contribution should be obtained by smoothing the cylinder pressure."

This paper marks a major change in the way the dynamic response of engine structures was analysed. Until this time the prediction of the displacement-time curve for an engine was the aim, but here the use of a measured Fourier series for both noise and cylinder pressure development indicated the correlation between the smoothness of a diagram and the levels of the high frequency components of a frequency analysis.

In 1960, Priede (2.5) continued this work by looking in more detail at the form of the cylinder pressure development and its spectrum and how this affected total engine noise. Because of the large number of harmonics required (some 1200), numerical methods and the use of electronic computers were found to be impracticable and the method of measuring with an electronic frequency analyser was used. It was found that a 'Critical cylinder pressure level curve' could be established by measuring the change in noise and cylinder pressure level at a given frequency. This was accomplished by varying the injection timing. Above this curve combustion noise was greater than mechanical and vice versa. In comparing the cylinder pressure spectra for a compression curve, smooth combustion, abrupt combustion and an electrical saw tooth waveform, it was found that the higher harmonics controlled the maximum noise in the 800-2000 Hz range. These were controlled by the form of the diagram; the more abrupt the diagram the higher the level of the higher harmonics. The degree of abruptness could be correlated with percentage of total fuel which was burned during the uncontrolled phase of combustion. Instead of describing a cylinder pressure development in terms of the pressure

rise and its derivatives, the capacity of the development to excite engine vibrations at any frequency throughout the audio frequency range could be described by a cylinder pressure spectrum, changes in which were directly reflected in the noise output of the engine. Priede concluded, "It is shown that the noise due to combustion in a diesel engine is determined by the form of pressure rise fully described by the cylinder pressure spectrum. This noise, however, is added to the mechanical noise of the engine, thus giving a resultant noise which is found to follow a known relation for the addition of two noise sources. A 'critical cylinder-pressure spectrum level' is introduced defining a condition when noise due to combustion equals that of the mechanical noise. This 'critical level' describes a characteristic of the engine and gives an indication of how far a 'smoothing' of cylinder-pressure diagram is required in a particular instant for the noise due to combustion not to penetrate the general mechanical noise. In practice, this condition is often achieved for steady running but combustion noise may exceed mechanical noise during acceleration."

"The low-frequency part of the cylinder pressure spectrum depends essentially on the peak pressure, whereas the high-frequency part depends on the form of the pressure rise. The cylinder pressure level of a diesel engine is normally markedly higher than that of a petrol engine from 800 Hz upwards. The difference in the form of pressure rise is ascribed to the difference of combustion processes in the two engines; steady propagation from the point source in the petrol engine as against the very rapid combustion following spontaneous ignition in the diesel engine."

"The rapid pressure rise in a diesel engine caused by the sudden combustion of an appreciable fraction of the fuel-air mixture (1.5 - 26.0 percent of the injected quantity at full load) initiates also pronounced gas oscillations in the combustion chamber. These oscillations produce a broad peak on the cylinder-pressure spectrum and thus enhance the emitted

noise in that frequency range."

Over this period (1949 onwards) the problems of abnormal combustion in petrol engines were still being investigated and by 1954 it was realised that the different terms used to denote such combustion could be defined in terms of their predominant frequency characteristics. A C.R.C. report (2.26) was issued in this year entitled 'Terms for use in Otto cycle engine combustion' and Starkman and Sytz (2.27) in 1960 used these terms to investigate 'Rumble' in petrol engines; "A recent problem associated with combustion in high-compression-ratio spark-ignition engines is the occurrence of two noises characterised by being of much lower audio frequency, about 600-2000 Hz, than the usual 5000-8000 Hz sounds of knock. While there is some confusion over the usage of the terms, one of these, called rumble, is associated with combustion chamber deposits and is aggravated by increasing compression ratio and engine speed. Another, called thud, while sounding the same as rumble, and reacting similarly to engine variables as rumble, can be brought about by advancing the spark setting."

Starkman and Sytz established that lateral bending vibrations of the crankshaft (at 600 Hz) were excited by, and coincided with, the rapid pressure rise associated with rumble. Noise and vibration oscillograms showed a similarity but the predominant noise measured was at 1200 Hz, the start of the two vibrations coinciding, but the duration of the noise being longer. They conclude: "The induced vibrations of the crankshaft are definitely linked to abnormally high rates of pressure rise. When these rates of pressure rise are far ahead of t.d.c. and could be called pre-ignition, there is sufficient instantaneous reversed torque to induce a restraint on the crankshaft. This gives rise to a torsional vibration and so-called Thudding. Advancing the spark is one way to induce this phenomenon. When the high rates of pressure rise occur near t.d.c., the crankshaft receives a bending impulse. This results in rumble. There is no reason to

believe that one phenomenon cannot blend into the other, and, furthermore, a coupled vibration of bending and torsion is highly possible."

Stebar, Wiese and Everett (2.28) in the same year published similar findings and suggested the mechanism of rumble as:

1) Multiple ignition of the fuel-air mixture by engine deposits;

2) abnormal pressure development;

3) shock excitation of engine parts;

4) resonant vibration producing rumble noise;

and observed that the characteristic sound frequencies did not change with engine speed, indicating resonant structural vibration.

Three years later, Andon and Marks (2.6) turned their attention to the problem of engine roughness and applied the frequency analysis techniques of Austin and Priede. The engine noise during rumble produced increased levels in the 500-2000 Hz range. They showed that a frequency analysis of a 'rumble' or 'fast burn' cylinder pressure development produced higher levels of harmonics from the 15th onwards as compared with a normal development. For normal combustion rates of pressure rise of 10-40 psi/degree were found; for fast burn rumble, 50-70 psi/degree. In the discussion to the paper, Austin and Priede showed measured cylinder pressure spectra for normal, fast burn rumble and knock cycles in a petrol engine. For fast burn, the spectra showed increased levels through the frequency range to 3000 Hz as Andon and Marks found. For a knock cycle, only the levels above 1000 Hz were increased with a substantial increase in the peak due to cylinder pressure oscillations at 6000 Hz. Janeway also re-proposed his method for predicting the structure deflection-time curve and re-iterated his belief that acceleration of pressure rise was the true criterion for this response.

It is clear that at this time there was still greatly divided opinion on what characteristic of cylinder pressure development was the prime cause in producing noise from both diesel and petrol combustion and Craig (2.7),

in 1963, set out to solve this problem. Craig decided to use the method proposed by Timoshenko, using a Duhamel integral (impulse response) method to calculate the peak velocity of a series of single degree of freedom systems when an applied pulse shape is imposed. He preferred this to the Fourier approach because the high number of harmonics needed could not be computed easily. He divided the applied cylinder pressure diagram into portions which could be represented by various simple algebraic expressions and then using Leibnitz's theorem represented these as a differential series. The results, for a constant mass system, were given as a 'relative sound intensity level' versus frequency spectrum. He showed for a typical petrol engine cylinder pressure development that:-

(a) Up to about 150 Hz, the response was controlled by the peak pressure.

(b) From 150 to about 1500 Hz the response was controlled by the rate of pressure rise and the rate of change of pressure rise on initiation of combustion.

(c) From 1500 Hz upwards the response was controlled by the maximum rates of change of pressure rise occurring in the cycle.

These results were the same as indicated by Priede (2.5), but added the result that very high frequency response was controlled by the maximum rate of change of pressure rise.

The results were of great interest and show why so many investigators had in the past come to what appear to be conflicting conclusions. The answer was that depending on the frequencies of noise assessed, 4000-6000 Hz for knock, 200-2000 Hz for rumble, etc., the controlling feature could be either maximum pressure, maximum rate of pressure rise or acceleration of pressure or combinations of all three.

In 1965, Priede (2.29) published a polished summary of the subject of noise due to combustion, covering his early work and adding further findings.

The effect of combustion chamber geometry on the cylinder pressure spectrum was shown to have a great effect on the cylinder pressure oscillation frequency and also the general level of the harmonics. The change in cylinder pressure spectrum with speed was shown to be the cause of the high rate of increase in noise with speed observed on both diesel and petrol engines. In a consideration of the form of a pressure diagram and its spectrum he showed that an approximate spectrum could be drawn by the addition of the spectra due to:

(a) compression curve

(b) spectrum associated with the mean rate of pressure rise

(c) a sawtooth wave spectrum with magnitude corresponding to the magnitude of any initial rapid rate of pressure rise upon initiation of combustion. As a consequence the reverse process could be used to identify the main source of high frequency excitation in the original pressure diagram.

Priede also turned his attention to the reduction of noise due to combustion, and showed that by reducing the number of spray holes or spraying fuel on to the wall of the combustion chamber the combustion excitation could be reduced.

In 1968, Bertodo and Worsfold (2.30) proposed a model of combustion noise based on a consideration of acoustical power. The power was shown to be given by three largely unknown system efficiencies, the square of b.m.e.p., a structure factor and inversely proportional to the number of strokes.

In the same year, Priede, Grover and Anderton (2.8) proposed a mechanism of combustion noise and used this to show how engine noise depended on speed and load for various combustion chamber types and fuel ignition systems. It was also shown that, because of advances in digital computer programming and speed, the cylinder pressure spectrum could be computed from a single oscillograph of cylinder pressure development. Use of this technique showed

that there was a fundamental difference between the cylinder pressure spectrum for two and four stroke diesel cycles. This showed that at the same cycle repetition frequency the excitation provided by two stroke combustion could be some 6 dB lower over the important frequency range of 500-2000 Hz. Thus, under certain conditions, the two stroke diesel engine cycle was shown to be inherently quieter. Also, in this paper, the phenomenon of cylinder pressure oscillations was expanded. It was found that the frequency of the oscillations decreased as the engine swept volume increased, and that the severity of these oscillations was determined by the damping to across-the-bore oscillations between piston and cylinder head. If this 'bump' clearance was low and there was no valve cutouts in the piston, then the oscillations were damped considerably.

Two years later, in 1970, Anderton, Grover, Lalor and Priede (2.10) showed that for a given rate of pressure rise in I.C. engines, the combustion noise could be very different according to the rate of change of pressure rise at the initiation of combustion, sharp changes producing an increase in noise above 1000 Hz, supporting the findings of Craig (2.7). The proposed mechanism of combustion induced noise (2.9), (2.34) and (2.10) was shown to be possible of expression in a mathematical form. A combustion noise model was proposed and from an empirical constant a series of noise prediction formulae, based on type of combustion system, bore and speed only, was established. This relationship was shown to predict current four stroke and two stroke diesel engine noise to within 2 dBA.

In the Indirect Injection Engine, the cylinder pressure oscillations occur at frequencies near 2000 Hz for half a litre per cylinder engine size. Combustion in these engines is rather less steady than that of the Direct Injection type. Burt and Troth (2.32) found that the maximum combustion noise frequency for a particular engine was at 2370 Hz and they characterised the combustion noise in terms of the noise response at this frequency

as the combustion was changed. Because of the unsteady combustion, a statistical approach was used and Burt and Troth found that the peak combustion noise intensity was not very dependent on rate of pressure rise but was dependent on the rate of change of pressure rise. Again this confirms the general findings of Craig (2.7).

In January 1973, a special session on Diesel Engine Noise Reduction at the International Automotive Engineering Congress of S.A.E., produced a large number of papers, most of which discussed combustion noise to varying degrees. The general content of the papers indicates a changing attitude to diesel noise in that it had now passed from a largely research attitude to a development of hardware to reduce noise, and summaries of the compromise solutions possible. Russell (2.32) showed that in trying to achieve good gaseous emissions, smoke and noise, if injection was retarded, so both Nitrous Oxides and noise were reduced. However, when considering smoke and noise it was found that smoke increased with retarded injection whilst noise decreased. Tiede and Kabele (2.34) showed that in a D.I. automotive diesel by changing from a shallow dished chamber with a five hole nozzle to a slightly deeper torroidal chamber with a four hole nozzle, an overall engine noise reduction of 3 dBA resulted. Scott (2.35) at the same conference, discussed the combustion noise of small I.D.I. diesel engines. Pilot injection was shown to provide a useful noise reduction at idle but to be impractical for such small injectors at load conditions where specific fuel consumption was increased as noise was reduced. He proposed the use of the Unit type injector to provide better control over fuel injection during the delay period and consequently lower combustion noise. Anderton and Baker (2.36), again at the same conference, showed that engine surface vibration and noise behaved in a linear manner and that for a given engine structure a comparison of combustion noise radiation can be made simply by comparison of the cylinder exciting force spectra. On this basis it was shown that two and four stroke

combustion noise characteristics were markedly different and that the higher the turbocharging of the four stroke cycle became the closer this approached the characteristics of the two cycle engine, i.e., higher low frequency excitation. Combination of engine performance calculations with the empirical noise prediction formulae indicated that in naturally aspirated form the two stroke cycle was inherently quieter for a given power. In the turbocharged case the two stroke advantage was not as great.

This Diesel Engine Noise Reduction Session illustrated that many of the research findings over the past 20 years were now finding their way into production but that there was still a long way to go before completely 'sociable' Internal Combustion Engines were the normally accepted rule rather than the exception.

REFERENCES

2.1 Pollack 'The Loudness of Bands of Noise' Journal of the Acoustical Society of America, 24, Sept. 1952, p. 533-538.

2.2 Robinson and Dadson ISO Standard R226 1961.

2.3 H. Fletcher and W.A. Munson. 'Loudness, its definition, measurement and calculation'. J.A.S.A., 24, 80.

2.4 A.E.W. Austen and T. Priede. 'Origins of Diesel Engine Noise'. Proc. Symp. on Engine Noise Suppression, London, Oct. 24, 1958, pp. 19-32.

2.5 T. Priede. 'Relation between the form of cylinder pressure diagram and noise in diesel engines'. Proc. I.M.E. Automobile Division (1960-61) 63-77.

2.6 J. Andon and C. Marks. 'Engine roughness - the key to lower octane requirements'. S.A.E. Trans. Vol. 72 (1964) p. 636-658.

2.7 W.S. Craig. 'Theoretical relationship between combustion pressure and engine vibration'. S.A.E. paper 647c, presented at S.A.E. Automotive Engineering Congress, Detroit, January 1963.

2.8 T. Priede, E.C. Grover, D. Anderton. 'Combustion Induced Noise in Diesel Engines'. Diesel Engine Users Association publication 317, March 1968.

2.9 D. Anderton, N. Lalor, E.C. Grover, T. Priede. 'Combustion induced noise in I.C. engines'. Combustion Engine Progress, 1969, London, England.

2.10 D. Anderton, E.C. Grover, N. Lalor, T. Priede. 'Origins of reciprocating engine noise - it's characteristics, prediction and control'. ASME paper no. 70-WA/DGP-3, December 1970.

2.11 J. Haasler. 'Gerauschverhalten von Viertakt-Dieselmotoren". Dusseldorf: VDI-Forschungsheft 505 (1964), p.10.

2.12 I.I. Slavin. "Industrielarm und seine Bekampfung". Berlin: Verlag Technik, 1960, p.346.

2.13 W. Pflaum and W. Hempel. "Gerauschverteilung bei Dieselmotoren." Forschungsbericht 2-215/3; Frankfurt am Main: Forschungsvereinigung Verbrennungskraftmaschinen E.V., 1966.

2.14 O. Cardier and G. Reyl. "The noise problems of air cooled diesel engines - measures towards its reduction, with general observations and specific results'. Paper 680405 presented at SAE Mid-year meeting, Detroit, January 1968.

2.15 H.R. Ricardo. 'The high speed internal combustion engine'. First edition, Blackie & Sons Ltd, Glasgow 1931.

2.16 P.M. Heldt. "Diesel Engines" - Blackie.

2.17 R.N. Janeway. "Combustion control by cylinder head design". SAE Journal, Vol. 24, p.498, 1929.

2.18 L.J. Le Mesurier and R. Stansfield. "Combustion in heavy oil engines", North East Coast Institution of Engineers and Shipbuilders, Feb. 26th, 1932.

2.19 D.R. Pye. 'The Internal Combustion Engine'. Vol. 1. Oxford University Press, Second edition, 1937.

2.20. J.O. Hinze. 'Effect of cylinder pressure rise on vibrations'. ASME Paper no. 49-OGP-3.

2.21 Fry, Stone and Withrow. "Analysis of shock excited transient vibration associated with combustion roughness". SAE Quarterly Trans. (1947), p.164.

2.22 L.J. Le Mesurier and R. Stansfield. "Vibration in engine structures". Paper read before North East Coast Institution of Engineers and Shipbuilders, Feb. 26th, 1932.

2.23 L. Withrow and A.S. Fry. "Physical characteristics of roughness in internal combustion engines". SAE Journal 52, 1944.

2.24 C.H. Bradbury. "The measurement and interpretation of machinery noise with special reference to oil engines". Proc. I. Mech. E. 1953.

2.25 J.E. Ancell, "A practical noise reduction treatment for diesel engines". J.A.S.A. Vol. 25 (1953), pp. 1163-1166.

2.26 "Terms for use in Otto cycle engine combustion". C.R.C. Report No. 278. June 1954.

2.27 E.S. Starkman, W.E. Sytz. "The identification and characterisation of rumble and thud". SAE Trans. Vol. 68/1960, p.93-100.

2.28 R.F. Stebar, W.M. Wiese and R.L. Everett. "Engine rumble - a barrier to higher compression ratios". SAE Trans. Vol. 68 (1960), p.206.

2.29 T. Priede. "Noise due to combustion in reciprocating internal combustion engines". Advances in Automobile Engineering, Part 3, edited by G.H. Tidbury, Cranfield International Symposium Series, Volume 7, Pergamon Press.

2.30 R. Bertodo and J.H. Worsfold. "Medium speed diesel engine noise". Proc. I.Mech.E., vol. 183, Pt. 1, no. 6, 1968-1969.

2.31 D. Anderton. 'Progress in I.C. engine noise assessment and suppression techniques'. Combustion Engine Progress, London, 1970.

2.32 R. Burt and K.A. Troth. "Combustion knock in pre-chamber engines". Paper submitted to SAE, 1970.

2.33 M.F. Russel. "Automotive diesel engines noise and its control". SAE paper 730243, Detroit, January 1973. Diesel Engine Noise Reduction Session.

2.34 D.D. Tiede and D.F. Kabele. "Diesel Engine Noise Reduction by Combustion and Structural Modifications". SAE paper No. 730245. Detroit, January 1973, Diesel Engine Noise Reduction Session.

2.35 W.M. Scott. "Noise of small indirect injection diesel engines". SAE paper no. 730242, Detroit, January 1973. Diesel Engine Noise Reduction Session.

2.36 D. Anderton and J. Baker. "Influence of operating cycle on noise of diesel engines'. SAE paper 730241, Detroit, January 1973, Diesel Engine Noise Reduction Session.

3.0 MEASUREMENT OF CYLINDER PRESSURE

3.1 Cylinder Pressure Transducers

The measurement of cylinder pressure in Internal Combustion Engines poses one of the most difficult tasks for instrument manufacturers. Not only do the transducers used need to be compact and stable with very fast response and good dynamic range, but these characteristics must be achieved and still withstand explosive and intense transient thermal loading, (refs. 3.1-3.5). Of the many types of pressure gauge used, variable resistance, variable inductance, variable capacitance, balanced disc and piezo-electric, only the balanced disc, variable resistance and piezo-electric types of gauge have proved robust and accurate enough (although some capacitance types have been reasonably successful). For engine cycle analysis the most accurate of these is the balanced disc type (Fig. 3.1) but this transducer is only capable of showing the average pressure development over a large number of cycles and so cannot be considered of use in dynamic response work, except as a calibration and error check. For high pressure dynamic cylinder pressure measurement the variable resistance (strain gauge (ref. 3.3, Fig.3.1) and piezo-electric (ref. 3.6) transducers, shown in Fig.3.2, are suitable. Both of these types of transducer have good response, good pressure sensitivity, low temperature sensitivity, low acceleration sensitivity and can be manufactured in a small enough size - less than $\frac{1}{2}$" diameter - to enable installation in combustion chambers. The work presented in this thesis is based largely on measurements using the piezo-electric type of gauge, although some use of strain gauge types has been made (Figs. 3.3 and 3.4).

3.2 Pressure Transducer Installation in I.C. Engines

There are three main requirements in pressure transducer installations:

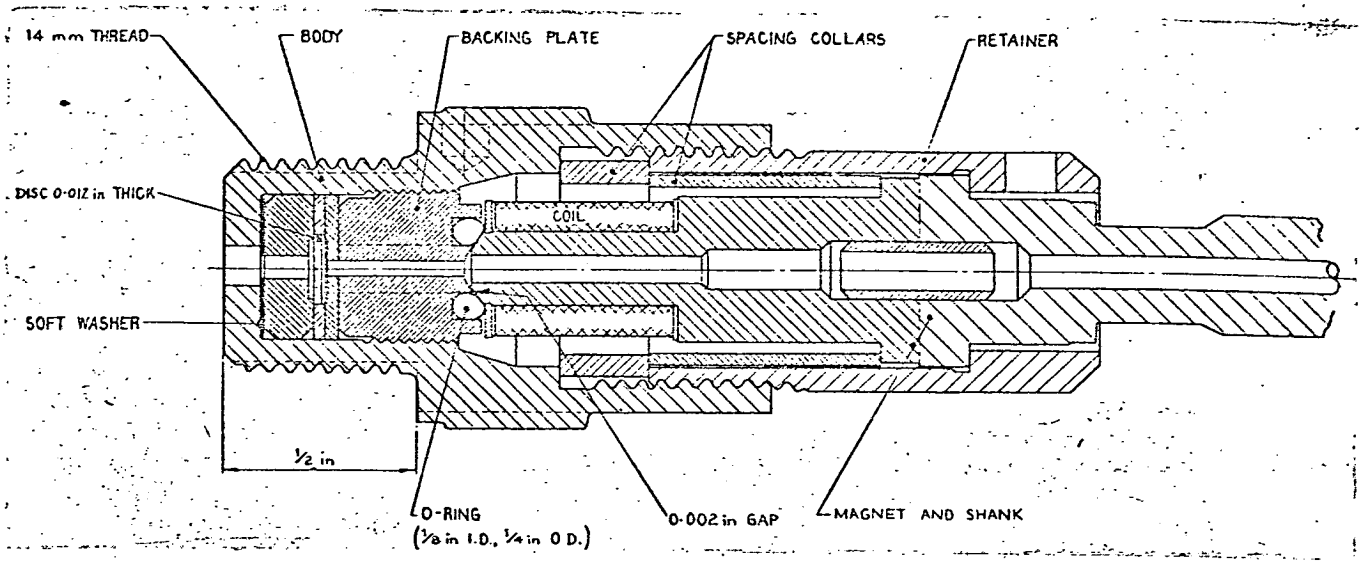

3.1a Balanced Disc Type.

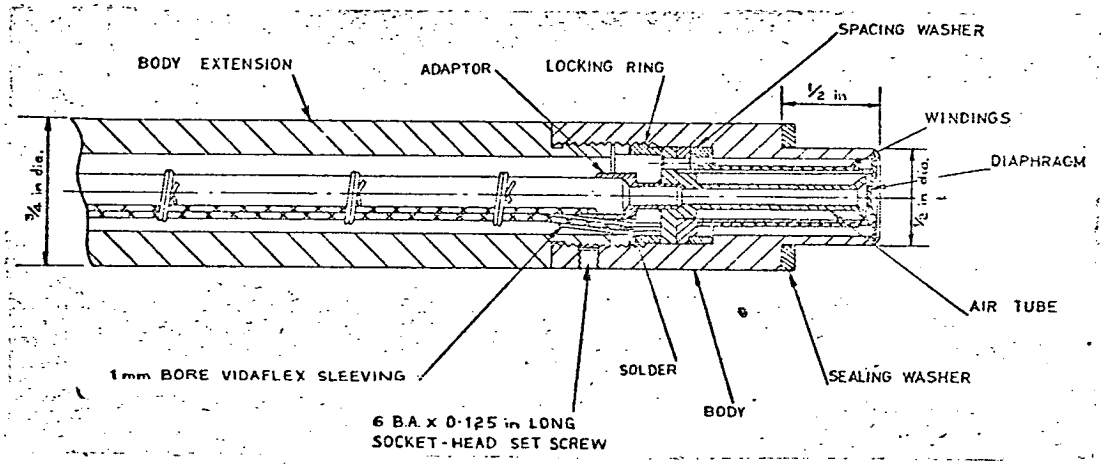

3.1b Strain Gauge Type.

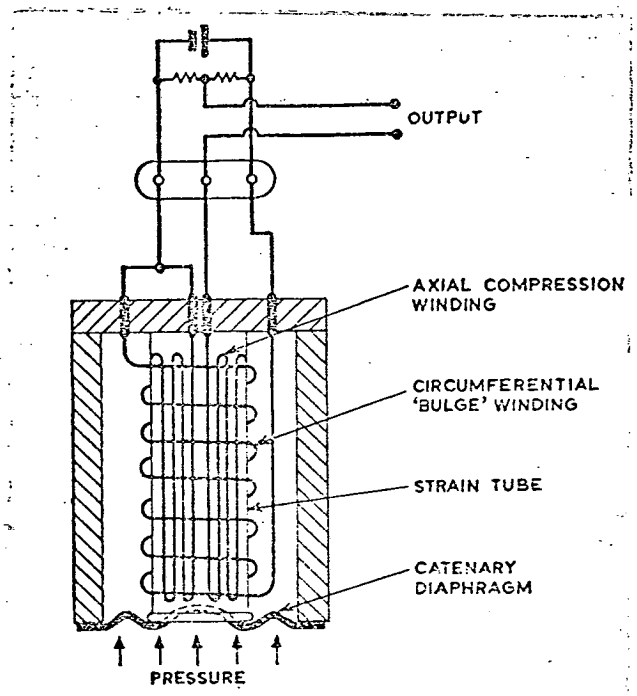

3.1c Schematic Diagram of Strain Gauge Type.

FIG. 3.1. BALANCED DISC AND STRAIN GAUGE PRESSURE TRANSDUCERS.

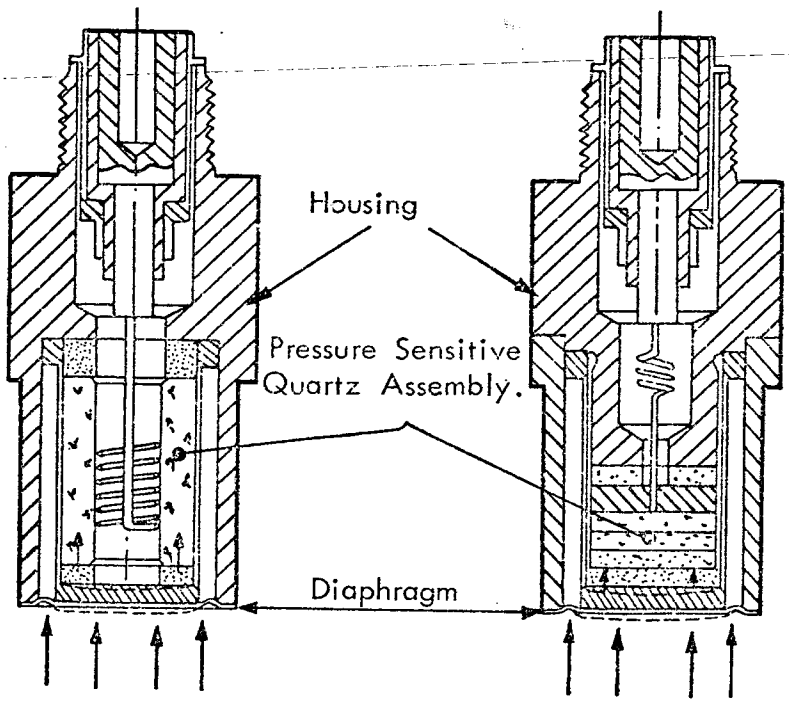

3.2 a) Longitudinal Crystal Alignment. 3.2 b) Lateral (Disc.) Crystal Alignment.

FIG.3.2. PIEZO-ELECTRIC PRESSURE TRANSDUCERS.

(1) A pressure transducer of adequate characteristics for the intended work.

(2) Installation of the transducer at a point where its output is representative of the overall cylinder pressure development.

(3) The transducer diaphragm must be flush mounted in the combustion chamber wall to avoid passage resonances.

The required transducer characteristics will vary according to application and these are discussed in the next section. The installation of the transducer in the combustion space is largely governed by the size of the transducer used and the bore size and detail head construction of the engine. In a large bore quiescent chamber engine, ignition of fuel will start at several centres of ignition at the edges of the fuel sprays. In this case it is unlikely that the cylinder pressure development will be uniform over the chamber volume. Thus, several pressure transducers should be installed (3.7). In the small indirect injection engine there is a difference between prechamber pressure and main chamber pressure and consequently two transducers should be used. In the general range of automotive direct injection engines of moderate swirl, the chamber size is such that a single pressure transducer can be representative of general pressure development. However, when considering the character of diesel 'knock' in respect of cylinder pressure oscillations, care must still be exercised in the positioning of the transducer.

Fig. 8.12 in section 8.7.1 shows the pressure distribution over a piston crown near top dead centre for the three lowest frequency acoustic modes. The lowest of these ($n_z = n = 0$, $m = 1$ mode) is basically a sloshing of the gas from side to side in the cylinder with one diametral nodal line. Since the position of this nodal line is only fixed by the application point of the first disturbance, in this case the combustion centre for the

cylinder in question, then there is no certain way of fixing a cylinder pressure transducer so that it will always record the maximum level of these oscillations. If the point of initiation of combustion is known, then this could be done. A pressure transducer near the cylinder centre will not show the first or third modes, but it will the second. A transducer placed towards the outside of the cylinder will show a high level for all three modes, unless it is situated on a nodal line for that mode. The choice, unless the combustion centre is known, is therefore somewhat arbitrary.

3.3 Development of Pressure Transducer Installations

The development of smaller transducers will always be a design aim. In the testing of engines at ISVR the installation size of pressure transducers has been progressively reduced, due largely to the increased ability of piezo-electric transducers to withstand high metal temperatures. The cylinder pressure transducer first used at the ISVR was the Draper-Li strain gauge type, which had been thoroughly assessed for performance during the original work of Priede at CAV Ltd., Acton (2.4). This gauge required a $\frac{1}{2}$" diameter hole. At the start of the present work (1965) a piezo-electric type of transducer was being manufactured by Kistler and the first engines run at the ISVR were fitted with a 'Universal Adaptor' to allow either type of gauge to be fitted. This adaptor, shown in fig. 3.4a, allowed either type of transducer to be fitted and of course the results could be compared. At that time it was not thought that a non cooled transducer would be reliable (the Draper-Li being air cooled). Cylinder pressure spectra obtained from the two guages were identical and so water-cooled adaptors for the piezo-electric type were used - fig. 3.4b. This increased the size required for fitting and so some transducers were run in adaptors where the only cooling was from the normal engine water surrounding the adaptor, fig. 3.4c. Transducer lives of over 50 hours were obtained. It has now been shown possible

to obtain good results for short periods of running (say 20 hours) with transducers fitted into uncooled parts of two-stroke engines as for the liner locating plug shown in Fig. 3.4d. The reduction in size of the fitting is clearly shown.

Three examples of piezo-electric pressure transducer installations which have proved satisfactory are shown in Figures 3.6, 3.7 and 3.8. Fig. 3.7 shows the installation of a Kistler 601A uncooled transducer in a horizontally opposed, three cylinder two stroke diesel engine. Adequate cooling is provided by the engine cooling water surrounding the sleeve. Transducer life of over 100 hours was obtained from this engine. Fig. 3.7 shows the installation in a Vee configuration, two-stroke diesel engine with high rating. A similar method is used but the sleeve is machined directly to accommodate the transducer and its locator. The installation is smaller and in this case a Kistler 6001 (high temperature) transducer was fitted. This was done in order to overcome the high metal temperatures measured in this position in the water jacket between the two exhaust ports. Metal temperatures of 320°C were measured, not during running but after shut down. This installation gave a transducer life of 70 hours - very good in these extreme conditions. The last installation shown is the smallest so far used. A Kistler 601A was fitted directly into a machined hole in the flame plate of an 8.6 litre, four-stroke diesel engine. The upper cylinder head surface was machined to take an extended locator, the join between transducer and locator being sealed against the engine water by non-set Locktite. Initially a problem arose in this case due to bending vibration of the locator, causing electrical interference - a 2000 Hz resonance - to the signal. However, modification of the locator cured this trouble and the installation is still running without gauge failure.

The small size of such an installation allows considerably more flexibility in the positioning of pressure transducers and this advantage has been

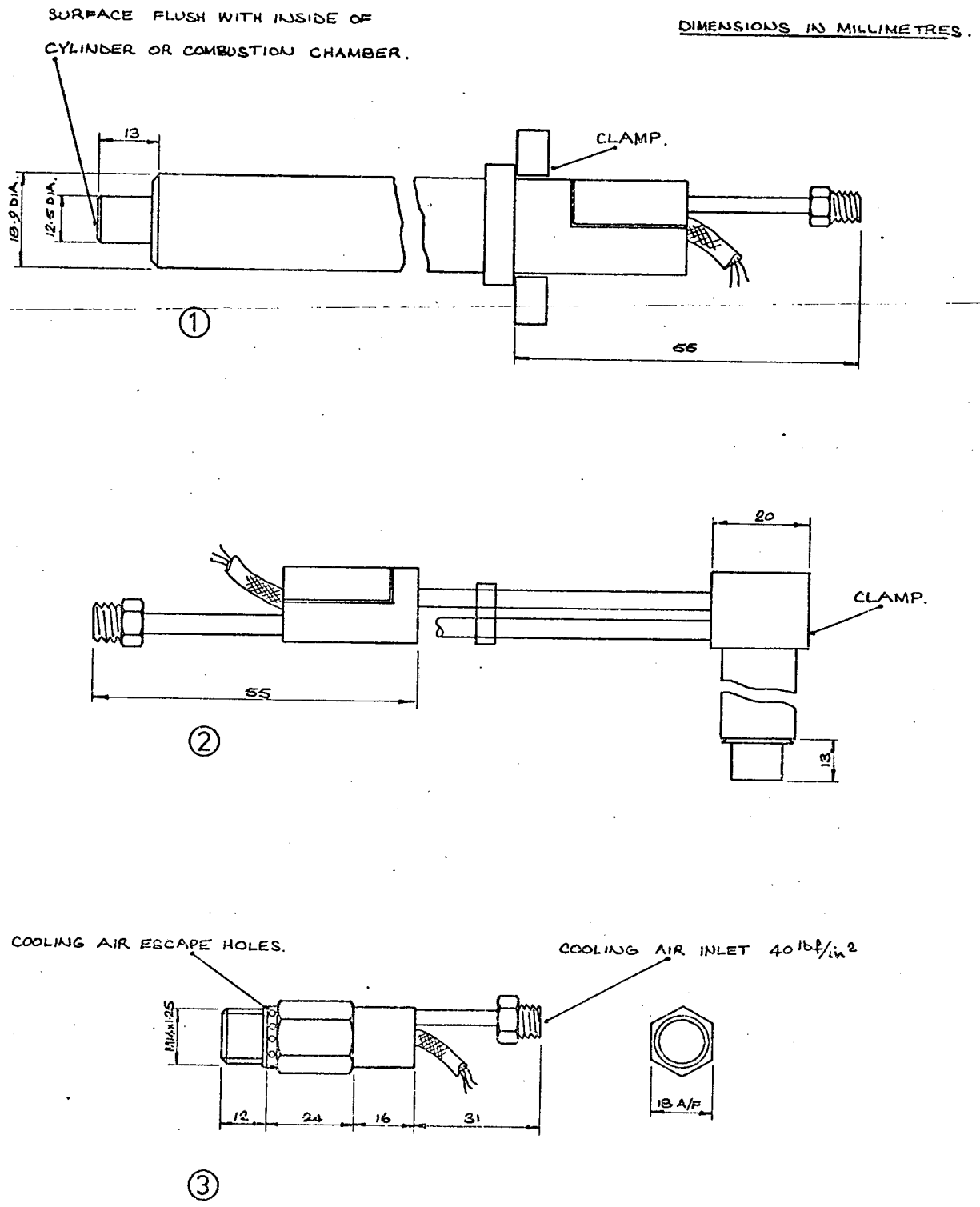

Fig. 3·3 TYPICAL STRAIN GAUGE CYLINDER PRESSURE TRANSDUCERS.

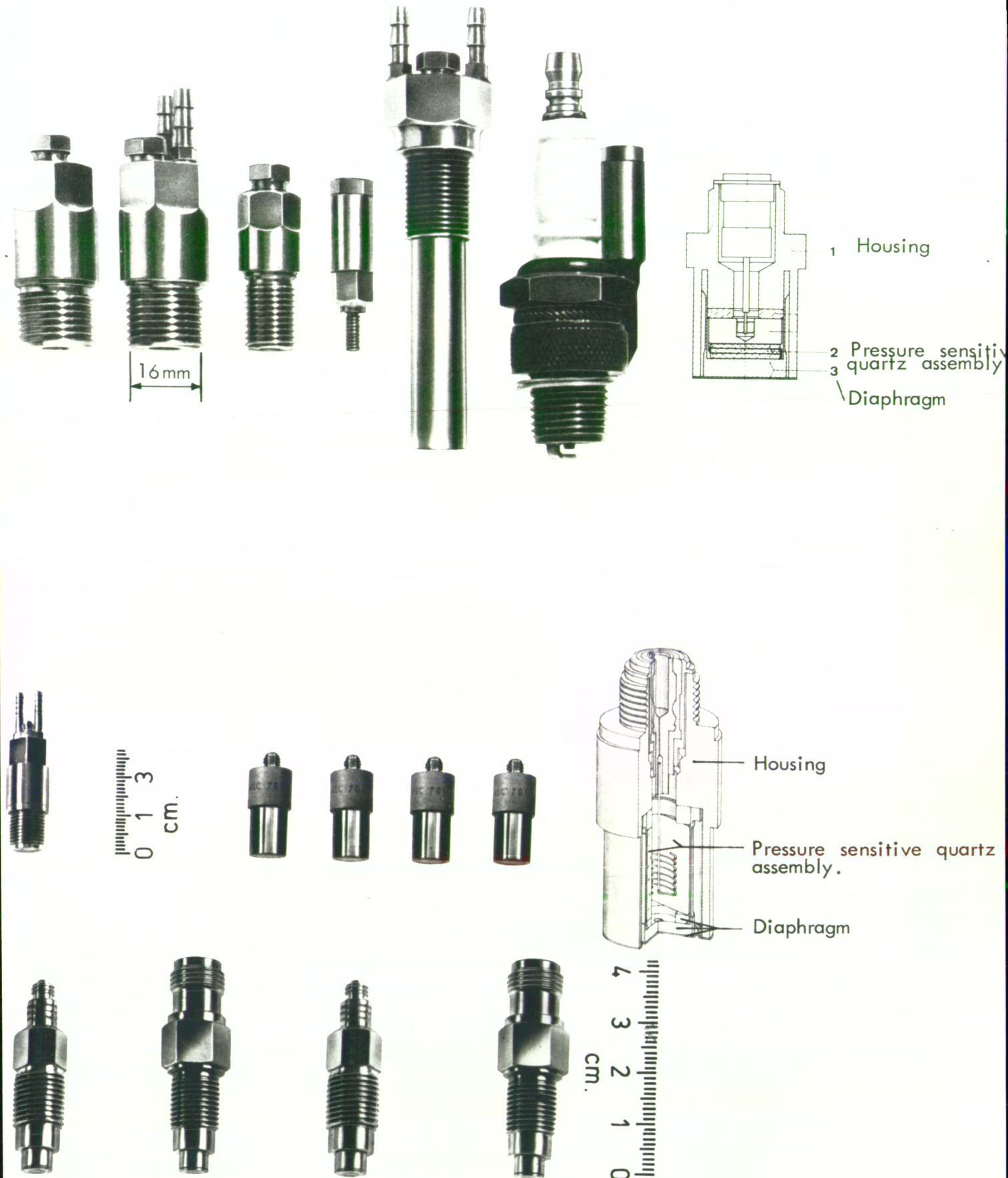

FIG.3·4. VARIOUS CONFIGURATIONS OF PIEZO-ELECTRIC PRESSURE TRANSDUCERS.

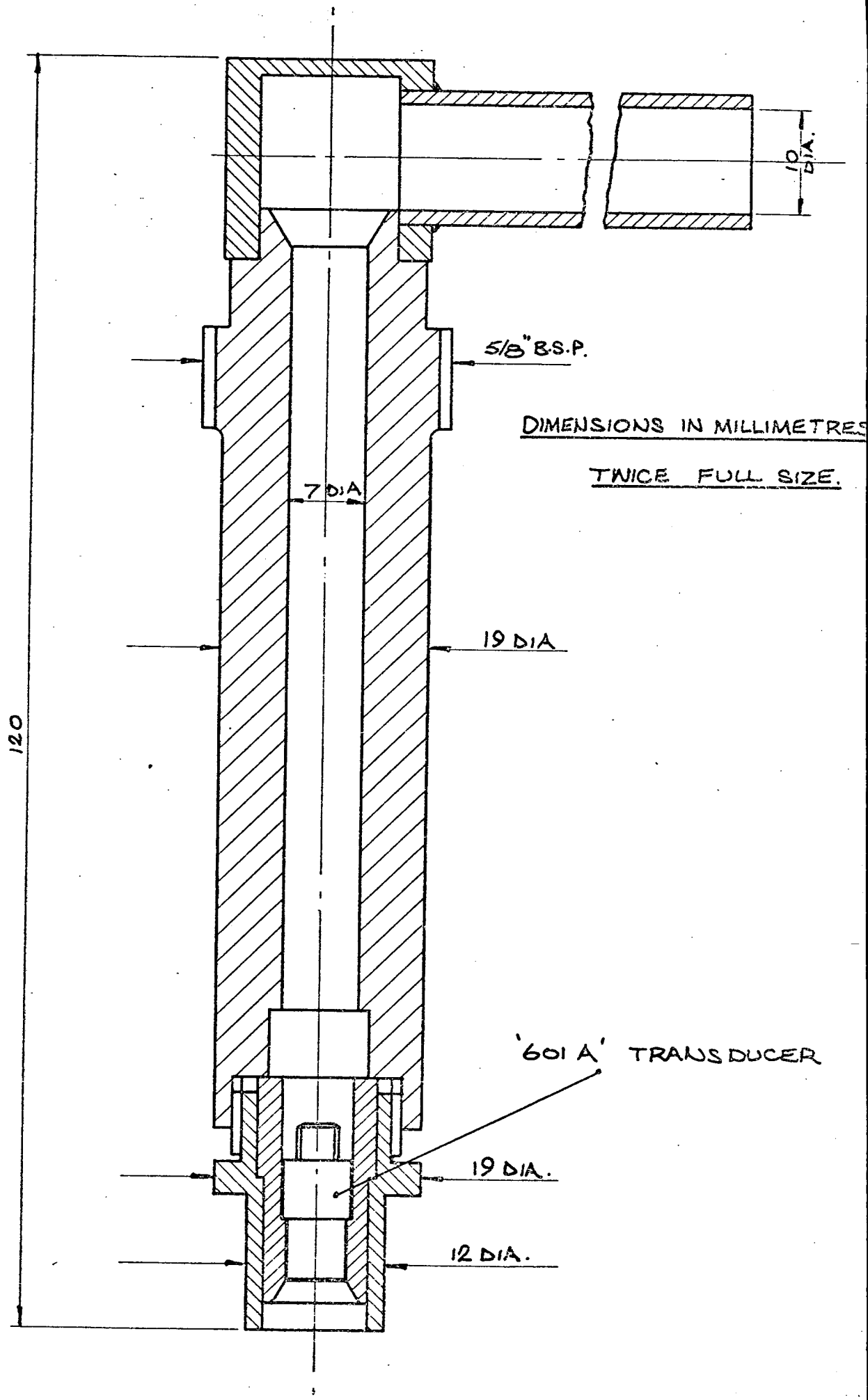

Fig. 3·5 a. Universal cylinder pressure adaptor for strain and piezo-electric types.

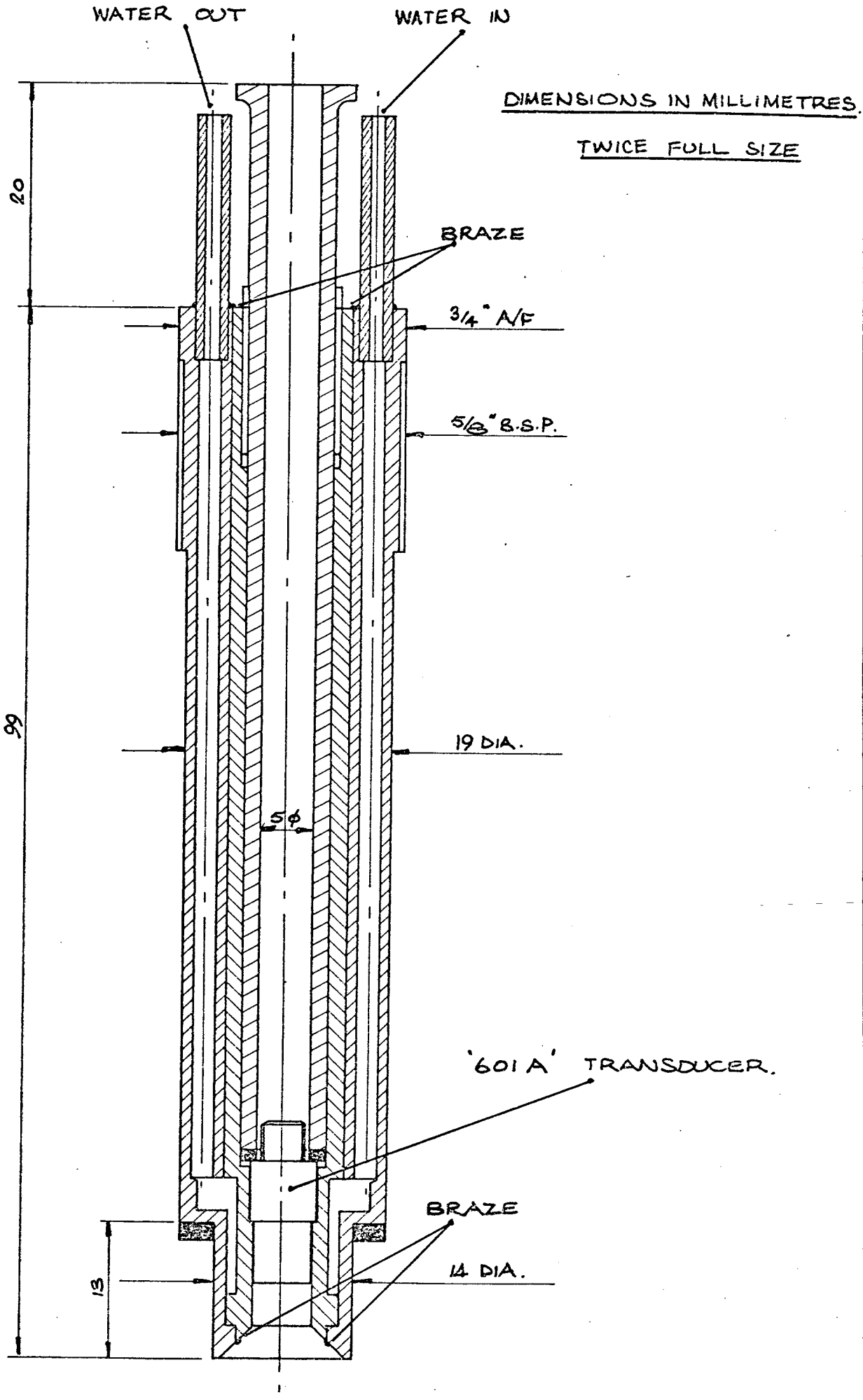

Fig. 3·5b. Water cooled pressure transducer adaptor.

DIMENSIONS IN MILLIMETRES.

TWICE FULL SIZE.

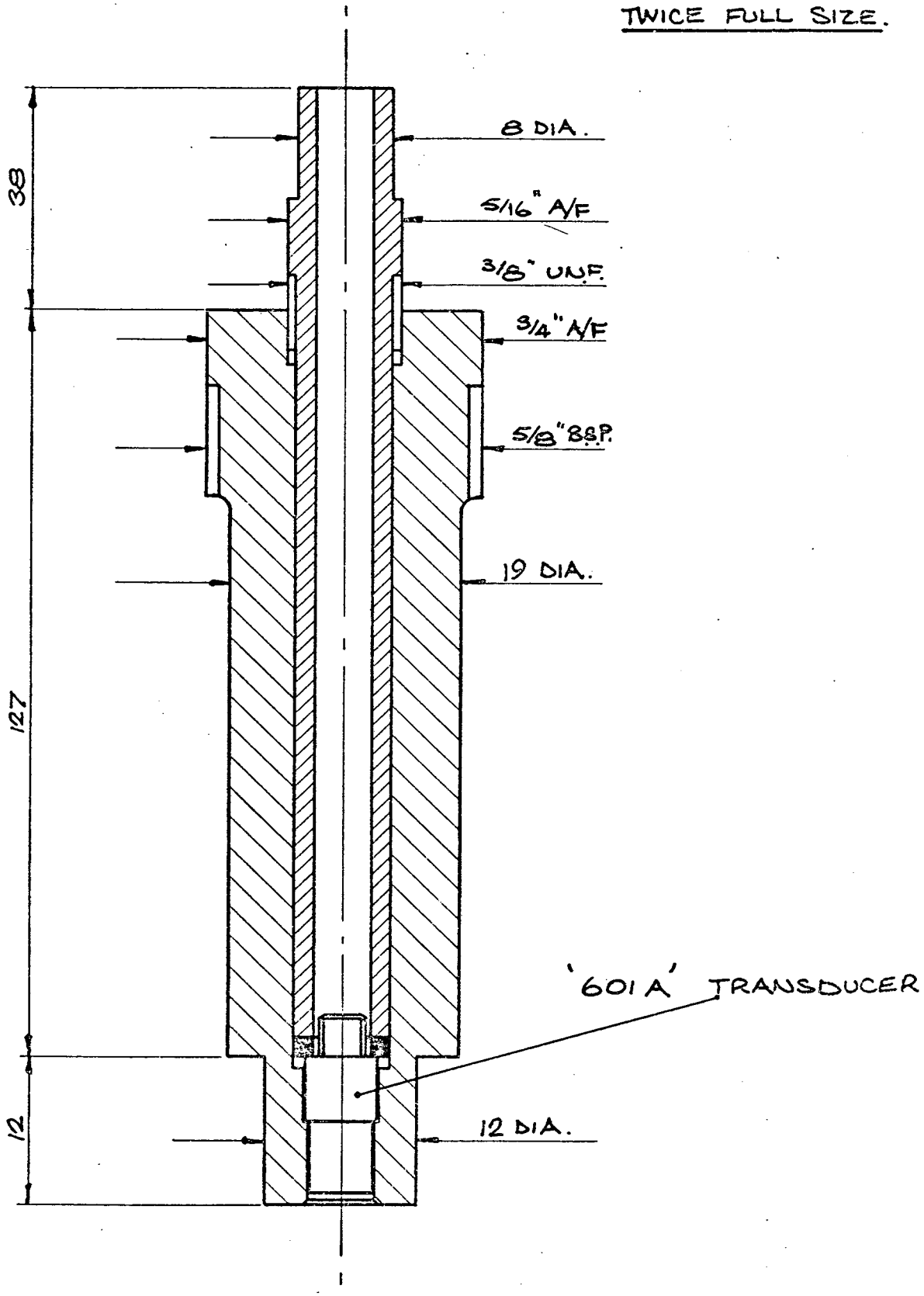

Fig. 3·5c. Uncooled cylinder pressure adaptor.

DIMENSIONS IN MILLIMETRES.

TWICE FULL SIZE

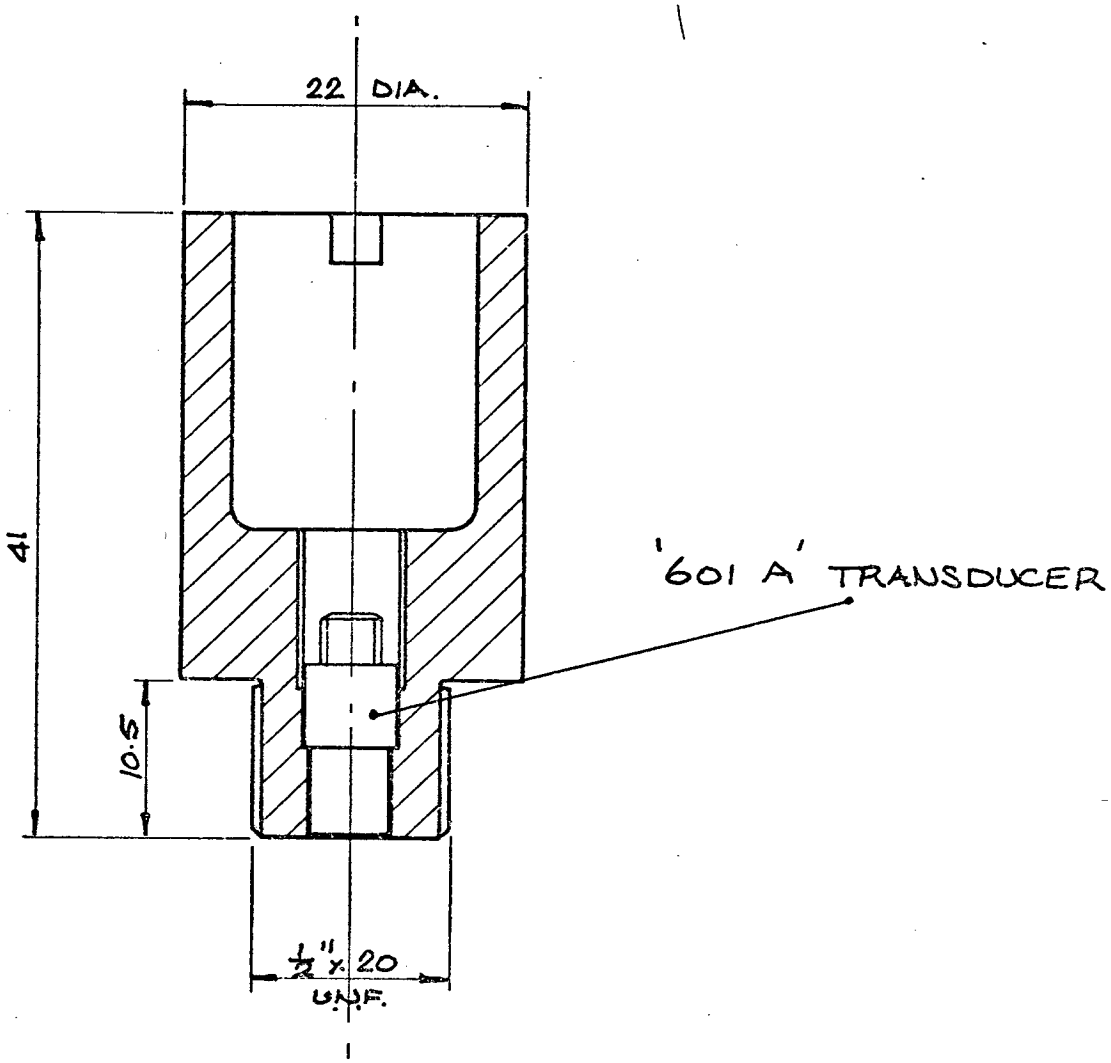

Fig. 3·5d. Uncooled cylinder pressure adaptor for opposed piston, two stroke diesel.

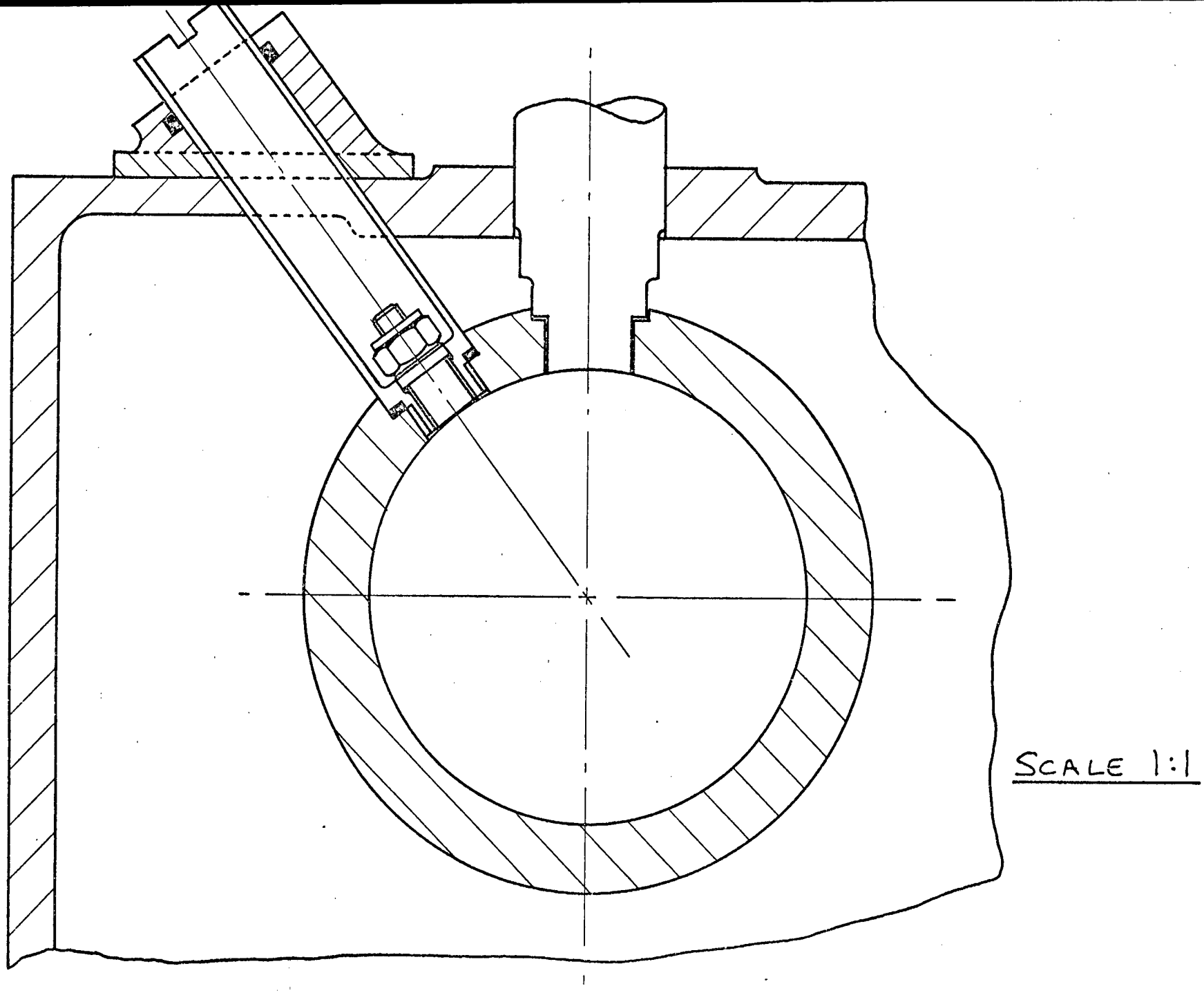

Fig. 3·6 Pressure transducer installation - horizontally opposed, two-stroke diesel engine.

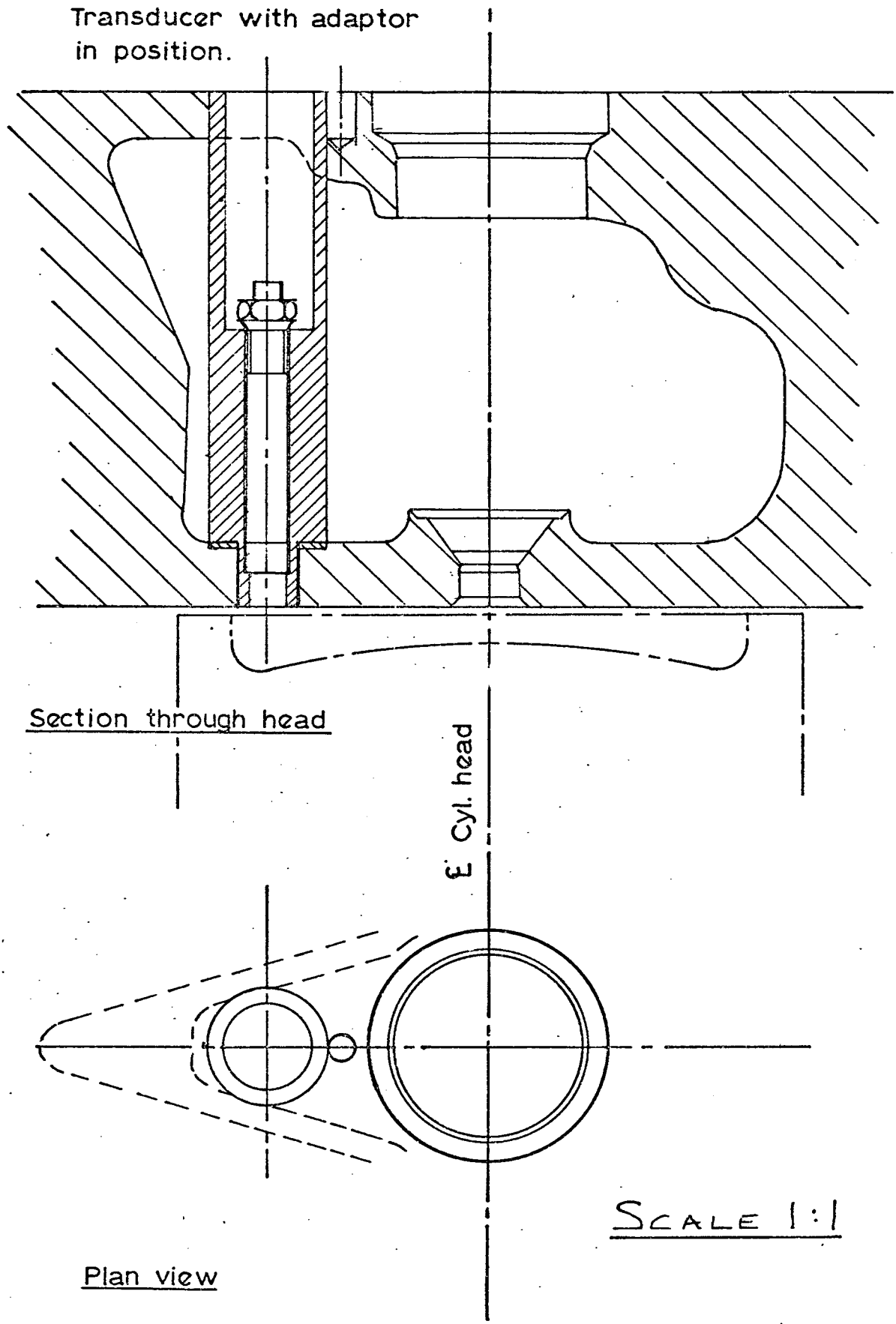

Fig. 3·7 Pressure transducer installation in 568 in^3 vee-eight, two-stroke diesel engine.

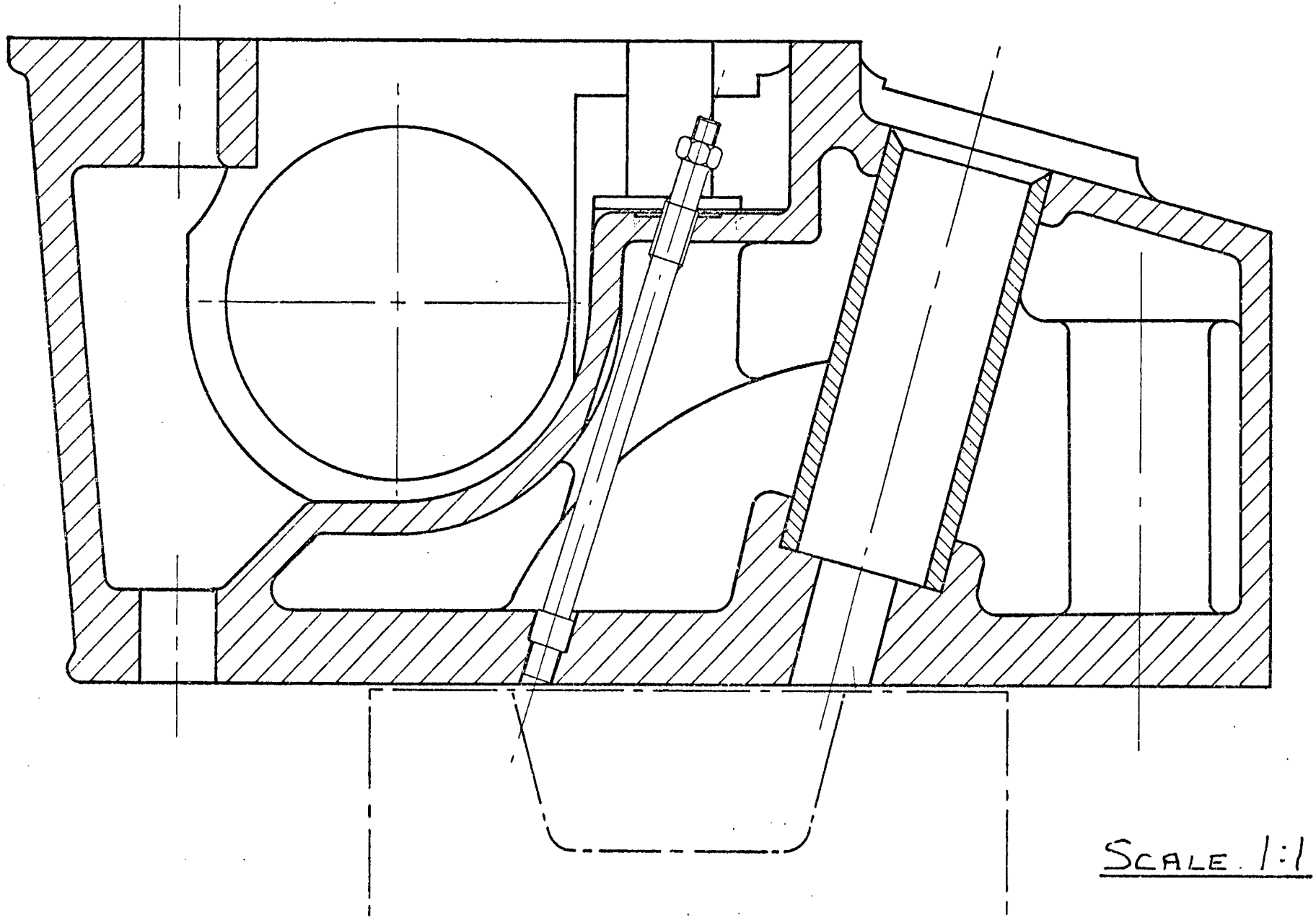

Fig. 3·8 Pressure transducer installation - 8·6 litre, four stroke, six cylinder diesel engine.

used to obtain good dynamic pressure measurements from a range of engines.

3.4 Characteristics of Cylinder Pressure Transducers

3.4.1 Frequency response

Lyn (3.5) has pointed out that for peak pressure measurement it is only necessary to have a frequency range of about 1.5 kHz. However, since the frequency analysis of a cylinder pressure spectrum must cover the audio-frequency range (D.C. to 15 kHz) then so must the pressure transducer. This in turn makes a fast rise time necessary - a minimum requirement being some 50 μsecs. Davies (3.4) shows that a pressure transducer can be considered as a single degree of freedom system excited by the pressure to be measured. Fig. 3.9 shows the harmonic response of such a system. From this analysis, and for a $\pm$ 1 dB accuracy, the limit to the useful frequency range of the transducer is about one half of the first system resonance. In addition to this requirement, particularly for engine work, very rapid impulsive pressures are to be measured. Thus the response of a transducer to a step impulse should be adequate. Fig. 3.10 shows, again for a single degree of freedom system, the response to a zero order step as a function of damping. An optimum damping ratio of about 0.6 should be aimed for and most transducers are made as near to this ideal as possible.

3.4.2 General characteristics

Table 3.1 shows a comparison of the typical characteristics of strain gauge and piezo-electric pressure transducers of various manufacture. In comparing the two types of dynamic transducer several points can be noted:

(1) The resonant frequency of the strain gauge type is much lower than for piezo-electric and in fact is only just enough to cover the audio frequency range. In fact, since the high frequency components of cylinder pressure spectra are of low magnitude, this range of about D.C. to 10 kHz is just sufficient.

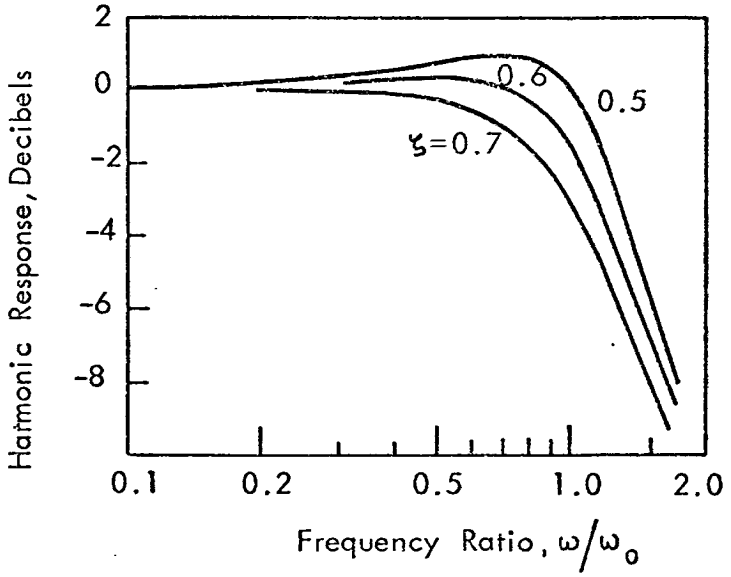

FIG. 3.9. HARMONIC RESPONSE OF A SINGLE-DEGREE-OF-FREEDOM SYSTEM.

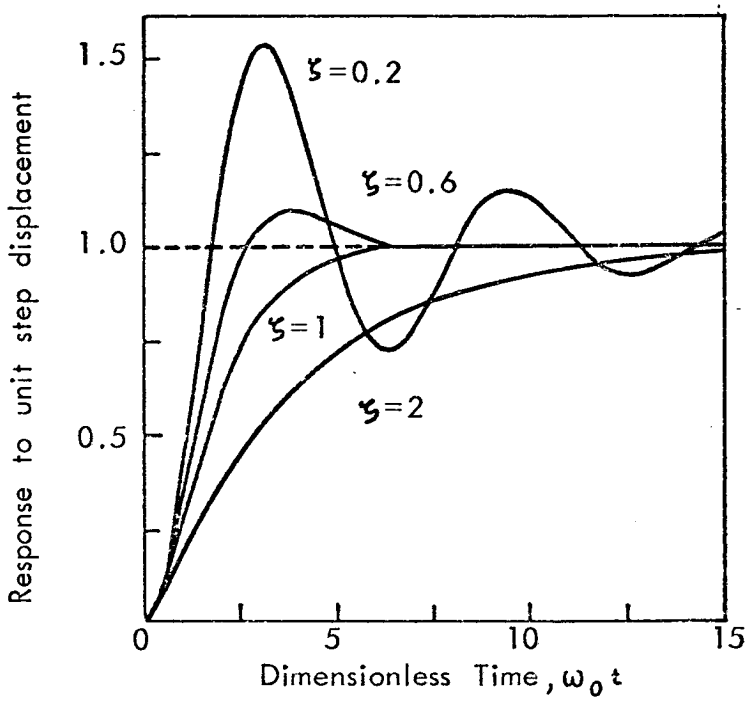

FIG. 3.10. RESPONSE OF SINGLE DEGREE-OF-FREEDOM SYSTEM TO A ZERO ORDER STEP.

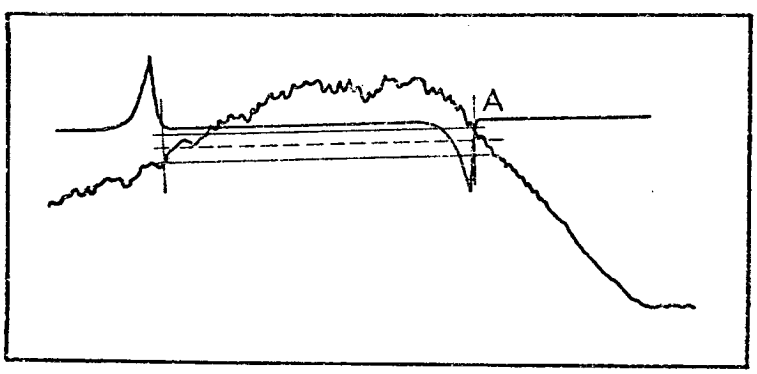

FIG.3.11. VARIATION IN CALIBRATION OBTAINED WITH BALANCED DISC PRESSURE TRANSDUCER.

Table 3.1. Typical Characteristics of Strain Gauge and Piezo-Electric Cylinder Pressure Transducers.

Characteristics	Units	Pressure Transducer			
		Kistler 601A (Piezo)	Kistler 701 (Piezo)	Vibrometer 6QP500a	Southern Instrumen G243 (Resistan
Max. pressure	psi	3500	3500	7100	2000
Resolution	psi	2.9×10^{-2}	5.6×10^{-3}	6.0×10^{-2}	1.0
Sensitivity	pc/at	16.0	80.0	8.0	0.67 mV/V
Resonant frequency	kHz	130	65	160	20
Rise time	μs	3	6	-	-
Linearity	psi	± 28	± 17	± 71	± 4
Temp. coefficient	%/°C	-0.01	-0.01	-0.01	-0.009
Acceleration coeff.	psi/g	1.42×10^{-2}	1.42×10^{-1}	1.1×10^{-2}	-
Diameter	mm	5.5	9.5	5.55	12.7
Dynamic range	dB	>100	>100	>100	66
Damping ratio	-	-	-	0.2	-

(2) The resolution (dynamic range) of the strain gauge type is lower than that of the piezo-electric type (60 dB against 100 dB)and this range for the strain type is only just sufficient. In practice, because of acceleration sensitivity and amplifier characteristics even the piezo-electric system dynamic range is reduced to some 85 dB in engine installations.

(3) In linearity the strain gauge transducer is superior and somewhat offsets the restriction of dynamic range.

(4) Temperature coefficients are the same for both types of transducer and the acceleration sensitivity, although important for gas exchange (low pressure) measurements, is not of much importance, in comparison to linearity, even for peak accelerations of 50 to 100g, where transient errors

of about 1 psi would be expected.

(5) The piezo-electric transducer is half the diameter of the strain gauge type.

From these characteristics it would appear that both types of gauge are suitable for high pressure I.C. engine cylinder pressure measurements, the main problem being in transducer linearity. This characteristic makes the balanced disc transducer more attractive for engine performance work although even the balanced disc has some errors due to the varying response of the disc to different rates of change of pressure (3.8), see Figure 3.11.

To test the characteristics of strain gauge and piezo-electric transducers three types of gauge were tested in an 8 litre Veeform four-stroke diesel engine. The results are shown in fig. 3.12. The agreement between the Kistler 601A piezo-electric transducer and the Draper-Li strain gauge type is remarkable and only diverges at very high frequency. As Priede's early work was completed using the Draper-Li transducer, the Kistler type 601A was used extensively during the work reported in this thesis.

A further test comparing the Kistler 601A with a Vibrometer transducer was undertaken in an 8.6 litre, six cylinder, in-line, four-stroke diesel engine and again good agreement was found but with some differences in the region of the high frequency gas oscillations - Fig. 3.13.

3.4.3 Effect of temperature coefficient

Very often installed transducers are subjected to constant metal temperatures of above 200°C, and therefore a reduced signal results. This reduction is applied to the whole pressure development and therefore can be considered as a constant correction. For a 601A transducer this correction would be 2% or 70 psi. In noise measurements an accuracy of $\pm$ 0.5 dB is the normally achieved limit. Since the decibel scale is a relative one, the addition of 70 psi to a peak pressure of 1000 psi would add only 0.6 dB to the measured levels and therefore account of this is not

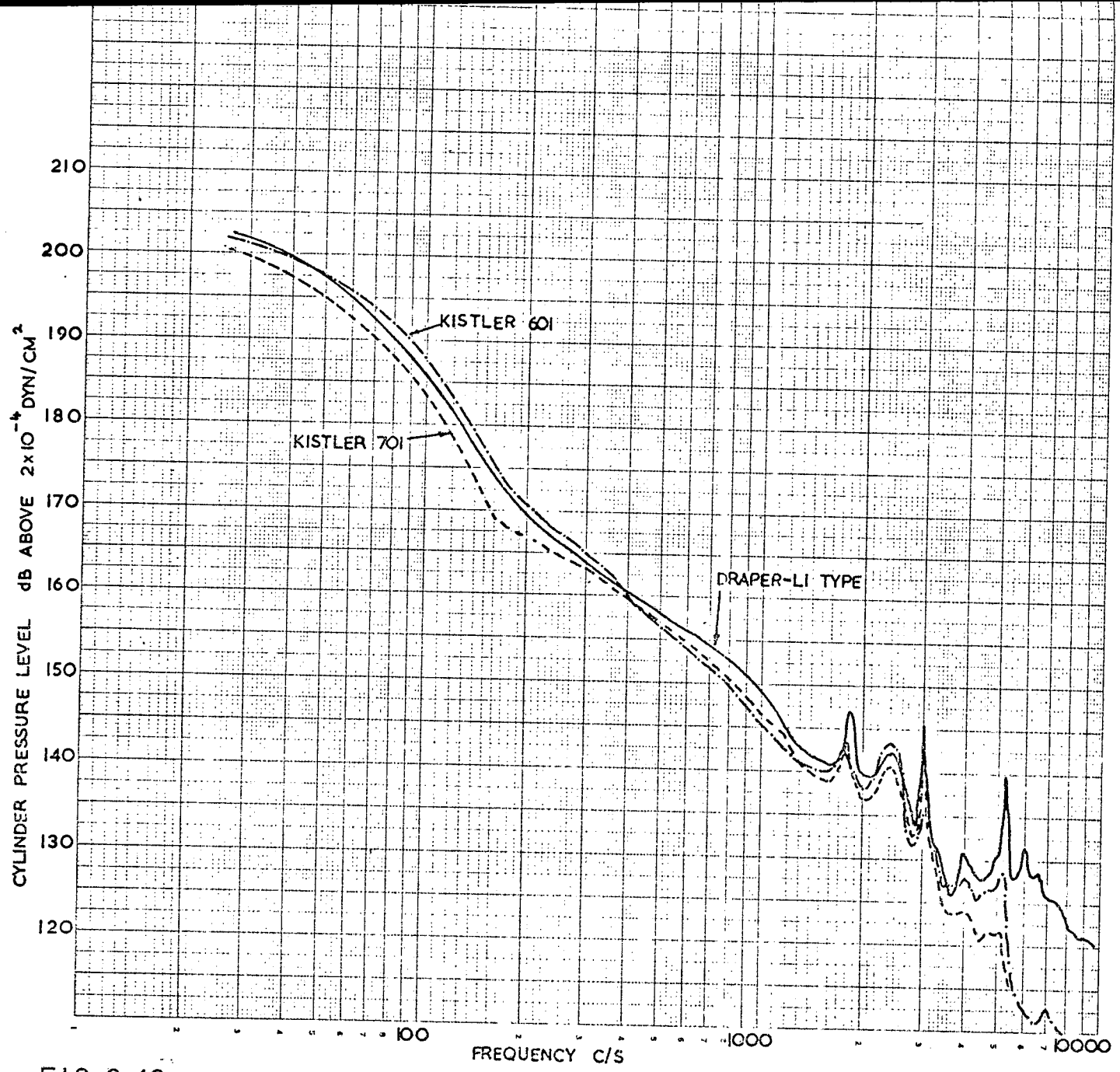

FIG. 3·12 - COMPARISON OF CYLINDER PRESSURE SPECTRA BY DIFFERENT GAUGES

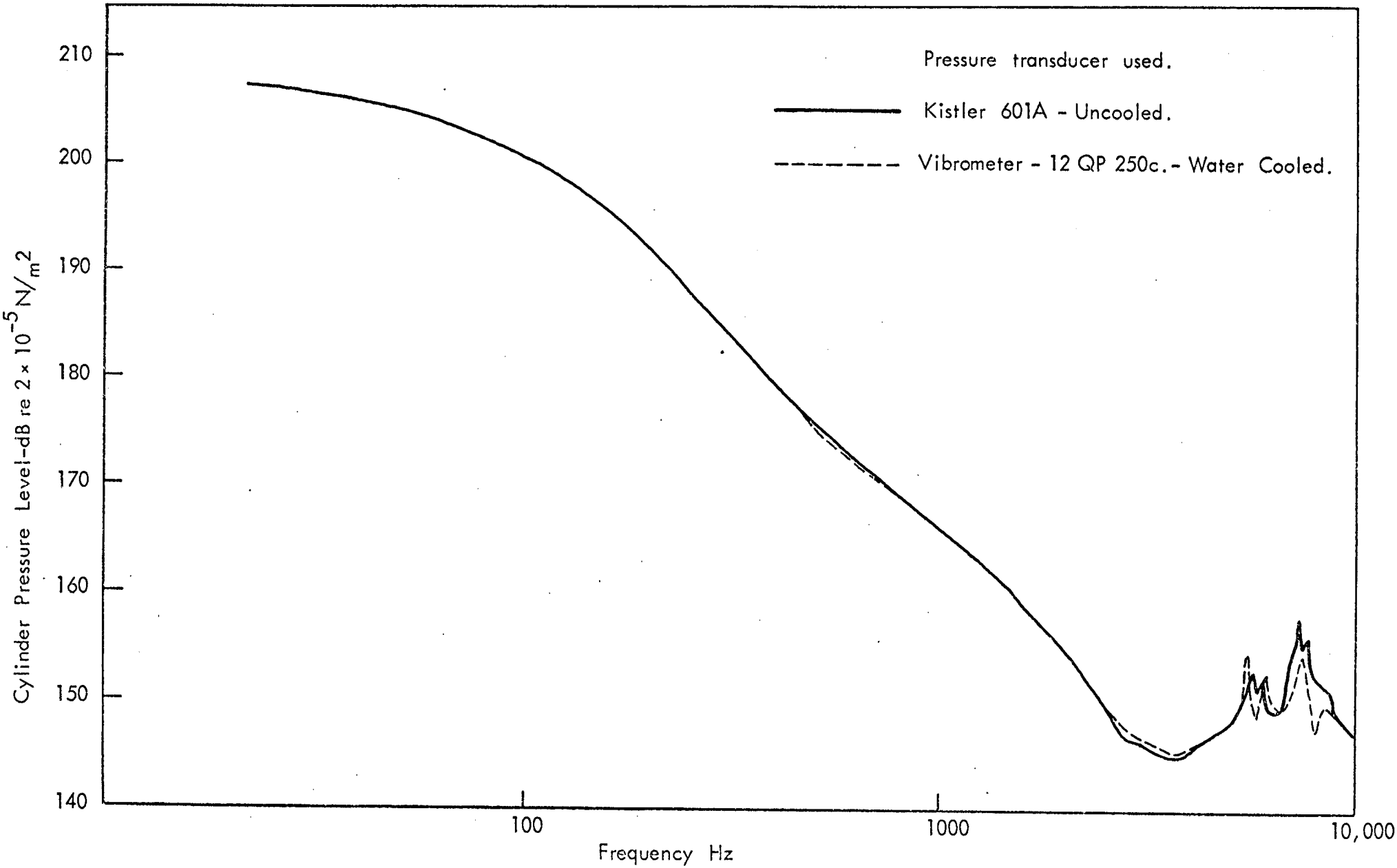

FIG. 3.13. COMPARISON OF CYLINDER PRESSURE SPECTRA MEASURED WITH TWO DIFFERENT PIEZO-ELECTRIC PRESSURE TRANSDUCERS- FOUR STROKE 2600 REVS/MIN.

usually taken in cylinder pressure spectra. For cylinder pressure developments, however, this is important and thus the temperature at which a transudcer runs at a given engine condition is recorded before installation by use of a dummy gauge instrumented with a thermocouple. This also serves to warn of the presence of excessive temperatures in a particular installation.

3.4.4 Flame sensitivity of transducers

Lyn, in reference 3.5, has shown that, in comparison to a balanced disc type of transducer, the output from a strain gauge transducer shows lower pressures during the period of heat release in an engine. Fig. 3.14 shows a comparison made in a running engine and indicates that errors as high as 30 psi can result from the effects of cyclic heat flux through the diaphragm of the transducer. This thermal shock will distort the measured pressure diagram throughout the period of heat release in the cycle. To investigate the magnitude of this problem in the Kistler 601A pressure transducer a special rig was made. This Thermal Shock Test Rig is shown in Fig. 3.15. Three types of pressure transducer installation are mounted at 120^{o} intervals at a two inch radius on a six inch diameter 7/16" mild steel 'flame plate' representing a cylinder head flame plate. This plate could be mounted horizontally in the tailstock of a lathe. A flame shield cut so that two opposite 45^{o} segments were removed could be mounted in the lathe and rotated close to the flame plate. As this shield rotated it alternately exposed and shielded the pressure transducer diaphragm to an Oxy-Acetelene torch flame to simulate the thermal shock condition. Thus an equivalent period of heat release of 90^{o} in 360^{o}, representing a two cycle stroke, was obtained. The flame temperature applied to the diaphragm was $1330^{o}C$. The results of the tests are shown in Fig. 3.16, where the same pressure gauge was used in each of the three transducer installations. In the first installation a standard Kistler water cooled adaptor type 6288 was used.

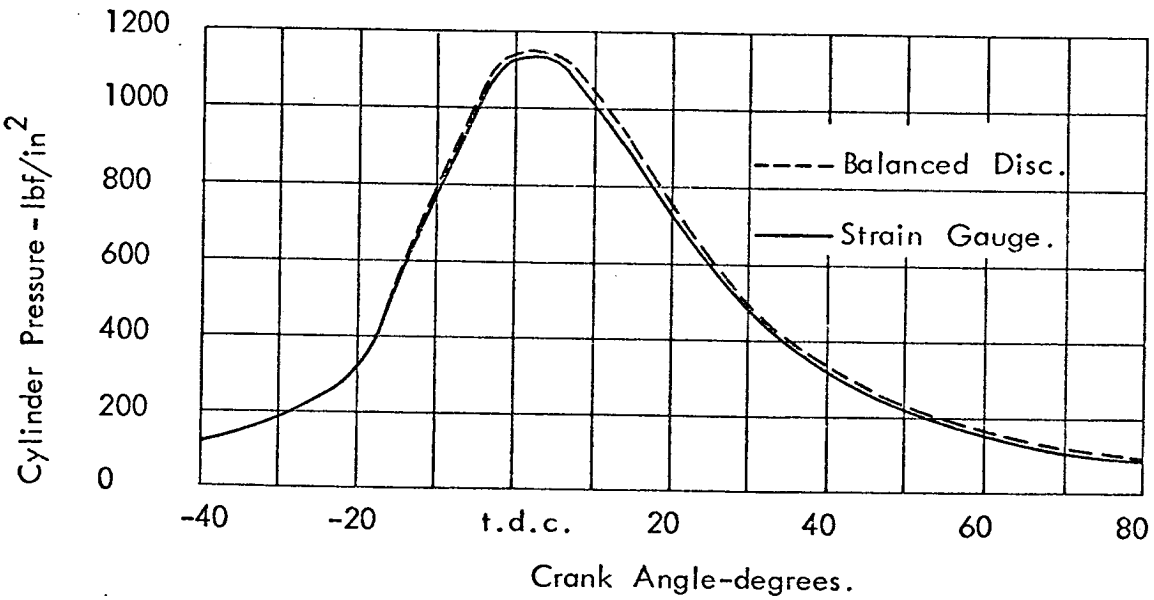

FIG. 3.14. COMPARISON OF PRESSURE DIAGRAM OBTAINED SIMULTANEOUSLY WITH TWO TRANSDUCERS AT 750 REVS/MIN.

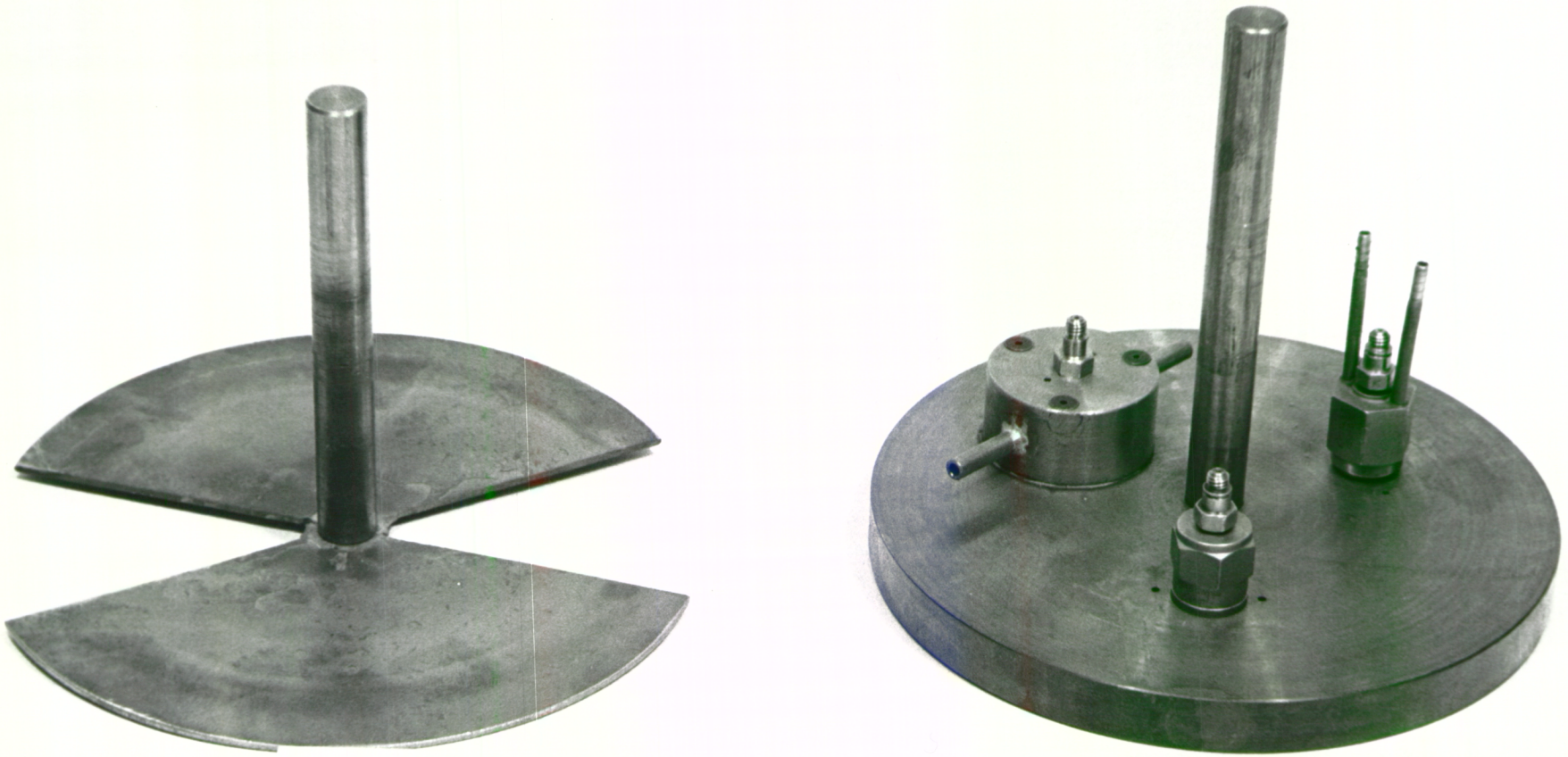

FIG. 3·16 - THERMAL SHOCK TEST APPARATUS.

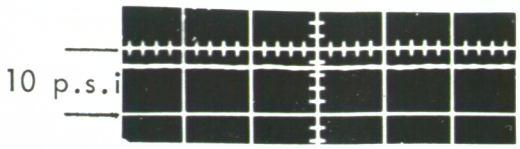

a) Water cooled adaptor with $\frac{1}{8}$" passage at 1000 revs/min. (Flame plate 200°C Flame 1330°C).

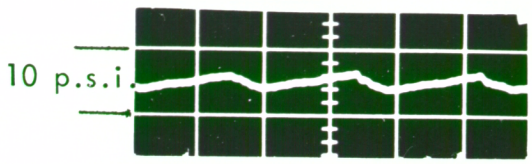

b) Uncooled flush mounted transducer at 1000 revs/min. (Flame plate 200°C Flame 1330°).

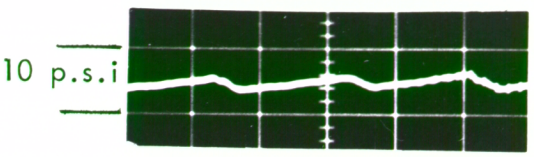

d) Uncooled flush mounted transducer at 1000 revs/min. (Flame plate 50°C Flame 1330°)

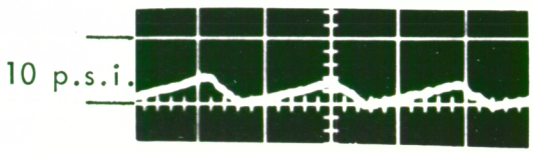

c) Cooled flush mounted transducer at 1000 revs/min. (Flame plate 200° C Flame 1330°).

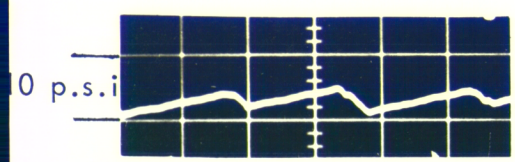

e) Uncooled flush mounted transducer 1000 revs/min. (Flame plate 200° C Flame 1330°).

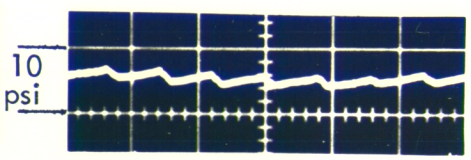

f) Uncooled flush mounted transducer at 2400 revs/min. (Flame plate 200° C Flame 1330°).

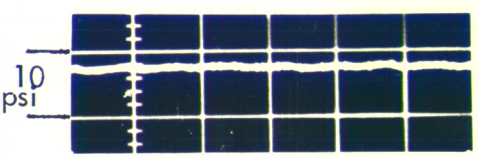

g) Cooled flush mounted transducer at 2400 revs/min (Flame plate 200° C Flame 1330°).

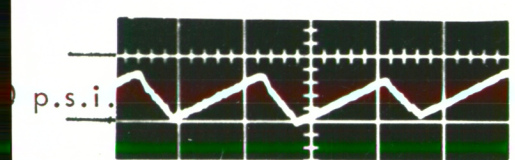

h) Cooled flush mounted transducer at 1000 revs/min. (Flame temp.1660°). (Flame plate 160° C).

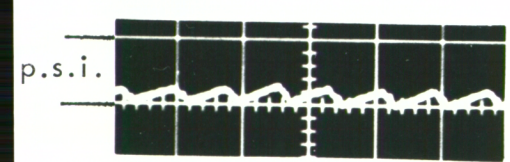

i) Cooled flush mounted transducer at 2400 revs/min. (Flame temp.1660°). (Flame plate 160° C).

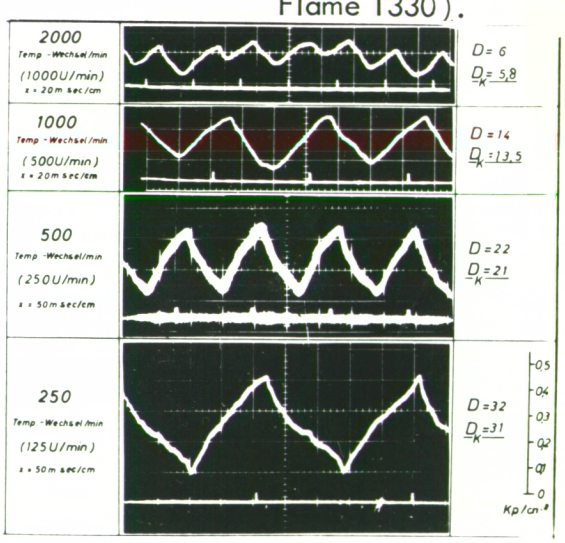

j) The results of Hatschek for vibrometer 12 QP 500 cl.

FIG. 3.16 THERMAL SHOCK CHARACTERISTICS OF KISTLER 601 A PIEZO - ELECTRIC CYLINDER PRESSURE TRANSDUCER.

For flame plate temperatures up to 250°C the transducer temperature (measured with a thermocoupled dummy) varied between 50° and 55°C. In this adaptor there is a short passage ($\frac{1}{8}$") to the diaphragm. Fig. 3.16a shows that at 1000 revs/min equivalent speed there was virtually no thermal shock (below 1 psi), presumably because of the protection provided by the passage. The second installation was a standard Kistler uncooled adaptor type 620. Here the temperature of the pressure gauge was found to follow very closely that of the flame plate. Fig. 3.16b shows that at 1000 revs/min with this flush diaphragm thermal shock of some 4 psi magnitude is present, the flame plate temperature being some 200°C. With the flame plate temperature reduced to 50°C, a thermal shock level of 3 psi is measured (fig. 3.16c). The third transducer installation (ISVR installation) is one in which the transducer fits into a machined recess in the flame plate and with a locator which passes through the water passage. Again thermal shock of some 4 psi magnitude is measured (fig. 3.16d). The effect of engine speed on thermal shock is shown in fig. 3.16e and f for the uncooled transducer and fig. 3.16g for the cooled flush mounted transducer. At 2400 revs/min the thermal shock has reduced to 2 psi, whilst for the ISVR cooled installation the value has fallen to 1 psi. It is clear that the effects of thermal shock reduce with increasing engine speed. In an effort to find the maximum effect of thermal shock the flame temperature at the diaphragm was increased to 166°C. Figs. 3.16h and i show the thermal shock levels at 1000 revs/min and 2400 revs/min to be 8 psi and 3 psi, respectively.

The results show thermal shock is present in installations where a Kistler 601A pressure transducer is flush mounted. With an $\frac{1}{8}$" passage before the transducer no thermal shock was measured. The effect of water cooling is to diminish the shock effect very slightly, whilst increasing engine speed also diminishes the effect. Thermal shock errors of up to 8 psi

can be expected at low engine speeds and high engine load conditions. Similar results were obtained on a Vibro Meter pressure transducer 12QP 500 c1 by Hatschek (3.9) and his results are reproduced in fig. 3.16j.

The effect of thermal shock is therefore present in the majority of results reported in this thesis, but is less for the Piezo-electric than for the strain gauge type of pressure transducer. However, the most important part of the pressure diagram from a noise analysis point of view is the compression and initial pressure rise. This part of the diagram will not suffer from thermal shock to the extent that the expansion stroke will. Comparison of a strain gauge and Piezo-electric pressure transducer has shown very similar results and since the thermal shock in a strain gauge transducer is some three or four times that of the Piezo-electric, then it can be concluded that for cylinder pressure spectrum analysis the effects of thermal shock are negligible.

References

3.1 Boiten, R.G. 'The mechanics of Instrumentation'. Proc. Inst. Mech. Engrs. London 1963, 177, 269.

3.2 Hempson, J.G.G. 'Instrumentation problems in internal combustion engine development'. Proc. Auto. Div. Instn. Mech. Engrs. 1961-62, 81.

3.3 Draper, C.S. and Li, Y.T. 'A new high-performance engine indicator of the strain gauge type'. J. Aero. Sci. 1949, 16, 593.

3.4 Davies, P.O.A.L. 'Measurement and recording of transient pressures in unsteady flow', paper 1. Symposium on 'Accuracy of Electronic Measurements in Internal Combustion Engine Development' - I. Mech. E. publication. January 1966.

3.5 Lyn, W.T., Stockwell, A.J., Wang, C.H.T. 'Accuracy in cylinder pressure measurement'. Paper 2 of Symposium in ref. 3.4.

3.6 Martini, K.H. 'Quartz Transducers in Practical Applications' Kister Instruments Technical Review.

3.7 J.A. Rogers. Undergraduate Thesis, 1968/69. Southampton University.

3.8 Bruffell, D. and Williams, D. 'Electronics applied to medium speed engines'. Paper 5 of symposium in ref. 3.4.

3.9 R. Hatschek. 'The suitability of Piezo-electric pressure transducers for engine applications'. Paper presented at 'Diesel and Gas Engine Power Conference'. Illinois Institute of Technology, USA.

4.0 FREQUENCY ANALYSIS OF CYLINDER PRESSURE DEVELOPMENT BY ELECTRICAL FILTERING

4.1 Introduction

In order to establish the exciting propensity of an I.C. engine cylinder pressure diagram it is necessary to be able to measure an appropriate physical characteristic. Of the two methods described in the literature, i.e.,

(a) Level-time response of a system to an applied cylinder loading,

(b) Level-frequency characteristics of applied loading and structure response,

only the frequency-time method can be utilised to give directly measureable physical characteristics. These characteristics are:

(a) The level-frequency spectrum of the applied cylinder pressure diagram;

(b) the level-frequency spectrum of the structure response;

and they can be assessed separately from one another. Priede (4.1) described the application of direct electrical filtering neatly. "Since the cylinder pressure is a recurrent phenomenon it can be described readily by a Fourier series. For the correlation of such a harmonic series with the emitted noise spectrum, however, this series would have to cover the whole audio frequency (AF) range. This means that for an engine (four stroke) running at 1000 rev/min (cycle repetition frequency 8.33 Hz) the amplitudes of some 1200 harmonics would have to be determined. Numerical methods and also electronic computers were considered but were found to be impracticable."

"In practice, however, such recurrent wave forms can be readily analysed by electrical wave form analysers. The results depend on the band width of the analyser and the characteristics of the indicating meter and must be interpreted and applied with some care."

4.2 Fourier Analysis and Electrical Filtering

Suppose we have a function f(t) which is periodic and suppose for simplicity that the period is 2π, i.e., $f(t + 2\pi) = f(t)$. Then f(t) can be represented as a series:

$$f(t) = \tfrac{1}{2}a_o + a_1 \cos t + a_2 \cos 2t + \ldots + b_1 \sin t + b_2 \sin 2t + \ldots$$

$$= \tfrac{1}{2}a_o + \sum_{n=1}^{\infty} (a_n \cos nt + b_n \sin nt) \qquad (4.1)$$

= constant term + sum of two sinusoidally varying terms.

This is the Fourier series representation of the function f(t). As might be expected, certain restrictions must be placed on f(t) for the expression to be valid. The conditions which must be satisfied, known as Dirichlet's conditions, are met by practically all of the functions which are of interest in the physical sciences.

An electrical filter is a system which will only allow electrical signals within a certain frequency range to pass it. Supposing that this range is small enough to allow only one harmonic frequency of a series to pass, this signal will be the combined sinusoidally varying quantity:

$$a_n \cos nt + b_n \sin nt. \qquad (4.2)$$

After passing through the filtering system the resultant waveform must be measured by a detector. This usually takes the form of a Root Mean Square Meter for A.C. signals. It can be shown that the root mean square value of the signal is given by:

$$\text{R.M.S. value} = \left\{\frac{1}{2\pi}\int_0^{2\pi} (a_n \cos nt + b_n \sin nt)^2 \, dt\right\}^{1/2} \qquad (4.3)$$

Therefore,

$$\text{R.M.S. value} = \frac{1}{\sqrt{2}}(a_n^2 + b_n^2)^{\frac{1}{2}} \qquad (4.4)$$

and hence the r.m.s. value of an electrically filtered signal can be related to the square root of the sum of the squares of the Fourier Coefficients. Note that phase information is lost and only the magnitude (modulus of the

resultant of the two Fourier coefficients can be measured by an ordinary electrical waveform analyser. Thus the original level-time history of a periodically varying signal cannot be obtained from a summation of the harmonic modulus series measured using an electrical analyser.

4.3 Electrical Analysis of Time Varying Signals

4.3.1 General system

The general system for harmonic analysis consists of three main parts, as shown in Fig. 4.1. Firstly, a transducer to produce an electrical output proportional to the physical parameter being measured. Secondly, an electrical filter which only allows signals within a certain frequency range to pass, and lastly, a detector to measure the value of the signal allowed through the filter section. If the filter can be adjusted to cover the frequency range, then a frequency spectrum can be built up.

The characteristics of the pressure transducers have been discussed in the previous section and therefore only the characteristics of filters and detectors will be discussed here, together with some comments on dynamic range.

4.3.2 Electrical filters

There are basically two types of electrical frequency filter, the constant bandwidth type with a fixed bandwidth and the constant percentage bandwidth type where the bandwidth is a certain percentage of the filter centre frequency. The two types can be obtained with either a continuously variable centre frequency or as a set of filters with fixed centre frequency. The wider bandwidth filters - octave and 1/3 octave (constant percentage) - tend to be made with fixed centre frequencies, whilst the narrower bandwidth analysers tend to be of the continuous sweep type. Noise analyses presented

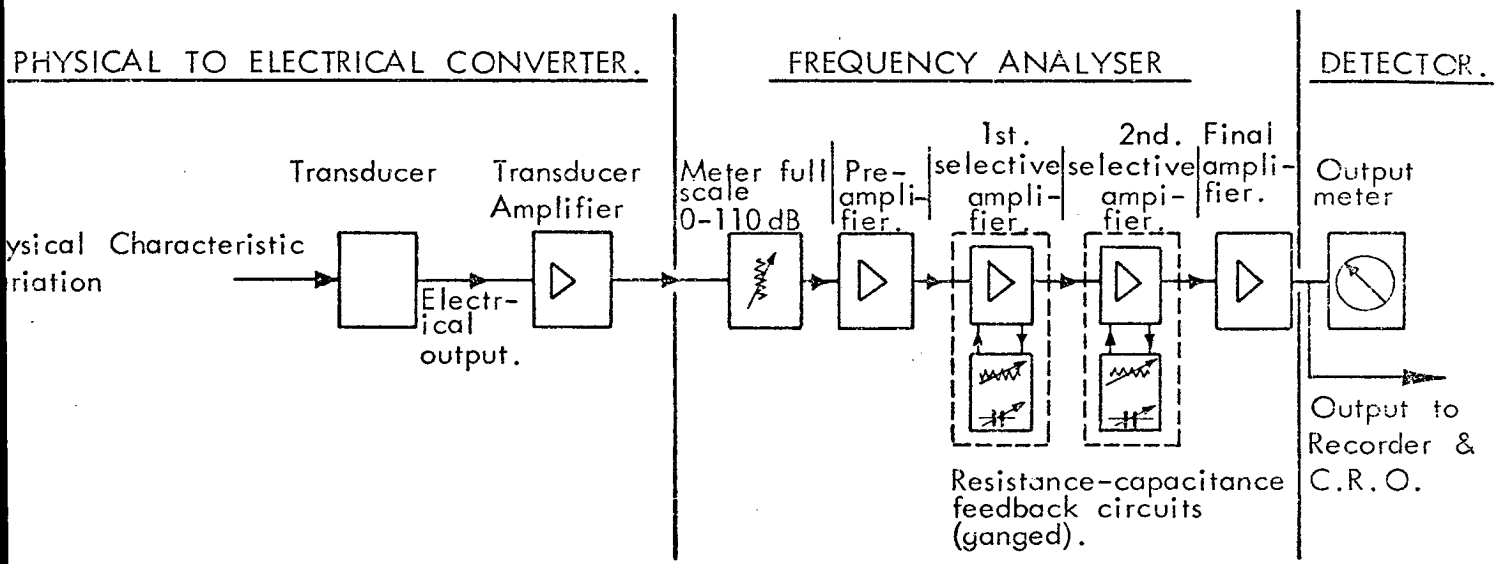

FIG. 4.1. SCHEMATIC DIAGRAM OF ELECTRICAL FREQUENCY ANALYSIS SYSTEM.

in this thesis are usually obtained using a 1/3 octave band analyser (approx. 22% bandwidth), whilst most cylinder pressure analysis has been obtained using a hand tuned Muirhead Parmetrada wave analyser with a 1.5% bandwidth. The type of analyser used is very dependent on the type of signal being recorded. Fig. 4.2 shows a comparison of diesel noise measured with a Spectral Dynamics SD101A analyser with 2 Hz and 20 Hz bandwidths. The vast amount of information obtained is apparent.

The time required for a 2 Hz filter to sweep through the frequency range 2 Hz to 10 kHz for a four stroke engine running at 1000 revs/min would be some 96 minutes, allowing ten engine revolutions to occur within the filter for accurate results. For the 10 Hz filter this time would be 19 minutes. Thus, narrow band analysis is time consuming and in practice for noise the third octave filter provides enough detail in a short analysis period.

Fig. 4.3 shows a 2 Hz constant bandwidth analysis (Spectral Dynamics SD101A) of a two stroke diesel engine cylinder pressure development at 1000 and 2000 revs/min. The harmonic form of the analysis is clearly seen as is the increased harmonic separation with speed. The pin-pointing of the harmonics is essential for this type of analysis and therefore, for research, a narrow band analyser is generally used for cylinder pressure spectra.

Another criterion for the filters is that they should respond quickly, since the explosive pressure build-up in an engine cylinder is very rapid. Fig. 4.4 shows the analysis of an electrically formed sawtooth waveform by three analysers. The theoretical spectrum reduces at the rate of 20 dB/decade and the two narrow band analysers follow this to within close limits. The B & K 1/3 octave filter follows at a lower rate of 10 dB/decade; the difference between this and the General Radio 3 Hz bandwidth analyser is due to the increasing bandwidth of the constant percentage analyser. The reduced slope, amounting to 10 dB/decade, will be the same for all normal

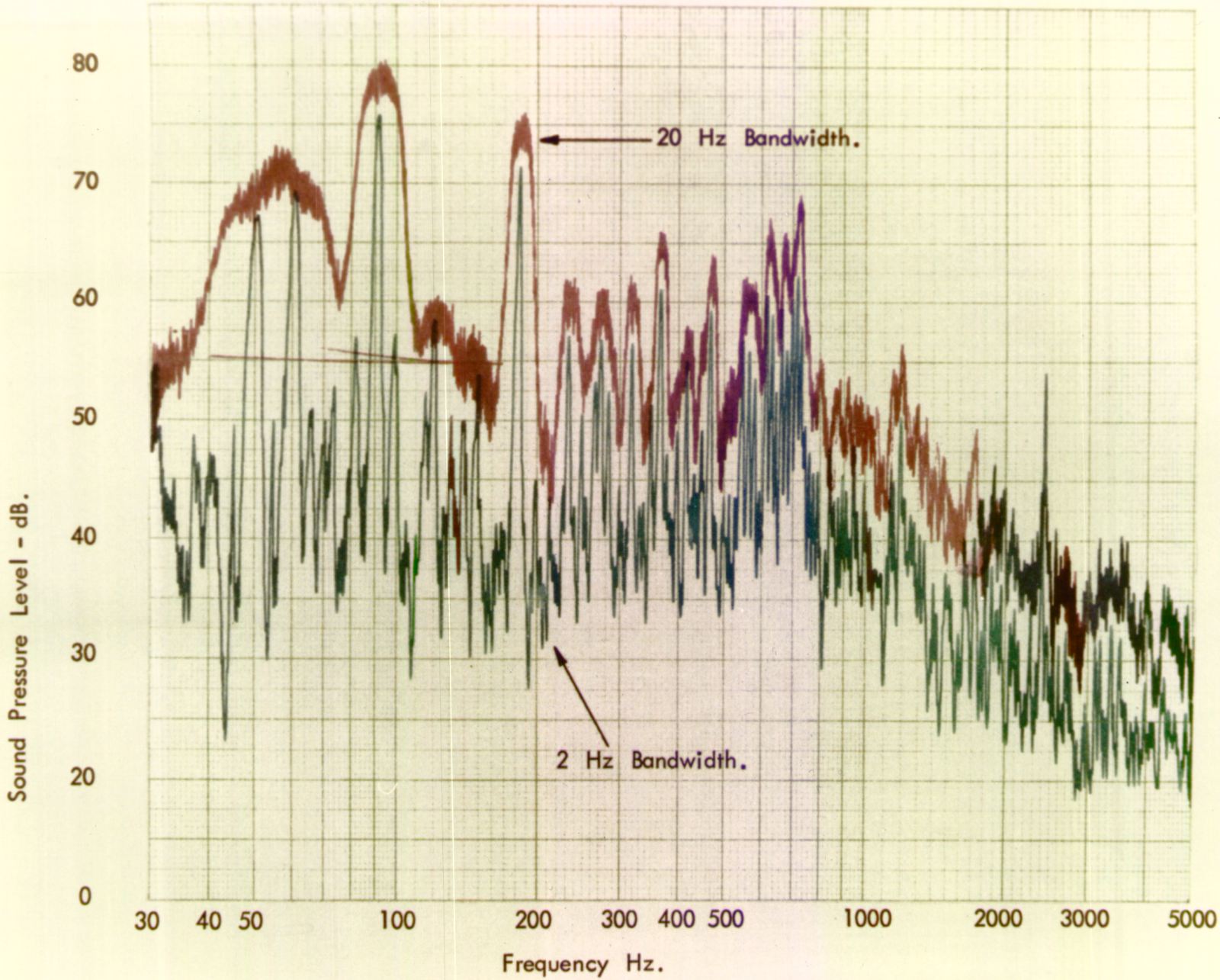

FIG. 4.2. 2 Hz. AND 20 Hz. CONSTANT BANDWIDTH ANALYSIS OF NOISE OF A DIESEL ENGINE.

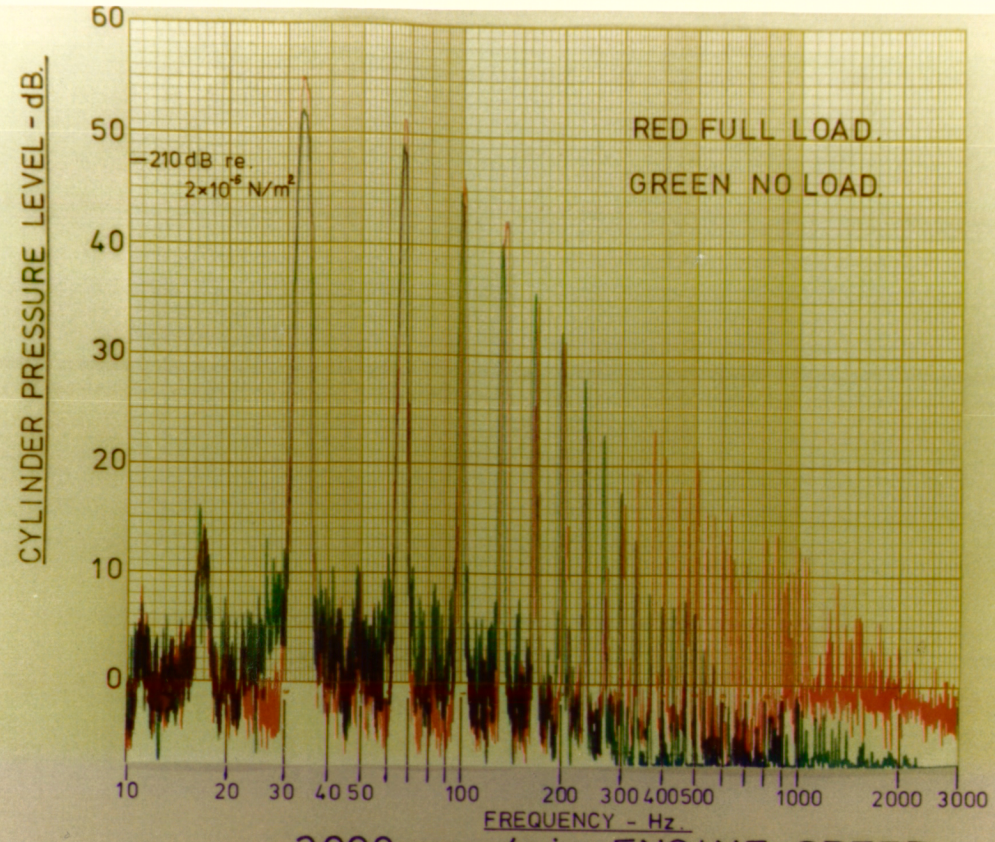

2000 revs/min. ENGINE SPEED.

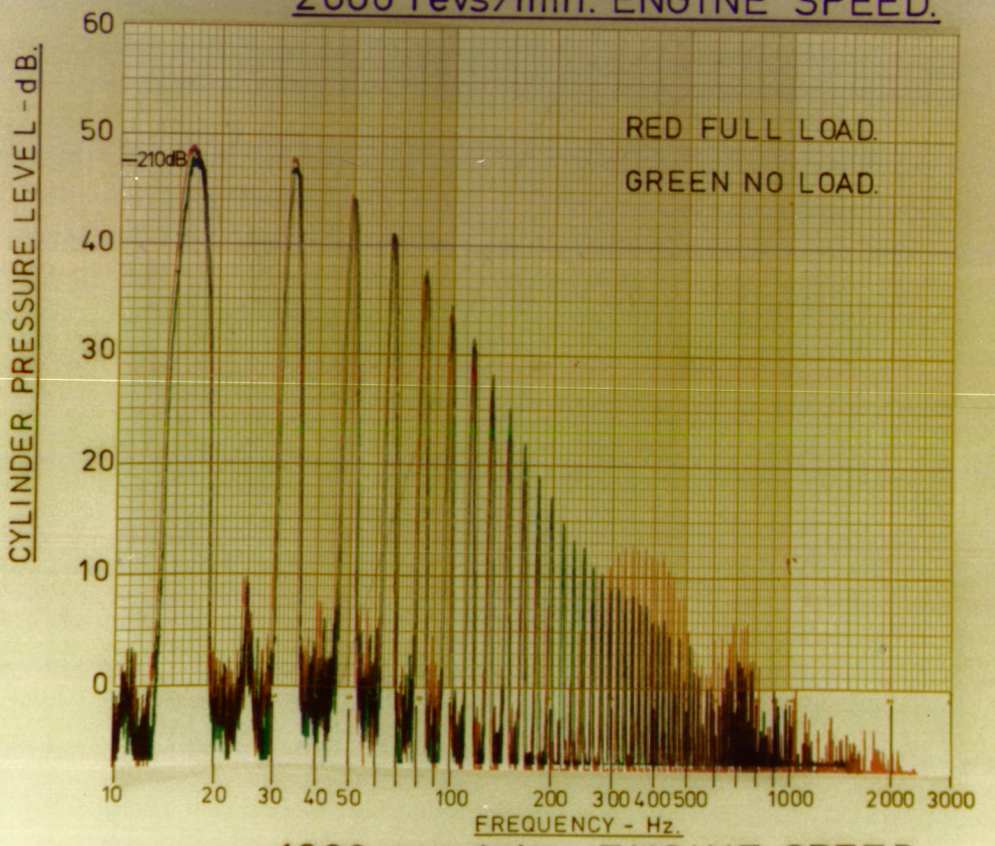

1000 revs/min. ENGINE SPEED.

FIG. 4.3 - 2 Hz. CONSTANT BANDWIDTH CYLINDER PRESSURE ANALYSIS FOR TWO STROKE DIESEL.

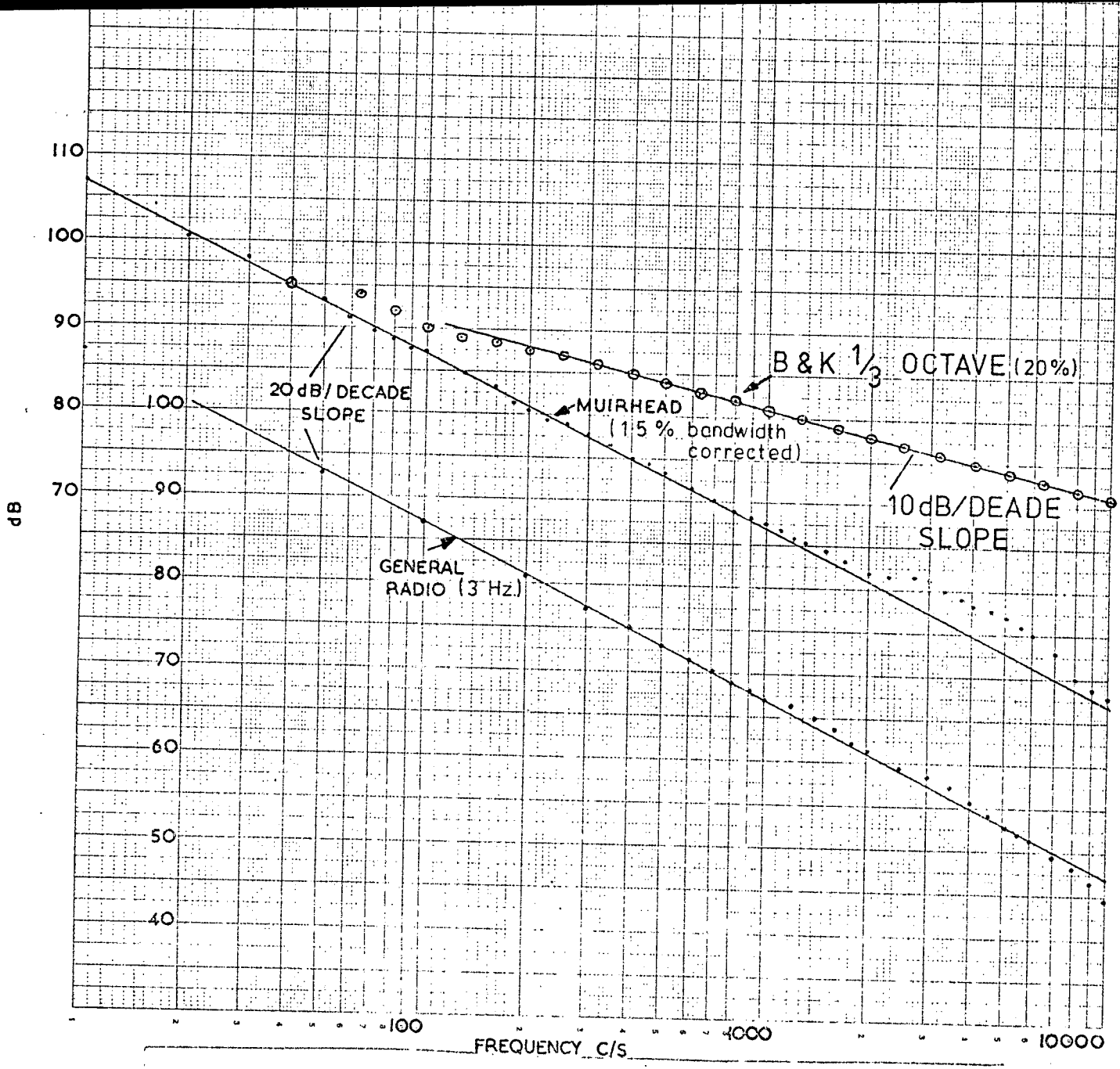

FIG. 4·4 COMPARISON OF ELETRICAL ANALISERS.

constant percentage analysers. The spectrum slope measured for the Muirhead Parmetrada 1.5% analyser is, however, also 20 dB/decade. This is because the metering circuit in this analyser effectively divides the output by the bandwidth, thus giving results more like a constant bandwidth analyser of 1 Hz bandwidth – direct power spectral density analysis.

Fig. 4.5 shows the measured cylinder pressure analysis of a four stroke diesel engine using the Muirhead and General Radio Analysers. The comparison is exceptionally good. For most of the measured cylinder pressure analyses presented here the Muirhead Parmetrada has been used. It has two main advantages over the General Radio type. Firstly being a constant percentage analyser, the time required for measurement is lower. Secondly, because harmonic analysis is being performed there is an advantage in manual operation – it being possible to skip from one harmonic to the next without having to measure through the trough between, again saving time.

4.3.3 Detectors

The detector should be capable of giving a true root mean square value. However, such detectors have been difficult to make and use of 'quasi-rms' meters is sometimes made. If a wide filter bandwidth is used this problem is likely to give rise to greater error than for narrow band filters. Two other factors can reduce the accuracy of electrical analysis. Firstly, the electrical filters do not reject all frequencies outside the measuring bandwidth. Fig. 4.6 shows these characteristics for the Muirhead Parmetrada. If the frequency spectrum slopes greatly, as it does for cylinder pressure spectra, then the filter 'skirts' will allow lower and higher frequencies to interfere with the signal being measured. Thus, even with a narrow band analyser, it is unlikely that the detector will only have one frequency present. Secondly, the detectors have a limited peak-to-rms ratio at which they will work correctly. For cylinder pressure analysis this ratio is

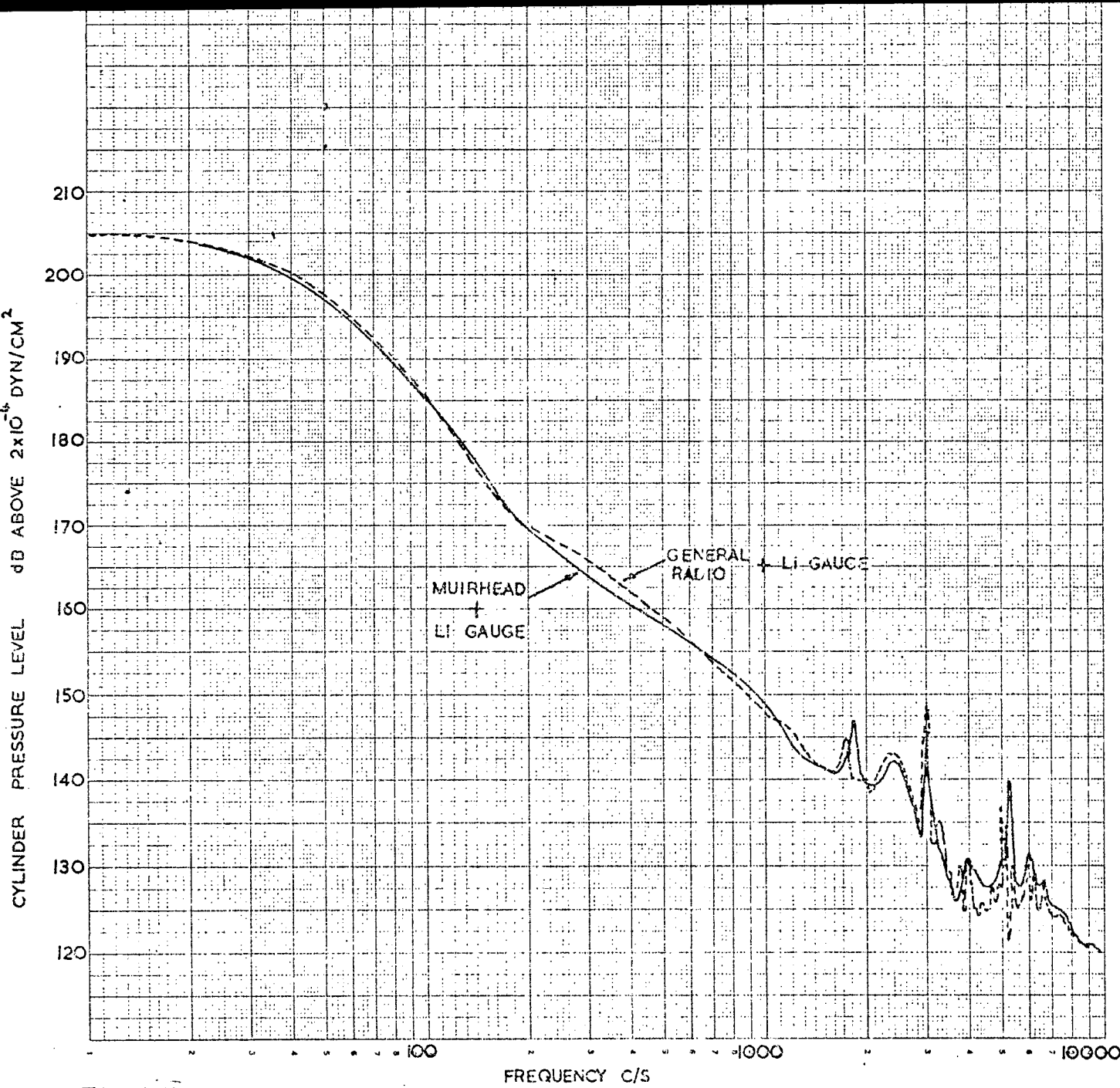

FIG. 4·5 - COMPARISON OF CYLINDER PRESSURE SPECTRA USING DIFFERENT ANALYSERS

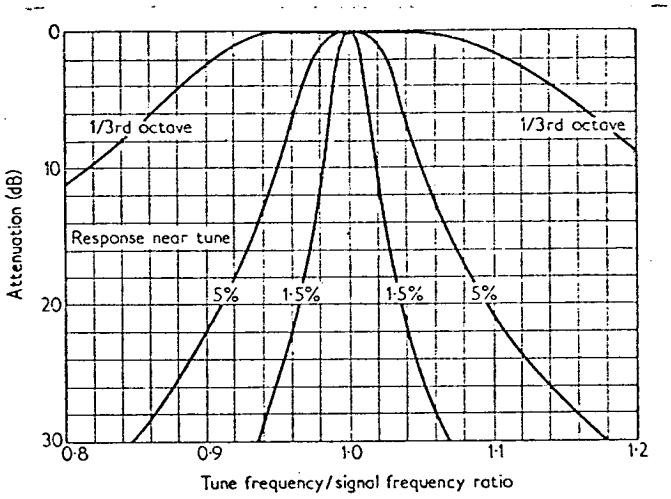

a) Static Response Near Tune.

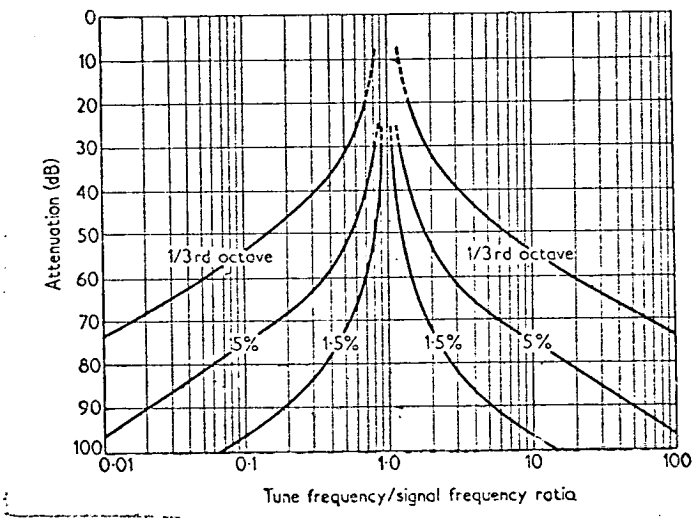

b) Overall Response Curves.

FIG. 4.6 FREQUENCY REJECTION CHARACTERISTICS OF TYPICAL RANGE OF ELECTRICAL FILTERS.

generally high, about 12:1, and therefore detector requirements are high.

There are, therefore, several factors which reduce the accuracy of electrical frequency analysis, but provided care is taken, good results can be obtained.

4.3.4 Dynamic range

Since the frequencies which are of prime interest in cylinder pressure spectra are those between 500 and 5000 Hz it can be seen from Fig. 4.5 that a very large dynamic range is required. The 60 dB dynamic range of the Spectral Dynamics SD101A is inadequate as can be seen from Fig. 4.3, where only values up to 1000 Hz could be obtained. A dynamic range of at least 80 dB (1 part in 10,000) is required from all component parts in a cylinder pressure analysis system. The use of a piezo-electric pressure transducer and associated charge amplifier together with the Muirhead Parmetrada or General Radio analysers have proved good systems.

4.3.5 Relation between narrow band and 1/3 octave band cylinder pressure levels

Because of the time required to complete a narrow band cylinder pressure spectrum (which can be completed at fastest in about 10 minutes on the Parmetrada) it is often required to use larger bandwidth analysers to reduce this time even further. Since noise is measured by 1/3 octave band analysis, this bandwidth of analyser would seem most suitable.

The characteristic of the Muirhead Parmetrada is that although a constant bandwidth analyser, the detector circuit automatically corrects for this so that a spectrum with levels equivalent to a 1 Hz bandwidth are produced (bandwidth corrected levels). In a similar manner, the same analyser, when set to 1/3 octave bandwidth, produces bandwidth corrected levels and the resulting spectrum is like that of a smoothed narrow band analysis. This is shown in Fig. 4.7a. In comparison, Fig. 4.7b shows the

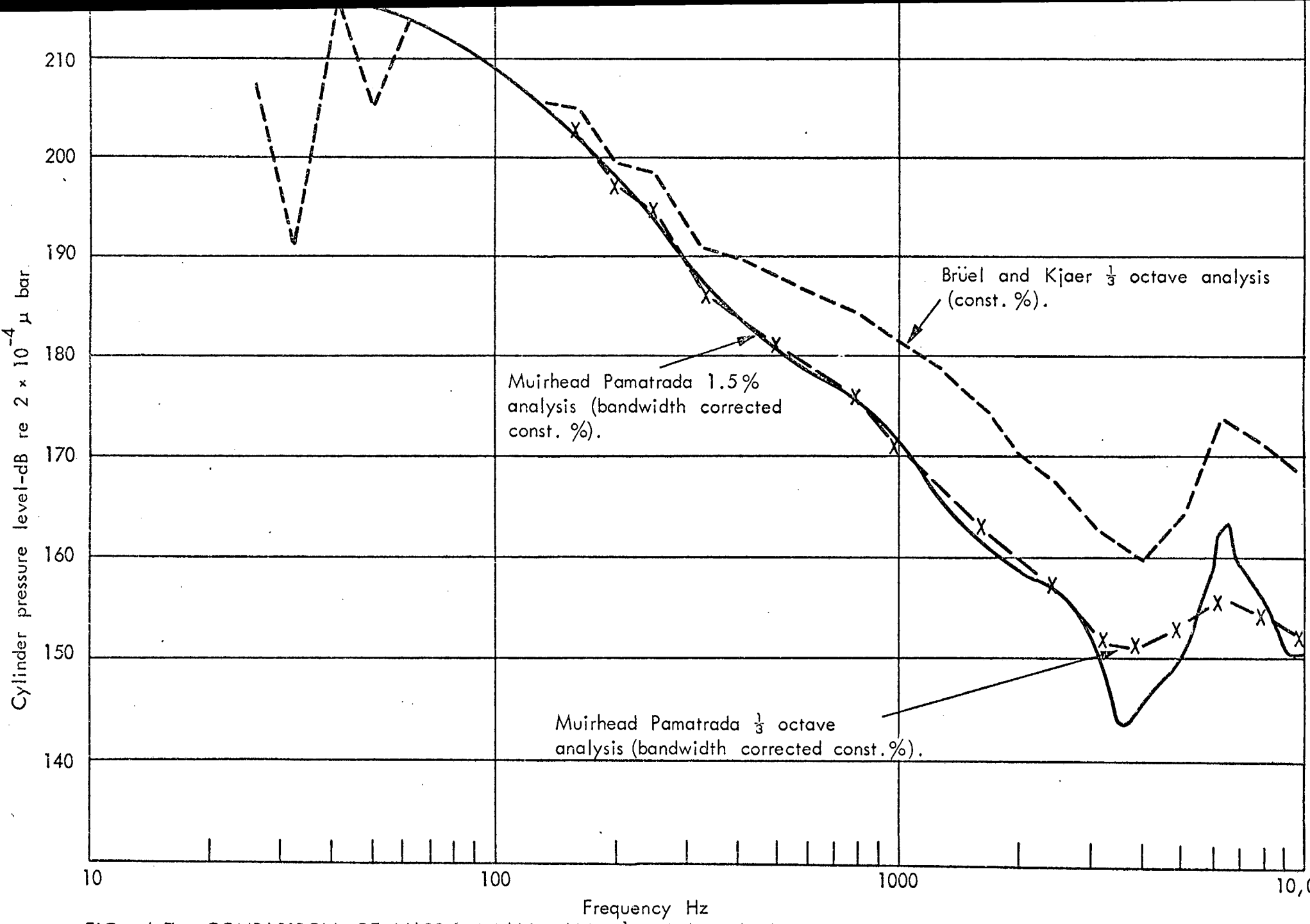

FIG. 4.7. COMPARISON OF NARROW BAND AND ⅓ OCTAVE ANALYSIS OF TWO STROKE DIESEL ENGINE-1200 R.P.M. FULL LOAD.

spectrum obtained using a B & K 1/3 octave band analyser with no bandwidth correction. Here the slope of the spectrum is changed as well as it being smoothed out. Since the rate of increase of combustion induced noise can be calculated from the slope of the cylinder pressure harmonic spectrum levels only, a way of converting from 1/3 octave band to narrow band data is needed.

The average level of the harmonics which fall within a particular 1/3 octave bandwidth will depend upon the number of harmonics contained within that band. The exact correction for a standard set of 1/3 octave filters to be applied to a four stroke engine running at 1000 revs/min is shown in Fig. 4.8. Where there are a reasonable number of harmonics in the band the correction is 10 dB/Decade, as it would be for a continuous spectrum. Below this the correction will vary according to the number of harmonics in the band. This will depend on the basic engine cycle repetition frequency which in turn is dependent on engine speed and cycle of operation (two or four stroke).

For a continuous spectrum the correction for a constant percentage filter over a decade will be the ratio of analyser bandwidths. This is (in log form):

$$\text{CORRECTION}_{\text{SPECTRUM}} = 10 \log_{10} \frac{10Kf_o}{Kf_o} \text{ dB/Decade}$$

f_o = band centre frequency

K = % bandwidth

$$= 10 \text{ dB/decade.}$$

The correction will start from 1 Hz.

For a harmonic function the correction will be the ratio of the number of harmonics within the bandwidth. This will be, for frequencies where there are at least 4 harmonics in a bandwidth,

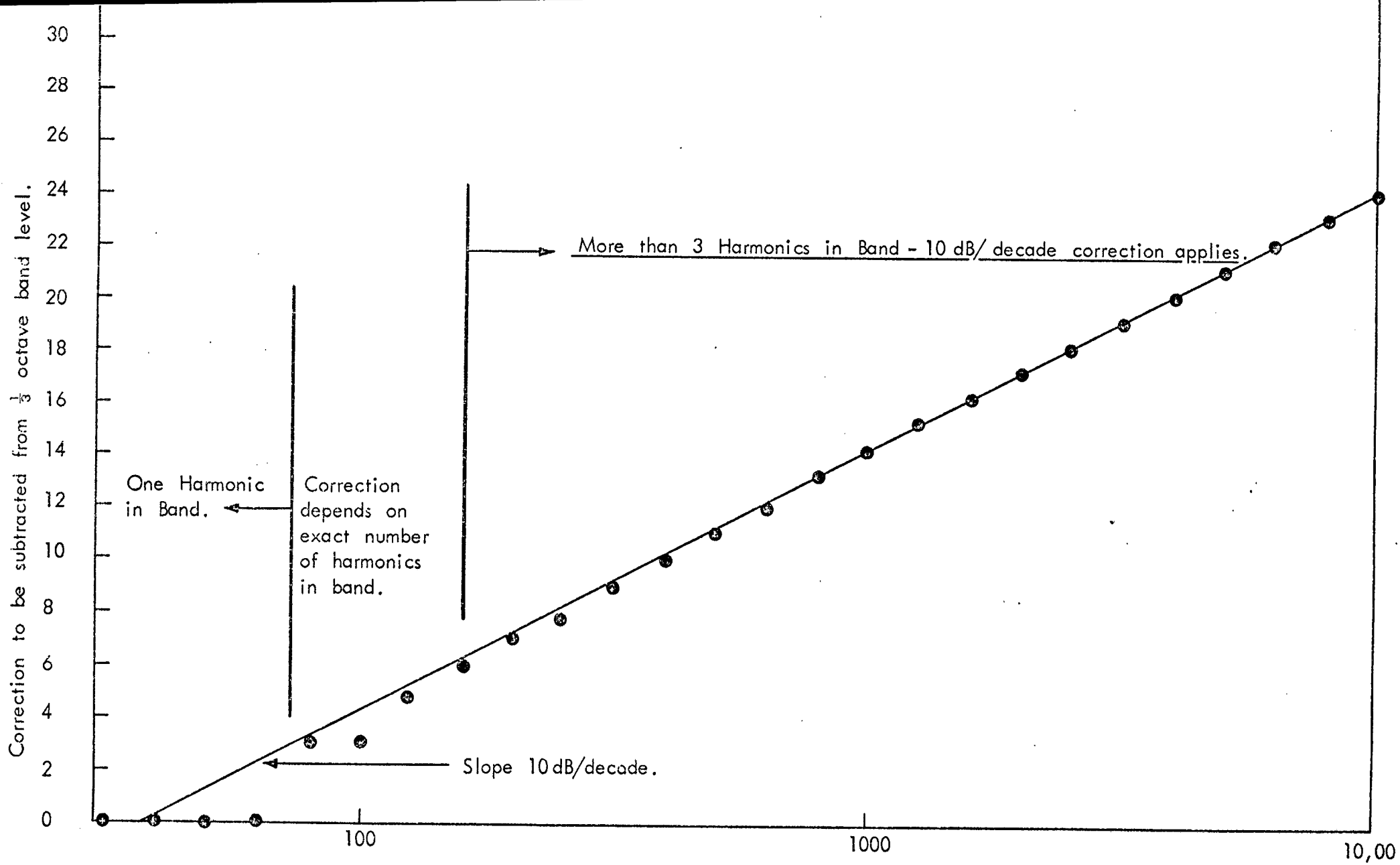

FIG. 4.8. CONVERSION FROM $\frac{1}{3}$ OCTAVE BAND ANALYSIS TO HARMONIC SPECTRA LEVEL - FOUR STROKE ENGINE RUNNING AT 1000 REVS/MIN.

$$\text{CORRECTION}_{\text{HARMONIC}} = 10 \log_{10} \frac{10Kf_o}{f_n} \cdot \frac{f_n}{Kf_o} \text{ dB/Decade}$$

$$= 10 \text{ dB/Decade}$$

f_o = band centre frequency

K = % bandwidth

f_n = basic engine cycle repetition frequency.

From Fig. 4.8 it can be seen that the exact correction, until some four harmonics are in a bandwidth, will depend upon engine speed and cycle. However, since the very low frequency portion of a cylinder pressure spectrum is not important for noise, the approximate correction of 10 dB/Decade can be applied, starting from the last band which contains only one harmonic. Table 4.1 shows these bands as a function of engine speed and cycle type.

Table 4.1: 1/3 octave band frequency above which 10 dB/Decade correction can be applied to convert 1/3 octave spectra to equivalent harmonic spectrum levels.

	FOUR STROKE CYCLE		TWO STROKE CYCLE	
Speed Revs/min	Cycle repetition frequency - Hz	Apply correction from 1/3 octave band - Hz	Cycle repetition frequency - Hz	Apply correction from 1/3 octave band Hz
1000	8.34	40	16.68	80
2000	16.68	80	33.3	160
3000	25.0	125	50.0	250
4000	33.3	160	66.6	315
5000	41.6	200	83.2	400
6000	50.0	250	100.0	500

4.3.6 Cylinder pressure analysis with limited dynamic range analysers

In the last section it was shown how the harmonic spectrum level could be obtained from 1/3 octave band analysers. In general the instruments commercially available are limited to a dynamic range of about 60 dB and are therefore not quite suited to cylinder pressure analysis where an 80 dB dynamic range is required. One way to reduce the dynamic range requirement

of an analyser is to use a differentiated signal for analysis rather than that of the original signal.

4.3.7 Cylinder pressure analysis using the differential of the cylinder pressure diagram

Consider the Fourier coefficients of a cylinder pressure diagram with repetition length ℓ:

$$a_k = \int_0^{\ell} f(x) \sin \frac{2\pi kx}{\ell} .dx \tag{4.5}$$

$$b_k = \int_0^{\ell} f(x) \cos \frac{2\pi kx}{\ell} .dx \tag{4.6}$$

Then the modulus harmonic spectrum levels obtained by electrical analysis will be

$$R_k = \frac{1}{\sqrt{2}} (a_k^2 + b_k^2)^{\frac{1}{2}} \tag{4.7}$$

In the same way let

$$a'_k = \int_0^{\ell} f'(x) \sin \frac{2\pi kx}{\ell} .dx \tag{4.8}$$

$$b'_k = \int_0^{\ell} f'(x) \cos \frac{2\pi kx}{\ell} .dx \tag{4.9}$$

and

$$R'_k = \frac{1}{\sqrt{2}} (a_k'^2 + b_k'^2)^{\frac{1}{2}} \tag{4.10}$$

where $y = f(x)$, $\quad y' = \frac{df(x)}{dx} = f'(x)$.

If the frequency analysis of $f'(x)$ is measured, what is the connection between a_k, b_k and a'_k, b'_k?

$$a'_k = \int_0^{\ell} f'(x) \sin \frac{2\pi kx}{\ell} .dx \tag{4.11}$$

Integrating by parts

$$a'_k = -\frac{2\pi k}{\ell} \int_0^{\ell} f(x).\cos\frac{2\pi kx}{\ell} .dx \tag{4.12}$$

or $$a'_k = -\frac{2\pi k}{\ell} b_k \tag{4.13}$$

and similarly,

$$b'_k = \frac{2\pi k}{\ell} a_k. \tag{4.14}$$

Thus the modulus value R'_k is given by

$$\underline{R'_k = \frac{\sqrt{2}\pi k}{\ell} . R_k.} \tag{4.15}$$

Since cylinder pressure level is expressed as $10 \log_{10} R_k$, then

$$20 \log_{10} R'_k = 20 \log_{10} R_k + 20 \log_{10} \frac{\sqrt{2}\pi k}{\ell} \tag{4.16}$$

and the reduction of slope will be 20 dB/Decade, compared to the straightforward cylinder pressure spectrum $20 \log_{10} R_k$.

Thus, if an engine fundamental is at 10 Hz then the required dynamic range of 80 dB is reduced by 60 dB to 20 dB - well within the capability of all frequency analysers. The use of a differentiated cylinder pressure signal for cylinder pressure analysis is therefore well suited to cases where 1/3 octave band analysers are the only available equipment.

There are two ways of producing a differentiated pressure signal:

1. Use of a direct measuring dp/dt transducer, such as the Sunbury type;
2. use of an electrical differentiation network applied to the output of a normal pressure transducer.

Figure 4.9 shows a cylinder pressure development and also rate of change of cylinder pressure development. The $\frac{dp}{dt}$ diagrams were obtained by using a Vibro-Meter TA-3/C charge amplifier with an electronic differentiation circuit. The $\frac{dp}{dt}$ diagrams for three different time constants

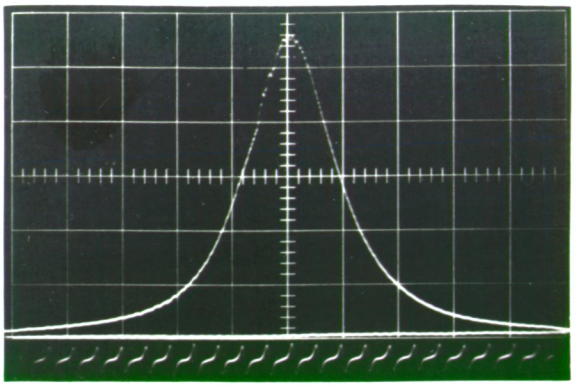

TIME CONSTANT
10 secs.

NO
DIFFERENTIATION.

CYLINDER PRESSURE DEVELOPMENT.

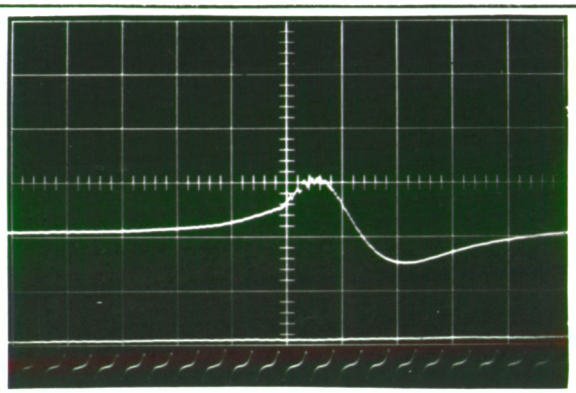

TIME CONSTANT
1 ms.

DIFF. TO 200 Hz.

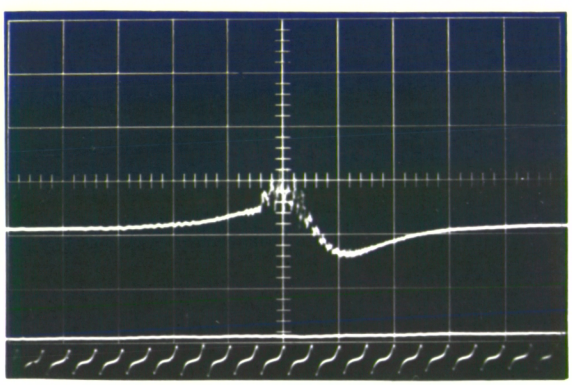

TIME CONSTANT
0·1 ms.

DIFF. TO 2000 Hz.

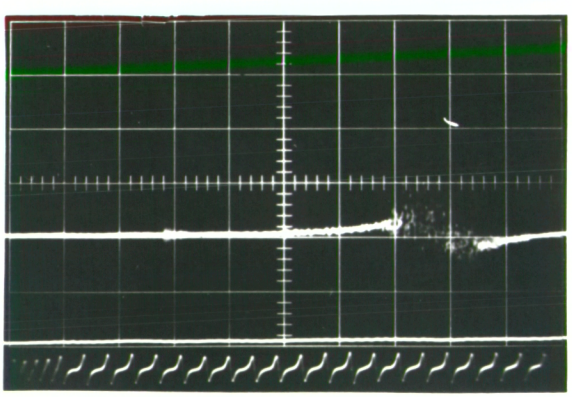

TIME CONSTANT
10 μsecs.

DIFF. TO 20,000 Hz.

RATE OF CHANGE OF CYLINDER PRESSURE.

FIG. 4·9 - RATE OF CHANGE OF CYLINDER PRESSURE FOR TWO STROKE DIESEL AT 2100 revs/min.

(increasing the frequency range of differentiation as the time constant is reduced) are also shown in Fig. 4.9.

It is difficult to relate a $\frac{dp}{dt}$ diagram to a pressure development by eye and this method has the advantage over the direct $\frac{dp}{dt}$ measuring transducer, that the pressure development can be displayed immediately by changing the time constant switch on the amplifier.

To obtain a $\frac{dp}{dt}$ output over the required frequency range, a time constant of one microsecond has been found necessary. Figure 4.10 shows a cylinder pressure spectrum obtained from an opposed piston two stroke diesel engine firstly by analysis of the direct cylinder pressure output and then from the differentiated cylinder pressure output. The spectrum levels obtained from the differentiated signal have a lower level but also a lower dynamic range. Using equation (4.16) the differentiated spectrum can be converted to give the correct cylinder pressure spectrum. The agreement is very good, although there are differences at high frequency where the spectrum is controlled by cylinder pressure oscillations.

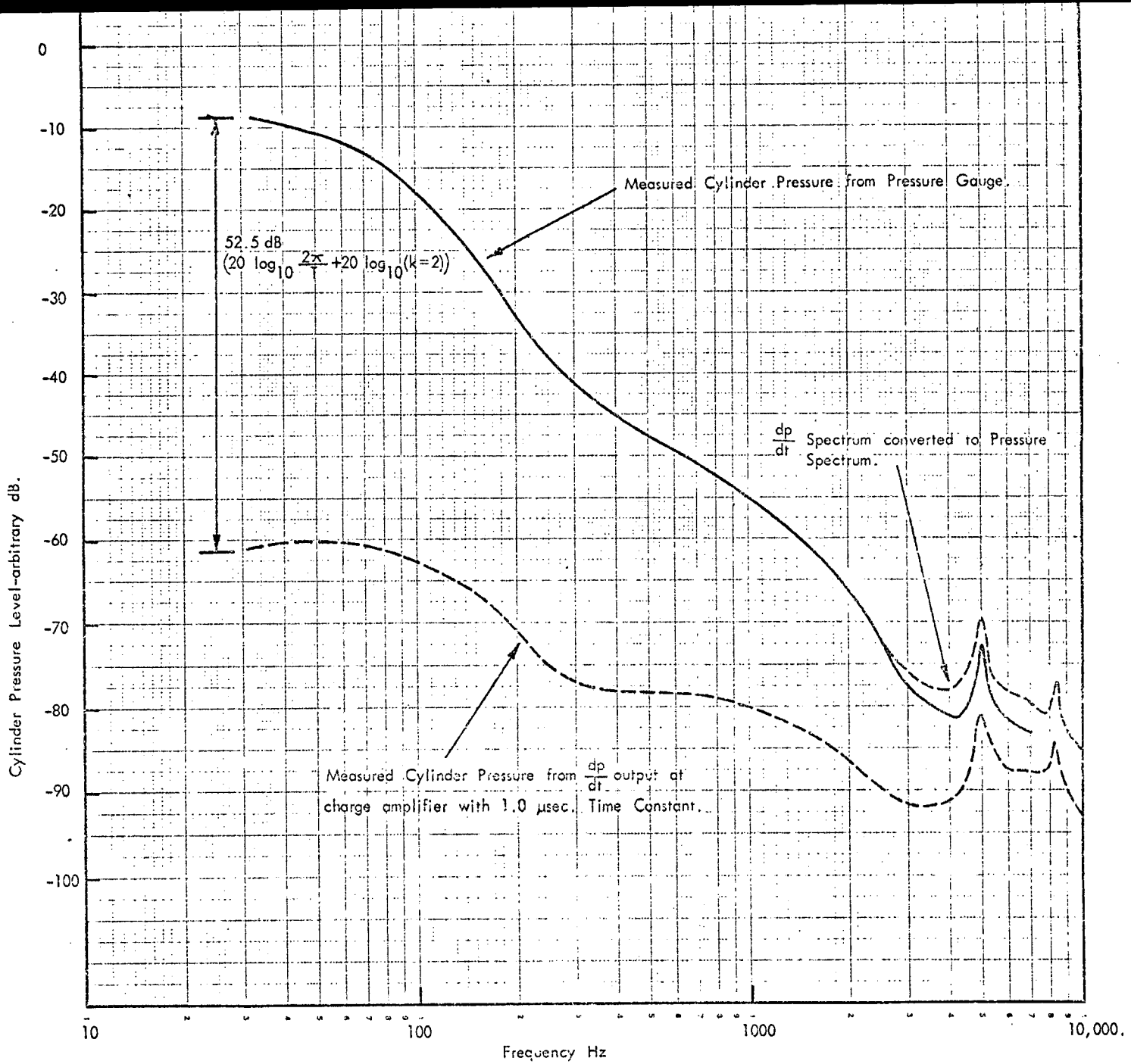

FIG. 4.10. COMPARISON OF MEASURED CYLINDER PRESSURE SPECTRUM USING PRESSURE AND $\frac{dp}{dt}$ SIGNALS-TWO STROKE DIESEL 1000 REVS/MIN NO LOAD.

References

4.1 T. Priede. "Relation Between Form of Cylinder Pressure Diagram and Noise in Diesel Engines". Proc. IME Automobile Division (1960-61), p.66.

5.0 FREQUENCY ANALYSIS OF CYLINDER PRESSURE DEVELOPMENT BY DIGITAL COMPUTER

In 1960, Priede, in his paper 'Relation between form of cylinder pressure diagram and noise in diesel engines' (ref. 2.5) stated that since some 1200 harmonics are required for a cylinder pressure spectrum, numerical methods and also electronic computers were found to be impracticable. By this he meant that the time (and consequent cost) for computation was too large. The development of the speed of commercially available electronic computers over the period 1960 to 1965 led to a new effort aimed at finding a method of computing the Fourier series for harmonic waveforms up to some 2000 harmonics. The work described in this chapter was started in September 1965.

Up to the early 1960's the majority of applications for Fourier series analysis were concerned with only a few harmonics - say up to 20 or so. For instance, engine torsional analysis or aircraft frame structure resonances. Manley (5.1) in his excellent book in 1950 describes the application and theory of Fourier analysis to periodic functions both of mathematical and analogue form, advocating a method for separating out the two or three main constituents of a waveform by the envelope method.

Even up to 1965 the bulk of the waveform analysis in mechanical engineering was based on a 24, 48 or 72 point system involving the calculation of some 10, 20 or 35 harmonics. Extension of these forms of analysis to compute a larger number of harmonics had not been reported in the literature at that time and the next sections describe one approach to this problem. It has resulted in the development of a Fast Fourier Analysis (FFA) computer programme for the Fourier analysis of complex, repetitive waveforms using standard FORTRAN programme language. The programme allows the computation of a large number of harmonics, any number in fact, depending on the specifi-

cation of input data. It is shown that calculation of at least 1000 harmonics can be computed from a limited amount of input data (70 - 150 points).

In its present form the programme is immediately suitable for the harmonic analysis of both cylinder pressure diagrams and noise oscillograms. Resultant harmonic amplitudes are calculated in decibels relative to 2×10^{-5} N/m^2. The Fourier analysis of complex noise oscillograms and cylinder pressure developments by this method is equivalent to a narrow band analysis of the waveform using a constant bandwidth analyser. The programme, designated V17E, is detailed in Appendix I. In the description of the development it is useful to specify four types of Fourier series:

1) FOURIER SERIES — A series of harmonically related sine and cosine waves where all waves have frequencies which are an integer number times the repetition period of the waveform.

2) DISCRETE FOURIER SERIES — As for (1) but values calculated from a set of data with discrete intervals between them.

3) FOURIER TRANSFORM — Continuous series of sine and cosine waves where waves are not necessarily an integer number times the repetition period of the waveform. Can be looked on as a Fourier series with infinitely long repetition period and is applicable to transients.

4) DISCRETE FOURIER TRANSFORM — As for (3) but values calculated from a set of data with discrete intervals between them.

5.1 Straightforward Calculation of Fourier Series

The Fourier series can be defined as follows (5.1):

If a function $f(x)$ of x has a finite number of points of ordinary discontinuity and a finite number of maxima and minima in the interval $0 \leq x \leq 2\pi$, and if the function be arbitrarily defined within this interval and defined by the relation

$$f(x + 2\pi) = f(x), \tag{5.1}$$

for values of x outside this interval, then

$$f(x) = \tfrac{1}{2}a_o + \sum_{k=1}^{k=\infty} (a_k \cos kx + b_k \sin kx) \tag{5.2}$$

where

$$a_k = \frac{1}{\pi}\int_o^{2\pi} f(x) \cos kx.dx$$

$$b_k = \frac{1}{\pi}\int_o^{2\pi} f(x) \sin kx.dx \tag{5.3}$$

$$k = 0, 1, 2, 3, \text{ etc.}$$

and at every point $x = X$ in the interval the series converges to the value

$$f(X) = \tfrac{1}{2}\left|f(X + 0) + f(X - 0)\right| \tag{5.4}$$

This is a statement of Fourier's theorem, named after the celebrated French scientist. Fourier's first paper on the subject of trigonometric series was read to the French Academy in 1807. He discovered the theorem in his researches into the conduction of heat (non periodic application). The series (5.2) is known as the Fourier series or Fourier expansion of the function $f(x)$; the coefficients a_k and b_k are termed the Fourier coefficients; and the process of determining these coefficients is called Fourier analysis or harmonic analysis.

If the function $f(x)$ can be described mathematically and the integrals (5.3) solved, then a harmonic analysis can be completed exactly. If, however,

the function is like a cylinder pressure development, then a numerical method of approximation must be found.

It is wished to find the integrals

$$a_k = \int_0^{\ell} f(x) \cos Akx \, dx$$

$$b_k = \int_0^{\ell} f(x) \sin Akx \, dx \qquad (5.5)$$

where the repetition period is now ℓ instead of 2π. This must be done by numerical integration. Using Simpson's rule, equations (5.5) become:

$$a_k = \frac{\Delta x}{3} \sum_{r=0}^{N} W(i) \, f(x_r) \cos Akr\Delta x$$

$$b_k = \frac{\Delta x}{3} \sum_{r=0}^{N} W(i) \, f(x_r) \sin Akr\Delta x \qquad (5.6)$$

where $W(i)$ is a weighting function, which can be applied to each value of $f(x_r)$, before the integration, thus forming a new input data set $\bar{f}(x_r)$. If this is done then:

$$a_k = \frac{\Delta x}{3} \sum_{r=0}^{N} \bar{f}(x_r) \cos Akr\Delta x$$

$$b_k = \frac{\Delta x}{3} \sum_{r=0}^{N} \bar{f}(x_r) \sin Akr\Delta x \qquad (5.7)$$

The number of coordinates $\bar{f}(x_r)$ is N and therefore the summation is for N coordinates N times for each harmonic k. The number of computations is thus proportional to $2N^2$. Fig. 5.1 shows the Discrete Fourier Analysis of a sawtooth waveform where one hundred data points were used. Up to the 25^{th} harmonic the theoretical and computed values agree, but after this point they diverge considerably. At the 50^{th} and 100^{th} harmonics there are huge errors. These errors are caused partly by alienation effects and partly because of

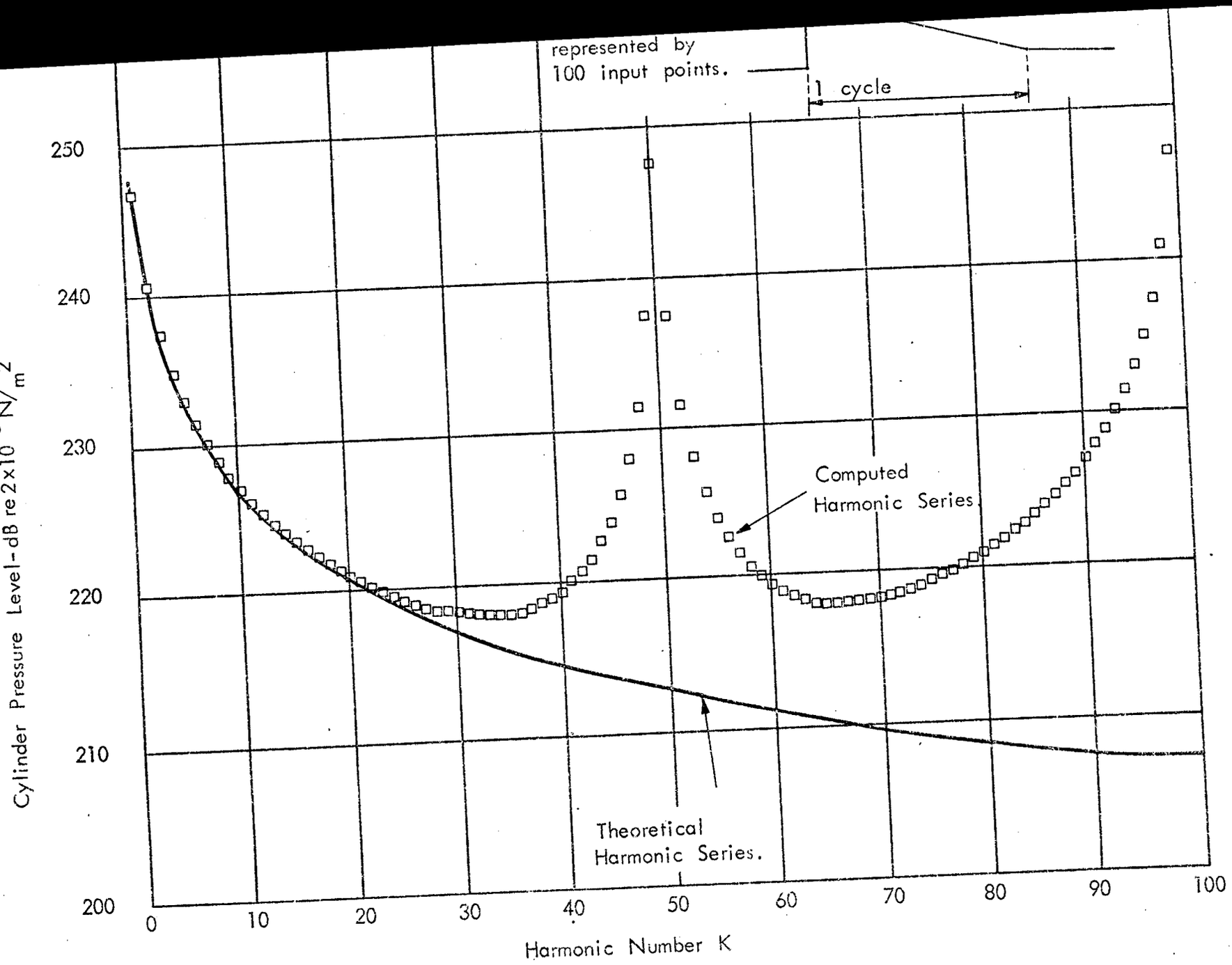

FIG. 5.1. CALCULATION OF HARMONIC ANALYSIS OF SAWTOOTH WAVEFORM USING SIMPSON'S RULE APPROXIMATION 100 INPUT DATA POINTS USED.

inaccuracies in the computation of sine and cosine values close to $\pi/2$ and π respectively. This simple example shows that for accurate computation to $\pm$ 0.5 dB the number of input data points must be four times the number of harmonic values to be calculated. This general rule applies to all data that is formed from unfiltered input data. On this basis, table 5.1 shows a comparison of the speed of computation for calculating the Fourier analysis to cover the frequency range D.C. to 10 kHz. This is based on the single operation of a sine calculation, which on the ICT 1907 takes approximately 0.002 seconds. It can be seen that the required computer time is in hours

Table 5.1 Speed of computation for straightforward Fourier analysis using Simpson's rule approximation.

Engine Cycle	Engine Speed Revs/ Min.	Cycle Fundamental freq. (Hz)	No. of harmonics in band DC to 10 kHz	Req'd no. of input data points N	Computation time $\propto N^2$ Seconds	Digitisation time sec/ point	Digitisation rate kHz
FOUR STROKE	500	4.17	2400	9600	9.2×10^7	25.0	40.0
	1000	8.34	1200	4800	2.3×10^7	"	"
	2000	16.68	600	2400	5.8×10^6	"	"
	3000	25.00	400	1600	2.6×10^6	"	"
	4000	33.3	300	1200	1.4×10^6	"	"
	5000	41.7	240	960	9.2×10^5	"	"
	6000	50.0	200	800	6.4×10^5	"	"
TWO STROKE	500	8.34	1200	480	2.3×10^7	25.0	40.0
	1000	16.68	600	2400	5.8×10^6	"	"
	2000	33.30	300	1200	1.4×10^6	"	"
	3000	50.0	200	800	6.4×10^5	"	"
	4000	66.6	150	600	3.6×10^5	"	"
	5000	82.3	122	488	2.4×10^5	"	"
	6000	100.0	100	400	1.0×10^5	"	"

rather than seconds, even on a comparatively fast machine like the ICT 1907. Despite this, some computations using this method were performed. Fig. 5.2

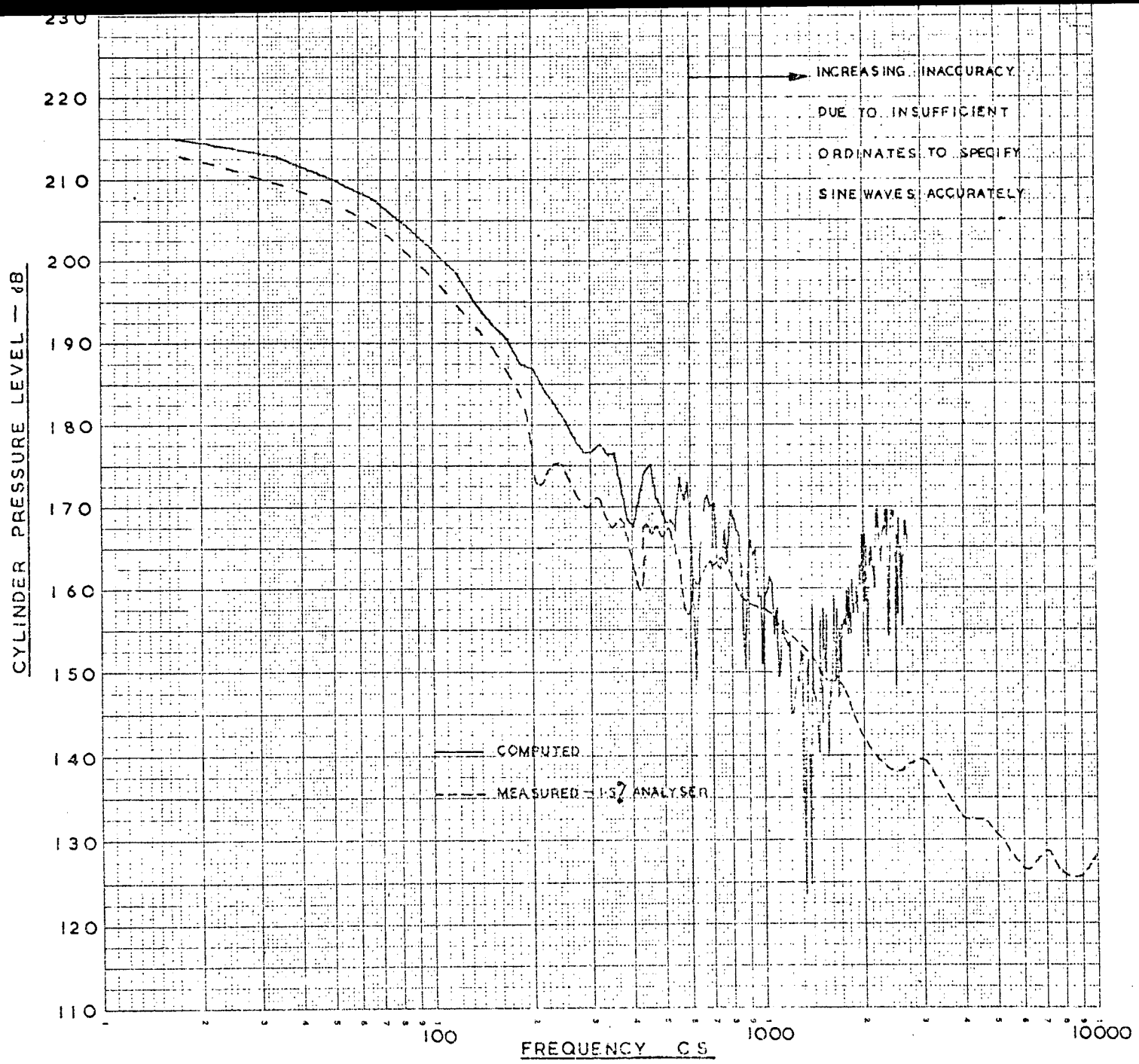

FIG. 5·2 — COMPARISON OF COMPUTED AND MEASURED CYLINDER PRESSURE SPECTRA

shows a comparison between the measured cylinder pressure spectrum for a horizontally opposed piston two stroke diesel engine and the computed spectrum obtained from a hand digitised single cylinder pressure development, digitised every degree of crankshaft rotation to produce 361 data input points. Again at the higher harmonics errors occur but up to the 90^{th} harmonic very good agreement is found. The important conclusion from this is that even with hand digitised data with an accuracy of at most 1% (or equivalent to 40 dB dynamic range input), the higher harmonics up to 90 could be computed accurately. The only limitation apparently being a lack of a sufficient number of input data.

5.2 Increasing the speed of Computation - Fast Fourier Analysis (FFA) Method

On the ICL 1907 series computer the time taken for addition and subtraction is some 3.5 μsecs, for multiplication some 20 μsecs and for sine/cosine some 2000 μsecs. Since each stage in the harmonic analysis involves a sine/cosine computation this is a controlling factor. An algorithm for computing the equations (5.7) which reduces the number of sine/cosine operations by a factor of 2N (N is the number of data points), was used to reduce the computation time. The origin of this algorithm cannot be traced and it must therefore have originated several years ago, its importance being unnoticed at the time.

If we define

$$C = \sum_{r=0}^{N} f(x_r) \sin(ry)$$

$$S = \sum_{r=0}^{N} f(x_r) \cos(ry) \qquad (5.8)$$

and if the loop

$$b_r = f(x_r) + 2b_{r+1} \cos y - b_{r+2}$$

$$b_{r+2} = b_{r+1} \qquad (5.9)$$

$$b_{r+1} = b_r$$

is completed r times where r = N, N-1, N-2, ..., 0 to form end values b_r', b_{r+1}', b_{r+2}' with b_r, b_{r+1}, b_{r+2} initially zero, then

$$C = b_r' - b_{r+2}' \cos y$$

$$S = b_{r+1}' \sin y \qquad (5.10)$$

Comparing equations (5.7) with (5.8) it can be seen that equations (5.9) and (5.10) provide a convenient form for computation of the original integrals required for Fourier analysis. In this method there are only one sine and N + 1 cosine calculations needed for each value of the harmonic number k. However, the total number of operations is still proportional to N^2.

Using this faster programme, 500 harmonics can be calculated on an ICL 1905 from input data of 2000 points in a time of 3½ minutes, as compared to 9 minutes for 180 harmonics with the straightforward programme, a reduction by a factor of about 20. With the 1907 (faster) computer, 800 harmonics could be calculated from 4011 input data points in 3 minutes 22 seconds.

These programme times were within the bounds of reason and further major time reductions were not attempted.

5.3 Analogue to Digital Data Conversion

In 1965 the use of electronic gates and storage to provide analogue to digital conversion was recognised and very expensive systems which operated at a rate of 18 kHz could be obtained. However, the accuracy of digitisation was poor (40 dB dynamic range) and this, coupled with the expense, ruled out the direct conversion of data at this time. Fig. 5.3 shows some results (obtained in 1970 with then new equipment) from two analogue to digital

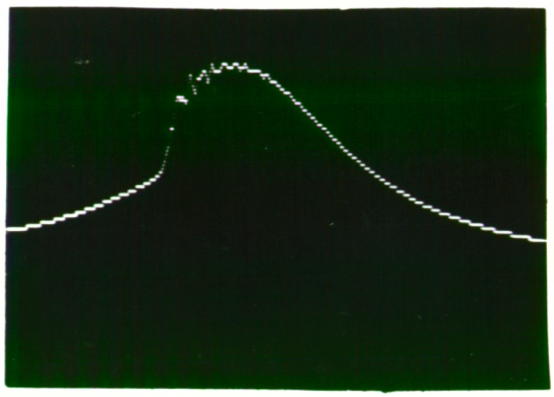

Biomec 1000 Analogue to Digital Converter.
10 μsec/point.
1 cycle.
40 dB dynamic range (1:100).

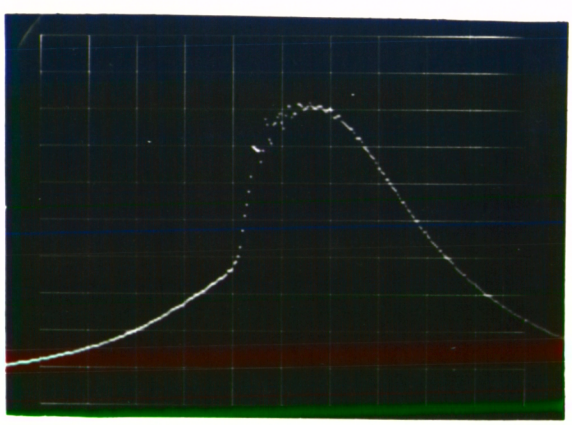

Intertechnique Physioscope Analogue to Digital Converter.
40 μsec/point.
1 cycle.
60 dB dynamic range (1:999).

FIG. 5.3. EFFECT OF DYNAMIC RANGE OF CONVERTER ON DIGITISED CYLINDER PRESSURE DEVELOPMENT FOR SHALLOW DISH CHAMBER FOUR STROKE 5.31" BORE DIESEL.

converters, one with a 40 dB dynamic range (one part in one hundred) and one with a 60 dB dynamic range (one part in one thousand). It is clear that a 40 dB dynamic range is unsatisfactory for cylinder pressure analysis.

The only method therefore available at the time was that of a hand operated X-Y reader (Benson-Lehner) which could punch an X and Y coordinate onto computer cards, the coordinates being read from a set of cross-wires. The X and Y scaling could be set to one part in 999 or equivalent to a 60 dB dynamic range and this was thought satisfactory. Photographic reproductions of cylinder pressure diagrams could be projected onto a ground glass screen on the machine so that they were of dimensions 24 in by 18 in and the digitising could therefore be completed quite accurately. Even with this process the time or crankangle scale could only produce 999 sets of input data and therefore only 250 harmonics could be calculated.

5.4 Extension of the Number of Harmonics Calculable from a Given Data Set by the Assumption of a Linear Variation Between Points

Since the number of points in a given data set determines the upper harmonic number which can be calculated, how can this range be extended? If it is assumed that the function $f(x)$, (a cylinder pressure diagram in this case), changes linearly between consecutive data points, then a new set of data points of any number can be generated. Thus, any number of harmonics can be calculated, the accuracy of the process being totally dependent on the accuracy of fit of this data as compared to the actual cylinder pressure diagram. Initial trials using such a system showed that to follow through 999 equal time intervals was difficult on the machine available, and that on the initial pressure rise portion of the diagram often equally spaced data did not follow exactly the trace, especially where gas oscillations occurred. Therefore unequally spaced data sets were tried, the digitising being done by using the minimum number of points which, when joined by straight lines,

followed the cylinder pressure diagram best. An example of this method, using a straight line approximation and unevenly spaced data is shown in Fig. 5.4. 87 input data points were used in this case and it can be seen that the results are similar to those obtained for the accurate portion of Fig. 5.2, where the number of data points was at least four times the number of harmonics. There is a scatter about the measured result which is the same in both cases. Thus in the unsymmetrical shape of a cylinder pressure diagram there is no advantage to be gained by equally spaced as opposed to unequally spaced data. Similar results were found in ref. (5.2), where specific forms of uneven spaced data were used. For symmetrical waveforms this is not so, as is shown later in this section. Fig. 5.5 shows a further comparison of measured and single cycle computed cylinder pressure spectra. The agreement between the mean computed values and those measured is very good especially when taking account of the fact that cyclic variations do occur and the measured value represents the mean of several hundred cycles.

5.5 Polynomial Variation Between Points

Some of the scatter shown in Figs. 5.4 and 5.5 could be due to the assumption of a linear variation between points. Therefore a third order polynomial approximation was made and tried. This was successful in increasing accuracy on smooth waveforms but was unsuitable for diesel cylinder pressure diagrams because it could not follow the initial pressure rise adequately, Fig. 5.6 illustrates this and the modification was dropped.

5.6 Extension of Discrete Fourier Analysis to the Computation of Discrete Fourier Transform Valves of Transient Waveforms

During the assessment of the Fast Fourier Analysis programme it was found convenient to use the computation of the Discrete Fourier transform of certain waveforms.

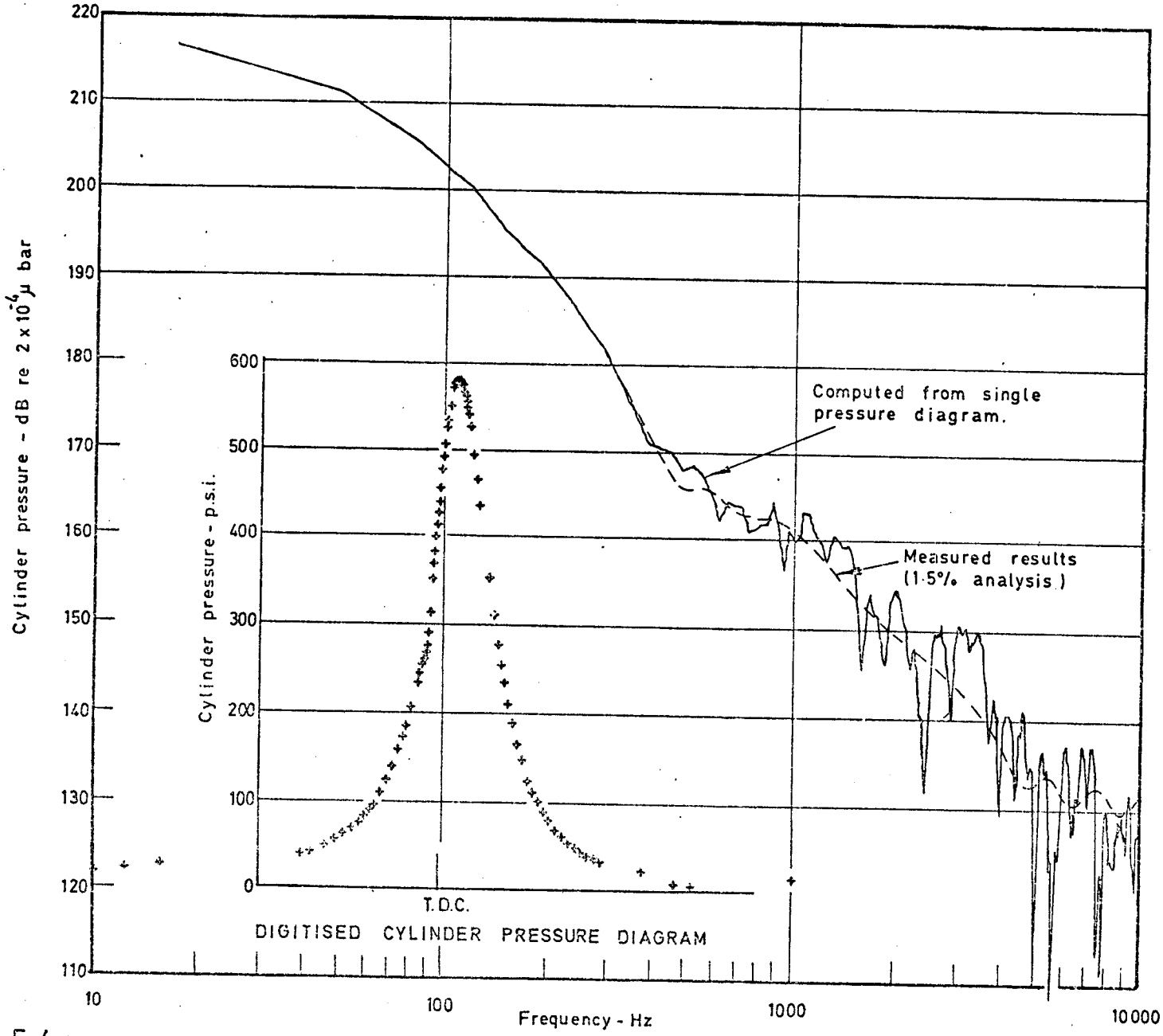

Fig. 5·4 Comparison of computed and measured narrow band cylinder pressure spectra for a two stroke diesel engine (1000 r.p.m.)

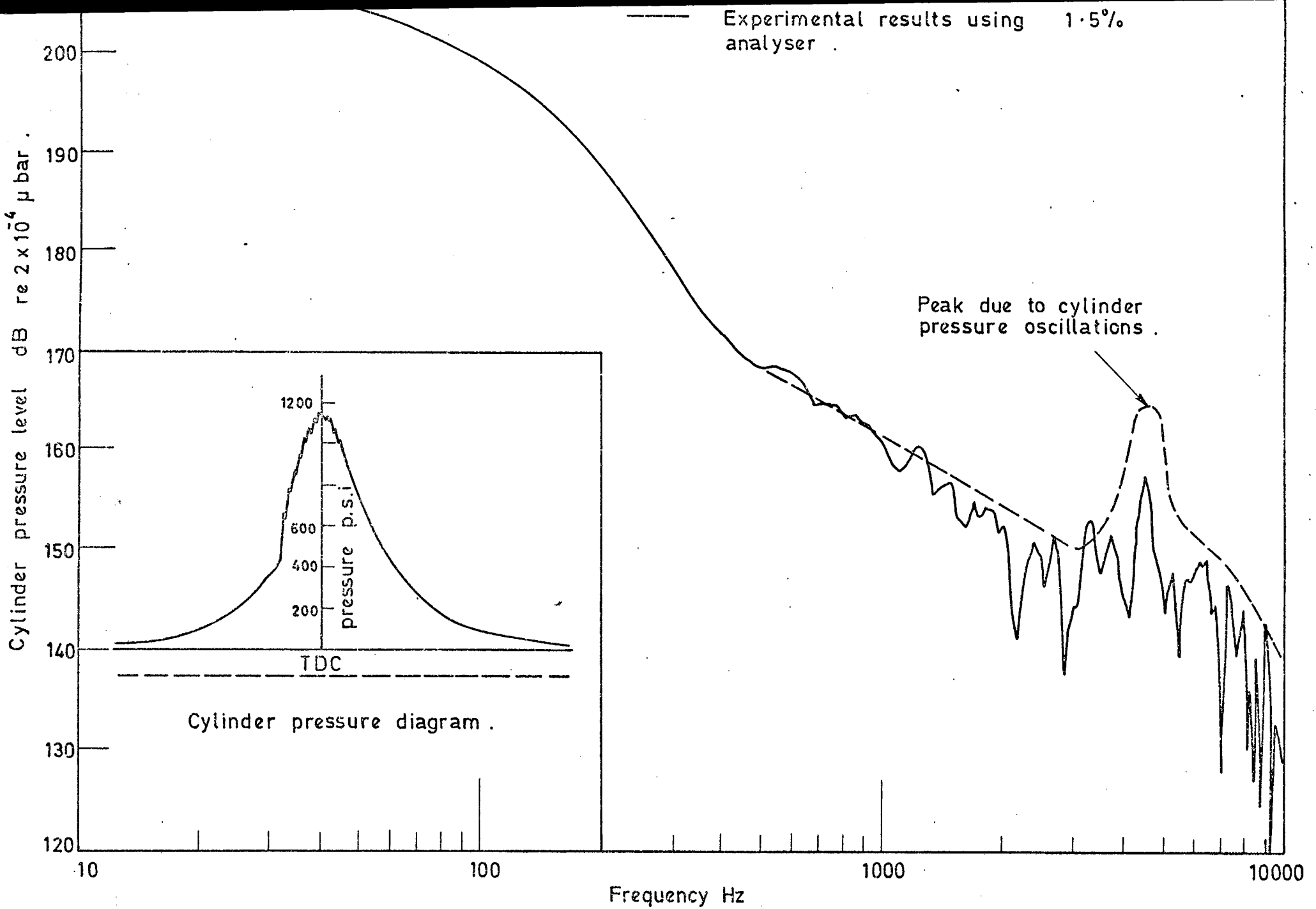

Fig. 5·5 Comparison of computed and measured cylinder pressure spectra for a direct injection four stroke diesel engine

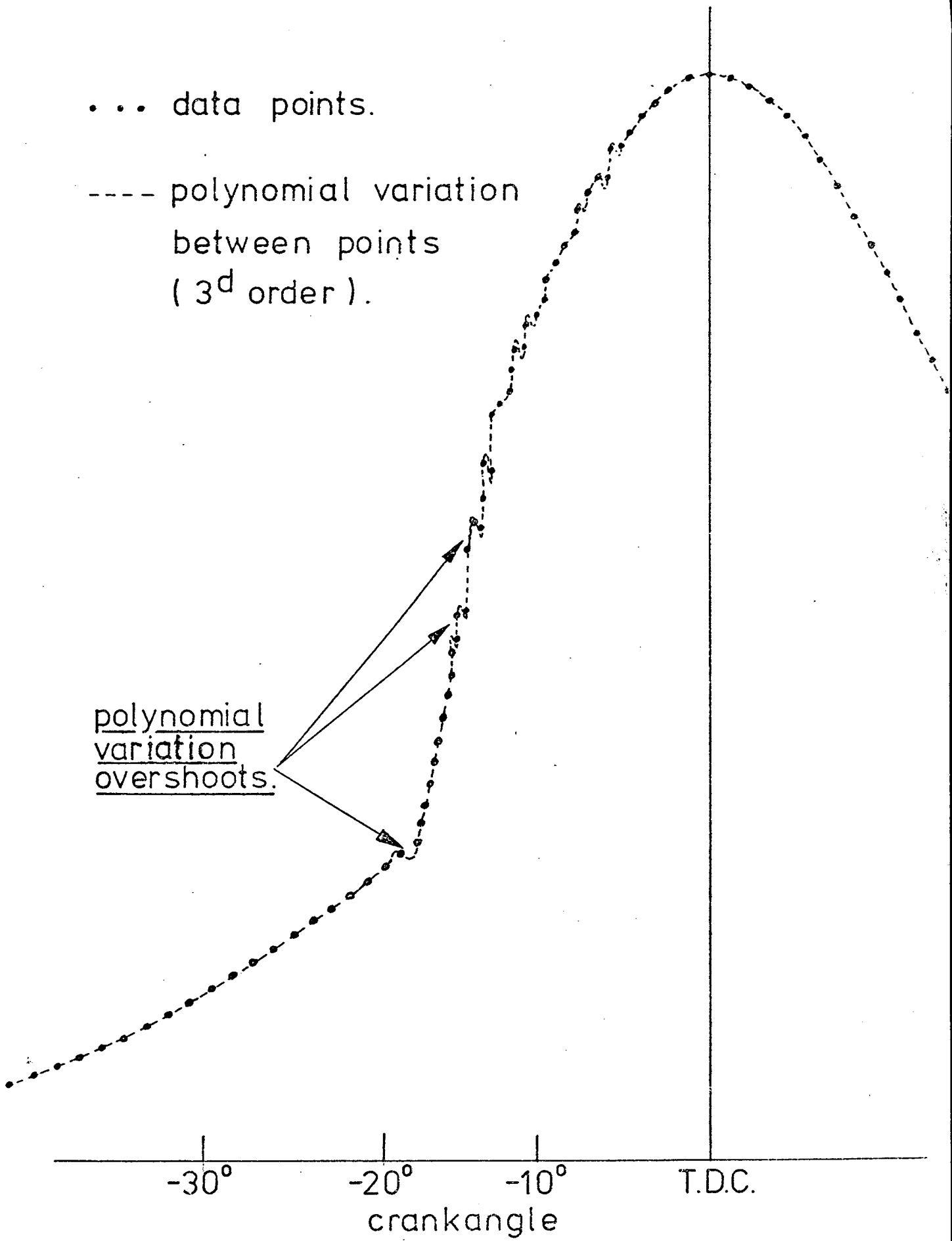

FIG. 5·6- OVERSHOOT CAUSED BY POLYNOMIAL APPROXIMATION.

If, in the normal Fourier series

$$x(t) = a_o + \sum_{r=1}^{\infty} (a_r \cos r\omega_1 t + b_r \sin r\omega_1 t) \tag{5.11}$$

we assume that the period of the waveform is infinite and the fundamental frequency ω is very small and equal to $\Delta\omega$ then

$$x(t) = \frac{\Delta\omega}{2\pi} \int_{-T/2}^{T/2} x(t)^{-ir\Delta\omega t}\, dt.ir\Delta\omega t \tag{5.12}$$

If we now let ω become the infinitesimal $d\omega$ the summation becomes an integral and $r\Delta\omega$ becomes simply ω.

Therefore,

$$x(t) = \int_{-\infty}^{+\infty} \left| \frac{d\omega}{2\pi} \int_{-\infty}^{\infty} x(t)e^{-i\omega t} dt.e^{i\omega t} \right|$$

Thus $x(t) = \frac{1}{2\pi} \int_{-\infty}^{\infty} A(i\omega)^{i\omega t} d\omega$

where $A(i\omega) = \int_{-\infty}^{\infty} x(t)e^{-i\omega t} dt$ (5.13)

and ω can have any value.

If we compare $A(i\omega)$ with the complex form for the Fourier series coefficients

$$C_n = \frac{2}{T} \int_{-\pi}^{\pi} x(t)\, e^{-in\omega_o t}\, dt \tag{5.14}$$

and C_ω is regarded as meaning the harmonic at frequency ω, it will be limited to the values $2\pi r/T$, where r is an integer number. Therefore, equation (5.14) can be rewritten

$$\frac{C_\omega T}{2} = \int_{o}^{T} f(t)e^{-i\omega t}\, dt \tag{5.15}$$

It is therefore obvious that there is an equivalence between C_ω (the complex harmonic amplitude) and $A(i\omega)$ (the complex transform) of any waveform $f(t)$. In the first case the waveform is assumed to repeat every 2π radians, i.e., $f(t) = f(t + 2\pi)$ and in the second the waveform occurs only once.

We can write that

$$A(i\omega) \equiv \frac{C_\omega t}{2} \tag{5.16}$$

For functions repeating every 2π radians this relationship only holds at values of ω of $\frac{2\pi r}{T}$ where r is an integer. For transient waveforms the relationship holds at all values of $\frac{2\pi r}{T}$ where r can now have any value.

It can be seen from equations (5.13) and (5.15) that any method of evaluating the integral common to both will be applicable to the calculation of either the Fourier series or the Fourier transform, depending on the values of ω chosen. Thus if the value of r in the expression $\frac{2\pi r}{T} = \omega$ is allowed NON-INTEGER values, the Fourier transform can be computed.

The relationship (5.16) must always be used when transforming from one set of coefficients to another.

It is interesting to note that the Fourier series values are always contained in the Fourier transform values, being those at which r is an integer.

Figure 5.7 shows the Fourier transform of a sine wave represented by 21 evenly spaced points and calculated from the Fast Fourier Analysis programme V17E, using non integer values of r. It is accurate to $\pm \frac{1}{2}\%$. Five figure log tables were used for the coordinate points.

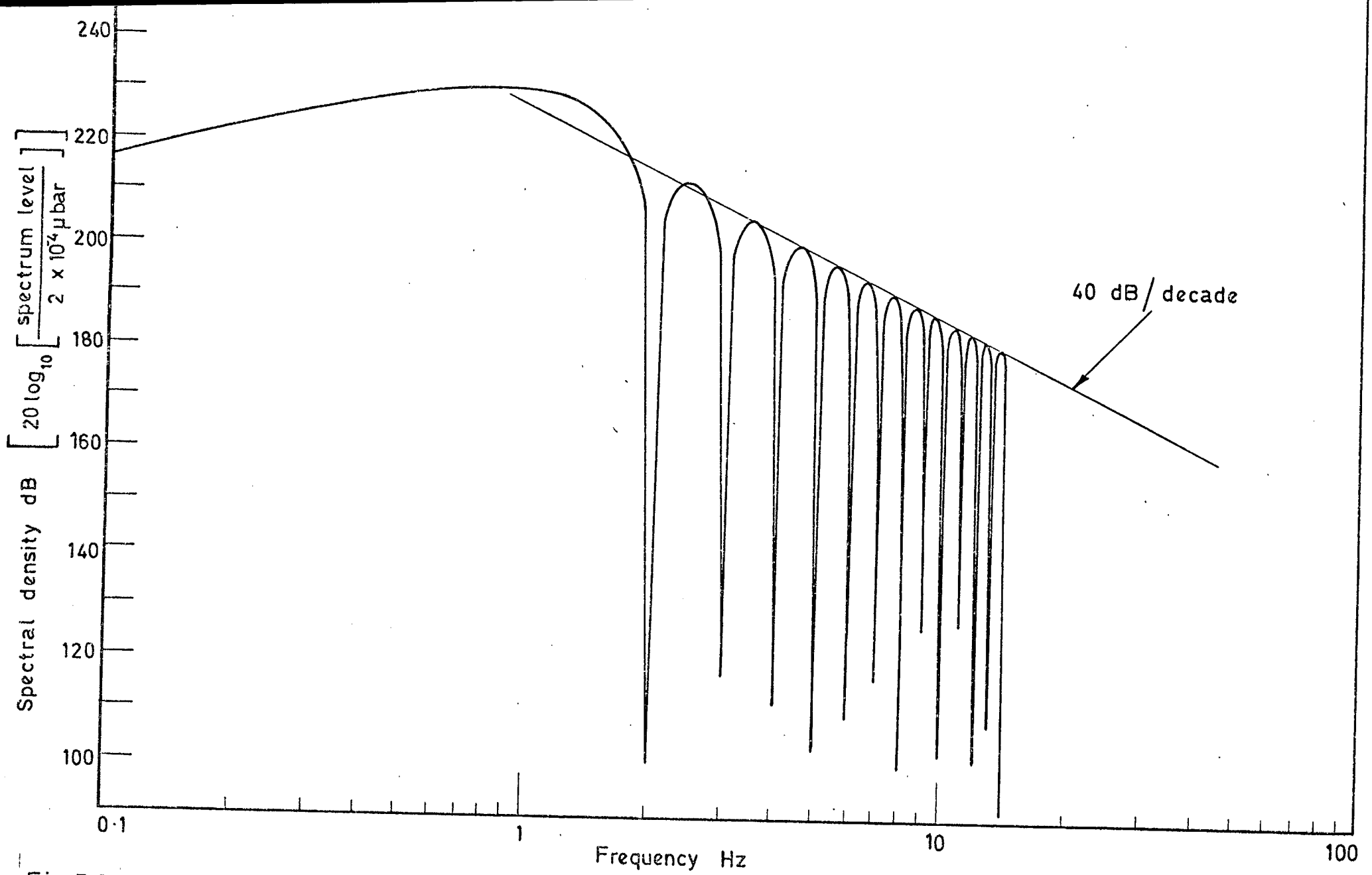

Fig.5·7-Fourier transform of a 1 c/s sinewave, amplitude 1000 p.s.i. computed from a 21 point representation. Linear variation between points assumed.

5.7 Accuracy of Fast Fourier Analysis Method

As soon as a continuous signal is digitised into a discrete data set, then the data set no longer truly represents the original and differences between original data and computed quantities are bound to arise. Once the spacing of consecutive points becomes comparable with the wavelength of a particular sine component, then several sine waves of differing higher frequency multiples will be identified as one combined component at a lower frequency. This occurs as the harmonic number approaches half the number of input data, and this folding of higher frequency harmonics back onto lower ones is termed aliasing. In the present method, Aliasing problems are eliminated by always having four times the number of input data points as harmonics to be calculated.

In the case of a sawtooth waveform, the assumption of a linear variation between data points produces the exact form of the input data. Figure 5.8 illustrates the computed spectrum up to the 100^{th} harmonic produced from two input data points. Since the input data is exact, this is a good test for calculation errors. The value of the hundredth harmonic should be 40 dB lower than the fundamental. The measured result is 39.96546 dB. Thus the only errors left in the Fast Fourier Analysis method are those due to:

a) The number of input data points;

(b) the straight line approximation;

(c) Accuracy of input data points;

(d) The uneven spacing of data points.

5.7.1 Effect of number of input data points

It was felt that the most severe test for the programme would be that of a smooth, symmetrical waveform. In this way the straight line approximation is exaggerated and the uneven spacing of data on a symmetrical waveform is

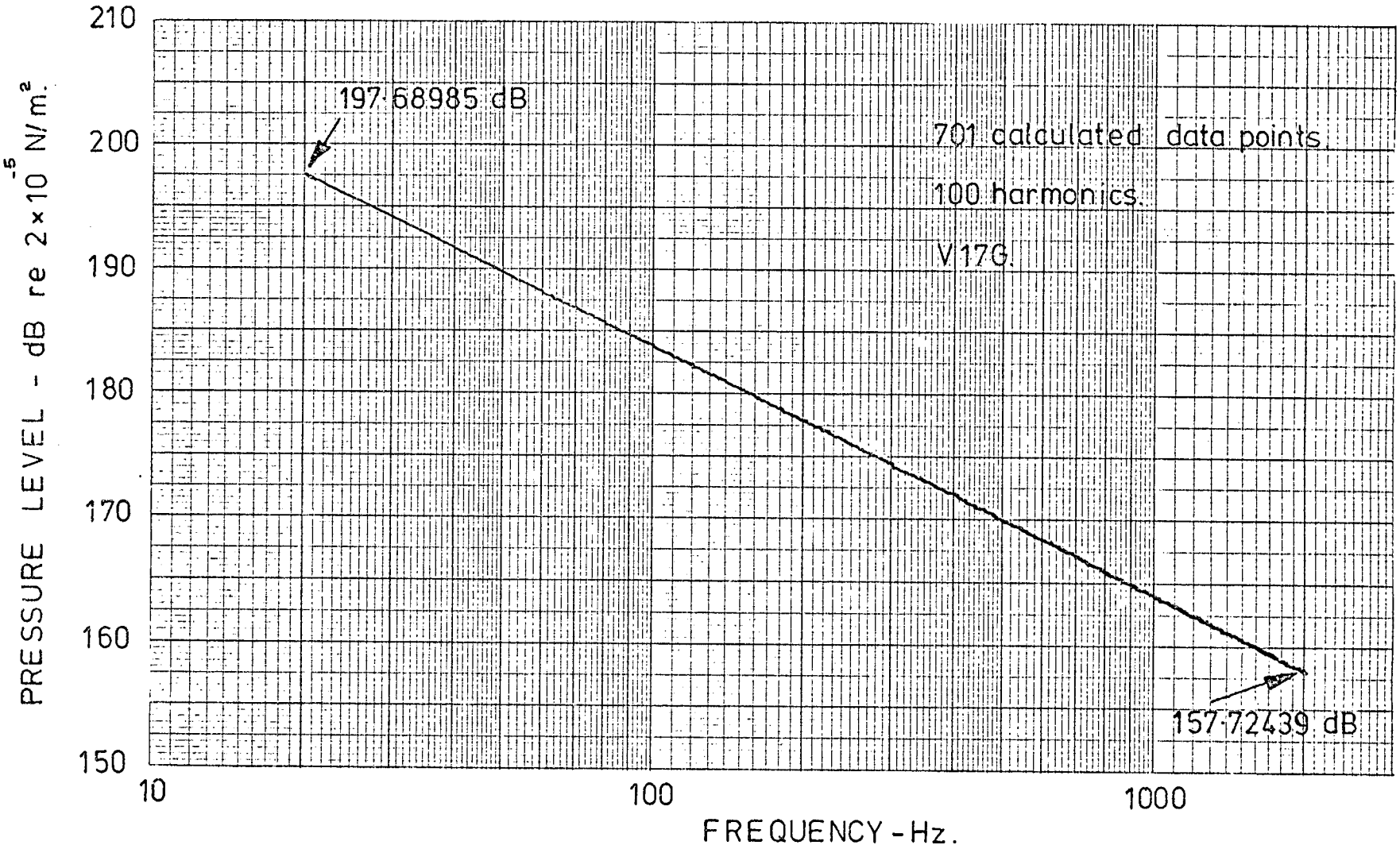

FIG. 5·8 - COMPUTED SPECTRUM FOR 100 p.s.i. SAWTOOTH WAVEFORM FROM TWO INPUT DATA POINTS.

the worst practical application. The analysis of a sine wave was therefore carried out both for the harmonic series, where only the fundamental should occur, and as a single transient, where a transform series as shown in Fig. 5.7 should result. For this purpose the transform values computed correspond to each maximum and minimum of Fig. 5.7. Fig. 5,9a shows such a computation for a 21 evenly spaced input data point sine wave representation, the period of the sine wave being assumed to be one second. The computation is taken up to 200 Hz. The important peak values follow the theoretical values very closely except at frequencies of 20, 40, 60 etc. Hz. These frequencies correspond to the harmonic numbers 20, 40, etc. and are therefore related to the number of input data points and its integer multiples. The values at the minima should be zero. Since they are generally some 60 to 100 dB below the maximum values this can be considered to be so. The fact that non zero values occur is probably due to rounding errors in the computer (5.3). Fig.5.9(b) shows a similar plot but for the case where 73 evenly spaced input data points were used. Results are only plotted to 70 Hz, but it can be seen that no appreciable increase in accuracy of maximum values has occurred, although the minimum values have been changed slightly. Most important, the obvious error occurring at 'harmonics' corresponding to multiples of the number of data input points have been changed. Thus, even a 21 point representation of a sine wave is sufficient to allow computation of at least 200 harmonics, corresponding in this transform case to 200 Hz, with errors occurring around integer multiples of the input data. Increasing the number of data points to 73 does not show a marked improvement in results but does move the error effect at integer multiples of the input data to higher harmonics.

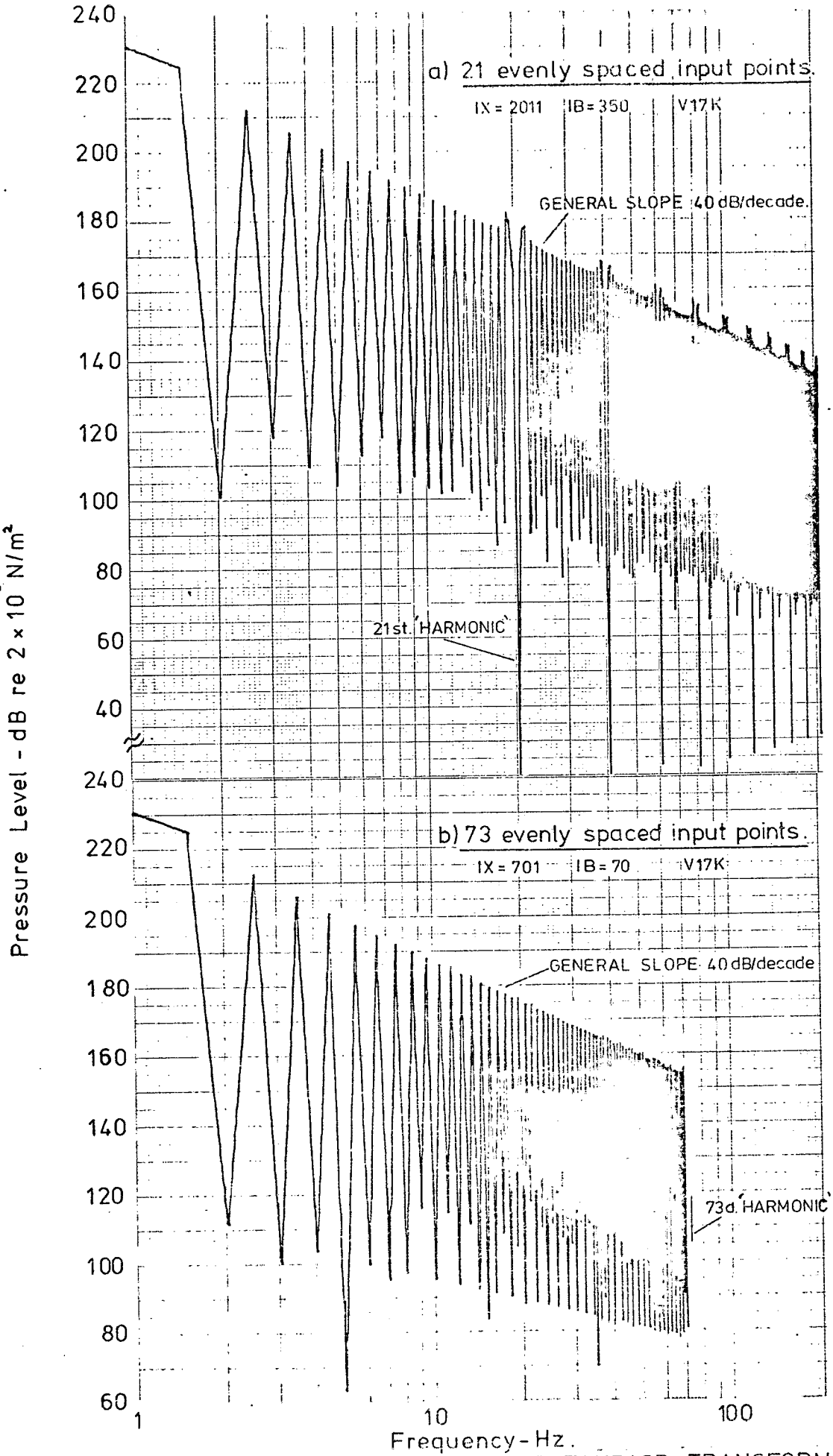

9 - EFFECT OF NUMBER OF INPUT DATA POINTS FOR FOURIER TRANSFORM OF ONE CYCLE OF 1Hz. SINE WAVE. (1000 p.s.i. peak)

5.7.2 Effect of straight line approximation

With a polynomial variation between input data points, the 21 input sine wave case was recalculated and the results are shown in Fig. 5.10. Only the maximum values are plotted. The error effect at the 'harmonic' corresponding to the number of input data points does not occur when the polynomial variation between points is used. Therefore it can be concluded that the error at integer multiples of input data is caused by the assumption of a linear variation between points. More important, it indicates that the error due to the linear variation assumption only occurs at these points and is not distributed through the spectrum. This result is amplified by calculations on a 73 even input point sine wave representation to find the Fourier series values. There should only be one value, at the fundamental frequency. Figure 5.11a shows the results. The harmonic levels above the fundamental can be considered as equivalent to electrical noise as in an electrical waveform analyser. This digital noise level is at least 110 dB lower than the fundamental value, except at harmonic values near integer multiples of the input data. Even at these points it is at least 35 dB lower. With this analogy one would only expect interference to calculated results at these points. Figure 11b shows the same computation but completed assuming a 3rd order polynomial variation between points. The general digital noise level is slightly lowered at the lower harmonic values but the error effect around multiples of the input data has vanished.

5.7.3 Effect of accuracy of input data points

The values used for the input data points for a sine wave variation were obtained from five figure logarithmic tables, and therefore represent an input dynamic range of 100 dB. The same data for a 21 even input point sine wave was reduced in accuracy to three significant figures or input dynamic range of 40 dB. A comparison of the results is shown in fig. 5.12a and b. The values at multiples of the input data remain the same but between

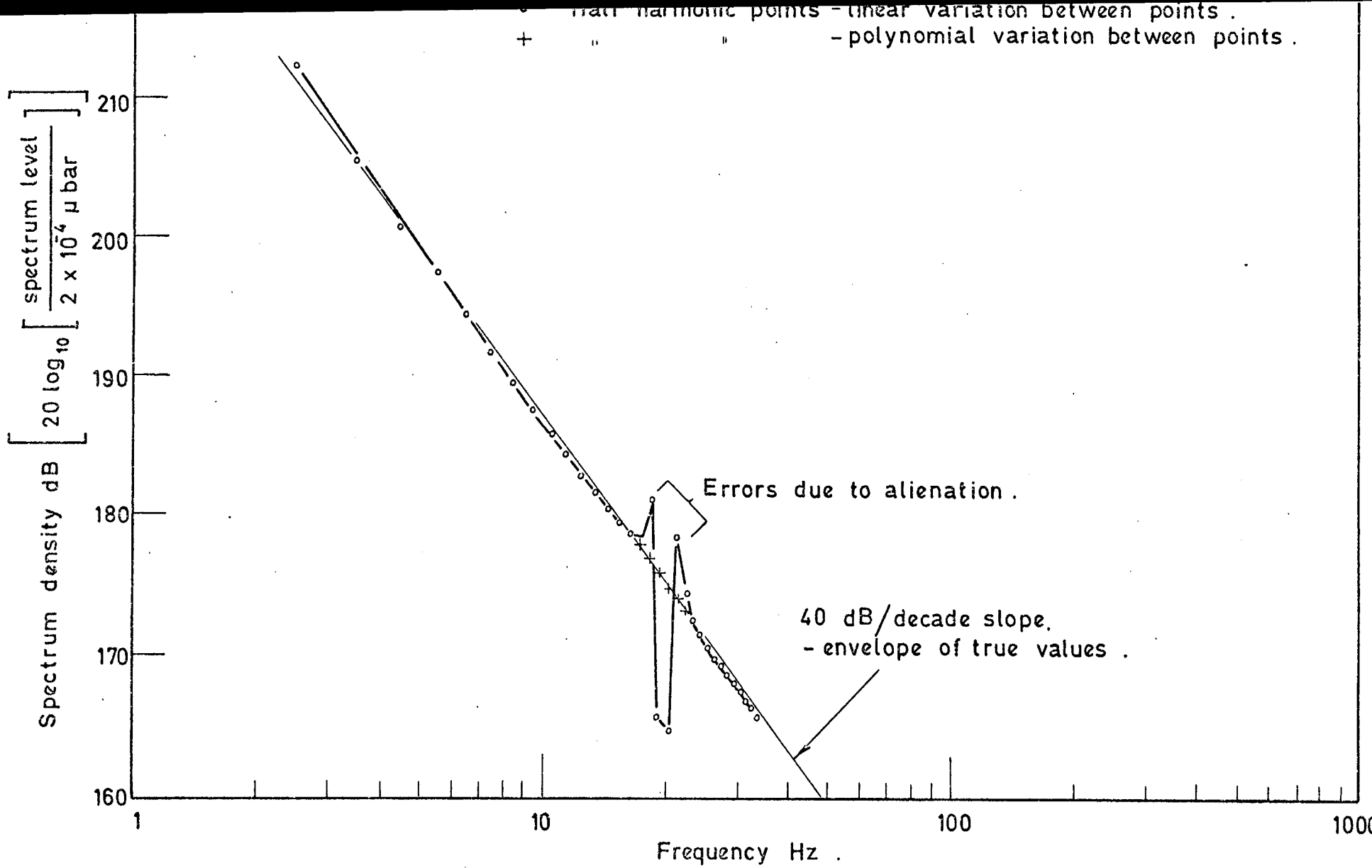

FIG. 5·10-EFFECT OF STRAIGHT LINE APPROXIMATION

('Half harmonic' points of fourier transform of a 1 c/s sinewave, amplitude 1000 p.s.i., computed from a 21 point representation).

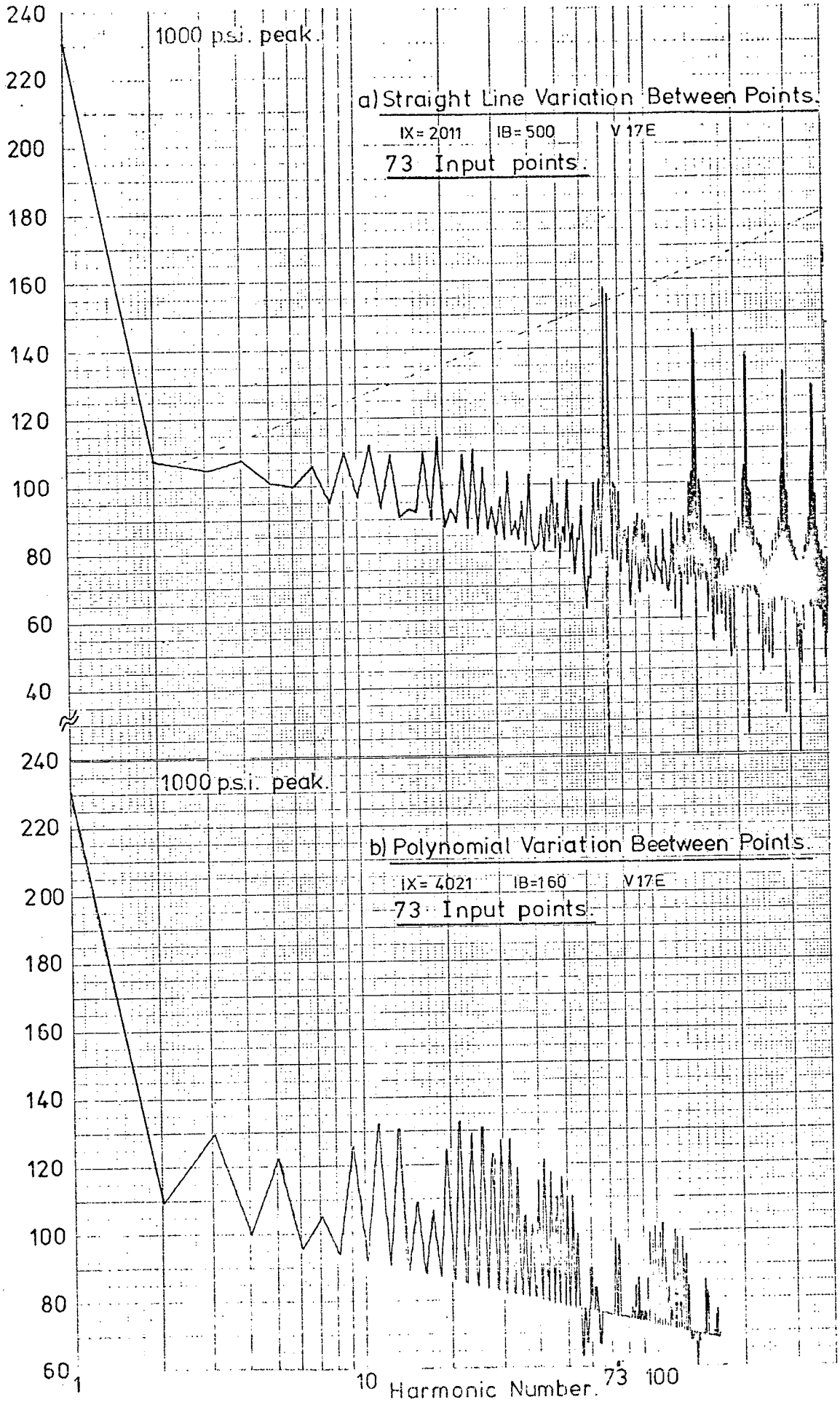

11-EFFECT OF POLYNOMIAL APPROXIMATION-FOURIER SERIES FOR 1 Hz. SINE WAVE.

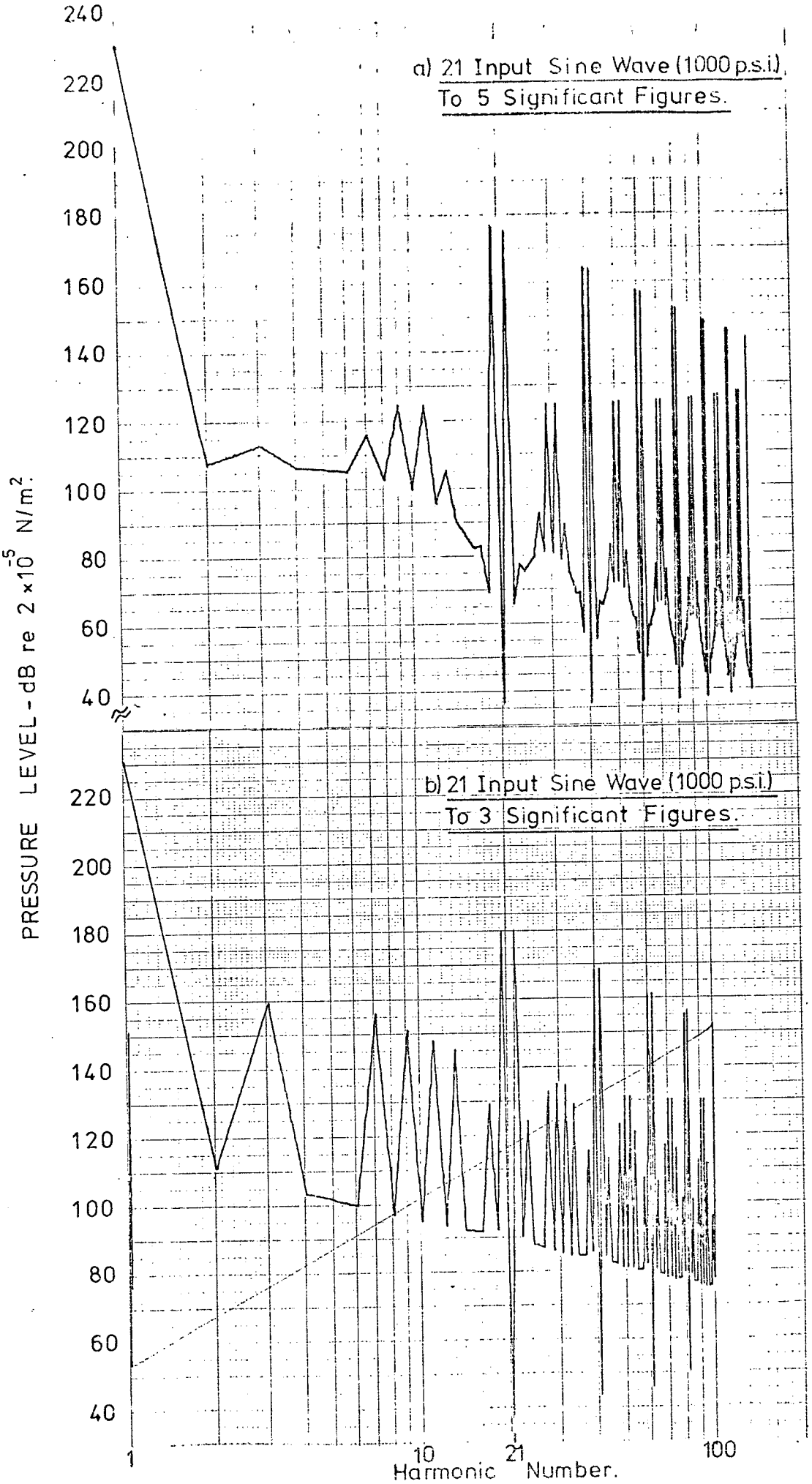

FIG. 5·12 - EFFECT OF ACCURACY OF INPUT DATA POINTS.

these values the digital noise level has increased 5 to 40 dB and the increase is spread generally through the harmonic range. Thus the effect of a lack of accuracy in the digitised pressure diagrams is similar to that of an increased noise level in an electrical waveform analyser.

5.7.4 Effect of uneven spacing of input data points

As discussed in section 5.4, unevenly spaced input data sets have been used extensively in this work. Fig. 5.13a and b shows the 'half harmonic' values of a discrete Fourier transform of a 21 point sine wave and also the same sine wave with reduced (3 significant figures) accuracy. The zero points (minima) are now grossly in error and the values of the maxima deviate to either side of the true values. Little effect can be seen from a reduced input data accuracy. Figs. 5.14a and b show a comparison for even and uneven spacing of a 73 input point sine wave representation. For uneven spacing the minimum values are changed significantly and from the 12th 'half harmonic' point there is a variation of maximum values either side of the true values. The mean error through a range of harmonics is shown in Table 5.2.

The first 20 'half harmonic' points are accurate to within $\pm$ 2%, but after this there is a developing scatter. However, very shortly the scatter settles down, the mean positive error being slightly smaller than the mean negative scatter. The maximum deviation is some $\pm$ 5 dB. If the mean error over ten half harmonic values is taken this remains constant and a maximum error of $\pm$ 1 dB results - just about measurement accuracy. Thus the mean error averaged over 10 'harmonics' does not increase with increasing harmonic number and a mean line will have values very close to the true values.

One very convenient method for performing the necessary averaging is to form a constant percentage bandwidth analysis of the computed harmonic

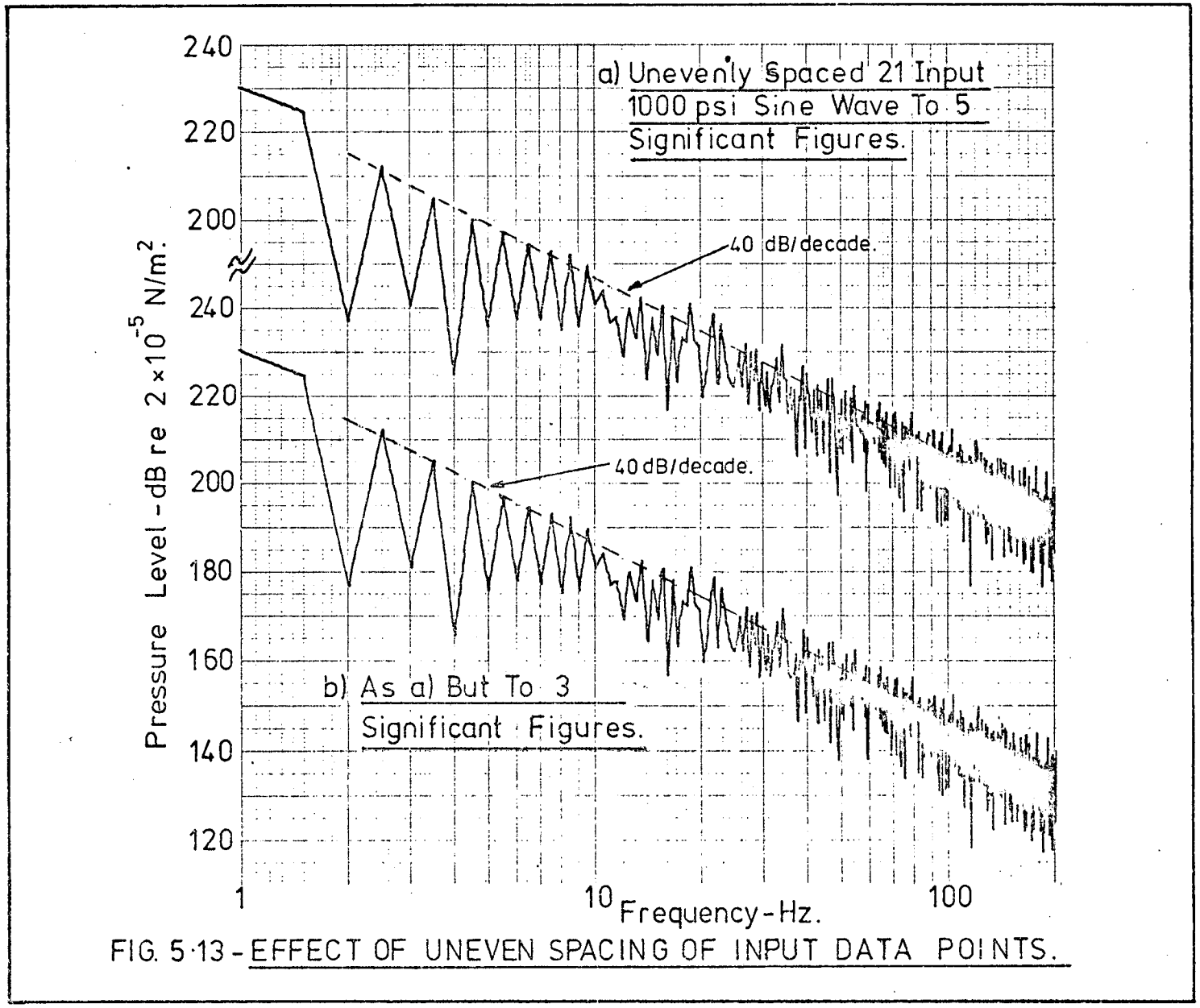

FIG. 5·13 - EFFECT OF UNEVEN SPACING OF INPUT DATA POINTS.

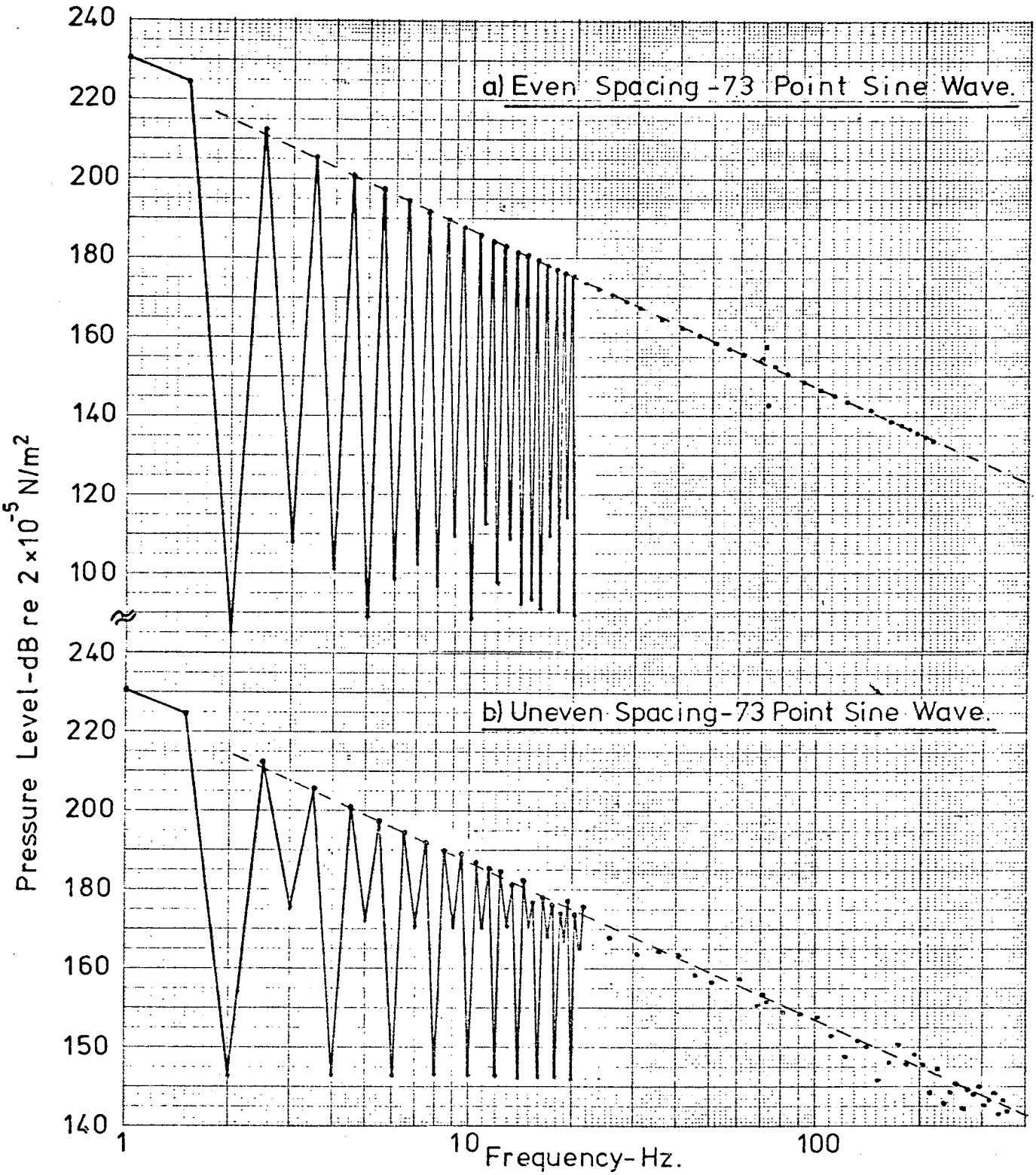

FIG. 5·14 - EFFECT OF UNEVEN SPACING OF INPUT DATA POINTS.

Table 5.2 Mean Error from True Maximum Values due to Uneven Data Point Spacing.

Half Harmonic Range	Maximum Positive Error dB	Maximum Negative Error dB	Maximum Scatter dB	Mean Error dB
0 - 12.5	0.8	0.5	1.30	+0.036
12.5 - 22.5	2.1	3.1	5.20	-0.340
22.5 - 32.5	2.4	3.9	6.30	+0.010
32.5 - 42.5	1.6	0.5	2.10	+0.470
42.5 - 52.5	3.1	5.2	8.30	-0.890
230.5 - 240.5	3.1	6.5	9.60	- 0.445
240.5 - 250.5	3.25	6.3	9.55	-0.085
250.5 - 260.5	1.7	5.6	7.30	-1.050
260.5 - 270.5	5.5	6.2	11.70	+0.675
225.5 - 235.5	2.7	4.0	6.7	-0.790
235.5 - 245.5	5.0	4.5	9.5	-0.370
245.5 - 250.5	2.4	1.3	3.7	+0.380

spectrum, since this is the process used in live analysis. Fig. 5.15 compares the measured cylinder pressure spectrum (1.5% bandwidth corrected) with the spectrum computed from a single cylinder pressure development. The computed results are in the form of the harmonic analysis, a 6% constant bandwidth (bandwidth corrected) and 16% constant bandwidth (bandwidth corrected) analysis. There is little difference between harmonic spectrum and the 6% analysis. However, the 16% analysis compares very favourably with the measured results.

Since the 1/3 octave band analysis has a bandwidth of 22% and is in common use, then in later work reported in this thesis the computed 1/3 octave band spectrum has been used to compare with measured results when an uneven data input set has been used. This process has the added advantage that the spectra can be compared easily. Comparison of 1/3 octave band computed data has also been used for evenly spaced input data sets where there is no such error.

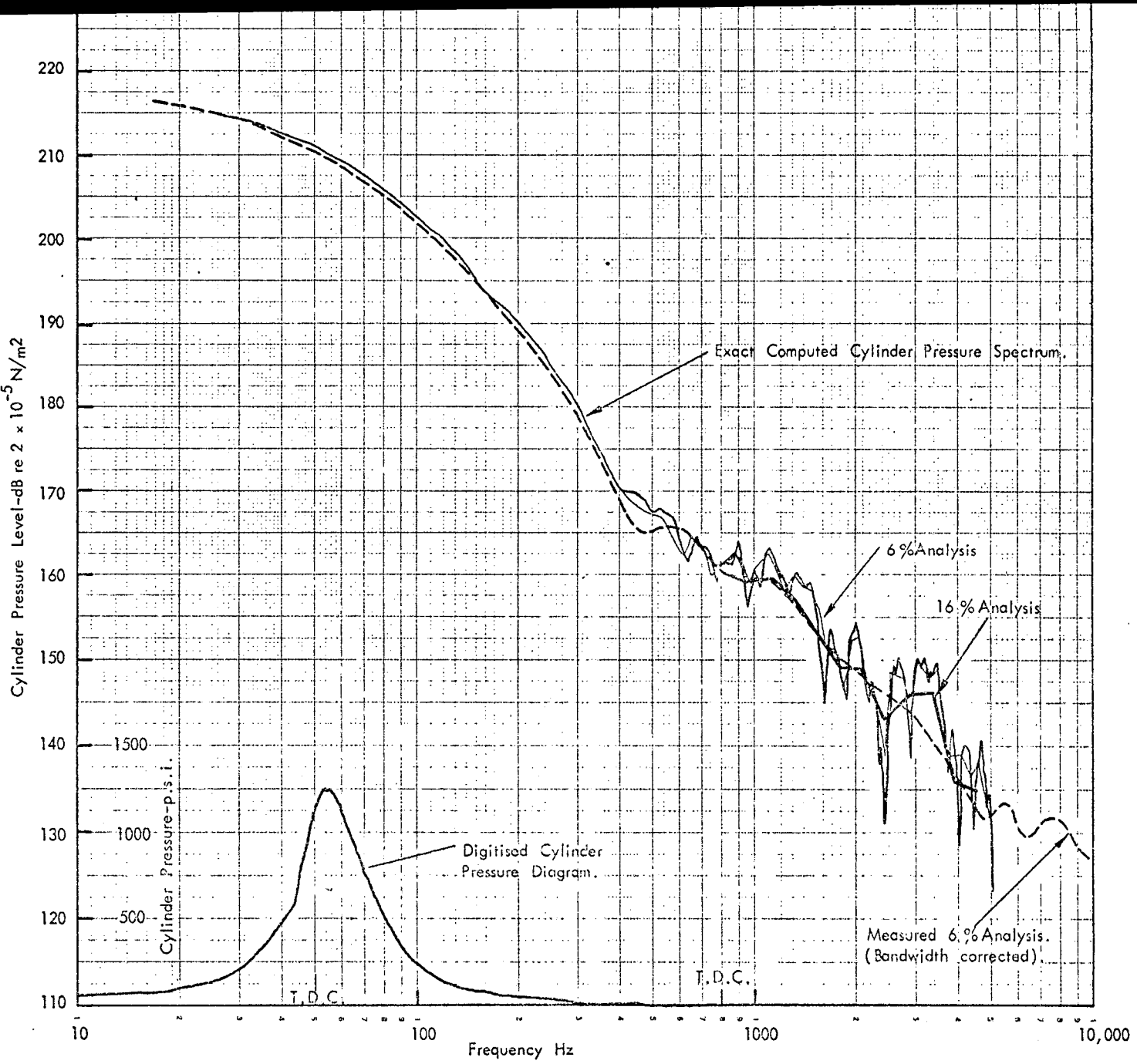

FIG. 5.15. COMPARISON OF VARIOUS ANALYSIS BANDWIDTHS FOR COMPUTED CYLINDER PRESSURE SPECTRA WITH MEASURED 6 % ANALYSIS.

5.8 Conclusions

It has been shown that if the Fast Fourier Analysis method is used with accurate (at least 60 dB dynamic range) input data, evenly spaced and with at least four times the number of data points as the required harmonic range then very accurate harmonic values can be computed up to any harmonic number. For harmonic numbers up to 2000 the programme time required is not ecessive.

The required input data for these calculations to be exact up to high harmonic numbers can only be obtained by the use of very fast analogue to digital converters. The digitising rate must be 40 kHz (25.0 μsec/point) and the equivalent dynamic range must be at least 60 dB. The required rate of digitisation is the same for two and four stroke cycles for all operating speeds (Table 5.1).

If this type of equipment is not available then results giving the spectrum maxima to an accuracy of ± 1 dB can be obtained from hand digitised data (equivalent input dynamic range 40 dB) using unevenly spaced data points and the assumption of a linear variation between points. A more sophisticated type of X-Y plotter (Benson-Lehner) with which hand digitised versions of photographically reproduced traces to an accuracy of one part in 3000 (69.5 dB dynamic range) has been used to give very satisfactory results for the special application of cylinder pressure spectrum computations. In general, therefore, the accuracy of the computed results depends on

(a) the degree of accuracy of the actual discrete data points

(b) the stationarity or cycle to cycle variation of the cylinder pressure diagram in question.

Figure 5.16 shows a typical comparison of measured and computed spectra using 189 and 203 unevenly spaced data points with a 1:999 digital accuracy for both X and Y coordinates.

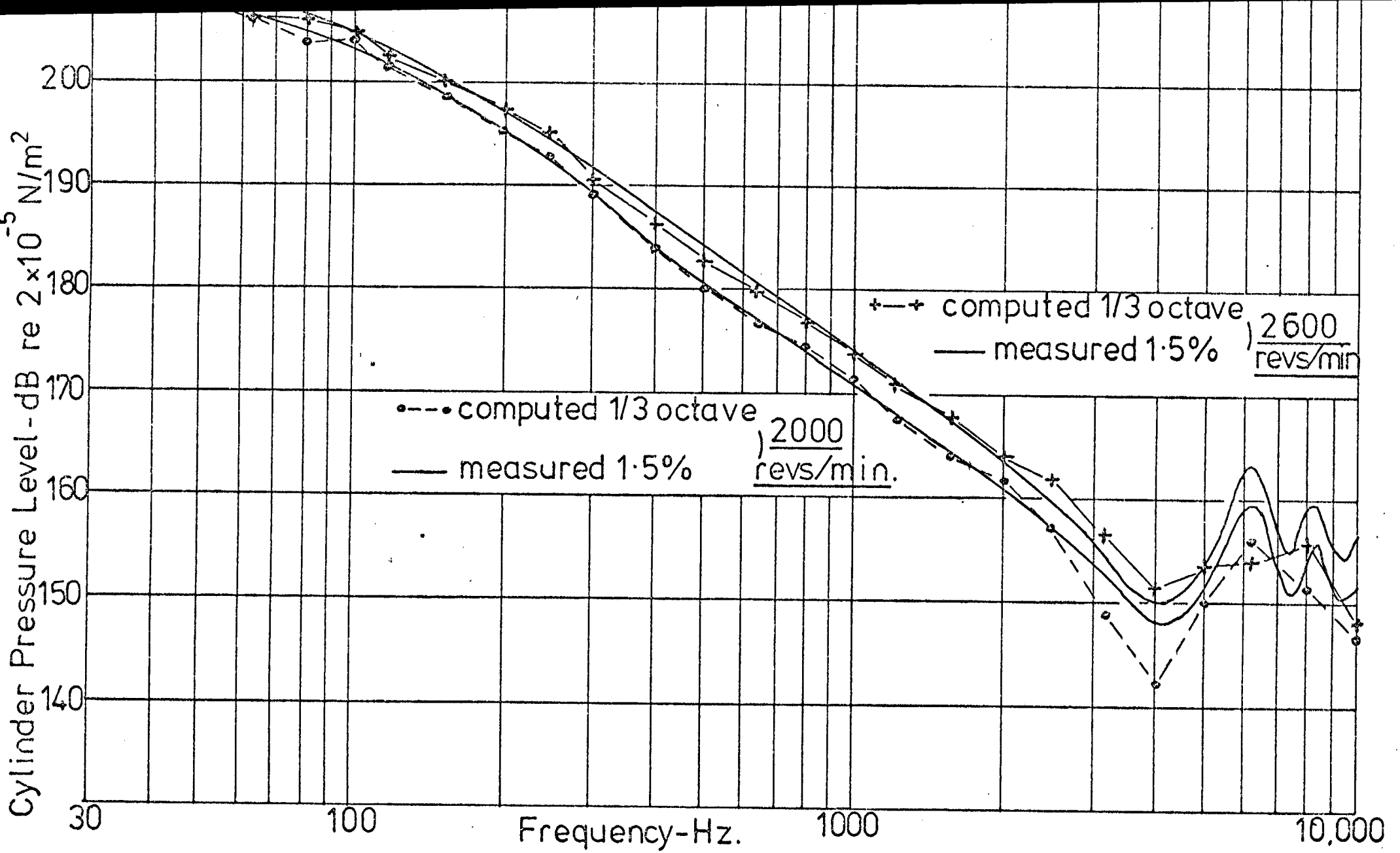

Fig. 5·16 - Example Of Computed and Measured Cylinder Pressure Spectra.

References

5.1 R.G. Manley 'Waveform Analysis' Chapman and Hall Ltd., 1950.

5.2 Lewis 'A Method of Harmonic Analysis' Trans. Amer. Soc. Mech. E., 1935, p.A137.

5.3 Reference to rounding errors in computers.

6.0 COMBUSTION INDUCED NOISE IN INTERNAL COMBUSTION ENGINES

The characteristic noise of diesel combustion is generally known as 'diesel knock' which distinguishes it from the smoother combustion of the spark ignition gasoline engine. Even for the gasoline engine well known terminology is ascribed to the noise produced by abnormal combustion processes such as 'pinking' (detonation noise). At the same time noises of mechanical origin can also be recognised such as 'piston slap', gear noise, tappet noise and bearing noise.

The forces producing these distinctive noises are of widely different character and require some classification. The gas force resulting from combustion can be assumed to be the direct exciting force of the engine. There are many indirect forces (causing some of the so called mechanical noises) which are dependent on the direct exciting force in some non-linear manner such as the forces producing piston impacts, impacts in bearings and timing gears. There are also secondary forces producing mechanical noise which are not related to the direct forces such as in the valve gear and fuel injection system.

Of all these exciting forces, the dominant one for the automotive diesel engine in its present form is that of the direct exciting force due to combustion. The work of Priede (6.1) has shown that when combustion controls noise wholly, then, in a given frequency band, there is a linear relationship between the cylinder pressure spectrum level and the noise level. The work of Priede (6.1), Austin and Priede (6.2) and Grover, Lalor, Priede and Anderton (6.3) and Anderton (6.4) has enabled the formulation of a combustion induced noise model which provides the basis for comparisons of internal combustion engines running with different operating cycles.

6.1 Combustion Noise Model

Comparison of the noise of two engines, both of equal power, and running at the same speed, tested at the ISVR showed a marked difference in overall noise level of 4 dBA. Examination of results from the ISVR 'Banger Rig' where an oxygen/propane mixture could be exploded in a non-running in-line engine (6.5 and 6.6) showed that substitution of a rubber strip for the normal shell big end bearing on the cylinder tested reduced the level of high frequency vibration substantially. This is shown in Figure 6.1 where even the vibration levels at the top of the engine block are reduced.

The conclusion is that most of the vibrational energy from combustion enters the in-line engine structure via the big end and main bearings. It is thus clear that the engine vibration (and hence noise) is dependent on the force input to these bearings, which is a combination of the forces of combustion and inertia. In the diesel engine combustion forces are greater than inertia and thus the peak force input to the bearing is dependent on engine bore. This was the major difference between the two engines tested.

The results of Chan (6.7) have shown that up to the force levels obtainable from electromagnetic shakers the variation of engine surface vibration and resultant noise with force input at the big end bearings are linear, as shown in Figure 6.2a and 6.2b.

The exciting force of combustion is applied to this linear system via the piston crown and then to the main bearings, causing deflections in the structure which will depend on the angular position of the connecting rod/crank mechanism. This resultant surface deflection will cause noise to be radiated. If only one side of the engine is considered then the noise can be considered to be radiated in a similar manner to that of a simple piston-in-baffle (6.8).

The mechanical impedance, Z, of the engine structure is defined as force divided by velocity. Thus, the structure surface velocity $V(\omega)$ at frequency ω:

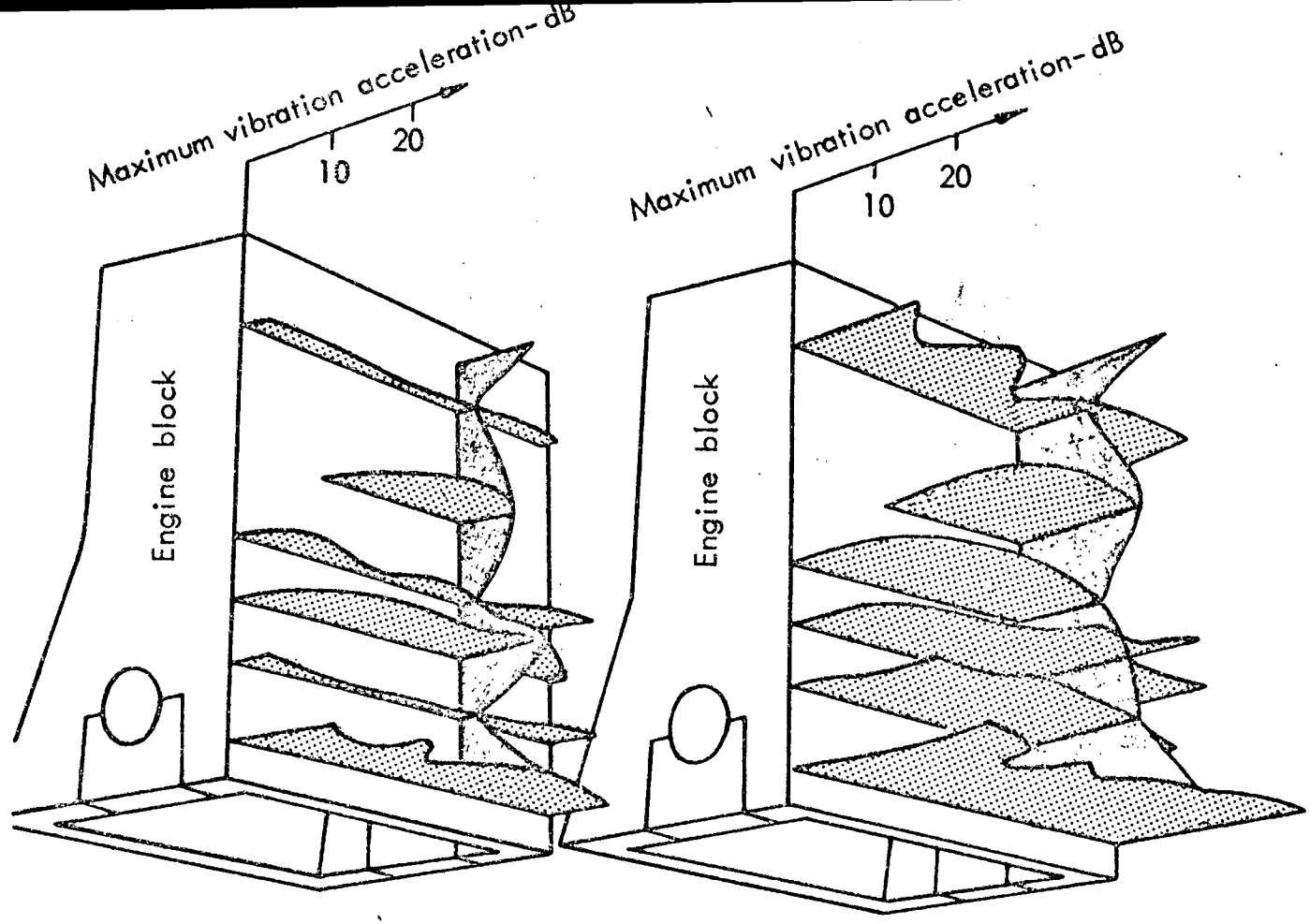

a) Structure response with rubber isolated big end bearing

b) Structure response with standard big end bearing

FIG. 6·1-STRUCTURE RESPONSE TO ONE FIRING OF ONE CYLINDER IN IN-LINE ENGINE

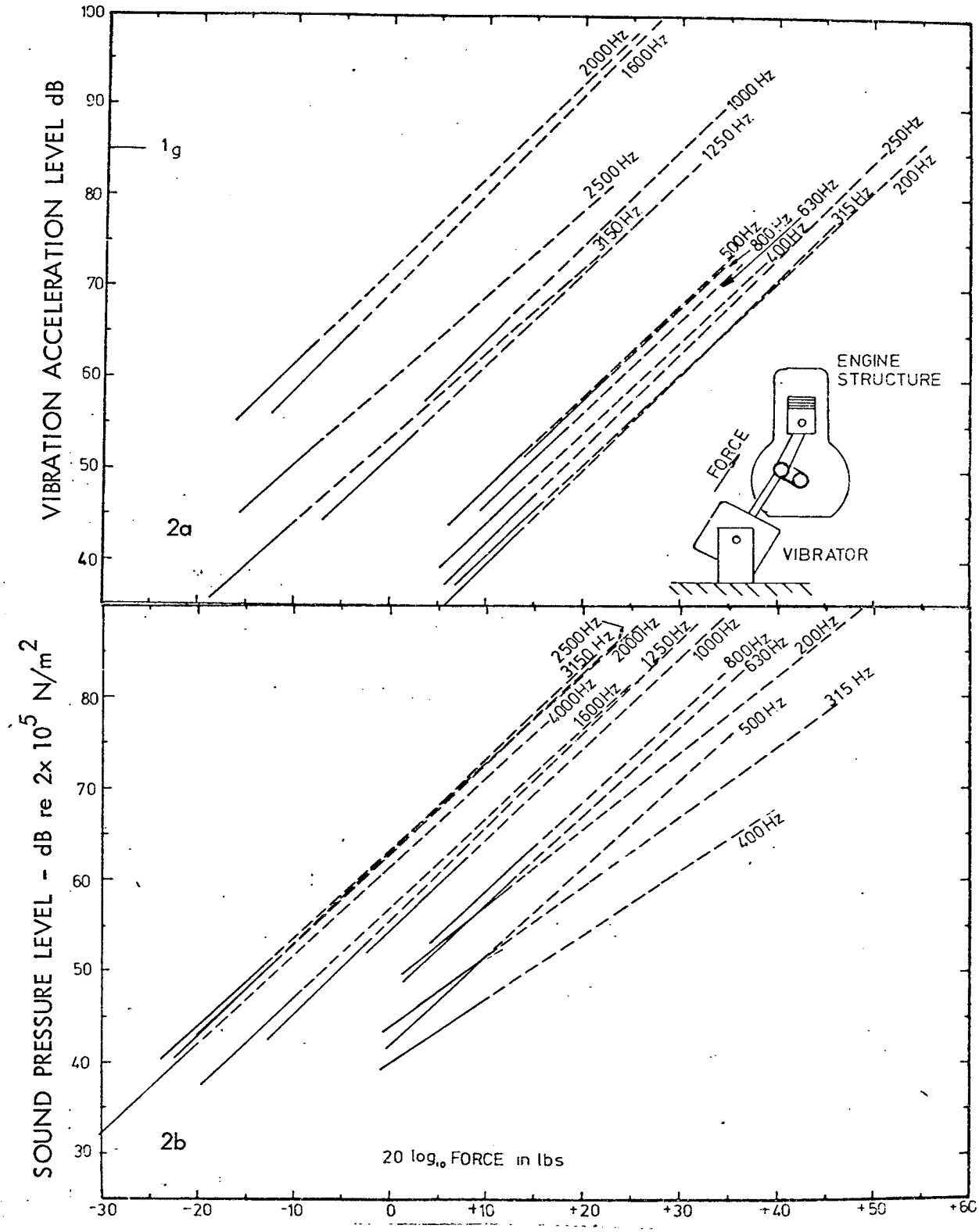

FIG. 6·2-(a&b) VARIATION OF NOISE AND VIBRATION OF AN ENGINE WITH A FORCE INPUT FROM A VIBRATOR.

$$V(\omega) = \frac{\text{force}}{Z(\omega)} \propto \frac{\text{cylinder pressure } (\omega) \text{ x } (\text{bore})^2}{Z(\omega)} \qquad (6.1)$$

and for acoustic radiation from a piston-in-baffle the noise intensity I at a given distance r is given by (6.8)

$$I(\omega) = \frac{\rho_o c k^2 V_o^2 (\pi a^2)^2}{8\pi^2 r^2} \left| \frac{2J_1(ka \sin\theta)}{ka \sin\theta} \right| \qquad (6.2)$$

where r = distance from piston

$\rho_o c$ = specific acoustic impedance

θ = angle at which noise radiated

a = piston area

k = wavelength constant = ω/c

J_1 = a Bessel function derived in reference 6.8

V_o = piston velocity

c = speed of sound in air.

In this case there is a complex directivity pattern. In practice, Chan and Anderton (6.9) have shown that the noise radiation from I.C. engines tends to have little directivity. In such a case the simple equations relating overall sound power radiated by a structure can be utilised. In anechoic conditions the acoustic power radiated $W(\omega)$:

$$W_{rad}(\omega) = \rho.c\ S_{rad}\sigma_{rad}(\omega)\ \langle U_o^2(\omega)\rangle \qquad (6.3)$$

S_{rad} = total area of radiating surface

σ_{rad} = radiation ratio

$\langle U_o \rangle$ = area average of the mean square velocity over the entire radiating area

f = frequency

Assuming that the engine tends to be non-directional the sound pressure level, p, measured 1 metre away from the engine can then be related to the acoustic power:

$$W_{ac}(\omega) = \frac{p^2(\omega)}{\rho c} \cdot S_{trav} \qquad (6.4)$$

where S_{trav} = surface area of measuring sphere. Hence the square of the sound pressure radiated at frequency w:

$$p^2(\omega) = (\rho c)^2 . \langle U_o^2(\omega) \rangle . \frac{S_{rad}}{S_{trav}} . \sigma_{rad}(f) \qquad (6.5)$$

and noise intensity $I(\omega)$.

$$I(\omega) = (\frac{\rho c}{2}) . \langle U_o^2(\omega) \rangle . \frac{S_{rad}}{S_{trav}} . \sigma_{rad}(\omega) \qquad (6.6)$$

Thus $$I(\omega) \propto \frac{S_{rad}}{S_{trav}} . \sigma_{rad}(\omega) \langle U_o^2(\omega) \rangle \qquad (6.7)$$

The noise radiated is dependent on the force input to the structure, the mechanical impedance of the structure, the area ratio, the acoustic radiation ratio and the average mean square surface vibration.

Combining equations (6.1) and (6.7), the noise intensity becomes:

$$I(\omega) \propto \frac{S_{rad}}{S_{trav}} . \sigma_{rad}(\omega) . (\frac{\text{cylinder pressure } (\omega) \text{ x } (\text{bore})^2}{Z(\omega)})^2 \qquad (6.8)$$

Fig. 6.3b shows a typical diesel engine cylinder pressure spectrum, obtained by electrical frequency analysis from the cylinder pressure development (Fig. 6.3a). The value of pressure at any frequency depends on engine speed and the average slope n (dB/decade) of the spectrum, or

$$(\text{cylinder pressure } (\omega))^2 \propto |\frac{\text{Engine speed N}}{\omega}|^n \qquad (6.9)$$

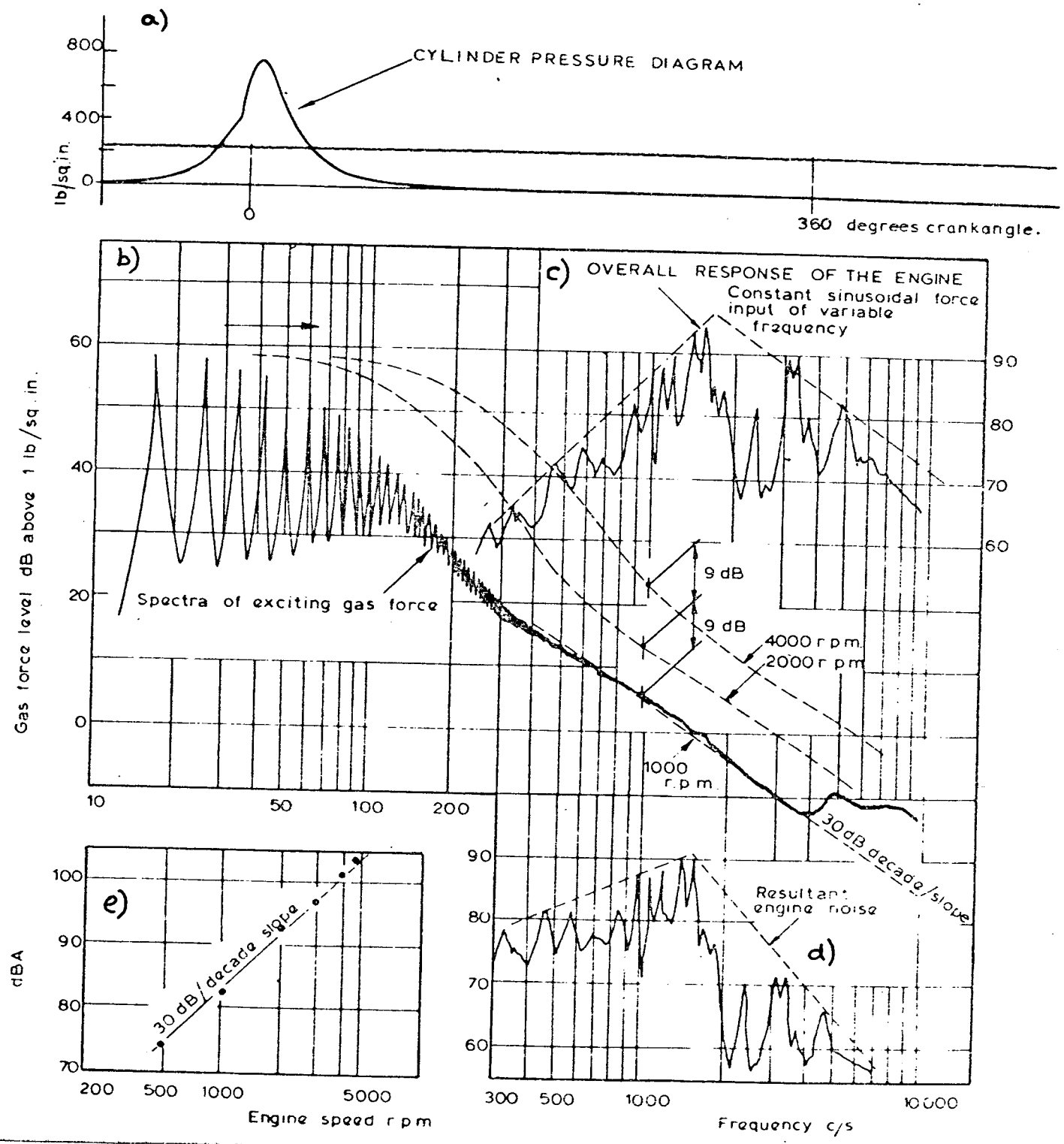

FIG. 6·3 - MECHANISM OF COMBUSTION NOISE SHOWING SPEED EFFECT.

Thus the average mean square surface vibration becomes:

$$\langle U_o^2 \rangle \propto \left| \left(\frac{N}{\omega}\right)^n . \frac{B^4}{Z^2(\omega)} \right| \qquad (6.10)$$

and therefore the resultant noise intensity $I(\omega)$; at frequency ω is given by

$$I(\omega) \quad \frac{S_{rad}}{S_{trav}} . \sigma_{rad}(\omega) . \left(\frac{N}{\omega}\right)^n . \frac{B^4}{Z^2(\omega)} \qquad (6.11)$$

If it is supposed that each frequency (Harmonic) is unaffected by its neighbour (low damping), then the principle of superposition can be used to find the overall noise intensity by summation over the audio frequency range:

$$\text{Overall noise intensity } I_o \propto \sum_{\omega=0}^{\omega=\omega_{max}} \left(\frac{S_{rad}}{S_{trav}} . \sigma_{rad}(\omega) \left(\frac{N}{\omega}\right)^n . \frac{B^4}{Z^2(\omega)} \right)$$

Therefore,

$$I_o \propto \frac{S_{rad}}{S_{trav}} . N^n B^4 \sum_{\omega=0}^{\omega=\omega_{max}} \frac{1}{\omega} . \frac{\sigma_{rad}(\omega)}{Z^2(\omega)} \qquad (6.12)$$

or

$$I_o \propto N^n . B^4 . \frac{S_{rad}}{S_{trav}} . C_{A.S.O} \qquad (6.13)$$

where C_{ASO} is the overall combined acoustical and structural factor.

A combined acoustic and structural factor $C_{AS(\omega)}$ is implied where

$$C_{AS}(\omega) = \frac{\sigma_{rad}(\omega)}{\omega Z^2(\omega)} \qquad (6.14)$$

which relates the noise produced by the structure per unit force input.

The mechanism of combustion induced noise can therefore be described in measured terms, as shown in Fig. 6.3. The force is the cylinder pressure development, as shown in Fig. 6.3a. In this example the rapid rise due to combustion occurs some 10^o b.t.d.c. Since this force time diagram is

repetitive, its exciting propensities can be fully described by a Fourier series. In the low frequency range the individual harmonics can be clearly distinguished; the level being primarily determined by the peak pressure. With increasing frequency, the individual harmonics can no longer be resolved and a spectrum of high density is obtained in the high frequency range. The level of these high frequency harmonics is determined by the actual form of the cylinder pressure diagram. The amplitude of harmonics shows a general decay at the rate of some 30 dB per tenfold increase of frequency.

The engine structure response, in terms of noise emitted by the engine structure (engine of automotive size) when subjected to a constant sinusoidal force input of varying frequency is shown in Fig. 6.3c. The maximum response is in the frequency range between 1,000 and 2000 Hz, which is typical for a machine employing a rigid cast iron structure (the maximum response of engines of larger size is in a somewhat lower frequency range).

As can be seen, the ratio of the frequency of maximum response to the repetition frequency of the force is of the order 50 to 100:1 and the relevant part of the force spectrum which is responsible for the predominant noise has a high density. The resultant spectrum of this diesel engine noise is shown in Fig. 6.3d, which is determined by both the characteristics of force and the characteristics of the structure.

It is of interest now to consider the effect of engine speed. Generally, the cylinder pressure diagram remains more or less constant when considered on the basis of degree of crankshaft rotation. Therefore, the force spectra at higher speeds will be geometrically similar, but with a shift parallel to the frequency axis corresponding to the change in speed (6.10). Because of this, the actual increase of the level of the gas force, and thus the engine noise, will depend on the general slope of the cylinder pressure force spectrum. For example, in this case the slope is 30 dB/decade and therefore

a 30 dB increase of noise with a tenfold increase of engine speed (or 9 dB for a two fold increase) can be expected. This is confirmed in fig. 6.3e, where measured overall sound pressure levels (dBA) of the engine are plotted versus the logarithm of the engine speed.

Thus it can be concluded that the form of the cylinder pressure diagram, as determined by the combustion process, is the primary factor which controls the rate of increase of combustion noise with engine speed.

If the combined acoustic and structural characteristics of engine structures are separated, then the basic mechanism of combustion noise generation can be amplified. The acoustic radiation ratio $\sigma_{rad}(\omega)$ describes the ability of the structure to radiated noise and the engine structure response $1/Z^2(\omega)$ describes the ability of the structure to withstand loading. Chan (6.11) has investigated the radiation ratio and structure response of in-line diesel engines. He finds that the radiation ratio tends to be of constant value above 400 Hz for engines in the automotive size range, and that the value does not depend on engine size, whereas the engine structure factor does depend on engine size, particularly in the frequency range 400-1000 Hz.

The mechanism of combustion induced noise is therefore the application of the cylinder pressure (figure 6.4a and 6.4b) to the engine structure causing deflections of the structure which can be expressed as structural velocity if the structure mechanical impedance or admittance is known (figure 6.4c, 6.4d). In a similar manner the resultant noise caused by the structural deflections (expressed as velocity) is specified by the radiation ratio (figure 6.4e, 6.4f) or acoustic radiation properties of the structure. Thus, if the cylinder pressure exciting force spectrum, the engine mechanical impedance and the acoustic radiation ratio are known, the engine noise can be specified. The general slope of the cylinder pressure spectrum has been found to be 30 dB/decade for four stroke normally aspirated diesels, 40 dB/

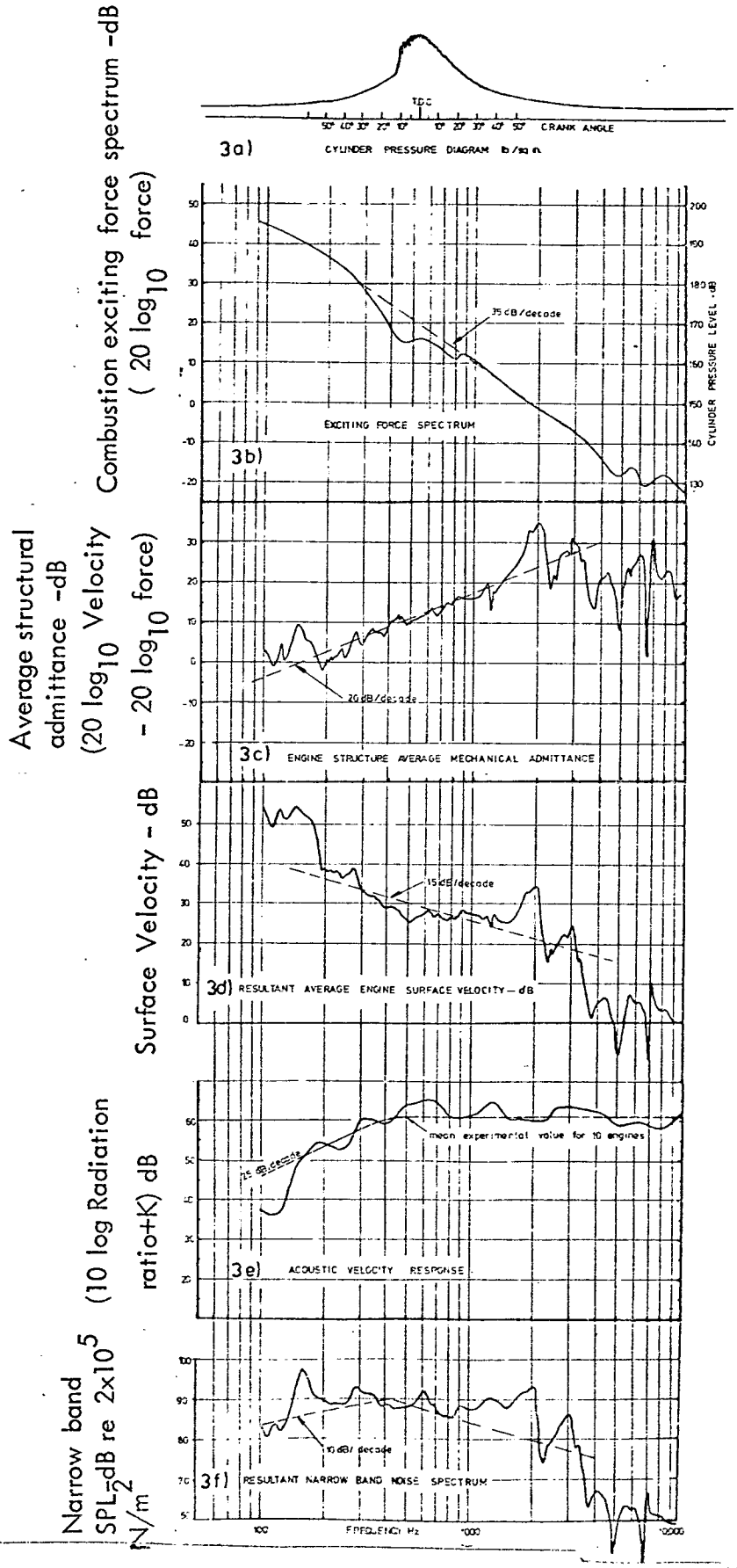

FIG. 6·4 - DETAIL MECHANISM OF COMBUSTION INDUCED NOISE.

decade for two stroke and turbocharged four stroke cycle diesels and 50 dB/decade for gasoline engines. The structural impedance of an engine structure is dependent on engine stiffness, mass and damping. The radiation ratio is dependent on engine detail vibration variation but appears to be constant above 400 Hz for automotive engines.

6.1.1 Effect of number of cylinders

The side area of the engine can be more closely equated to

$$S \propto (n \times B \times L) \tag{6.15}$$

where n = number of cylinders

B = engine bore

L = engine height

Thus the increase of noise with number of cylinders for engines of similar bore and stroke will be as shown in Table 6.1, where a substantial effect is only seen for engines with less than three cylinders.

Table 6.1

Effect of Number of Cylinders on Engine Noise

No. of cylinders	Overall Noise Reduction Compared to 6 cylinder in-line engine - dBA
1 in-line	8.0
2 in-line	5.0
3 in-line	3.0
4 in-line	2.0
5 in-line	1.0
6 in-line	0.0
8 vee	2.0

6.2 General Relations Between Engine Design Variables and Combustion Noise

Noise investigations show that the detail characteristics of noise spectra of automotive engines are closely related to the modes of vibration which are dictated by the particular form of the engine design. The overall noise level in dBA, however, does not appear to be influenced to any great extent by these differences, but depends largely on cylinder bore and rated speed. This is illustrated by Figs. 6.5a and 6.5b, which shows the noise spectra of three different engines running at the same speed and each having the same cylinder bore. Despite considerable differences in design, the overall noise levels of all three are within 1 dBA of 103 dBA.

Fig. 6.5a shows the noise spectra of a four- and a six-cylinder in-line engine. The six-cylinder engine has two pronounced noise peaks: a low frequency peak around 315 Hz due to the fundamental horizontal bending mode and another peak at around 1000 Hz due to its first overtone. Due to its shorter length, the four-cylinder engine has the two equivalent noise peaks at 800 and 1600 Hz. It may, therefore be concluded that two more cylinders can be added to the engine without an increase of overall noise level.

Fig. 6.5b shows the spectra of noise of the six-cylinder engine compared with a V8 engine of the same bore running at the same speed. There are significant differences in the characteristics of noise, but the overall levels of noise again are the same, namely 103.5 dBA, showing that still another two cylinders can be added to the engine without an increase of noise.

In Fig. 6.5c, the noise spectra of three six-cylinder in-line engines produced by different manufacturers are shown. As can be seen, the relevant design details influence the characteristics of noise, but the overall noise levels again remain within 1 dBA.

Fig. 6.5d shows the noise spectra of two V8 engines of the same cylinder capacity but of different stroke/bore ratio compared when running at the same

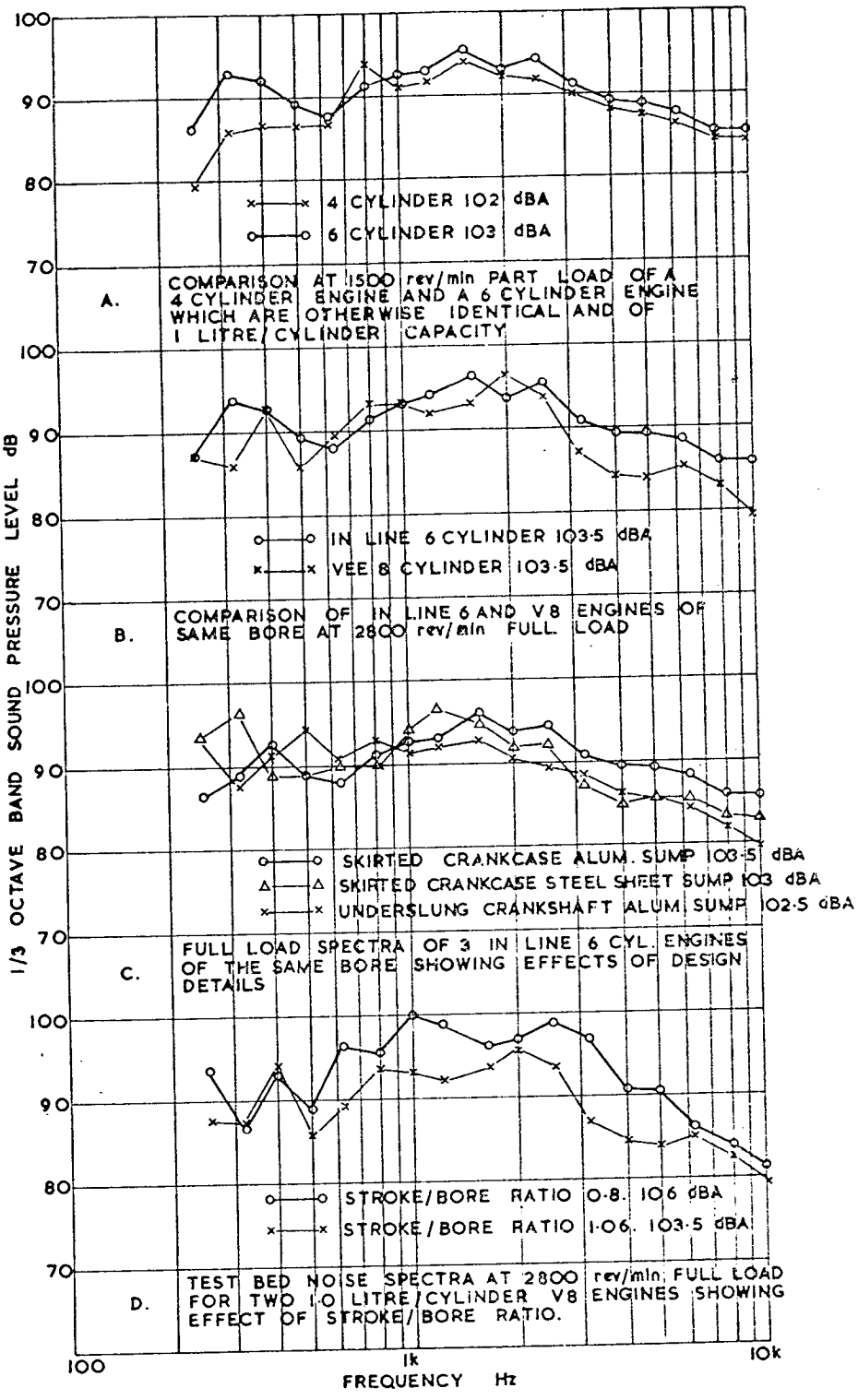

Fig.6·5 COMPARISON OF NOISE SPECTRA FOR VARIOUS TYPES OF ENGINES.

speed. A considerably greater overall level of noise is measured from the larger bore engine which corresponds directly to the larger total gas force applied to the pistons.

Thus it can be concluded for conventional design diesel engines that the overall combined acoustic and structural factor does not vary greatly, and therefore to a first approximation the overall combustion noise intensity, I_o:

$$I_o \propto N^{n_B 4} \frac{S_{rad}}{S_{trav}} \cdot C_{A.S.O.}$$

can be expressed as

$$I_o \propto N^{n_B 4} \frac{S_{rad}}{S_{trav}} \qquad (6.16)$$

6.2.1 First empirically derived relations (1969)

Using this approach an empirical formula was found which related noise intensity to bore and engine speed, the size effect $(\frac{S_{rad}}{S_{trav}})$ being at that stage included in the empirically found constant, ref. (6.3). For contemporary engines, unless the engine structure design is radically changed (e.g. ISVR crankframe engine) and assuming that the cylinder pressure spectrum level is constant at rated speed for all engines, it was found that the overall noise intensity, I_o

$$I_o \propto N^{n_B 5} \qquad (6.17)$$

and three general relationships for predicting the overall diesel engine noise at rated speed due to combustion, in dBA at 1 metre distance and depending on the form of combustion, were formulated:

(a) Four stroke normally aspirated diesel engine

$$dBA = 30 \log_{10} N + 50 \log_{10} B - 31.5 \text{ dB}$$

(b) Four stroke turbocharged diesel engine

$$dBA = 40 \log_{10} N + 50 \log_{10} B - 66.5 \text{ dB} \qquad (6.18)$$

(c) Two stroke diesel engines

$$dBA = 40 \log_{10} N + 50 \log_{10} B - 54.5 \text{ dB}$$

where N = engine revs/min

B = bore in inches.

Table 6.2 shows a comparison between predicted and measured results for a range of engines, the agreement generally being between $\pm$ 2 dBA.

It is clear from the relationship given that the noise produced by an engine is independent of the power produced, and Fig. 6.6 shows the similarity in noise levels for a range of engine volumes from 0.375 to 30 litres/cylinder. The reason for this has been shown by computing the power output of an engine cylinder from the Fourier series representations of cylinder pressure and piston motion. It was found that the first two harmonics accounted for 99 percent of the power produced (see section 7.3). Since the harmonics which control noise are those largely above the 25th, then the low-frequency components of the cylinder pressure spectrum control power, while the high-frequency components control noise.

6.2.2 Modification of original relations to include the effect of radiating area

The extremely good results provided by the empirical relations (6.18) indicated that the approach taken was a realistic one. Even so, discrepancies were found. These were mostly for very small high speed indirect injection diesels and very large bore diesels - those at the extreme ends of the range tested.

From the work of Chan and Anderton (6.9) and Chan (6.11) the effect of the engine surface area was established and Chan (6.11) showed that the area ratio term in equation (6.16) was

$$\frac{S_{rad.}}{S_{trav}} \propto B^2 \qquad B = \text{bore size} \qquad (6.19)$$

and hence the relation for the overall noise intensity due to combustion becomes,

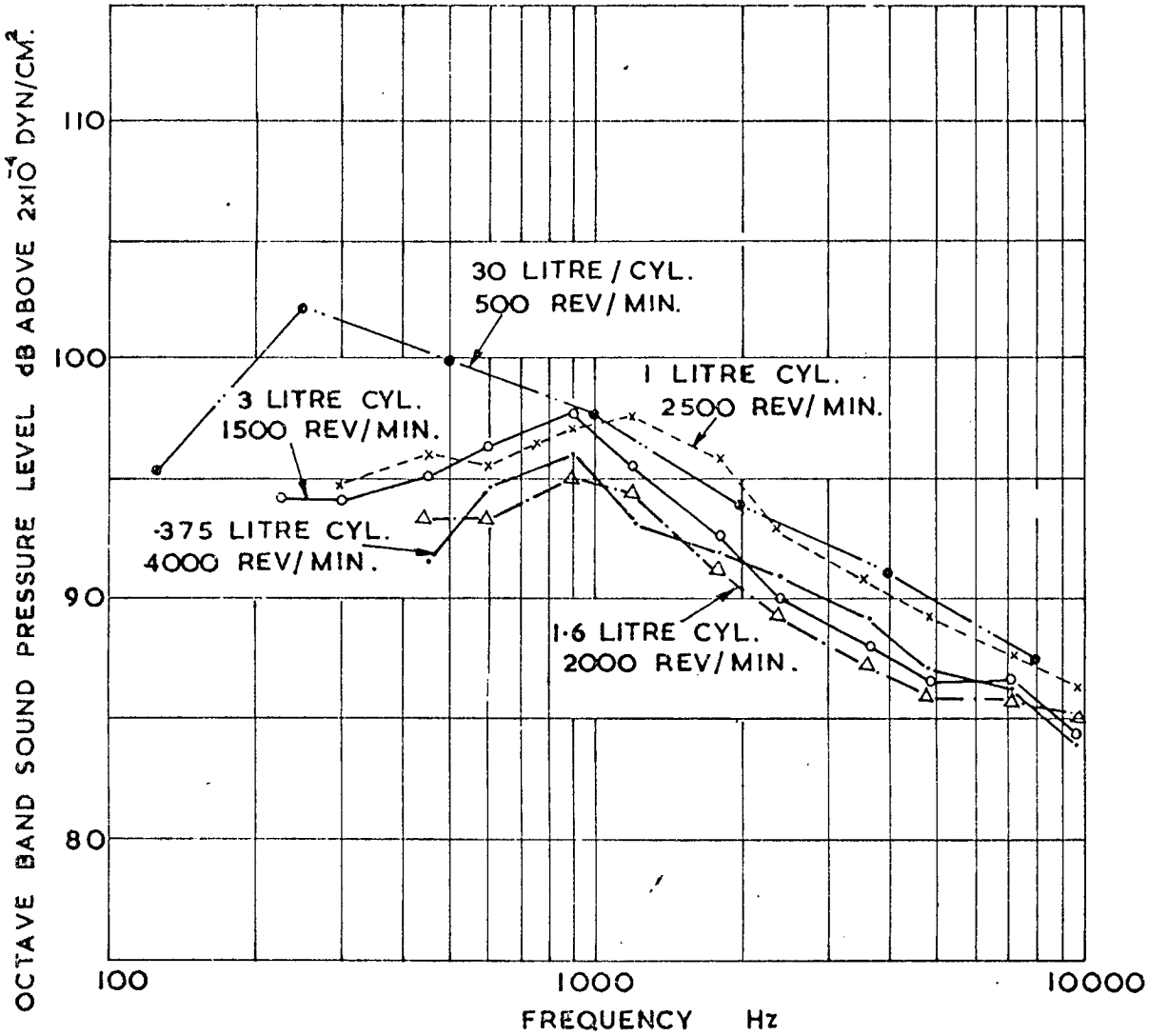

Fig. 6·6 – NOISE OF VARIOUS DIESEL ENGINES AT RATED SPEED

Table 6.2

Predicted and Measured Noise Levels of Automotive Diesel Engines

Engine Type	Induction	Bore - Inches	Rated Speed - Rev/Min	Overall Noise Level - dBA	
				Calculated	Measured
	Four-stroke				
V FORM 8 Cyl.	N.A.*	4.625	3300	107.2	108
" "	"	4.625	3300	107.2	109
" "	"	4.5	3000	105.5	106.5
" "	"	4.25	2800	103.3	103.5
" "	"	5.31	2600	107.2	109
In-line 6 Cyl.	"	5.5	2100	105.5	106
" "	"	4.65	2600	104.4	102
" "	"	4.56	2800	104.9	105
" "	"	4.125	2800	102.7	102.5
" "	"	3.875	2800	101.3	103
" "	"	3.81	2800	101	102
" "	"	3.875	2800	101.3	103
" "	"	3.688	4000	104.9	107
" "	"	3.125	4000	101.3	101.5
" "	"	3.5	3500	102	101.5
	Four-stroke T.Ch.+				
V FORM 8 Cyl.	"	5.5	2600	107.3	107
In-line 6 "	"	5.5	2100	103.3	102
" "	"	4.75	2200	101	100
Opposed piston single crank with rocker arms - 3 cyl.	Two stroke	3.25	2400	109.3	108.5
Opposed piston double crank - shaft in-line 6 cyl.	"	3.4375	2400	110.5	109.5
Opposed piston double-crank-shaft in-line 6 cyl.	"	4.625	2100	114.9	113.5
In-line 6 cyl.	"	3.620	2200	102.2	102

* N.A. - Normally aspirated.

+ T.Ch. - Turbocharged.

Overall Noise Intensity, $I_o \propto N^n.B^6.C_{ASO}$ (6.20)

or $I_o \propto N^n.B^6$

assuming that the overall acoustic and structural response remains constant. A new set of prediction relations, similar to those of equation (6.18), can now be put forward, (see chapter 10). Overall noise at 1 metre at rated speed in dBA:

(a) Four stroke D.I. normally aspirated diesel engines

$$dBA = 30 \log_{10}N + 60 \log_{10}B - 38.0$$

(b) Four stroke I.D.I. normally aspirated diesel engines

$$dBA = 36 \log_{10}N + 60 \log_{10}B - 60.0$$

10.9

(c) Two stroke D.I. Roots Scavenged diesel engines

$$dBA = 20 \log_{10}N + 60 \log_{10}B + 18.0$$

(d) Turbocharged Rotor and two stroke D.I. diesel engines

$$dBA = 20 \log_{10}N + 60 \log_{10}B + 13.0$$

where N = engine speed revs/min

B = engine bore in inches

This produces the interesting result that when considering a comparison of engines of different size the relation:

$$I_o \propto m\, N^n\, B^6\, C_{ASO}$$

holds. If, however, engines of the same engine surface area are compared, then:

$$I_o \propto N^n B^4.$$

6.2.3 Combustion noise in engines with the same overall acoustic and structural response

Since the combustion exciting propensity of an engine can be measured independently from its construction, then the effect that variations in the form of combustion will have on an engine structure which has the same overall acoustic and structural response can be assessed. A standard acoustic and structural response curve must therefore be established to enable this comparison to be made. Equation (6.13) can be rewritten:

$$\text{Overall Noise Intensity} \propto (\text{Force Input})^2 \times (\text{Surface Area Ratio}) \times C_{ASO} \tag{6.23}$$

and consequently an assessment of the overall acoustic and structural response can be obtained from measured data:

$$(\text{Surface Area Ratio}) \times C_{ASO} \propto (\text{Noise Intensity}) - (\text{Combustion Force Level}) - \text{dB} \tag{6.24}$$

Or, in terms of a structure attenuation factor S (6.12)

$$S = \frac{1}{(\text{Surface Area Ratio}) \times C_{ASO}} \tag{6.25}$$

and

$$S = 10 \log_{10} (\text{Surface Area Ratio}).C_{ASO} = (\text{Combustion force level}) - (\text{Noise intensity}) - \text{dB} \tag{6.26}$$

Some measured 1/3 octave band structure attenuation factors for various configurations of both two cycle and four cycle engines are presented in figure 6.7. The curves show high attenuation at low frequencies and the lowest attenuation in the 1500-4000 Hz range. There appears to be no definite grouping of the attenuation factors for the various configurations of two cycle and four cycle engine structures and it must be concluded that the detail structural design of each engine is more important than the configuration. The only important effect of configuration other than that of changing

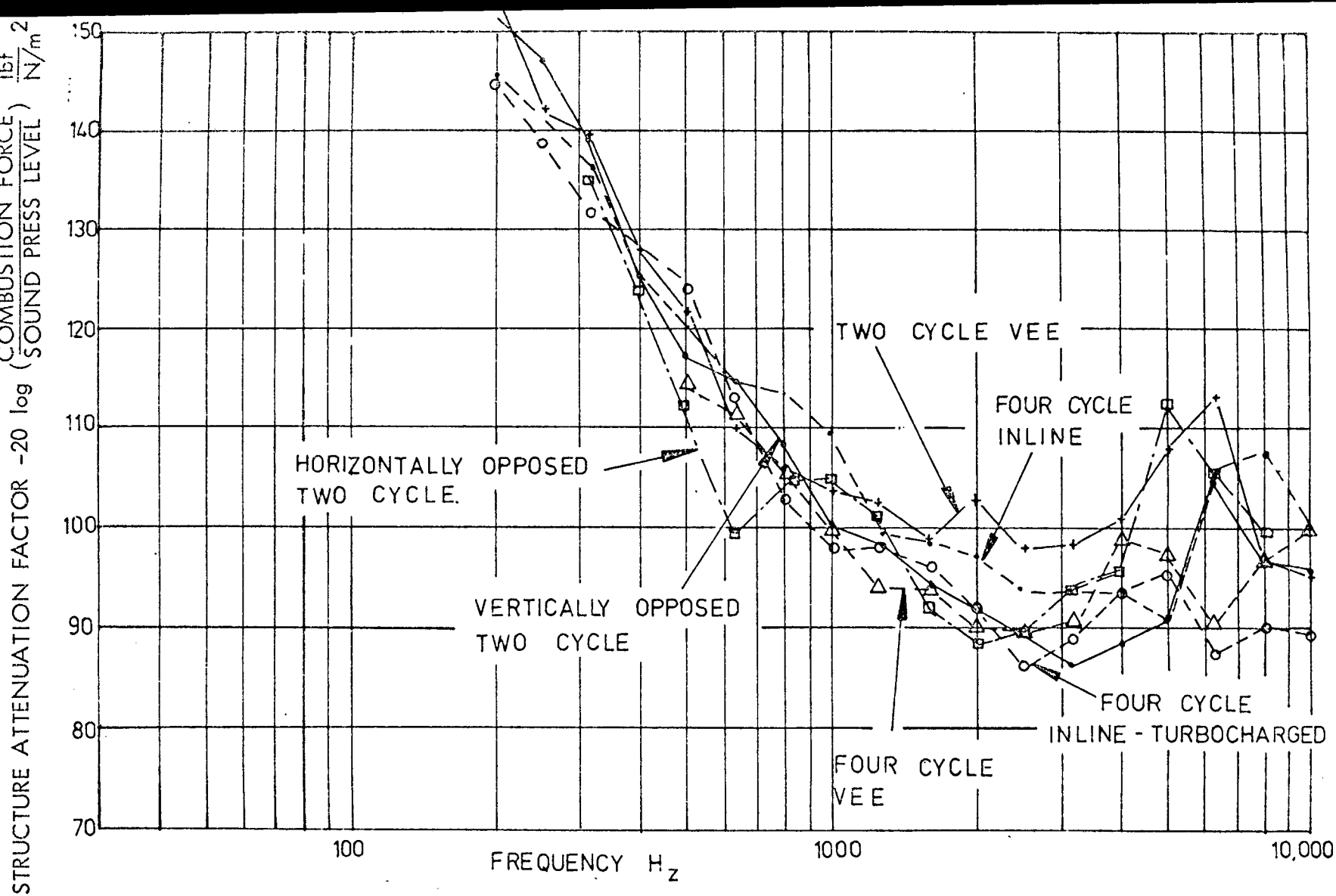

FIG. 6·7- STRUCTURE ATTENUATION FACTOR FOR VARIOUS ENGINE CONFIGURATIONS

the precise frequency and form of the structural resonances is in the opposed piston design where because the force input to the structure is doubled the resultant overall noise is some 6 dBA higher than for conventional engines.

A mean structure attenuation factor curve can be drawn through these results and will provide a suitably realistic value which can then be used to assess the effect of combustion changes on a 'standard' engine. Such a mean structure curve is shown in fig. 6.8, both for 1/3 octave bands and corrected to a constant bandwidth of 1 Hz. This can be regarded as the Standard Structure Attenuation Factor.

6.2.4 Calculation of combustion induced noise using the standard structure attenuation factor

At present it is very difficult to compare the combustion exciting properties of various engines directly since usually the cylinder pressure spectrum, bore, engine speed, engine surface area, etc., vary. By putting the applied force (cylinder pressure spectrum) and combined acoustic and structure response into simplified forms it is possible to calculate the combustion induced noise which would be produced by a 'standard' engine from a knowledge of the level and slope of the exciting pressure spectrum.

6.2.4.1 Simplified cylinder pressure spectrum

Figure 6.9 shows the cylinder pressure spectra at various engine speeds for a 4.65" bore Direct Injection four stroke diesel. Over the critical frequency range of 500 to 5000 Hz, the spectra can be represented by straight lines of n dB/decade. Figure 6.10a illustrates this. The slope is n dB/decade and a representative level is given by the cylinder pressure level at 1000 Hz ($C.P.L._{(1000)}$). The cylinder pressure (C.P.) is given by

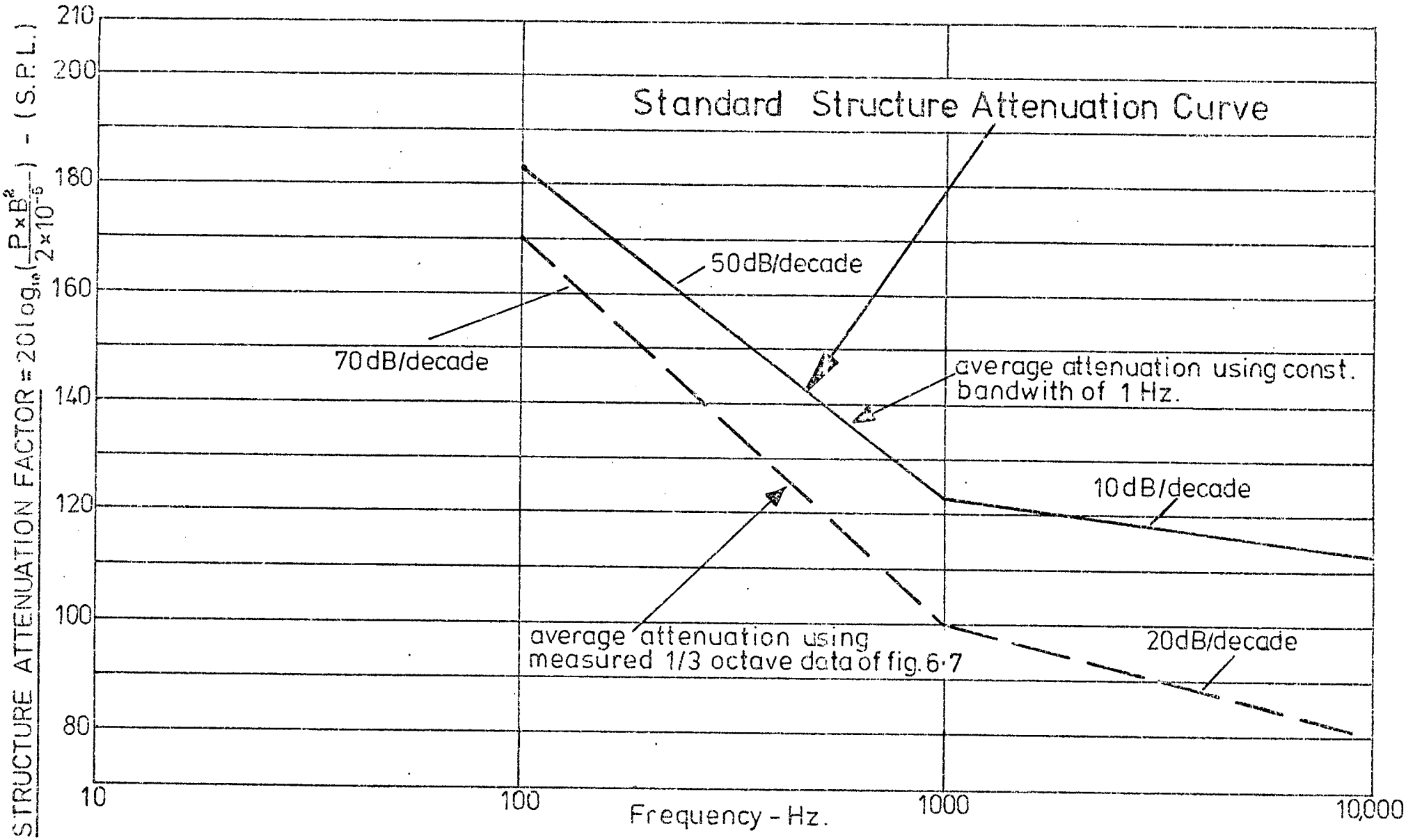

FIG. 6·8- STANDARD STRUCTURE ATTENUATION FACTOR.

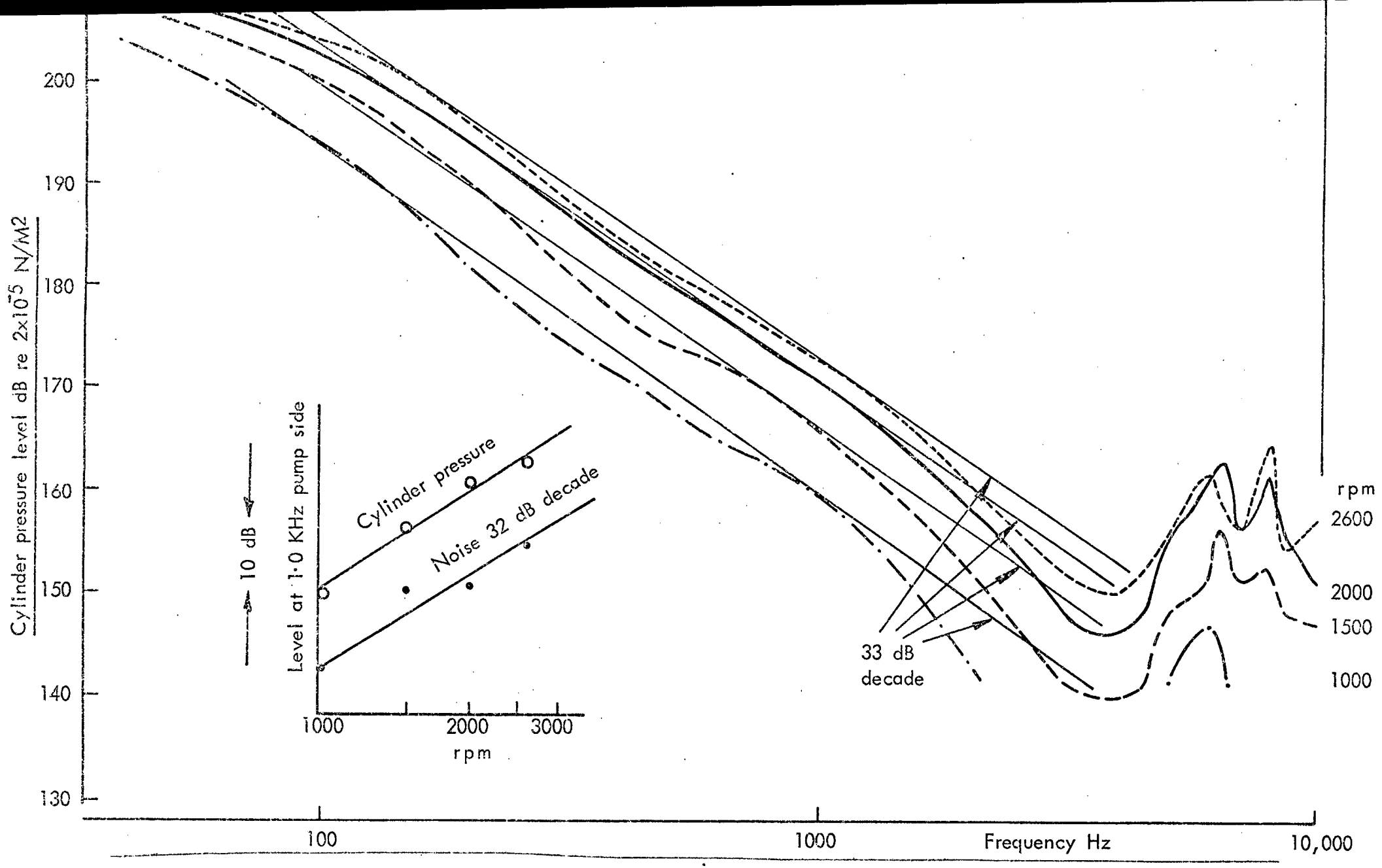

FIG. 6·9 - CYLINDER PRESSURE SPECTRA VERSUS SPEED D.I. 4 STROKE FULL LOAD.

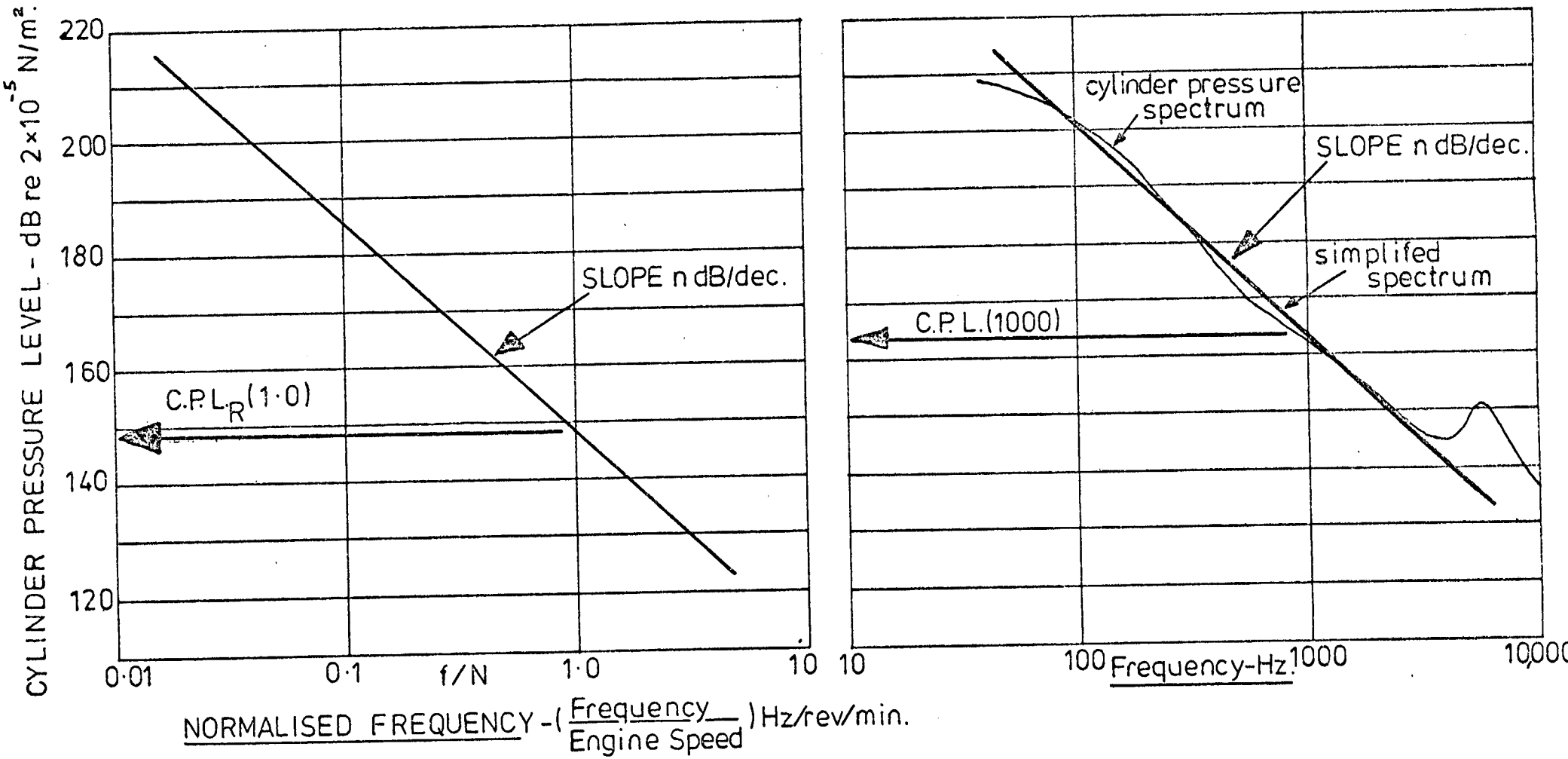

a) Simplified and Reduced Spectra. b) Simplified Spectra.

FIG. 6·10 - SIMPLIFIED AND REDUCED CYLINDER PRESSURE SPECTRA.

$$(C.P.)_f^2 = \frac{(C.P._{(1000)})^2 \; A \log_{10}(3n)}{f^n} \quad (N/m^2)^2/Hz \qquad (6.27)$$

$(C.P.)_f$ = cylinder pressure at frequency f Hz in N/m^2

$C.P._{(1000)}$ = cylinder pressure at 1000 Hz

n = slope dB/decade

f = frequency Hz

and

$$C.P.L.(f) = 10n \log_{10} \frac{1}{f} + C.P.L._{(1000)} + 30n \quad dB \qquad (6.28)$$

6.2.4.2 Reduced cylinder pressure spectrum

If the cylinder pressure diagram, on a degree basis, does not change with speed then the four spectra shown in fig. 6.9 can be reduced to one spectrum plotted against the ratio f/N to take account of the speed effect. The data of fig. 6.9 are replotted in fig. 6.11 on this basis. From fig. 6.10 (b) it can be shown that the cylinder pressure $(C.P.)_f$ at frequency f calculated from the reduced spectrum is

$$(C.P.)_f^2 = (C.P._R(1.0))^2 \; A \log_{10}(3n) . (\frac{N}{f})^n - (\frac{N}{m^2})^2/Hz \qquad (6.29)$$

and cylinder pressure level

$$C.P.L. = 10n \log_{10} (\frac{N}{f}) + C.P.L._R(1.0) \quad dB \qquad (6.30)$$

where

$C.P._R(1.0)$ = cylinder pressure on reduced spectrum at f/N = 1.0

$C.P.L._R(1.0)$ = cylinder pressure level on reduced spectrum at f/N = 1.0.

6.2.4.3 Standard structure attenuation factor

The structure attenuation factor S:

$$S = 20 \log_{10}(\frac{\text{combustion pressure x bore}^2}{\text{reference pressure}}) - 20 \log_{10}(\frac{\text{sound pressure}}{\text{reference press.}}) \qquad (6.31)$$

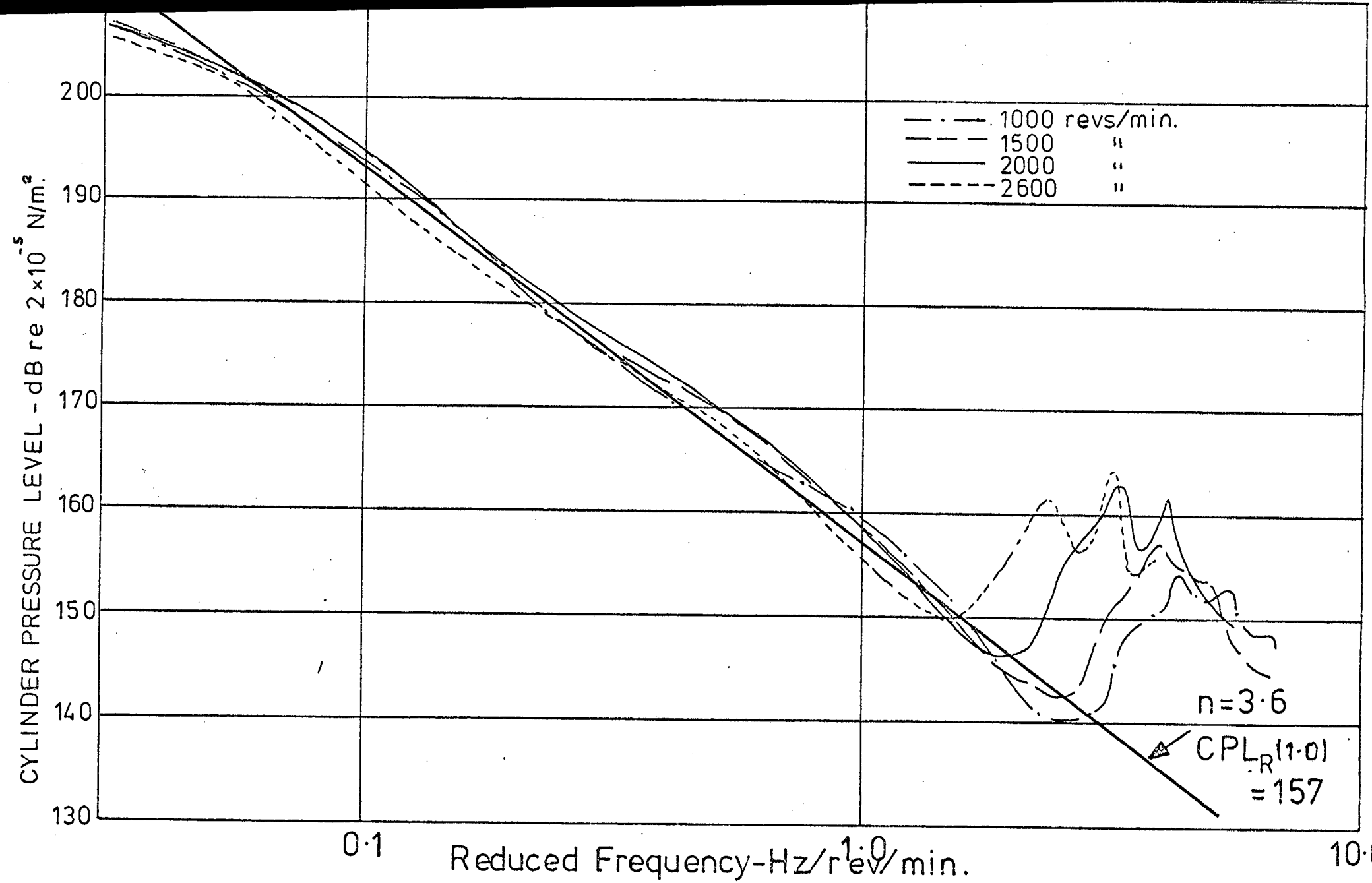

FIG. 6·11 - REDUCED CYLINDER PRESSURE SPECTRA FOR D.I. DIESEL AT FULL LOAD.

and therefore each straight line portion of the standard structure attenuation can be treated in a similar manner to the previous two sections

$$S = 10q \log_{10} \frac{1}{f} + S_{1000} + 30q \text{ dB} \tag{6.32}$$

where

S_{1000} = attenuation at 1000 Hz

q = slope of attenuation curve dB/decade

f = frequency Hz

and

$$S = \frac{A \log_{10}(S_{1000}/10)\ A \log_{10}(3q)}{f^q} \tag{6.33}$$

and from equation (6.23)

$$(\text{Sound Pressure, P})^2_{(f)} = \frac{(\text{cylinder pressure x bore}^2)^2}{S}$$

$$P^2(f) = \frac{(\text{cylinder pressure x bore}^2)^2 \times f^q}{A \log_{10}(S_{1000}/10)\ A \log_{10}(3q)} \tag{6.34}$$

6.2.4.4 Calculation of overall level from known cylinder pressure spectrum

From equations (6.27) and (6.34) the sound pressure P at frequency f

$$P^2(f) = \frac{(C.P._{(1000)})^2\ A \log_{10}(3n)\ B^4}{A \log_{10} S_{1000}/10\ A \log (3q)}\ f^{q-n} \tag{6.35}$$

The overall pressure level is therefore

$$P^2\ (\text{Overall}) = \int_{f_1}^{f_2} P^2\ df \tag{6.36}$$

where the integral extends over the audio frequency range.

$$P^2\ (\text{Overall}) = \frac{(C.P._{(1000)})^2\ A \log_{10}(3n).B^4.K}{(q - n + 1)\ A \log_{10}(3q)} \left[f_2^{(q-n+1)} - f_1^{(q-n+1)} \right] \tag{6.37}$$

where

$$K = \frac{1}{A \log_{10}(S_{1000}/10)}$$

and the overall Sound Pressure Level due to combustion

$$(S.P.L.)_{Overall} = 20 \log_{10} \left(\frac{P_{(Overall)}}{P_{reference}}\right).$$

6.2.4.5 Overall level assuming two part standard structure attenuation curve

If a standard structure attenuation curve of the form

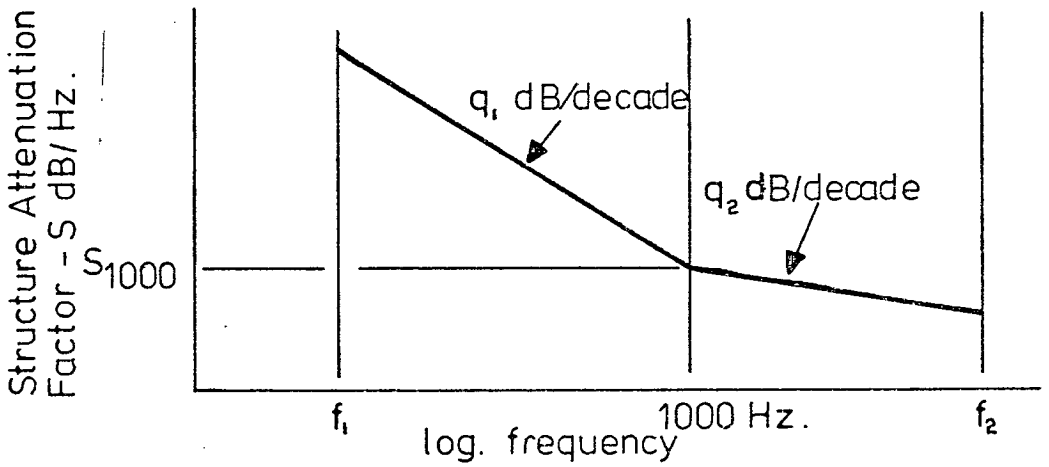

STANDARD STRUCTURE ATTENUATION FACTOR.

is used then from sections 6.2.4.3 to 6.2.4.5 the overall combustion noise level as calculated from a measured or computed simplified cylinder pressure spectrum at engine speed N revs/min will be

$$(S.P.L.)_{Overall} = 20 \log_{10} \left[\frac{(C.P._{(1000)})^2 . A \log_{10}(3n) . B^4}{P_{ref} . A \log_{10}(S_{1000}/10)} \left(\frac{(1000^{(q_1-n+1)} - f_1^{(q_1-n+1)})}{(q_1 - n + 1) A \log_{10}(3q_1)} + \frac{(f_2^{(q_2-n+1)} - 1000^{(q_2-n+1)})}{(q_2 - n + 1) A \log_{10}(3q_2)} \right) \right] \quad (6.38)$$

And the overall combustion noise level as calculated from a measured or computed simplified and reduced cylinder pressure spectrum at an engine speed N revs/min will be:

$$(S.P.L.)_{Overall} = 20 \log_{10} \left[\frac{(C.P._R(1.0)^2 . A \log_{10}(3n) . B^4 . N^n}{P_{ref.} \cdot A \log_{10}(S_{1000}/10)} \times \left(\frac{[1000^{(q_1-n+1)} - f_1^{(q_1-n+1)}]}{(q_1-n+1) A \log_{10}(3q_1)} + \frac{[f_2^{(q_2-n+1)} - 1000^{(q_2-n+1)}]}{(q_2-n+1) A \log_{10}(3q_2)} \right) \right] \text{ dB.} \quad (6.39)$$

By using the standard structure attenuation the values of q_1 and q_2 and S_{1000} (50 dB/decade, 10 dB/decade, S_{1000} = 122.5 dB respectively), equations (6.38) and (6.39) can be simplified to include only a representative cylinder pressure spectrum level, slope, engine bore, speed and a factor Y which depends on the slope of the cylinder pressure spectrum n. The factor Y can be regarded as a Spectrum Shape Factor relating the excitation and response spectra. In this way the predicted overall combustion noise, in dBA at 1 metre, of a standard structure response engine becomes:

$$dBA = C.P.L._{(1000)} + 40 \log_{10} B - Y \text{ dB} \quad (6.40)$$

and

$$dBA = C.P.L._R(1.0) + 40 \log_{10} B + 10n \log_{10} \frac{N}{1000} - Y \text{ dB}$$

from a known reduced cylinder pressure diagram.

The values of Y as a function of the cylinder pressure spectrum slope n are shown in fig. 6.12. Inherent in the value of Y is the effect of engine radiating area, which has been established as being proportional to the square of cylinder bore. For a true comparison of combustion noise then account of this factor should be taken. By assuming that the standard structure attenuation factor represents an average engine, then it can be represented by an average bore size. For automotive engines the choice of average bore is 4 inches.

Thus the predicted combustion noise of a 'standard' engine, including the effect of radiating area, becomes:

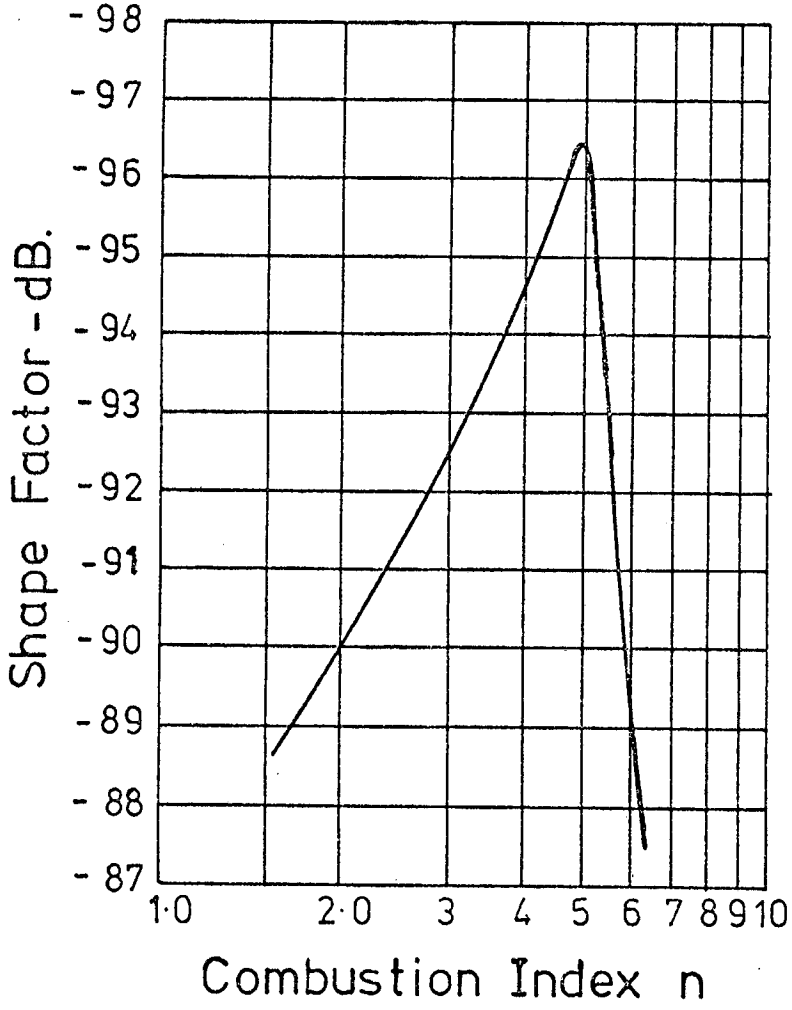

FIG. 6·12- SPECTRUM SHAPE FACTOR 'Y'

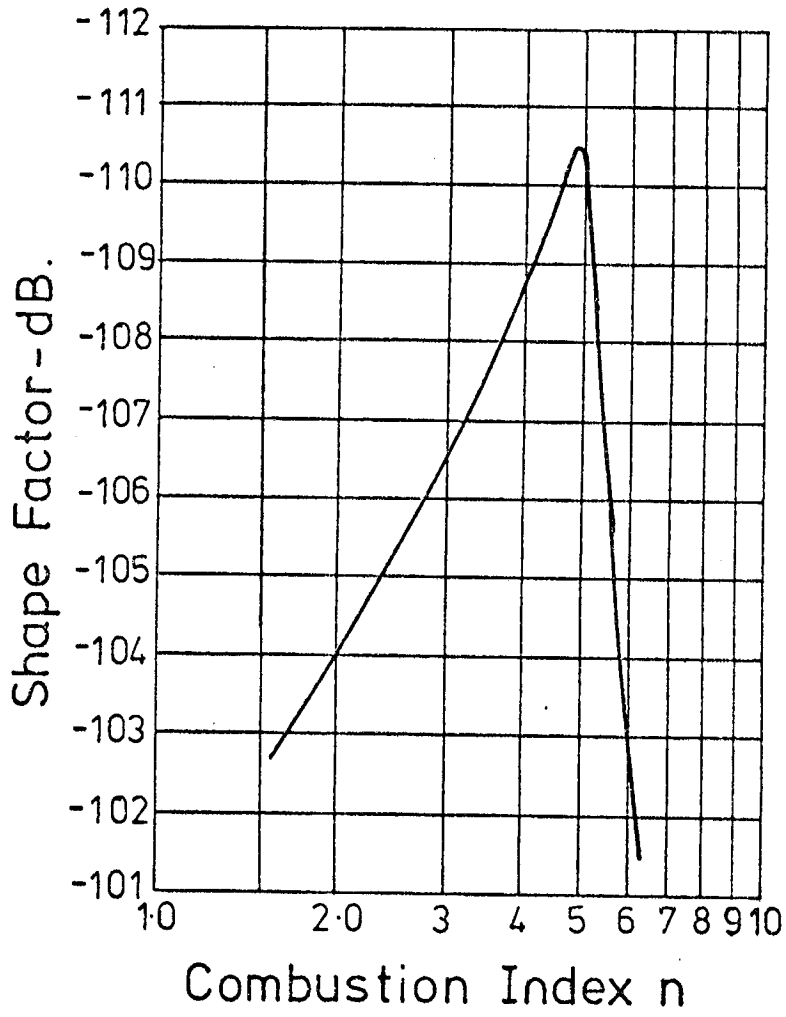

FIG. 6·13- SPECTRUM SHAPE FACTOR 'X'

PREDICTED COMBUSTION NOISE FROM KNOWN CYLINDER PRESSURE SPECTRUM - dBA AT 1 METRE

$$dBA = C.P.L._{(1000)} + 60 \log_{10} B - X \quad dB \tag{6.41}$$

PREDICTED COMBUSTION NOISE FROM KNOWN REDUCED CYLINDER PRESSURE SPECTRUM - dBA AT 1 METRE

$$dBA = C.P.L._{R}(1.0) + 60 \log_{10} B + 10n \log_{10} \frac{N}{1000} - X \; dB$$

and the values of the Spectrum Shape Factor X are shown in Fig. 6.13.

This method of calculating the noise which would be radiated by a standard engine due to combustion excitation has the advantage that it takes account of the actual level of the cylinder pressure spectrum as well as the Combustion Index (slope). It can therefore be used at any engine condition, unlike the previously mentioned relations which can only be applied at rated speed since it is assumed that only the spectrum slope varies from engine to engine. The relations (6.41) apply to all forms of I.C. engine for the calculation of Combustion Induced Noise.

The application of the three sets of prediction formulae given in this chapter (equations (6.18), (6.21) and (6.41)) is described in Chapter 10.

It can be concluded that the sound pressure level produced by combustion in I.C. engines (equation 6.16) is dependant upon the force input to the structure resulting from combustion, the radiating area, and the combined acoustic and structural response of the engine.

References

6.1 T. Priede. 'Relation between the form of cylinder pressure diagram and noise in diesel engines'. Proc. I.M.E. (A.D.) No. 1, 1960-1961.

6.2 A.E.W. Austen and T. Priede. 'Origins of diesel engine noise'. Symposium on engine noise suppression. Proc. Instn. Mech. Engrs. London, 1959, 173, 19.

6.3 D. Anderton, E.C. Grover, N. Lalor, T. Priede. 'Origins of Reciprocating engine noise - its characteristics, prediction and control'. ASME paper 70-WA/DGP-3, 1970.

6.4 D. Anderton. 'Progress in I.C. engine noise assessment and suppression techniques'. Combustion Engine Progress, London 1970.

6.5 G.C. Darby. 'Response of an in-line diesel engine structure to impulsive gas forces'. Thesis, 1968/69. Southampton University.

6.6 D. Anderton, E.C. Grover, N. Lalor, T. Priede. "Assessment and control of combustion induced noise in I.C. engines". Combustion Engine Progress, 1969.

6.7 C.M.P. Chan. 'Electromagnetic excitation of engine structures'. ISVR Memorandum no. 475, September 1972.

6.8 L.E. Kinsler and A.R. Frey. 'Fundamentals of Acoustics'. Wiley, 1962.

6.9 C.M.P. Chan and D. Anderton. 'The correlation of machine structure surface vibration and radiated noise'. Internoise 72 Proceedings, Washington D.C., October 4-6, 1972.

6.10 T. Priede. 'Noise due to combustion in reciprocating internal combustion engines.' Symposium A.S.A.E. Cranfield - Advances in Automobile Engineering, Part III, Noise and Vibration, 1964.

6.11 C.M.P. Chan. 'In-line diesel engine surface vibration and its radiated noise'. Ph.D. Thesis, Southampton University, 1974.

6.12 D. Anderton, J. Baker. 'Influence of operating cycle on noise of diesel engines'. S.A.E. paper 730241, January 1973.

7.0 EFFECT OF OPERATING CYCLE ON COMBUSTION-INDUCED NOISE

When a single engine structure is considered, then the mechanical and acoustic radiation characteristics remain constant and any changes in the combustion noise spectrum will be caused by changes in the cylinder pressure spectrum. A comparison of cylinder pressure spectra for various types of combustion will then also provide a direct comparison of the relative combustion noise levels which would be radiated for unit piston area. This comparison can be accomplished in three ways.

(a) By analysis of mathematical approximations to cylinder pressure development.

(b) By computer analysis of digitised cylinder pressure development.

(c) By direct electrical analysis of cylinder pressure development.

This last method is the most accurate but it is also very difficult to change in a specific way. If good cylinder pressure development records are available then the digital technique lends itself best to the study of specific combustion changes.

7.1 Theoretical Considerations of Two and Four Stroke Operating Cycles

7.1.1 Representation by intermittent sine wave function

The basic difference between the two stroke and four stroke cycle of operation is the difference in cycle length in terms of its crank angle (360° for two-stroke and 720° for four stroke).

Figure 7.1 shows a comparison of two and four stroke cylinder pressure development. The compression pressure is higher in the two stroke due to the Roots blower. A sharper rise of pressure occurs in the four stroke and also the expansion pressure remains higher for a longer period due to the later exhaust valve opening. In general and to a first approximation they are the same on a degree basis. On this assumption, Fig. 7.2(a) shows

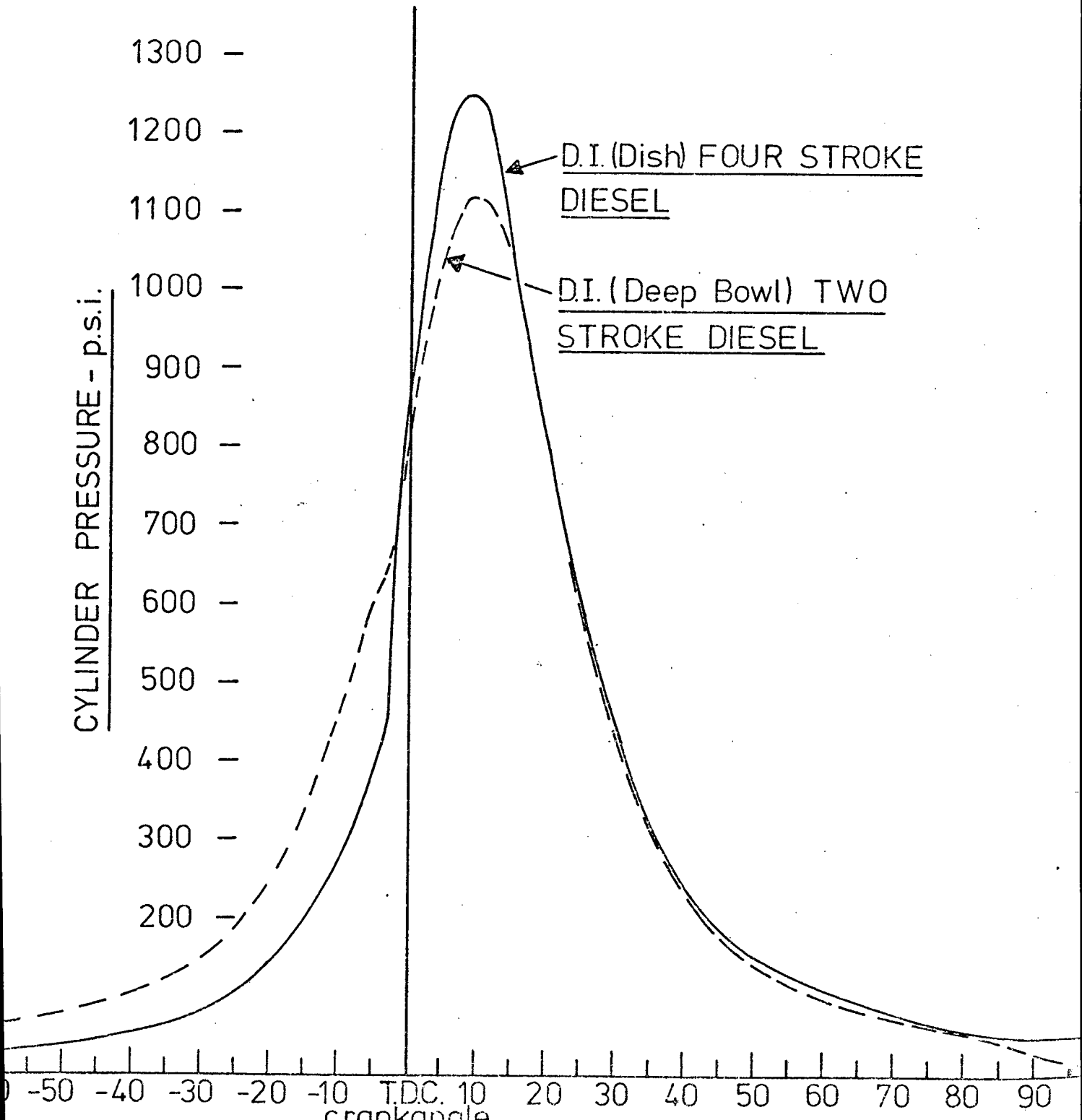

FIG. 7·1 - COMPARISON OF FOUR AND TWO STROKE ON A DEGREE BASIS.

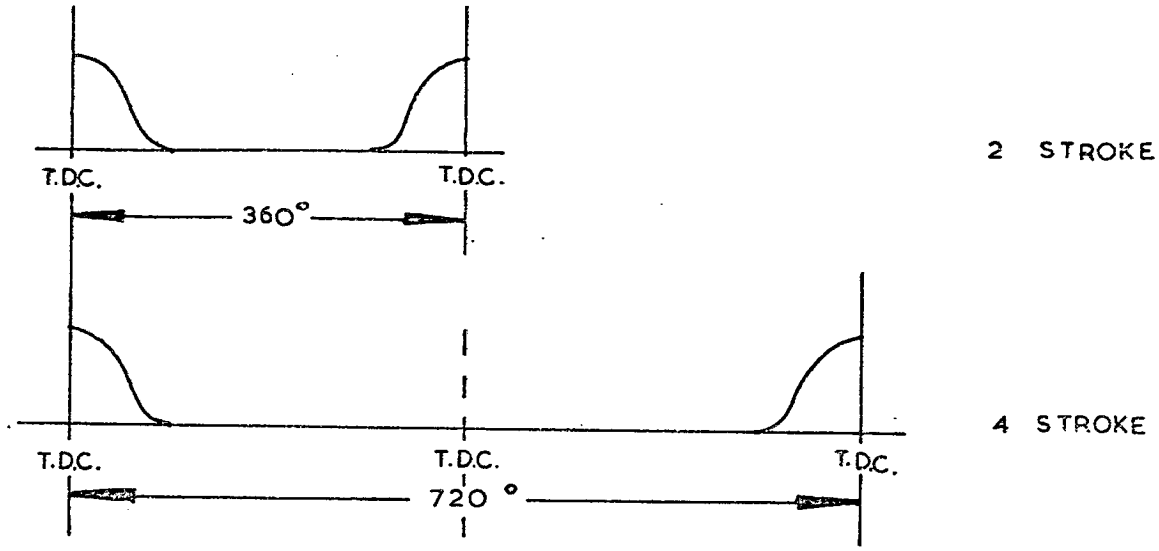

FIG. 1a.- PRESSURE DIAGRAMS ON DEGREE BASE.

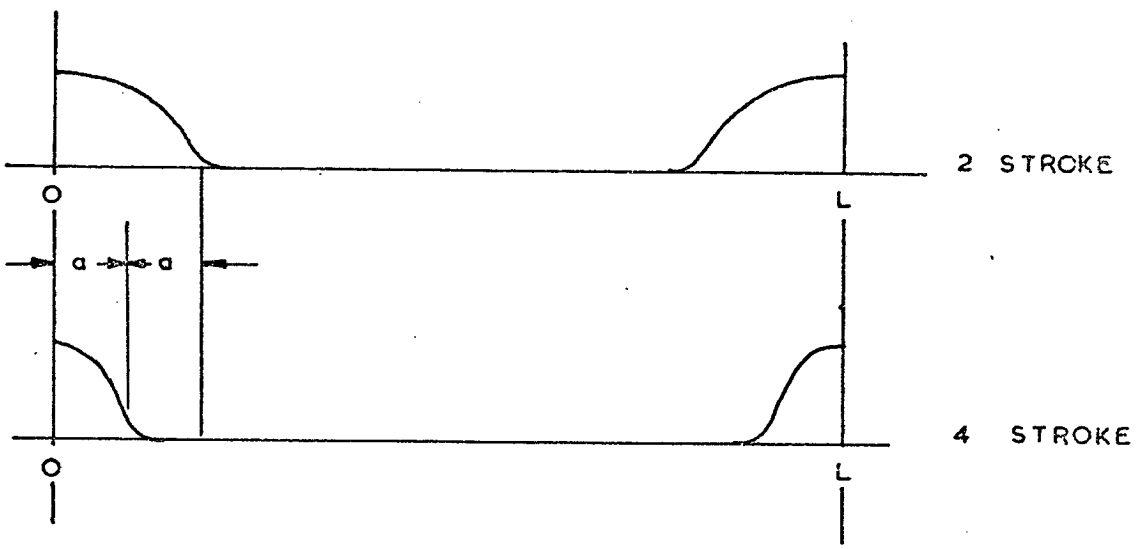

FIG. 1b. — PRESSURE DIAGRAMS ON REPETITION PERIOD BASE

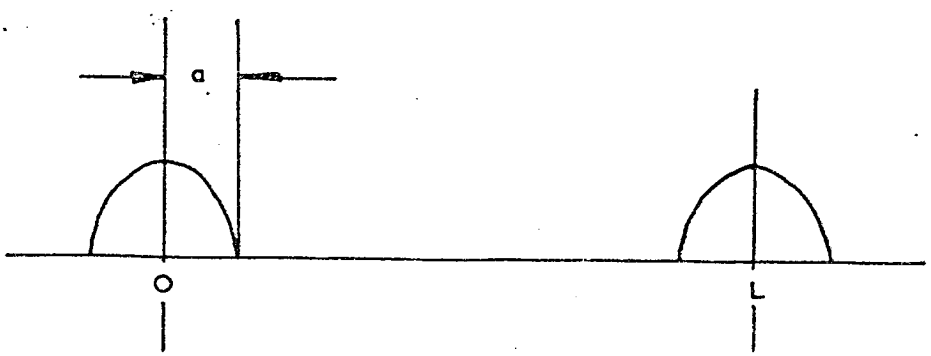

FIG. 7·2 - HALF SINE WAVE REPRESENTATION OF 2 & 4 STROKE CYCLES.

the comparison of one cycle on a degree basis. The high pressure portion of the development has a greater separation in the four stroke cycle. Figure 7.2(b) shows a comparison on the basis of repetition length. The frequency of the harmonic spectrum fundamental is not involved in the computation of the harmonic series as the whole series is multiplied by this frequency to form the spectrum. The actual spectrum values are controlled by the variation of the waveform within the cycle and their relationship to the repetition length L. On this basis the four stroke cycle high pressure 'pulse' is narrower than that of the two stroke by a factor of two. This has a considerable influence on the values of the harmonic series. Figure 7.2(c) shows a mathematical idealisation of the cylinder pressure developments into a half sine wave of width a such that the width to repetion length ratio a/L can be varied.

The cycle can be defined as:

$$y = \cos \frac{\pi x}{2a} \quad \text{for} \quad 0 \leq x \leq a \tag{7.1}$$

$$y = 0 \quad \text{for} \quad a \leq x \leq \pi \tag{7.2}$$

and in the general case the harmonic series is given by

$$a_n = \frac{2C}{\pi(C^2 - n^2)} \cos na \quad \text{for } n = 0,1,2,3,.., \text{ except } n = C \tag{7.3}$$

$$b_n = 0$$

where $C = \pi/2a$.

As can be seen, the pulse width a is a very important factor in determining the harmonic amplitudes.

From equation (7.3) it can be shown that the amplitude of the fundamental for the four stroke cycle, where $2\pi/a = 1.2$, is given by

$$a_1 = \frac{3.25}{5\pi}$$

and for the two stroke cycle, where $2\pi/a = 6$, is

$$a_1 = \frac{6}{5\pi}$$

Thus the amplitude of the fundamental is higher in the two stroke cycle by a factor of 1.85, or 5.34 dB when expressed as a pressure level, than in the four stroke cycle.

At high harmonic numbers n is large compared to C and

$$a_n \simeq \frac{2C}{\pi n^2} \cos na \qquad (7.4)$$

and the slope of the harmonic envelope joining the spectrum maxima will be 40 dB/decade, and for the four stroke cycle the level of these maxima will be exactly twice those of the two stroke cycle. This occurs when the fundamental cycle frequency is the same for both cases. Figure 7.3 shows a comparison of the cylinder pressure spectra envelope when compared on the basis of equal engine speed and also equal cycle repetition frequency.

7.1.2 Comparison at the same engine speed

The engine speed is taken to be 2000 revs/min. In Fig. 7.3(b) the general shape of the spectra are similar except that the level of the two stroke harmonics are some 5.34 to 6 dB higher than those of the four stroke cycle. The fundamental firing frequency for the four stroke cycle is 16.7 Hz while the two stroke cycle is 33.4 Hz. Thus in a given frequency band there are twice as many harmonics in the four stroke spectrum.

7.1.3 Comparison at the same firing frequency

For the same cycle firing frequencies the two stroke must run at half the speed of the four stroke and in the case chosen the speeds are 2000 and 4000 revs/min respectively. Thus the harmonic separation is the same for both cases. From Fig. 7.3(a), the differences in the harmonic spectrum caused by the change in the pulse width a are now apparent. At the funda-

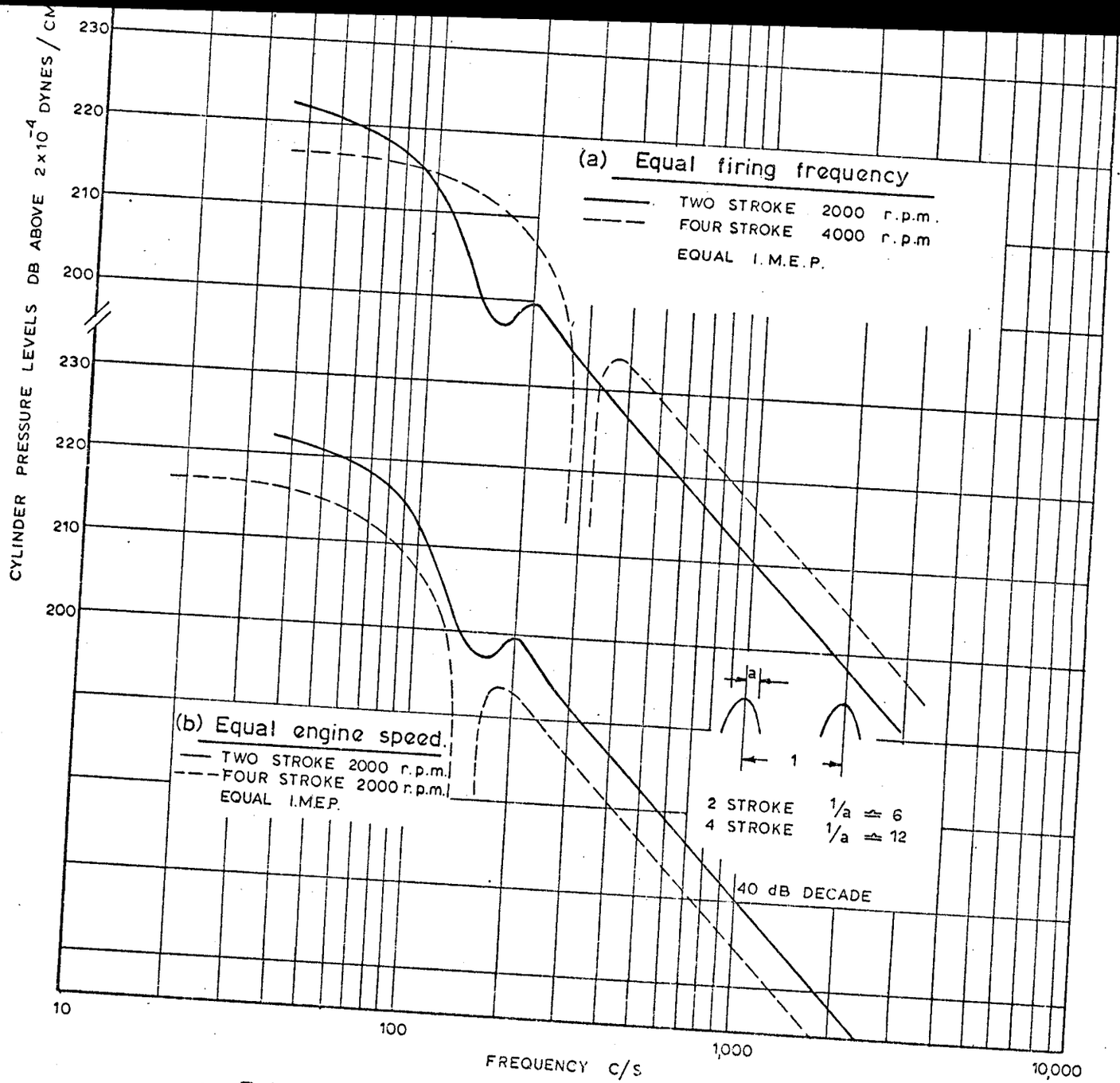

Fig 7·3 – [illegible] half sine repetitive pulse.

mental the two-stroke harmonic level is 5.34 dB higher than the four stroke whilst at higher harmonics the level of the four stroke spectrum is some 6 dB higher than the two stroke. In both cases in the high frequency range the envelope of the harmonics decreases at a rate of 40 dB/decade.

It can be concluded that the pulse width a affects both the form and level of the low frequency part of the spectrum but only the level of the high frequency part. The slope and the form of the high frequency part of the spectrum are affected by the shape of the pulse itself.

A similar result is found for actual cylinder pressure developments. Figure 7.4 shows the result of a harmonic analysis, using the Fast Fourier Series programme, for the case of a smooth two stroke diagram. By adding 360^{o} of zero data the spectrum for precisely the same cylinder pressure development on a degree basis can be computed as a two or four stroke cycle. A similar result to that of the sine pulse is found. However, there is a general change of spectrum shape in both cases due to the different basic diagram shape.

These same results are found when comparing two measured diesel engine spectra, one from an automotive D.I. four stroke of 4.125" bore and an opposed piston two stroke of 3.25" bore. Figure 7.5 shows the comparison at the same engine speed. The two stroke cylinder pressure spectrum levels are some 6 dB higher up to about 1000 Hz, when the two spectra gradually converge. This indicates that the two stroke cylinder pressure development is smoother than that of the four stroke.

Figure 7.6 shows a comparison of the engines at the same firing frequency - 1000 revs/min and 2000 revs/min engine speeds. At frequencies above 40 Hz the four stroke cycle cylinder pressure spectrum levels are higher than those of the two stroke.

Thus it has been shown that the fundamental cycle difference between the

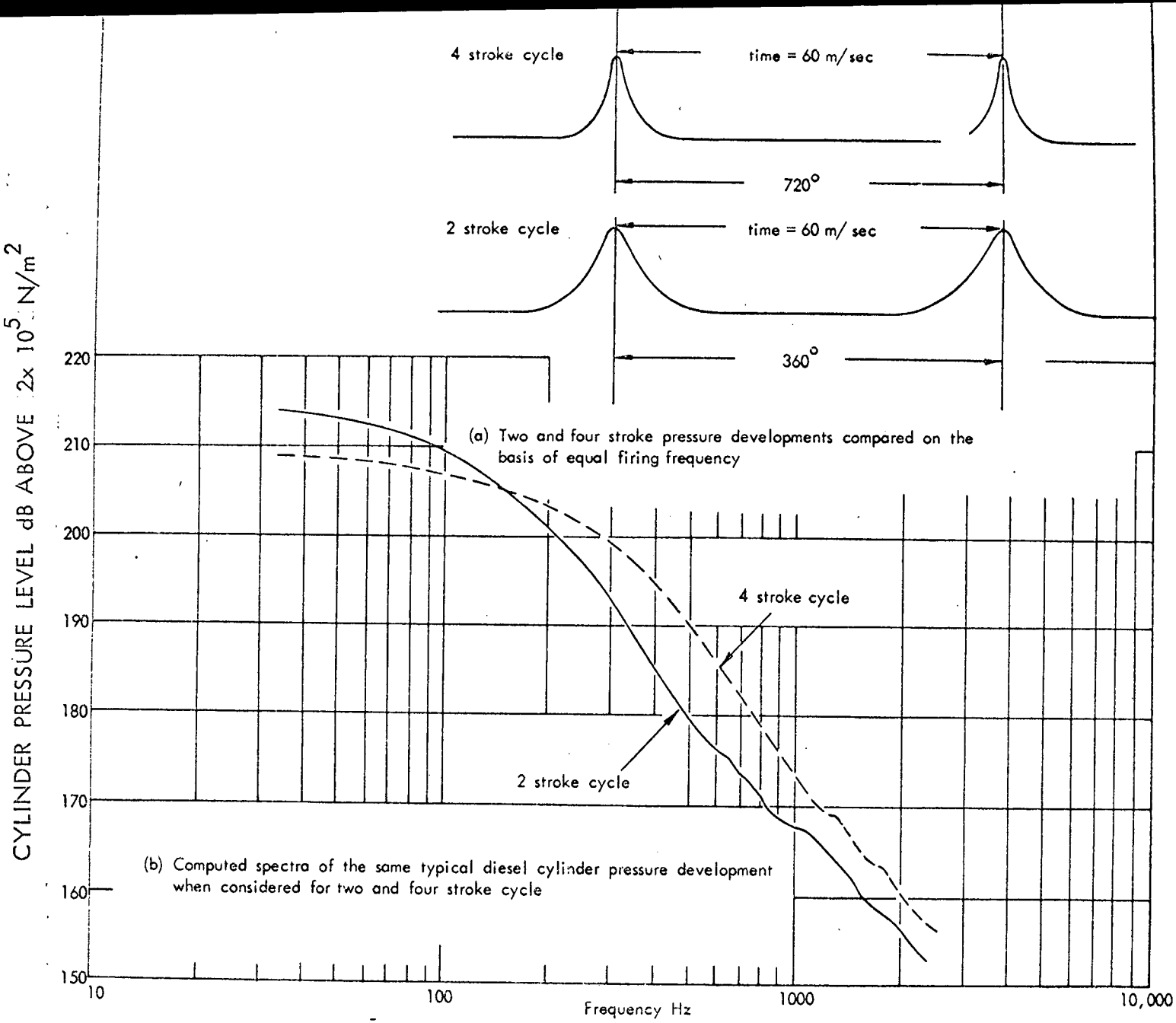

FIG. 7·4- COMPARISON OF TWO AND FOUR STROKE CYCLE AT EQUAL FIRING FREQUENCIES (Computed).

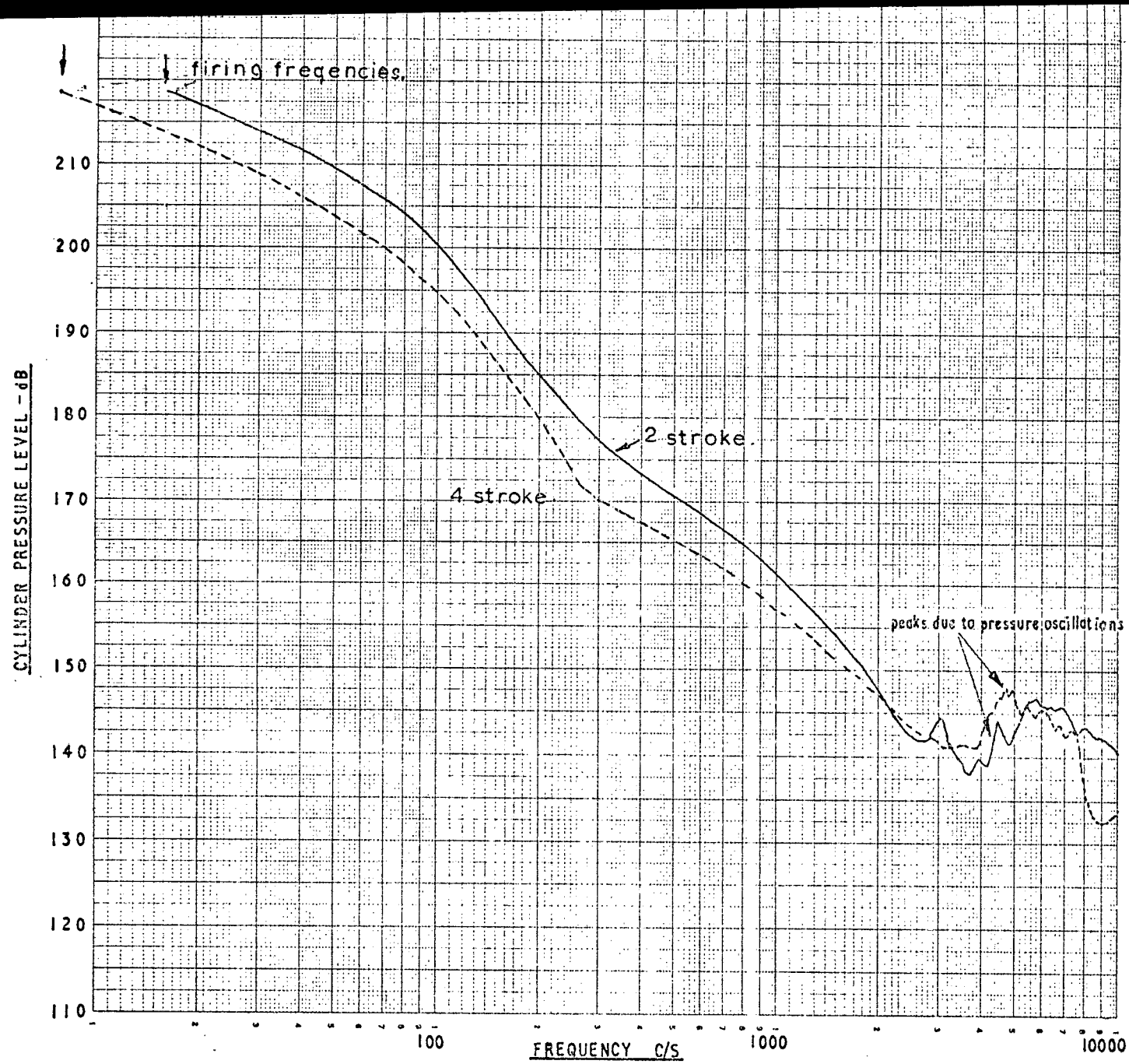

FIG. 7·5 – COMPARISON OF 2 AND 4 STROKE ANALYSES AT 1000 R.P.M.

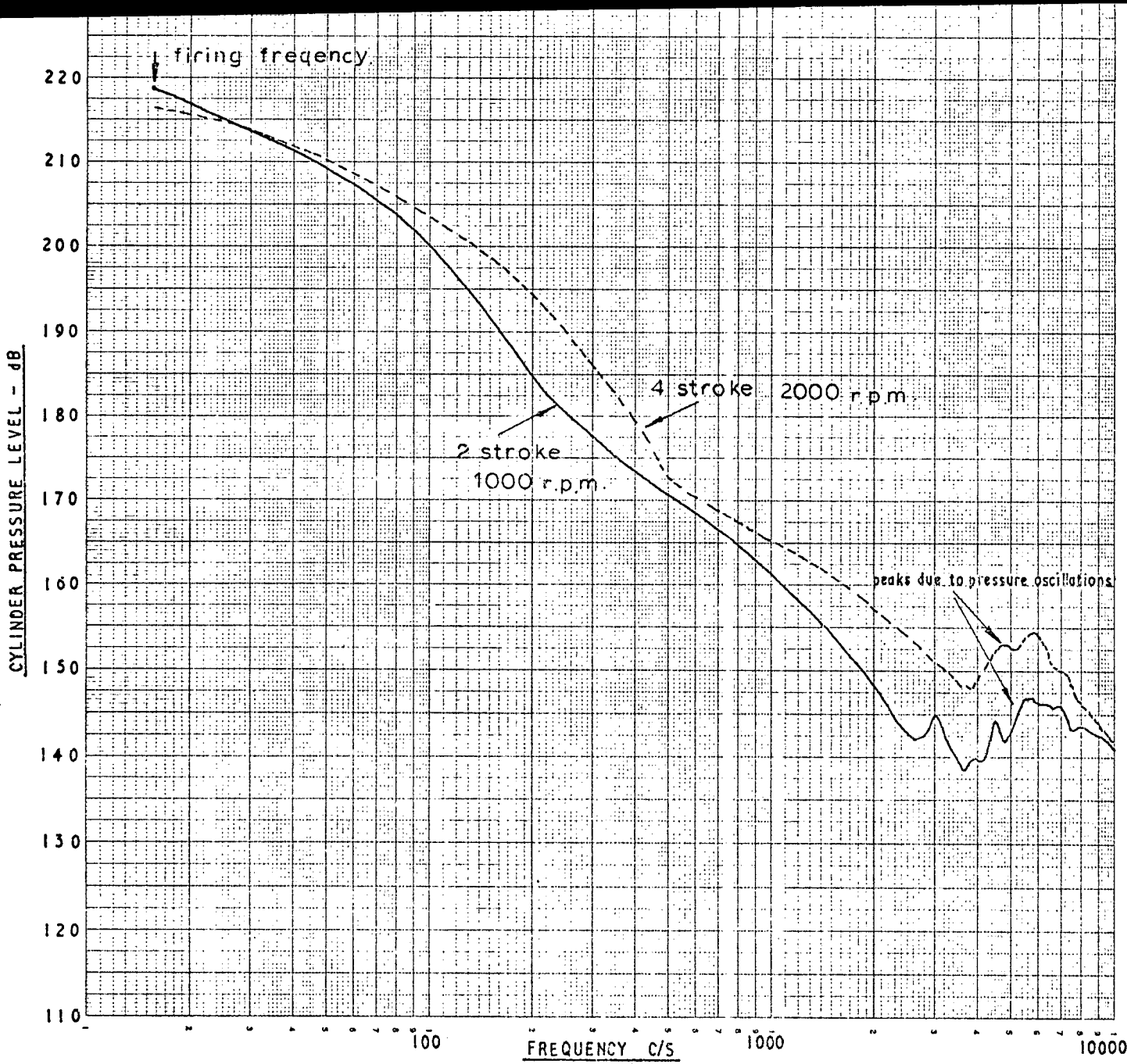

FIG. 7·6 – COMPARISON OF 2 AND 4 STROKE ANALYSES AT SAME FIRING FREQUENCY

two and four stroke cycle of operation results in a fundamental difference between the combustion noise exciting propensities of the two cycles.

7.1.4 Comparison of the two cycles at equal power output

The last section gives a comparison of the direct exciting propensities of the cylinder pressure development in the two and four stroke cycles. However, as is shown in Chapter 5, the noise output and power output of the engines are dependent upon the physical characteristics of the particular engine - namely rotational speed, bore, stroke, b.m.e.p. and cycle. In comparing the combustion noise characteristics of two and four cycle engines the balance between noise and power output provides the only fair means of comparison. The power output of the engines is given by

$$\text{Power of four stroke} = \frac{P.L.A.N.}{33,000} \quad \text{b.h.p.} \qquad (7.5)$$

$$\text{Power of two stroke} = \frac{P.L.A.2N}{33,000} \quad \text{b.h.p.} \qquad (7.6)$$

P = b.m.e.p. - lb/in^2

L = stroke - ins.

A = piston area - in^2.

N = engine speed - revs/min.

Theoretically the two stroke engine should give twice the power output of a four stroke engine of the same swept volume and engine speed. In practice, largely because of the necessary Roots blower for the two stroke, the power output is about 1.9 times that of the four stroke under these conditions. For the purpose of this comparison it is convenient to assume the theoretical value of two.

Under this assumption the ratio of the powers is given by:

$$\frac{\text{POWER}_2}{\text{POWER}_4} = \frac{2P_2L_2A_2N_2}{P_4L_4A_4N_4} \qquad (7.7)$$

and for the same assumed b.m.e.p. (same cylinder pressure diagram on a degree basis) and same stroke to bore ratic,

$$\frac{\text{POWER}_2}{\text{POWER}_4} = \frac{2B_2{}^3N_2}{B_4{}^3N_4} \qquad (7.8)$$

Therefore, for equal power output,

$$2B_2{}^3N_2 = B_4{}^3N_4 \qquad (7.9)$$

Two extreme engine running conditions can result in the same power output. If the engine bore is the same (equal swept volume), then the two stroke will run at half the speed of the four stroke for equal power. If the engines run at the same speed the two stroke cylinder bore will be smaller,

$$B_2 = \frac{B_4}{3\sqrt{2}} = \frac{B_4}{1.26} \qquad (7.10)$$

and the engine swept volume will be half that of the four stroke. In between these values there are an infinite number of combinations of bore and speed to provide equal power. In practice, because high specific output is usually sought, the two types of engines are usually operated at the same engine speed.

The cylinder pressure spectra shown in Fig. 7.3 provide a suitably representative result on which basis the combustion noise of the two cycles can be compared. The envelope of the spectra at frequencies above 500 Hz can be approximated by a straight line and

for the two stroke:

$$\text{CYLINDER PRESSURE LEVEL} = 20 \log_{10} \frac{P}{P_{ref}} = 40 \log_{10}(\frac{N_2}{f}) + 158 \qquad (7.11)$$

and, for the four stroke:

$$\text{C.P.L.} = 20 \log_{10} \frac{P}{P_{ref}} = 40 \log_{10}(\frac{N_4}{f}) + 152 \qquad (7.12)$$

N_2, N_4 = engine speed, revs/min

f = frequency, Hz.

It was shown in Chapter 5 that for the same engine structure the noise intensity, I,

$$I \propto (\text{COMBUSTION FORCE})^2$$

$$\propto (\text{CYLINDER PRESSURE} \times \text{BORE}^2)^2 \qquad (7.13)$$

and therefore with simple acoustic assumptions, that

$$\text{SOUND PRESSURE LEVEL (S.P.L.)} \propto (\text{CYLINDER PRESSURE} \times \text{BORE}^2)^2 \qquad (7.14)$$

at any frequency f.

Thus

for two stroke:

$$\text{S.P.L.}(f) \propto 40 \log_{10}\left(\frac{N_2 B}{f}\right) + 158 \qquad (7.15)$$

and for four stroke:

$$\text{S.P.L.}(f) \propto 40 \log_{10}\left(\frac{N_4 B}{f}\right) + 152 \qquad (7.16)$$

Since the engine structural and acoustical response is linear then the overall change in noise will be the same as that at any frequency f. On this basis, the overall combustion noise for the two cycles can be calculated.

7.1.5 Comparison of engines of equal bore size

From equations (7.15) and (7.16):

$$\frac{(\text{S.P.L.})_4}{(\text{S.P.L.})_2} = 40 \log_{10}\left(\frac{N_4}{N_2}\right) - 6 \text{ dB} \qquad (7.17)$$

If the two stroke engine is running at half the speed of the four stroke then the power output will be equal, and:

$$\frac{(\text{S.P.L.})_4}{(\text{S.P.L.})_2} = +6 \text{ dB} \qquad (7.18)$$

the four stroke will be 6 dB more noisy as compared to the two stroke.

If, however, the engines run at the same speed, the power output of the two stroke will be twice that of the four stroke, and:

$$\frac{(S.P.L.)_4}{(S.P.L.)_2} = -6 \text{ dB} \qquad (7.19)$$

and the two stroke engine will be 6 dB more noisy as compared to the four stroke engine.

7.1.6 Comparison of engines at equal rotational speed

At equal engine speeds for a given power output

$$B_2 = \frac{B_4}{3\sqrt{2}} = \frac{B_4}{1.26} \qquad (7.20)$$

and

$$\frac{(S.P.L.)_4}{(S.P.L.)_2} = 40 \log_{10}\left(\frac{B_4}{B_2}\right) - 6 \text{ dB}$$

$$= 40 \log_{10}(1.26) - 6 \text{ dB} \qquad (7.21)$$

$$= -2 \text{ dB}$$

and the two stroke will be 2 dB more noisy as compared to the four stroke.

For equal noise

$$B_2 = \frac{B_4}{4\sqrt{2}} \qquad (7.22)$$

and the comparative power outputs will be

$$\frac{(POWER)_2}{(POWER)_4} = \frac{2}{(1.414)^3} = 0.706 \qquad (7.23)$$

and the power of the two stroke will be some 30% lower than that of the four stroke.

Thus it is shown that for the same cylinder pressure development on a degree basis the effect of the cycle difference on combustion induced noise is very marked. For the same power output from the two cycle engine the choice of design parameters can produce an overall combustion noise variation of some 12 dB. The inherent quietness of the two stroke cycle is therefore apparent, it being possible to produce two stroke engines with a combustion noise level some 6 dB lower than that of the four stroke for a given power

output. With currently produced two stroke engines advantage of this characteristic is not taken fully because of the design choice putting specific output before that of noise.

7.2 Practical Comparison of Two and Four Stroke Operating Cycles

In practice there are many variations between individual engines and particularly between the two stroke and four stroke. These are discussed in Chapter 9. However, despite these differences, the general trends indicated by a theoretical consideration of combustion excitation are borne out in practice. Because of the limited availability of two stroke engines it has not been possible to make a direct comparison of a two stroke and four stroke diesel engine with the same power output at the same rated speed. However, a comparison is possible for two engines with the same bore. A normal six cylinder, In Line Direct Injection, normally aspirated, four-stroke diesel engine of 4.125 inches bore is compared to a conventional six cylinder, In Line, Direct Injection, Roots blown valve in head, two stroke diesel engine of 4.25 inches bore. The results are shown in figs. 7.7 and 7.8. Figures 7.7 show the two engines when compared at the same engine speed of 2000 revs/min, where the two stroke produces 210 bhp, the four stroke 103 bhp. The low frequency excitation is higher for the two stroke, as it is from 1500 Hz up to 4000 Hz. The resultant noise shows the same trend except that the high frequency (above 2000 Hz) noise produced by the four stroke engine is relatively low. The overall level of the two stroke is 101 dBA and that of the four stroke 99 dBA - exactly as would be predicted theoretically. Figure 7.8 shows the comparison for equal power - the two stroke engine now running at 1000 revs/min. Here the cylinder pressure excitation is much lower in the two stroke and this is reflected in the noise spectrum, the overall level of the two stroke now being some 4 dBA lower than that of the four stroke for the same power output.

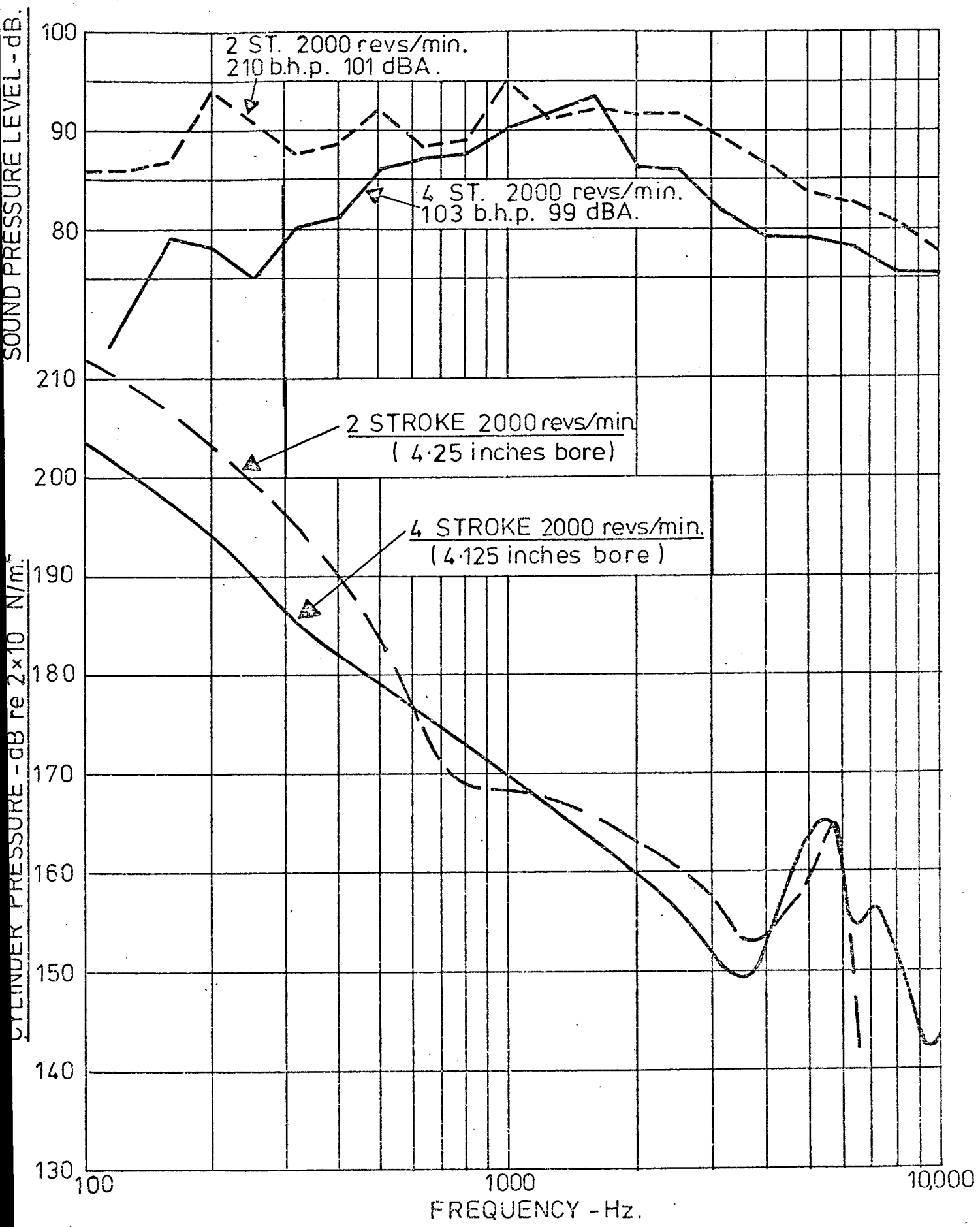

FIG. 7·7- COMPARISON OF EQUAL BORE ENGINES AT THE SAME SPEED.

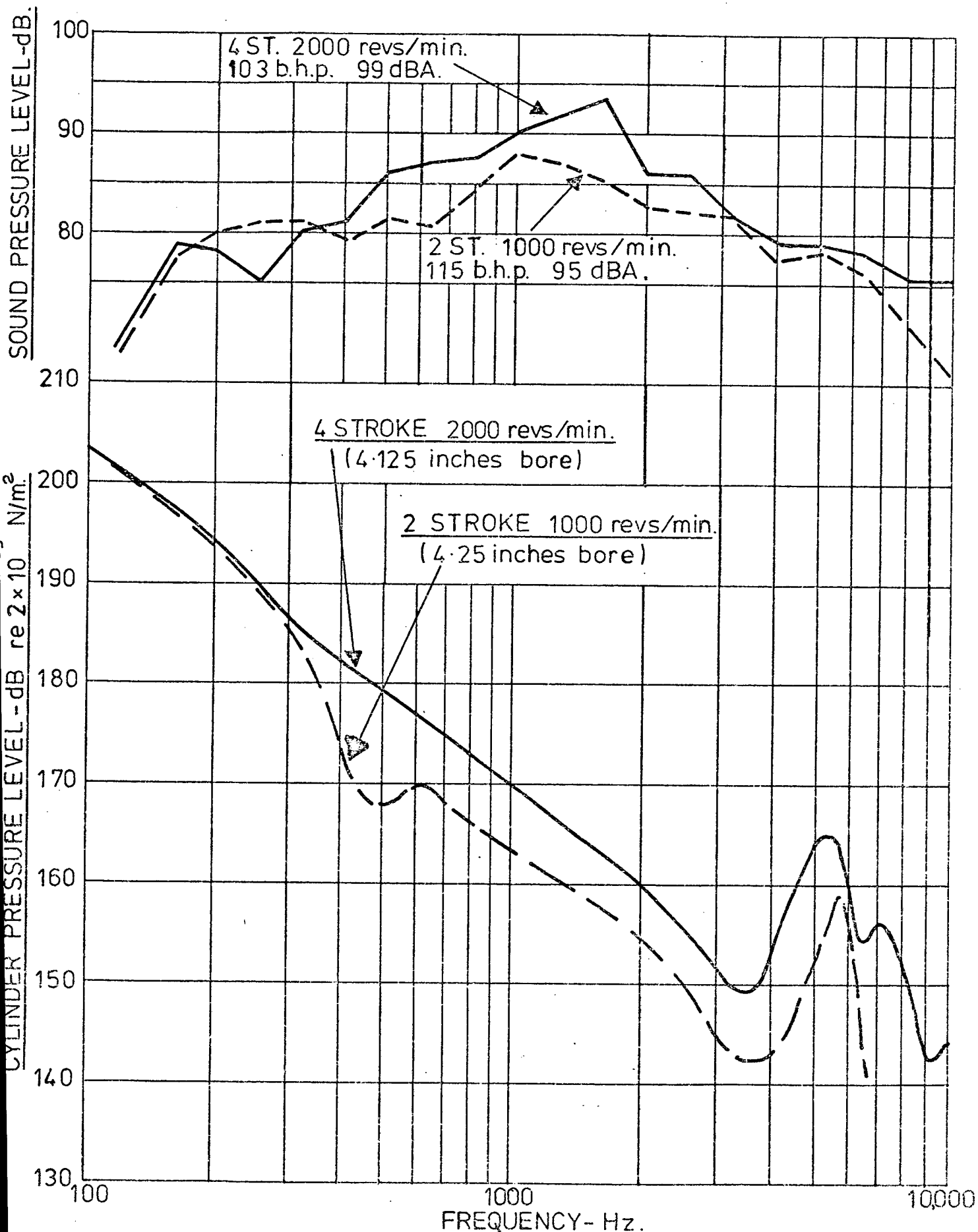

FIG.7·8- COMPARISON OF EQUAL BORE ENGINES AT THE SAME POWER.

7.3 Application of Fourier Analysis Methods to the Calculation of Indicated Horse Power in I.C. Engines

As has been shown, one cannot separate power output from noise when making a comparison between the combustion noise characteristics of the two and four stroke diesel cycles. This prompts the viewpoint, still widely held, that noise and power are synonamous in the I.C. engine and even machines in general. That this is an absurd view is very obvious when the noise levels of a small chain saw and a large marine diesel engine are compared. Generally the chain saw will have a higher noise level at perhaps 3 h.p. than the marine diesel at 10,000 h.p.

It was thought, therefore, that the application of the Fourier method to calculate I.C. engine power would furnish results which would indicate in which frequency ranges the major portion of power was transmitted from combustion pressure to crank mechanism.

7.3.1 Work done in I.C. engines

Generally the work done per cycle for any internal combustion engine is given by

$$\text{W.D./cycle} = A \oint_{A}^{B} p(x)dx \qquad (7.24)$$

where $p(x)$ = cylinder pressure as a function of piston displacement,
A = piston area.

Generally it is more convenient to express both the cylinder pressure and piston displacement as a function of time. Then equation (7.24) becomes

$$\text{W.D./cycle} = A \int_{o}^{T} p(t).\frac{dx}{dt}\,dt \qquad (7.25)$$

where $p(t)$ = cylinder pressure as a function of time

$x(t)$ = piston displacement as function of time

T = time for one cycle.

Thus the work done is the net area under the cylinder pressure times piston velocity graph. The Fourier series representation of both $p(t)$ and $x(t)$ can be written as:

$$p(t) = \frac{a_o}{2} + \sum_{p=1}^{\infty} \left(a_p \cos \frac{2\pi pt}{T} + b_p \sin \frac{2\pi pt}{T}\right) \qquad (7.26)$$

which repeats every T seconds

$$x(t) = \frac{a_o}{2} + \sum_{n=1}^{\infty} \left(a_n \cos \frac{2\pi nt}{T'} + b_n \sin \frac{2\pi pt}{T'}\right) \qquad (7.27)$$

which repeats every T' seconds

For the four stroke cycle $T = 2T'$, but for the two stroke cycle $T' = T$. From (7.27)

$$\frac{dx(t)}{dt} = \frac{2\pi}{T'} \sum_{n=1}^{\infty} n\left(B_n \cos \frac{2\pi nt}{T'} - A_n \sin \frac{2\pi nt}{T'}\right) \qquad (7.28)$$

Hence, substituting (7.26) and (7.28) in (7.25), we obtain:

$$\text{WORK DONE/cycle} = A \int_o^T \left\{\left|\frac{a_o}{2} + \sum_{p=1}^{\infty} \left(a_p \cos \frac{2\pi pt}{T} + b_p \sin \frac{2\pi pt}{T}\right)\right| \times \frac{2\pi}{T'} \left| \sum_{n=1}^{\infty} n\left(B_n \cos \frac{2\pi nt}{T'} - A_n \sin \frac{2\pi nt}{T'}\right)\right|\right\} dt \qquad (7.29)$$

7.3.2 The four stroke cycle

In this case $T = 2T'$, and hence (7.29) becomes:

$$\text{W.D./cycle} = \frac{4\pi A}{T} \int_o^T \left\{\left| \frac{a_o}{2} + \sum_{p=1}^{\infty} \left(a_p \cos \frac{2\pi pt}{T} + b_p \sin \frac{2\pi pt}{T}\right)\right| \left| \sum_{n=1}^{\infty} n \left(B_n \cos \frac{4\pi nt}{T} - A_n \sin \frac{4\pi nt}{T}\right)\right|\right\} dt.$$

Therefore,

$$\text{W.D./cycle} = \frac{4\pi A}{T} \left| \int_0^T \frac{a_o}{2} \left| \sum_{n=1}^{\infty} n\left(B_n \cos \frac{4\pi nt}{T} - A_n \sin \frac{4\pi nt}{T}\right)\right| dt \right.$$

$$+ \int_0^T \sum_{p=1}^{\infty} \sum_{n=1}^{\infty} \left(a_p \cos \frac{2\pi pt}{T} \; B_n.n \cos \frac{4\pi nt}{T}\right) dt$$

$$- \int_0^T \sum_{p=1}^{\infty} \sum_{n=1}^{\infty} \left(a_p \cos \frac{2\pi pt}{T} \cdot A_n.n.\sin \frac{4\pi nt}{T}\right) dt$$

$$+ \int_0^T \sum_{p=1}^{\infty} \sum_{n=1}^{\infty} \left(b_p \sin \frac{2\pi pt}{T} \cdot B_n.n.\cos \frac{4\pi nt}{T}\right) dt$$

$$- \int_0^T \sum_{p=1}^{\infty} \sum_{n=1}^{\infty} \left(b_p \sin \frac{2\pi pt}{T} \cdot A_n.n.\sin \frac{4\pi nt}{T}\right) dt \qquad (7.30)$$

Now it can be shown that (ref. 7.1)

(a) $\int_0^{2\pi} \sin mx. \sin nx \, dx = 0$

(b) $\int_0^{2\pi} \sin mx. \cos nx \, dx = 0$ if m and n are unequal integers

(c) $\int_0^{2\pi} \cos mx. \cos kx \, dx = 0$

(d) $\int_0^{2\pi} \sin kx. \cos kx \, dx = 0$ (7.31)

(e) $\int_0^{2\pi} \sin kx \, dx = 0$

(f) $\int_0^{2\pi} \cos kx \, dx = 0$ if k is an integer

(g) $\int_0^{2\pi} \sin^2 kx \, dx = \pi$

(h) $\int_0^{2\pi} \cos^2 kx \, dx = \pi$

From equations (7.31) it can be shown that all the terms in equation (7.30) are zero except when $\sin^2 kx$ or $\cos^2 kx$ are involved. This is only so for two terms and then only when $p = 2n$. Thus, the double summation is reduced to a single infinite sum of values for $p = 2n$.

Thus

$$\text{WORK DONE/CYCLE} = \frac{4\pi A}{T} \sum_{n=1}^{\infty} n.\frac{T}{2} (a_p B_n - b_p A_n)$$

or put in terms of harmonics of the engine speed

$$\text{W.D./cycle} = \pi A \sum_{m=1}^{\infty} (a_{2m} B_m - b_{2m} A_m) \qquad (7.32)$$

Therefore,

$$\text{INDICATED POWER} = \frac{\pi.A.N.}{33,000} \sum_{m=1}^{\infty} 2m(a_{2m} B_m - b_{2m} A_m) \quad \text{h.p.} \qquad (7.33)$$

where N = camshaft revs/min.

Now the general expression for power in a four stroke I.C. engine is

$$\text{POWER} = \frac{\pi.N.\ T.}{33,000} \qquad (7.34)$$

Thus,

$$A\left| \sum_{m=1}^{\infty} m(a_{2m} B_m - b_{2m} A_m) \right| = T \qquad (7.35)$$

where, in this case, T is the <u>indicated torque</u> of the engine.

In terms of engine speed then:

$$\text{INDICATED POWER IN FOUR STROKE CYCLE} = \frac{\pi.A.N.}{33,000} \sum_{m=1}^{\infty} m(a_{2m} B_m - b_{2m} A_m) \qquad (7.36)$$

N = engine revs/min.

Thus the indicated power output of a four cycle I.C. engine can be obtained from a summation of products of the Fourier coefficients of cylinder pressure and piston motion functions. Because the cycle repetition frequency is one half that of the piston motion, then in the four stroke cycle

only the even numbered harmonics will contribute to the engine power.

7.3.3 The two stroke cycle

The analysis is the same for the two stroke cycle except that the piston displacement

$$x(t) = \frac{A_o}{2} + \sum_{n=1}^{\infty} \left(A_n \cos \frac{2\pi nt}{T} + B_n \sin \frac{2\pi pt}{T}\right) \qquad (7.37)$$

Thus the non-zero terms in equation (7.30) form a single infinite series in which p = n. Thus,

$$\text{W.D./cycle} = \frac{2\pi A}{T} \sum_{m=1}^{\infty} m.\frac{T}{2} (a_m B_m - b_m A_m)$$

$$= A \sum_{m=1}^{\infty} m(a_m B_m - b_m A_m) \qquad (7.38)$$

and

$$\text{INDICATED POWER IN TWO STROKE CYCLE} = \frac{\pi.A.N.}{33,000} \sum_{m=1}^{\infty} m(a_m B_m - b_m A_m) \quad \text{h.p.}$$

N = engine revs/min.

A similar result for indicated power is found for the two stroke cycle except that in this case all the harmonics, whether odd or even, contribute to the engine power.

7.3.4 Power produced when the connecting rod is very long

In the conventional crank mechanism if the connecting rod is very long the piston displacement is given by

$$x(t) = R.|1 - \cos \phi| \qquad (7.39)$$

In this case there is only one A.C. harmonic component:

$$A_1 = R_o \qquad (7.40)$$

Therefore,

$$(I.H.P.)_{2st.} = \frac{\pi.A.N.}{33,000}\ b_1 R_o = \frac{\pi.A.R_o.N}{33,000}\ (b_1)_{2st.}$$

$$(I.H.P.)_{4st.} = \frac{\pi.A.N.}{33,000}\ 2b_2 R_o = \frac{\pi.A.R_o.N}{33,000}\ (b_2)_{4st.} \qquad (7.41)$$

where suffix 2st. indicates 2 stroke cycle and 4st. indicates 4 stroke cycle. It can be shown that for the same pressure diagram on a degree basis that the values of the harmonics of the cylinder pressure diagram when treated as a two and four stroke cycle are

$$(b_1)_{2st} = 2(b_2)_{4st} \qquad (7.42)$$

Hence, from (7.41)

$$(I.H.P.)_{2st.} = 2(I.H.P.)_{4st} \qquad (7.43)$$

Equation (7.43) is only true for the same crank mechanism and the same cylinder pressure development on a degree basis for both cycles of operation.

7.3.5 Indicated power produced in the two types of cycle

Consider a fixed bore and stroke engine.

The piston displacement for a normal crank mechanism is given by

$$x(t) = R_o\left|1 - \cos\phi + \frac{L_{CR}}{R_o}\left(1 - \sqrt{\left(1 - \frac{(R_o)^2}{L_{CR}}\sin^2\phi\right)}\right)\right|. \qquad (7.44)$$

Therefore, as the connecting rod length L_{CR} is reduced the piston motion becomes a distorted sinusoid and will then have a large number of harmonic components. This is shown in fig. 7.9 where the harmonic analysis of piston motion for various L/R ratios is shown. The modulus results are plotted in decibels so that the level of the higher order harmonics can be seen. Zero piston motion occurs at top dead centre and so, relative to this phasing, it is seen that the series is mainly a cosine one. Only the first, second, fourth, sixth, etc., harmonics have substantial levels, the third, fifth, seventh, etc., being suppressed. The connecting rod to crank

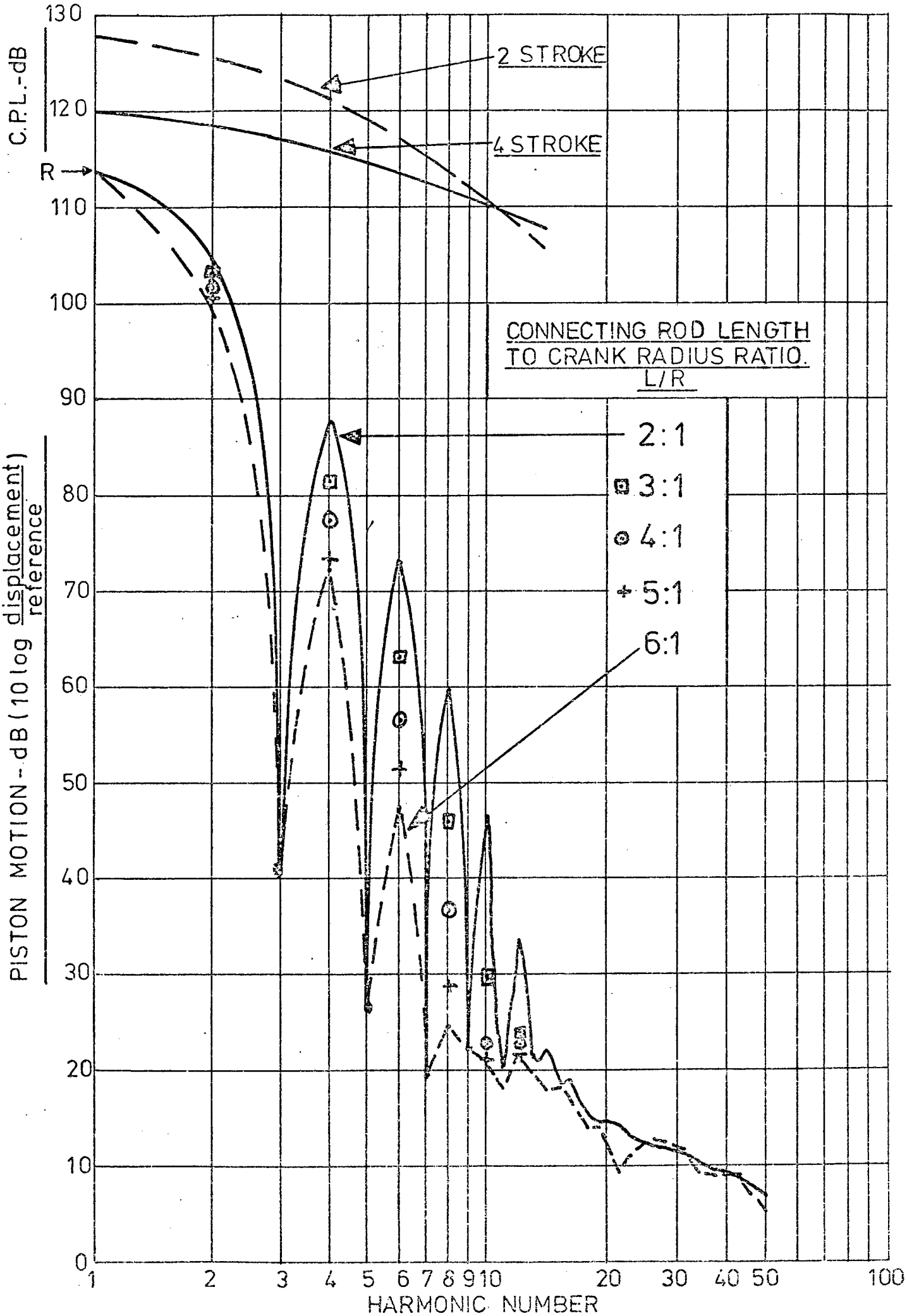

FIG. 7·9 - HARMONIC ANALYSIS OF PISTON MOTION.

radius ratio, as it reduces from 6:1 to 2:1, increases the levels of the even harmonics substantially. Also shown in fig. 7.9 are typical cylinder pressure spectrum level values for the two and four stroke diesel cycles. It can be seen that both show decreasing levels with increasing harmonic number. Thus in the computation of indicated power using the relationships derived in the previous section (equations (7.36) and (7.38)) it will be observed that as the summation of Fourier coefficient products progresses the values of the coefficients are rapidly reducing. Computations of typical values have shown that even with several hundred harmonics contributing to the summation it reaches a steady value after only a few harmonics. If the amplitude values for the piston motion are taken, the reason for this becomes more clear. Table 7.1 illustrates the values of the modulus, cosine and sine components for two L/R ratios. At an L/R ratio of 6:1 the fourth harmonic amplitude is 0.0073% of the fundamental, and it is clear that, with values for the cylinder pressure Fourier coefficients reducing, there will only be major power transferred at the first and second harmonic. Even then the second harmonic will contribute only some 5.2% of the fundamental. As the engine is shortened in height and the L/R ratio approaches 3:1, then the contribution of the second harmonic increases to 8.4% with the fourth harmonic contributing 0.063%. It is thus clear that in general the power will be mostly transferred at the first two harmonics of piston motion (i.e., engine rotational speed).

The modulus, cosine and sine component values for typical two and four stroke diesel engine cylinder pressure spectra are shown in Table 7.2. The values do not decrease as rapidly as those of the piston motion, but it is shown that the values for the two stroke cycle fall off more rapidly than those of the four stroke. This indicates that changes in pressure development as a result of changing L/R ratio will be more marked in the four stroke cycle than the two stroke.

Table 7.1: HARMONIC SERIES VALUES FOR PISTON MOTION FOR TWO EXTREME VALUES OF L/R RATIO

Connecting Rod Length to Crank Radius Ratio	Harmonic Number	Cosine Component A(K) inches	Sine Component B(K) inches	Modulus R(K) inches	% of R(1)
6:1	1	1.999440	0.000011	1.999944	100
	2	0.083818	0.000000	0.083818	4.2
	3	0.000000	"	0.000000	0
	4	0.000147	"	0.000147	0.0073
	5	0.000000	"	0.000000	0
	6	0.000000	"	0.000000	0
3:1	1	1.999440	0.000011	1.999944	100
	2	0.171550	0.000000	0.171550	8.57
	3	0.000000	"	0.000000	0
	4	0.001262	"	0.001262	0.063
	5	0.000000	"	0.000000	0
	6	0.000000	"	0.000000	0

Table 7.2: HARMONIC SERIES VALUES FOR TYPICAL TWO AND FOUR STROKE DIESEL ENGINES

Harmonic Number K	Direct Injection 4-Stroke			Valve-in-head 2-Stroke		
	Cosine Component A(K) lb/in^2	Sine Component B(K) lb/in^2	Modulus R(K) lb/in^2	Cosine Component A(K) lb/in^2	Sine Component B(K) lb/in^2	Modulus R(K) lb/in^2
1	+68.9	+99.11	120.71	-241.24	+154.81	286.65
2	-38.23	+93.84	101.34	+117.41	-174.57	210.38
3	-81.89	+12.56	82.85	-5.96	+150.27	150.39
4	-44.32	-53.70	69.63	-48.82	-98.10	109.58
5	+18.35	-55.38	58.34	+62.95	+46.33	78.16
6	+45.55	-11.25	46.92	-55.12	-5.02	55.35
7	+26.38	+26.09	37.11	+37.93	-20.82	43.27
8	-6.71	+29.37	30.13	-17.08	+28.24	33.01
9	-23.43	+8.40	24.89	-0.86	-24.12	24.14
10	-16.01	-12.65	20.40	+12.25	+15.10	19.44

From this analysis we can conclude that the indicated horse power in I.C. engines is given by

$$\text{INDICATED HORSE POWER IN FOUR STROKE CYCLE} = \frac{\pi.A.N.}{33,000}\left(a_2B_1 - b_2A_1 + 2a_4B_2 - 2b_4A_2\right)$$

where N = engine, revs/min

a_n, b_n = Fourier coefficients of cylinder pressure spectrum

A_n, B_n = Fourier coefficients of piston motion spectrum (7.45)

and

$$\text{INDICATED HORSE POWER IN TWO STROKE CYCLE} = \frac{\pi.A.N.}{33,000}\left(a_1B_1 - b_1A_1 + 2a_2B_2 - 2b_2A_2\right) \quad (7.46)$$

which is a comparatively simple operation once the Fourier coefficients are determined. It also shows quite clearly that the harmonics which produce power are the very low order harmonics, whilst the harmonics responsible for noise are those above this range (generally 10th harmonic and above). Thus there is no direct relation between combustion induced noise and engine power. This is illustrated in fig. 7.10 for both I.C. engines and some general machines.

7.3.6 Continuous monitoring of I.M.E.P.

The relations given for indicated power could form the basis of a continuous I.M.E.P. monitoring system. Equations (7.45) and (7.46) could be calculated continuously by a modified form of electronic hand calculator. The electrical analysis of the necessary Fourier coefficients could be carried out by a modified form of hetrodyne analyser and fed to the calculator. The electrical pressure signal could be obtained in the usual way and the piston motion generated electronically. This would have the advantage that the two signals could be dynamically timed to make sure that they were exactly phased, which is necessary for accurate measurements and is a difficulty often encountered in I.C. engine work. The engine timing requirements are exactly the same as for the standard method of measurement.

RELATION BETWEEN NOISE AND POWER

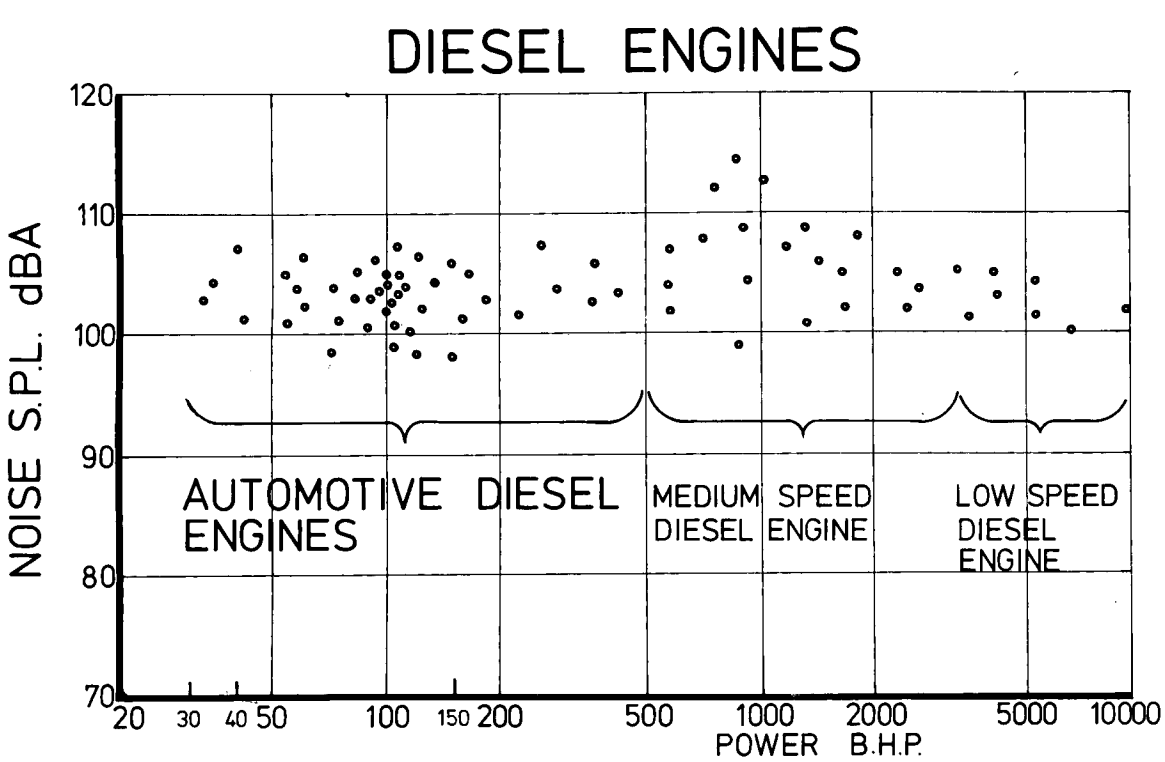

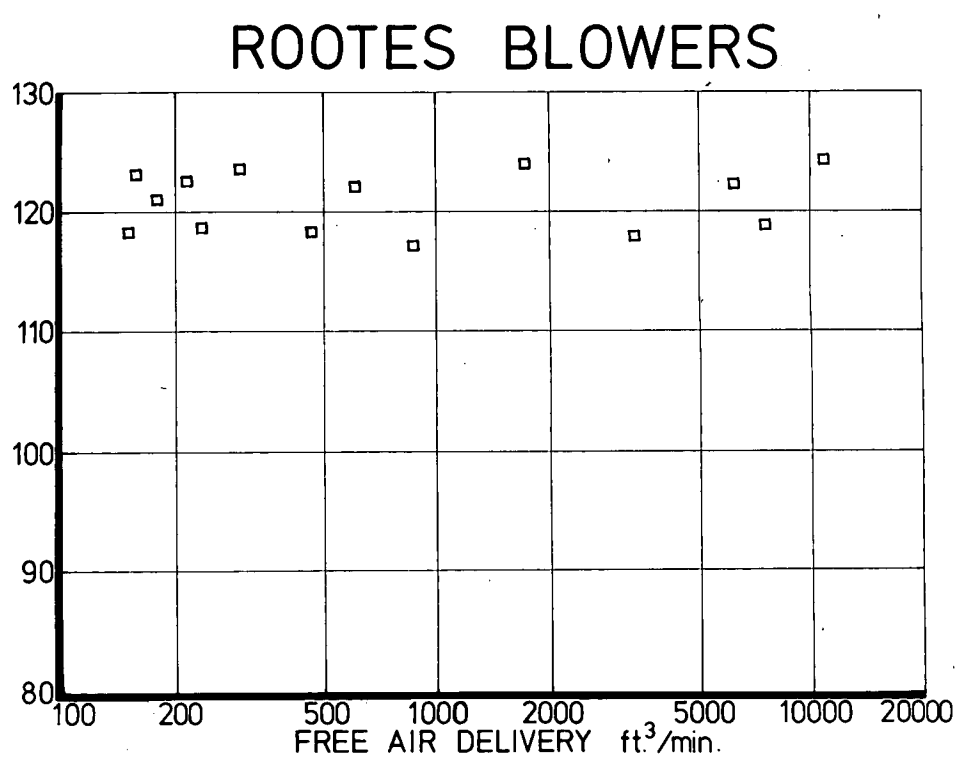

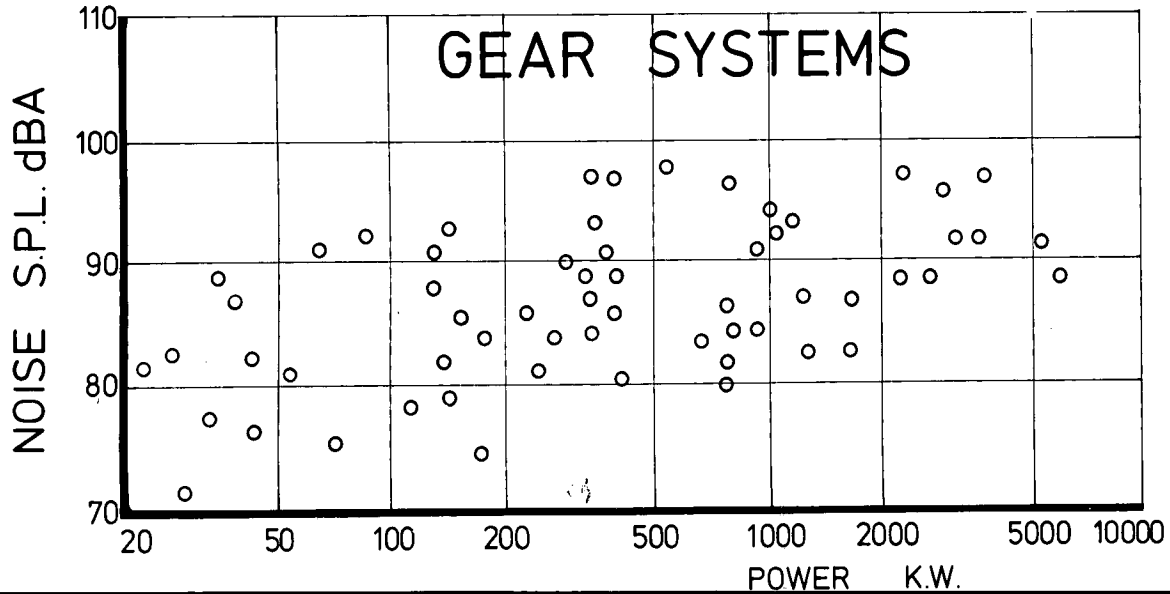

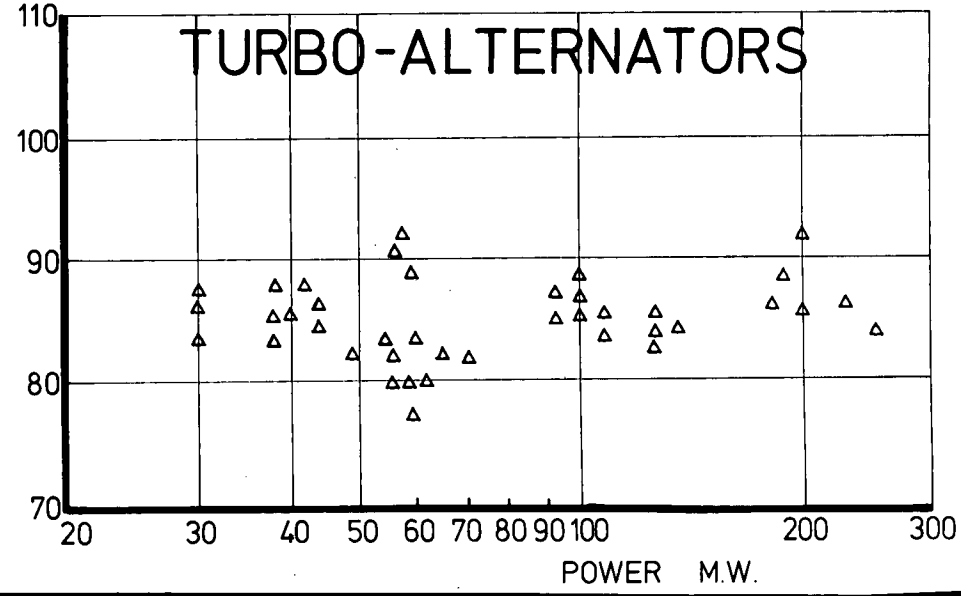

7.4 Effect of Cylinder Pressure Diagram Width on Fundamental Harmonic Value

Since the cylinder pressure diagram width affects the values of the cylinder pressure spectrum, this can be used to compare the various engine cycles. The level of the cycle fundamental provides a convenient measure, and the effect that the cylinder pressure diagram width has on the fundamental or first harmonic of the cylinder pressure analysis is shown in Fig. 7.11. The four stroke engines group together at the lower end and the two stroke engines at the upper end. Turbocharged four cycle engines will tend towards the two stroke region, the effect of turbocharging being to increase rapidly the first harmonic amplitude - both because of a diagram width increase and additional peak pressure. The higher into the two stroke region the value of a fundamental reaches, then the higher will be the specific power output of that engine. The figure can therefore be regarded as an indication of power output per unit piston area.

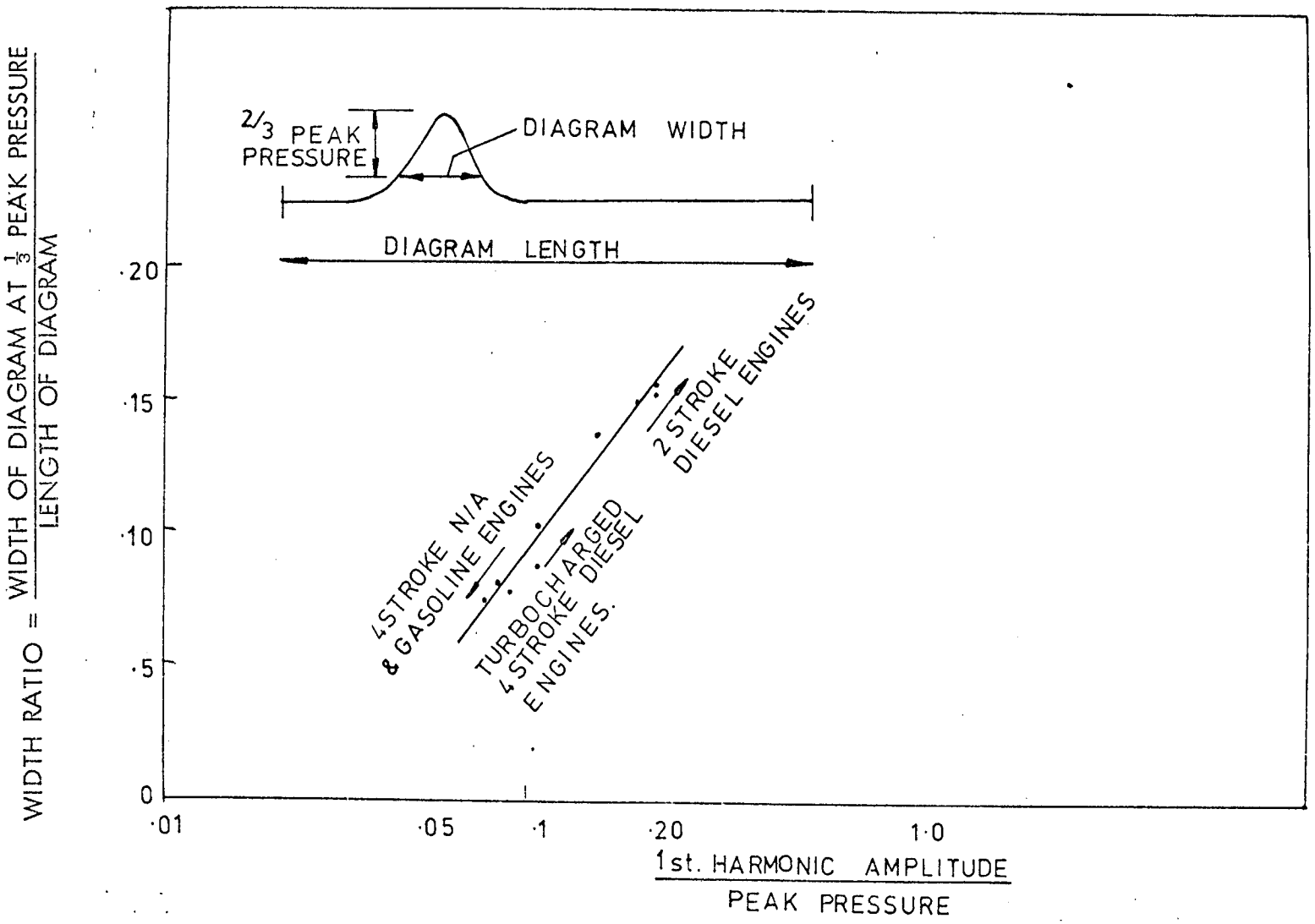

FIG. 7·11 - EFFECT OF CYLINDER PRESSURE DIAGRAM WIDTH ON AMPLITUDE OF 1st HARMONIC OF CYLINDER PRESSURE ANALYSIS.

REFERENCES

7.1 R.D. Stuart - 'An introduction to Fourier analysis'. Methuen, London

8.0 EFFECT OF PEAK PRESSURE, RATE OF PRESSURE RISE AND ACCELERATION OF PRESSURE RISE ON COMBUSTION EXCITATION

As is made clear in the literature survey of Chapter two, there is, even now, a considerable variation of test data and opinion as to which of the three main variables of a cylinder pressure diagram (peak pressure, rate of pressure rise or acceleration of pressure rise) control combustion excitation. It is important to know this if quieter and more vibration free Internal Combustion engines are to be developed. The fact that so much variation of opinion exists indicates the complexity of the task, and in this chapter an attempt is made to explain why so many different results have been obtained in practice.

The tool which has not been available previously is that of the computer, and in particular the ability to compute, by Fast Fourier Analysis, the cylinder pressure spectra of cylinder pressure developments in which completely known changes can be introduced.

8.1 Interpretation of the Fourier Analysis Method

The basic definition and calculation of the Fourier analysis method has been described in chapters four and five. If the Fourier coefficients, together with their phase information can be calculated, the summation of these according to equation (4.1) will exactly specify the level-time history of the waveform which has been analysed (if enough coefficients are used) whether this is transient or repetitive. The same is true for a similar analysis of structure response, noise, etc. Therefore, the spectrum of sine and cosine Fourier coefficients is truely representative of the original function, converting it from a level-time to a level-frequency history. However, care must be taken in accepting this mathematical relation too literally when describing the response (or input) to a system. The value of the harmonics in the spectrum is the root mean square value of a sine wave

at a frequency which exists only for the period T of the transient or repetition period T_R of a cyclic function. Thus if in the original level-time history a strong frequency component is present, at a constant amplitude, then the Fourier coefficient will represent both its maximum and r.m.s. value. If, however, the strong frequency component exists only for a portion of the period then the r.m.s. value will still be truely represented by the Fourier coefficient r.m.s. value but the peak value of the component is not. To obtain this peak value then the level-time history must be formed by summation of the Fourier coefficients and examination of the result. This then is the crux of the difference between the Fourier approach and that of calculating the deformation of a structure to a given load. In the former the r.m.s. values of response can be obtained: in the latter the peak values (and subsequently, the r.m.s. values). The difference can be clearly seen in a comparison of the peak to peak value for cylinder pressure oscillation in Fig. 9.5 of 125 lb/in^2 and the spectrum r.m.s. value at 6300Hz of 0.35 lb/in^2.

Since measurement, for the purpose of noise assessment, is carried out using the r.m.s. value of the signal, then the Fourier approach is justified. If the resultant peak amplitudes are of concern then the response of a system to the actual loading presents a better approach.

8.2 General Considerations

As Hinze observed in his paper in 1949 (2.20) 'It is fundamentally impossible to express the effect of the particular shape of the pressure time curve on the response of the vibrating system in terms of one single time derivative of the pressure time curve, for the same reason that it is fundamentally impossible to express the particular shape of the pressure-time curve in terms of one single derivative'. In other words, the complete Fourier Series representation is needed.

In practice it is useful to possess such information as to be able to determine what is in fact the best overall shape to aim for, given certain boundary conditions. Therefore, the main observable characteristics are put forward here for this reason.

For cyclic functions, the Fourier series is described in terms of harmonics, the frequency of each harmonic being determined by the cycle period. Therefore, for a given harmonic series the frequency range occupied by a range of harmonics will vary. Because of this characteristic, a more general presentation of results can be given in terms of harmonics.

On this basis the comparison of rate of pressure rise, etc., are specified in terms of their relation to the cycle period, and can therefore be related to crankshaft degrees rather than time. Thus the harmonics affected by a rate of pressure rise of n lb/in^2/degree will always be the same. However, the frequency range will depend on the engine speed and a frequency band covered by all normal operating speeds for I.C. engines can therefore be specified.

8.3 Effect of Peak Cylinder Pressure

If the scaling on a cylinder pressure diagram is changed then the effect is to increase or reduce the whole spectrum by the log ratio of the change and in this case the shape of the development is unaffected. If, however, the peak pressure alone is increased, then to obtain such a diagram the rate of pressure rise or acceleration of pressure rise must also increase. Therefore, the shape of the diagram relative to its repetition period will be changed and a general increase in the level of the spectrum is expected, the exact change depending on the new diagram shape.

In general it is found that the first few (10-20) harmonics change their amplitude directly as the peak pressure. The actual amplitude will depend on the peak pressure and also the diagram width (fig. 7.11) and shape. Doubling

the diagram width, as changing from four stroke to two stroke operation, and doubling the peak pressure will both approximately double the levels of the first four or five harmonics (increasing cylinder pressure spectrum levels by 6 dB). The shape factor will vary the level of the fundamental from one tenth peak pressure for a typical normally aspirated four stroke engine to peak pressure for a pure sine wave.

The value of these low frequency harmonics is not important from the point of view of engine surface radiated noise. However, they are important from a consideration of engine power output and engine structure vibration transmitted to, for example, a car body and radiated into the car passenger space as structure borne noise.

8.4 Effect of Acceleration of Cylinder Pressure Rise

In Fig. 8.1 are shown cylinder pressure diagrams from engines with widely differing combustion systems: (a) a diesel engine with toroidal combustion chamber employing four hole injector, (b) M.A.N. diesel employing a combustion system where the fuel is sprayed on the wall of the combustion chamber to reduce the amount of fuel/air mixture which ignites spontaneously at the onset of combustion, and (c) a high performance petrol engine. In all three engines, the timings were set so that approximately the same main rate of pressure rise was obtained, i.e:, between 44 and 50 lb/in^2/Deg. and about the same peak pressure, 1000 to 1200 lb/in^2.

Figure 8.1(a) shows the diagram of the conventional D.I. engine. This diagram is characteristic of a normally aspirated type showing a rapid initial pressure rise abruptly breaking away from the compression curve. From this initial point the rate of pressure rise gradually decreases. The mean rate is about 50 lb/in^2/deg.

The smoothing of this discontinuity (the part of the pressure diagram indicated by a circle) has been a problem with which many investigators have

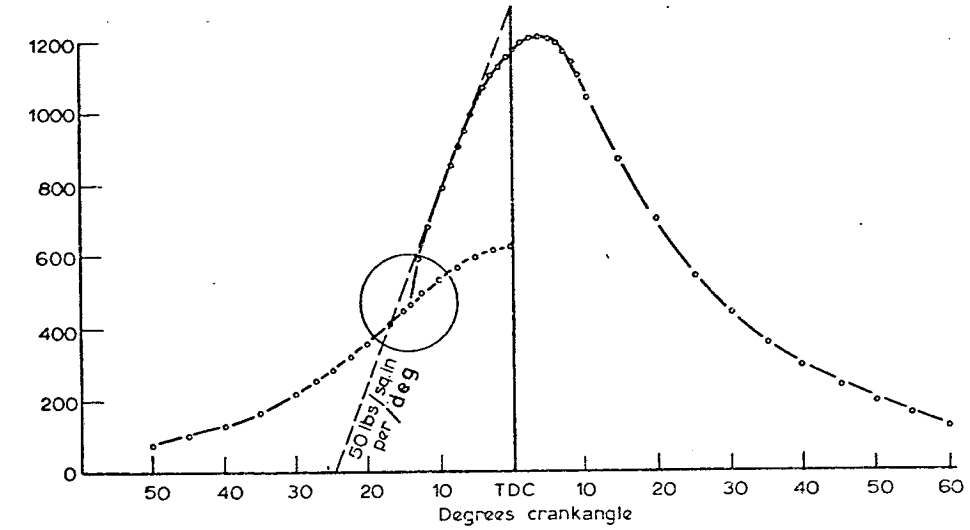

(a) Direct injection engine with toroidal chamber - four hole injector.

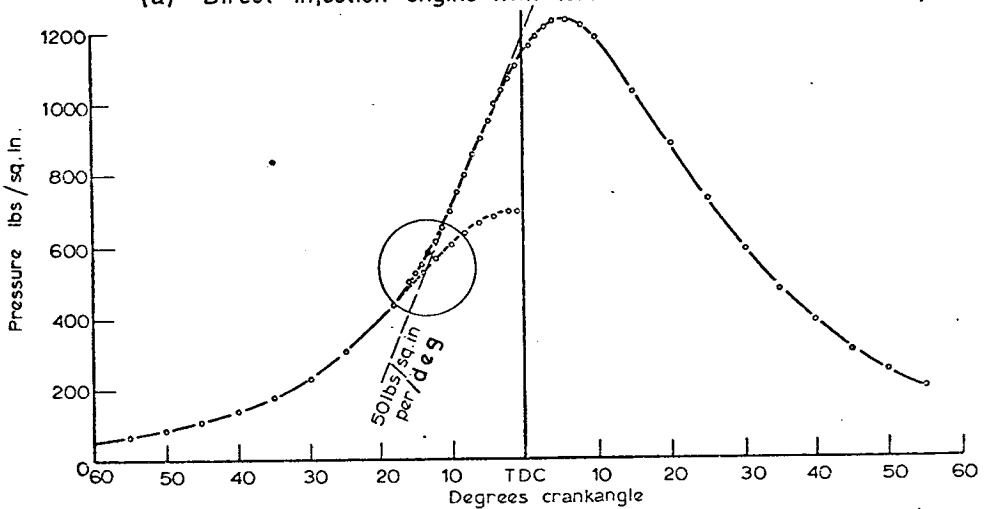

(b) M.AN combustion system - two hole injector - fuel sprayed on the wall of combustion chamber.

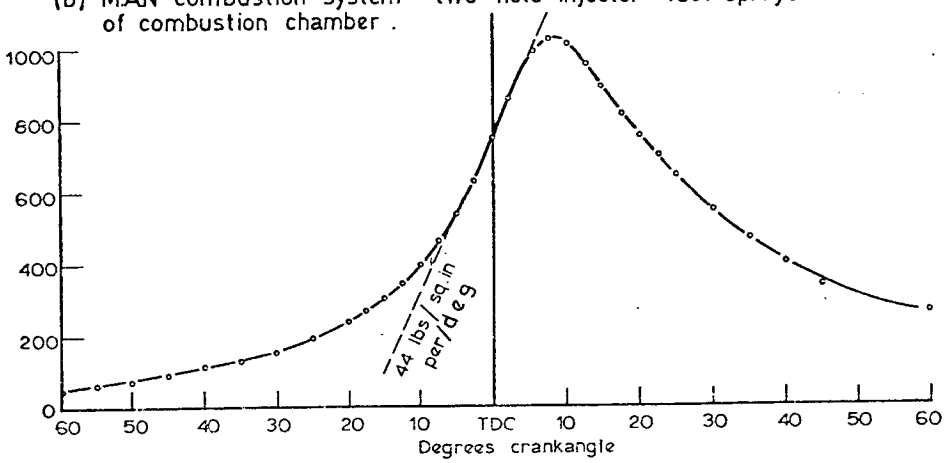

(c) High performance petrol engine

Fig.8·1 Comparison of cylinder pressure development of conventional D.I., M.A.N. and petrol engine. Engine speed 1000 r.p.m. full load.

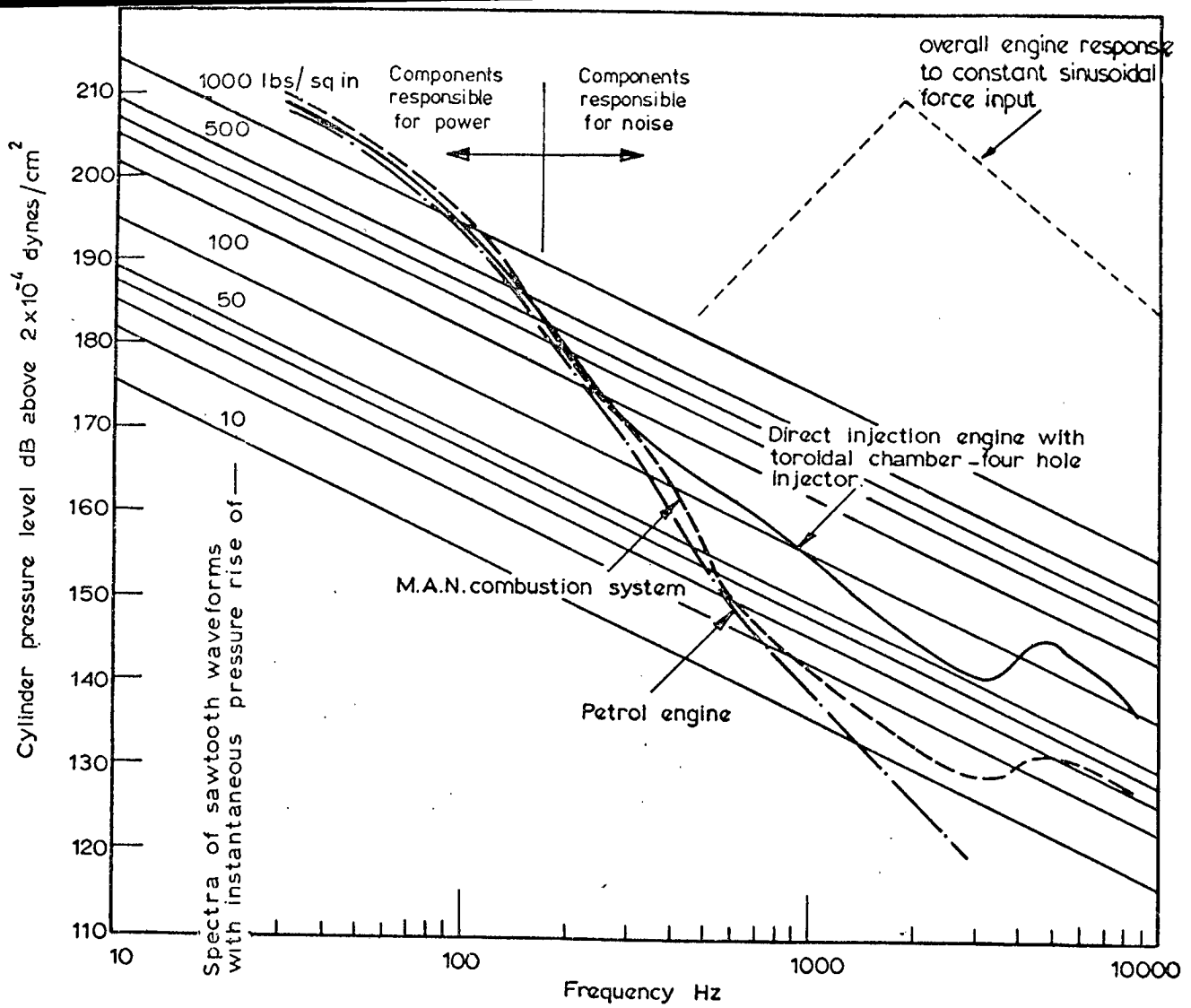

Fig. 8·2 Cylinder pressure spectra of a conventional D.I., M.A.N. and petrol engine. Engine speed 1000 r.p.m full load.

attempted to deal. Injection characteristics, swirl, and compression ratio have certain effects on this part of the diagram. Lyn (ref. 8.1) demonstrated that, by inducing paraffin fuel spray into the engine air intake, smoothing takes place accompanied by a pronounced reduction of engine noise. This illustrates the important role of this initial pressure rise. Similar effects have also been observed with a pilot injection system.

Meurer (ref. 8.2) developed the M.A.N. combustion system, which has been used successfully in automotive engines, giving extremely smooth pressure development over the whole operating range of the engine. Fig. 2(b) shows a pressure diagram from the M.A.N. engine which is almost identical to the conventional D.I. engine diagram except for the small part indicated by the circle.

Figure 8.2 shows the comparison of the spectra. It is interesting to observe that the spectra up to 300-400 Hz are exactly the same, indicating that harmonics up to this frequency are determined by the general shape of the pressure development and the value of the peak cylinder pressure. From 400 Hz a marked reduction of cylinder pressure components by as much as 15 dB is noted in comparison with the D.I. engine.

Figure 8.2(c) shows the pressure diagram of a high-performance petrol engine which has about the same peak pressure and rate of pressure rise. As can be seen from Fig. 8.2, the M.A.N. cylinder pressure spectrum is about the same as that of the petrol engine.

This enormous difference in cylinder pressure level in the high frequency range is due to the small discontinuity and rapid initial pressure rise. The acceleration of pressure rise is some 157 psi/deg/deg and magnitude of pressure rise some 100 psi at 160 psi/deg. To reduce this high level of excitation in the high frequency range, smoothing is only necessary in the

area indicated by a circle in Fig. 8.1(a) and (b). For the M.A.N. engine by this means the maximum rate of acceleration of pressure rise occurs near peak pressure (20 psi/deg/deg) whilst the maximum rate of pressure rise is reduced to 50 psi/deg. The high frequency components of cylinder pressure spectra are largely responsible for the predominant noise of the diesel engine and excite the frequency range of maximum response as shown in Fig. 8.2. In Fig. 8.2 are also shown the calculated cylinder pressure levels for various degrees of instantaneous pressure rise which confirms that a small (only about 100 psi) instantaneous pressure rise is sufficient to produce the whole high-frequency noise of the engine. This is verified very clearly in gasoline engines when, due to detonation, a small rapid pressure rise produces high intensity audible noise.

More insight into the relative importance of the three parameters can be gained from a comparison of the characteristics of Very High Output (V.H.O.) diesel engines.

During the last decade considerable success has been made on developing (V.H.O.) diesel engines for military applications, and engines up to 400 lb/in^2 b.m.e.p. have been developed.

The Caterpillar Tractor Company has achieved this output with a fixed compression and designed engine structures which can readily withstand peak pressures of the order of 3,000 lb/in^2 (refs. 8.3 and 8.4). Research at the British Internal Combustion Engine Research Institute has shown that with B.C.E.R.I. variable compression ratio pistons, high outputs are feasible by limiting the peak cylinder pressure to a value consistent with the strength of the engine by automatically increasing the cylinder clearance volume with increase of engine load (refs. 8.5 and 8.6). The successful development of this engine has been fully described (ref. 8.7).

It is therefore of interest to consider the effects of the two developments on combustion induced noise. Computer studies were made based on the

data of cylinder pressure diagrams published by Robinson and Mitchel (ref. 8.8) for a fixed ratio piston and variable ratio piston supplied by B.I.C.E.R.I.

Figs. 8.3 and 8.4 compare these two methods of obtaining 360 lb/in^2 b.m.e.p. In both cases the rate of pressure rise is the same at about 65 lb/in^2/degree. The corresponding peak pressures are 1,500 and 3,300 lb/in^2, at 1500 revs/min.

The following variables are considered:-

(i) In both cases a smooth blending of pressure rise with the compression curve is assumed as shown in Fig. 8.3. The variable compression ratio piston offers a considerable reduction of cylinder pressure level (6 dB) over the whole frequency range.

(ii) In this case a smooth pressure development is assumed for a fixed compression ratio engine and an abrupt pressure development for a variable ratio piston engine.

The spectra shown in Fig. 8.3 illustrates that even in this case there is a considerable advantage in favour of the variable ratio piston. Over the whole low-frequency range extending up to 400 Hz the fixed ratio cylinder pressure level is by 8 dB higher, while in the high frequency range the level of both the systems is about the same. This indicates that the general shape of the pressure diagram with very high peak pressure, despite its smoothness, results in higher values of the high-frequency harmonics.

(iii) For the fixed ratio engine the effect of the smoothing at the same peak pressure of 3,300 lb/in^2 is illustrated in Fig. 8.4. The effect is similar to that observed on normally-aspirated D.I. engines. Low-frequency harmonics are the same; from 200 Hz smoothing becomes noticeable but the main effect becomes apparent from 600 Hz upwards. In this case the maximum rate of pressure rise was kept constant and the increase in levels is due solely to the increase in acceleration of rate of pressure rise.

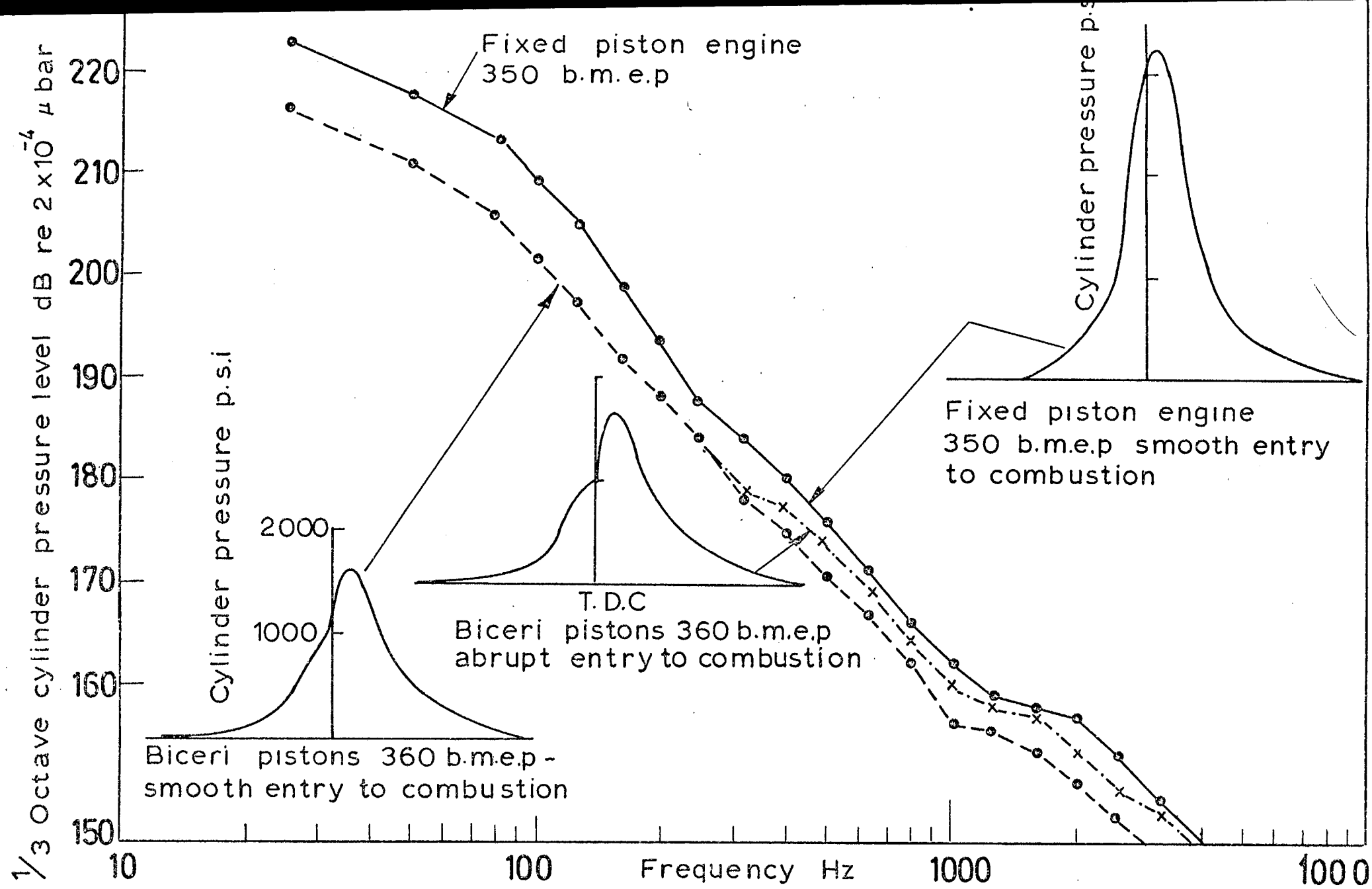

Fig. 8·3-Comparison of computed cylinder pressure spectra for a fixed piston engine and a Biceri piston engine at high b.m.e.p and 1500 r.p.m.

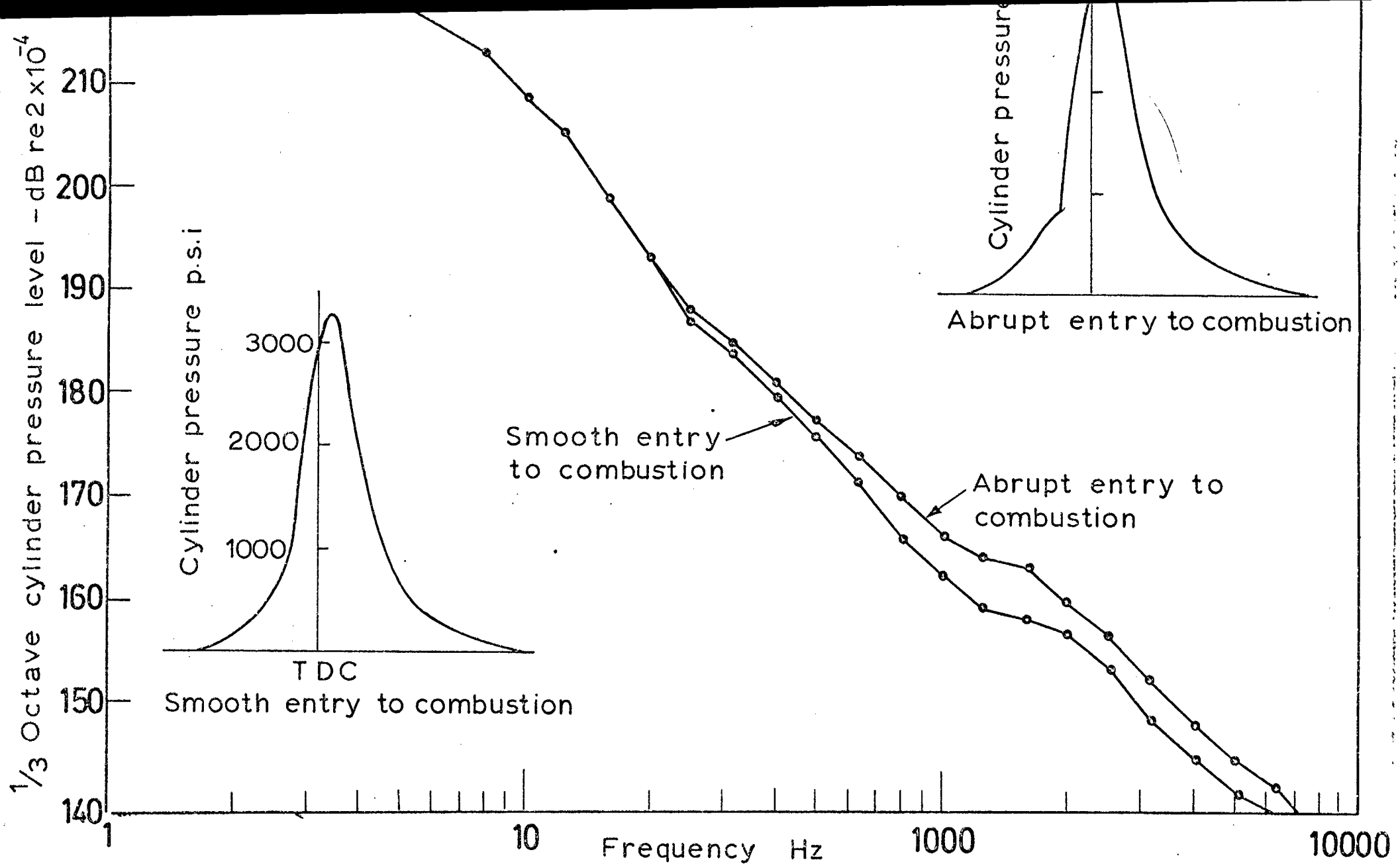

Fig.8·4-Effect of smoothing entry to combustion on an extremly high peak pressure diagram giving 350 b.m.e.p.

The smooth entry fixed piston spectra shows the effect of increased peak pressure, even with smooth entry to combustion, to be a general increase in spectrum level through the audio frequency range.

Referring back to Fig. 8.2, the increase in high frequency spectrum levels for the D.I. was attributed to a 100 psi instantaneous pressure rise. Actually the rate of rise was 160 psi/deg. and thus, since from Fig. 8.3 and 8.4 the effect of acceleration in pressure rise extends from 200 Hz (16th harmonic) upwards it can be deduced that the increase in spectrum level is due to a combination of high rate of pressure rise and high acceleration of pressure rise.

It can be concluded that high acceleration of pressure rise (above 20 psi/deg/deg) at any part of the diagram will introduce an increase in the cylinder pressure spectrum levels at all harmonics above the 16th.

8.5 Effect of Rate of Pressure Rise

By comparing the general form of a sawtooth waveform as shown in Fig. 8.5 to the repeating form of cylinder pressure development, the effect of overall rate of pressure rise can be assessed.

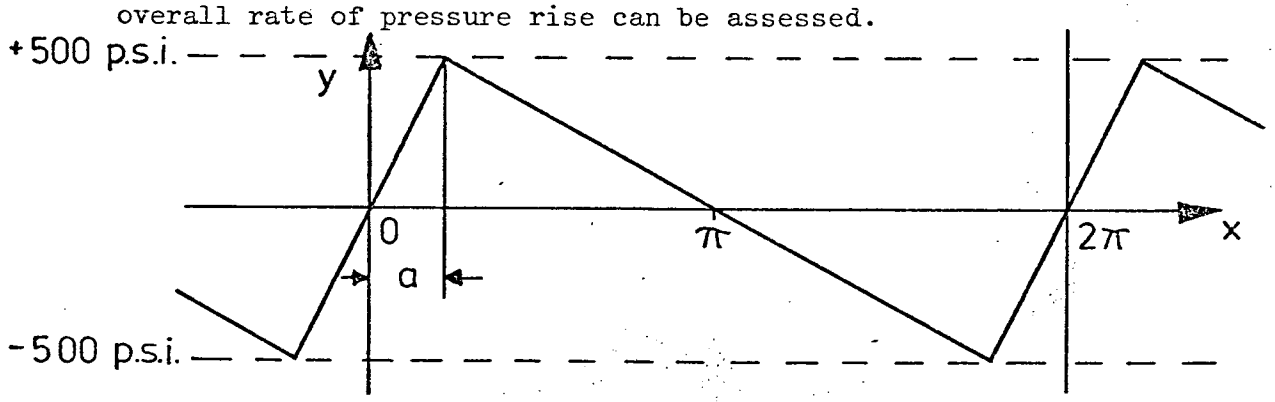

FIG. 8·5 - GENERAL FORM OF SAWTOOTH WAVEFORM.

The general expression for the Fourier components of this waveform is

$$b_k = \frac{2000}{k^2 a(\pi - a)} \sin ka \qquad (10.1)$$

Figure 8.6 shows the computed frequency spectra for a number of sawtooth waveforms with rates of pressure rise varying from 5 psi/deg to instantaneous. The waveform repeats every 1/10 second (equivalent to four stroke running at 1200 revs/min), and thus has a harmonic spectrum with a fundamental of 10 Hz. For the instantaneous pressure rise the fundamental level is 197.6 dB and the spectrum slopes regularly at 20 dB/decade. When the rate of pressure rise reduces to 5 psi/deg, the spectrum possesses peaks and troughs and also the envelope of the maximum values fall off at the increased rate of 40 dB/decade.

Figure 8.6(b) shows the effect of making the instantaneous pressure rise into a finite one of value 125 psi/deg. At a frequency of the increase of the rise time the Fourier coefficient is zero, and moreover, the peak harmonic values change to a slope of 40 dB/decade. This is illustrated in Fig. 8.6(c), where the rise time is only 25 psi/degree. In each case the transition from a 20 to 40 dB/decade slope occurs below 200 Hz (20th harmonic) for this four stroke cycle at 1200 revs/min.

Figure 8.7 shows a comparison between the sawtooth spectrum for a range of rates of pressure rise (constant peak pressure of 1000 psi) with 1200 rev/min 'engine' speed and a direct injection four stroke cylinder pressure spectrum for 1000 revs/min engine speed. Even for such a high sawtooth pressure rise, only at 125 psi/degree pressure rise do the harmonic values lie above those of the engine at frequencies above 1 kHz. However, in the lower frequency range (200-800 Hz or 20th-80th harmonic) there is a marked intrusion. It is likely, therefore, that the rate of pressure rise will only substantially affect the cylinder pressure spectrum below 1000 Hz, except for the case of very high speed operation (above 3000 revs/min). If the rate of rise is substantially higher than 125 psi/degree then the harmonics which will affect the cylinder pressure level will extend past the 80th, e.g., up to 180th harmonic for 250 psi/degree rise rate, etc.

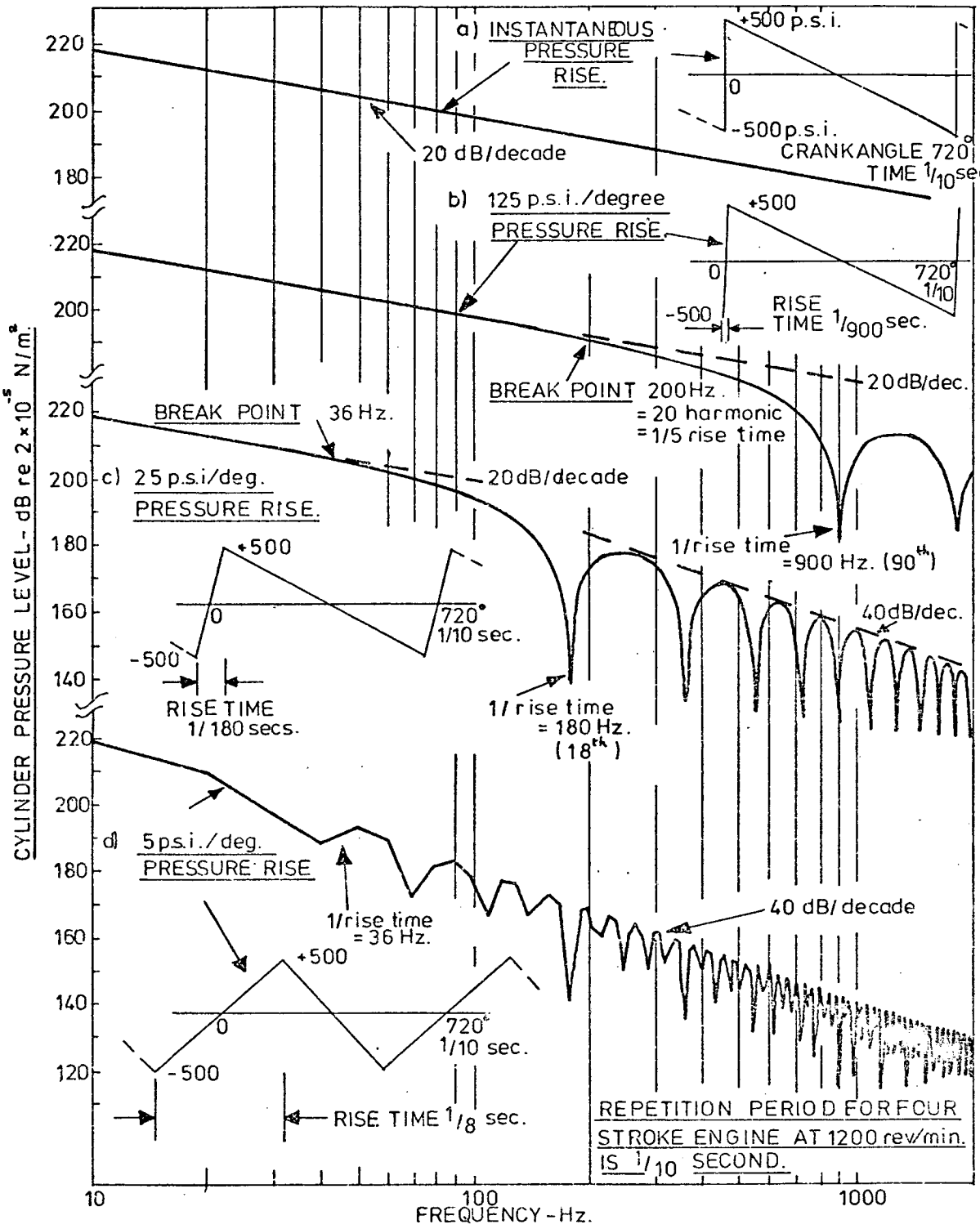

FIG. 8·6 - EFFECT OF RATE OF PRESSURE RISE ON SAWTOOTH WAVEFORM SPECTRA.

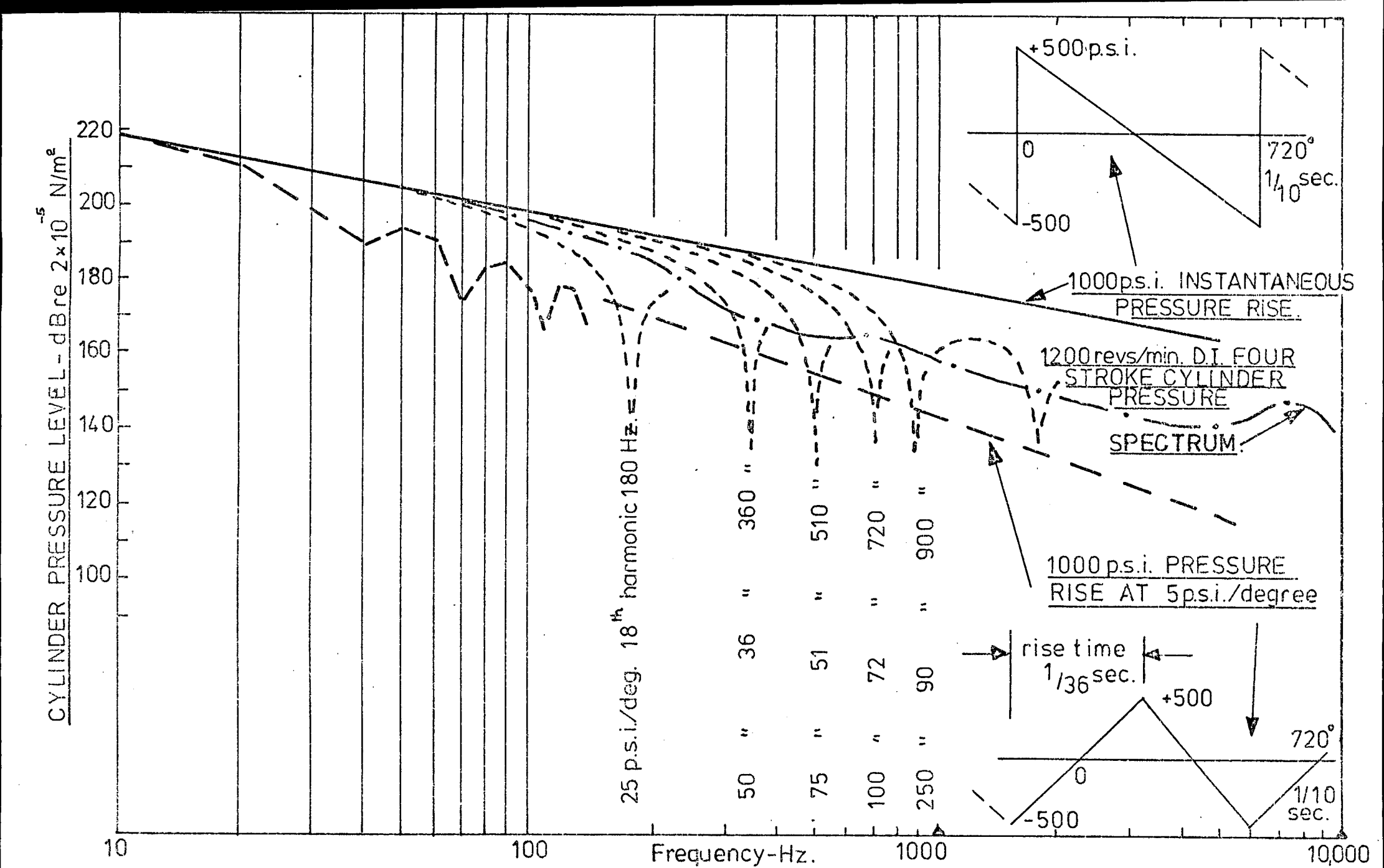

FIG. 8·7 - COMPARISON OF SAWTOOTH AND DIESEL SPECTRA.

In conclusion it is shown that for a finite rate of pressure rise the exciting spectrum levels are the same as those of the instantaneous rise up to the frequency corresponding to one fifth of the rise time. Above this value the spectrum levels are lower than for the instantaneous noise. In comparison to a typical cylinder pressure spectrum the influence of rate of pressure rise will be limited to a range from the fundamental to the frequency corresponding roughly to the rise time (36th harmonic for 50 psi/deg rise rate, 90th harmonic for 125 psi/deg rise rate, etc.).

8.6 Effect of Changing Specific Portions of Cylinder Pressure Development for Diesel and Petrol Combustion

Two representative cylinder pressure diagrams, one for diesel and one for petrol operation, were digitised accurately. Subsequently the diagram shape was modified around the initiation of combustion portion to form six different developments, in which:

(a) Diesel

(i) Smooth combustion - rate of pressure rise 70 psi/deg
acceleration of pressure rise 15 psi/deg/deg.

(ii) Typical combustion - rate of pressure rise 100 psi/deg
acceleration of pressure rise 130 psi/deg/deg

(iii) Abrupt combustion - rate of pressure rise 200 psi/deg
acceleration of pressure rise 280 psi/deg/deg.

(b) Petrol

(i) Smooth normal combustion - rate of pressure rise 25 psi/deg
acceleration of pressure rise 3 psi/deg/deg

(ii) Fast Burn Combustion (Rumble) - rate of pressure rise 70 psi/deg
acceleration of pressure rise 6 psi/
deg/deg.

(iii) Fast Burn with Increased dp/dt - rate of pressure rise 70 psi/deg

acceleration of pressure rise

15 psi/deg/deg.

The cylinder pressure developments are shown in Fig. 8.8.

The resulting spectra obtained by using the Fast Fourier Series programme are shown in Fig. 8.9 as 1/3 octave bandwidth corrected spectra.

For the diesel cycle (Fig. 8.9a) the general rate of decay of cylinder pressure spectrum level with frequency is 30 dB/decade. The smooth diesel combustion has a more rapid decay than this in the 400 to 2000 Hz (48 to 240th harmonics) range. The effect of increasing rate of pressure rise from 70 psi/deg. to 100 psi/deg., which also automatically increases the acceleration of pressure rise from 15 to 130 psi/deg/deg is to increase substantially (10-15 dB) the spectrum levels in the harmonic range 38 to 200 (315 Hz to 1800 Hz). The levels above this range remain substantially the same. Increasing the rate of pressure rise again to 200 psi/degree, with its consequent increase in acceleration of pressure rise to 280 psi/deg/deg, results in an increase in the spectrum levels in the range 80 to 400 harmonics (800 to 3000 Hz) but leaving the higher and lower harmonics unaffected. If the engine speed were 3000 revs/min, then the frequency range affected by the last change would be 2000 Hz to 1000 Hz and for the previous change 950 Hz to 5000 Hz.

Figure 8.9(b) shows the effect of similar changes made to a petrol engine diagram. The general slope of the cylinder pressure spectrum is some 50 dB/decade. Increasing the rate of pressure rise from 25 psi/deg to 70 psi/deg, to simulate normal and fast burn cycles, the acceleration of pressure rise as a consequence increases from 3 psi/deg/deg to 6 psi/deg/deg. The result is significantly increased spectrum levels (10 dB) over the harmonic range 9 to 120 (80 Hz to 1000 Hz). For a petrol engine running at 6000 revs/min this frequency range would be 450 Hz to 6000 Hz. If the acceleration of pressure rise is increased, keeping the rate of pressure rise at 70 psi/deg, then the spectrum levels over the harmonic range 90 to 200 are increased by some 3 dB.

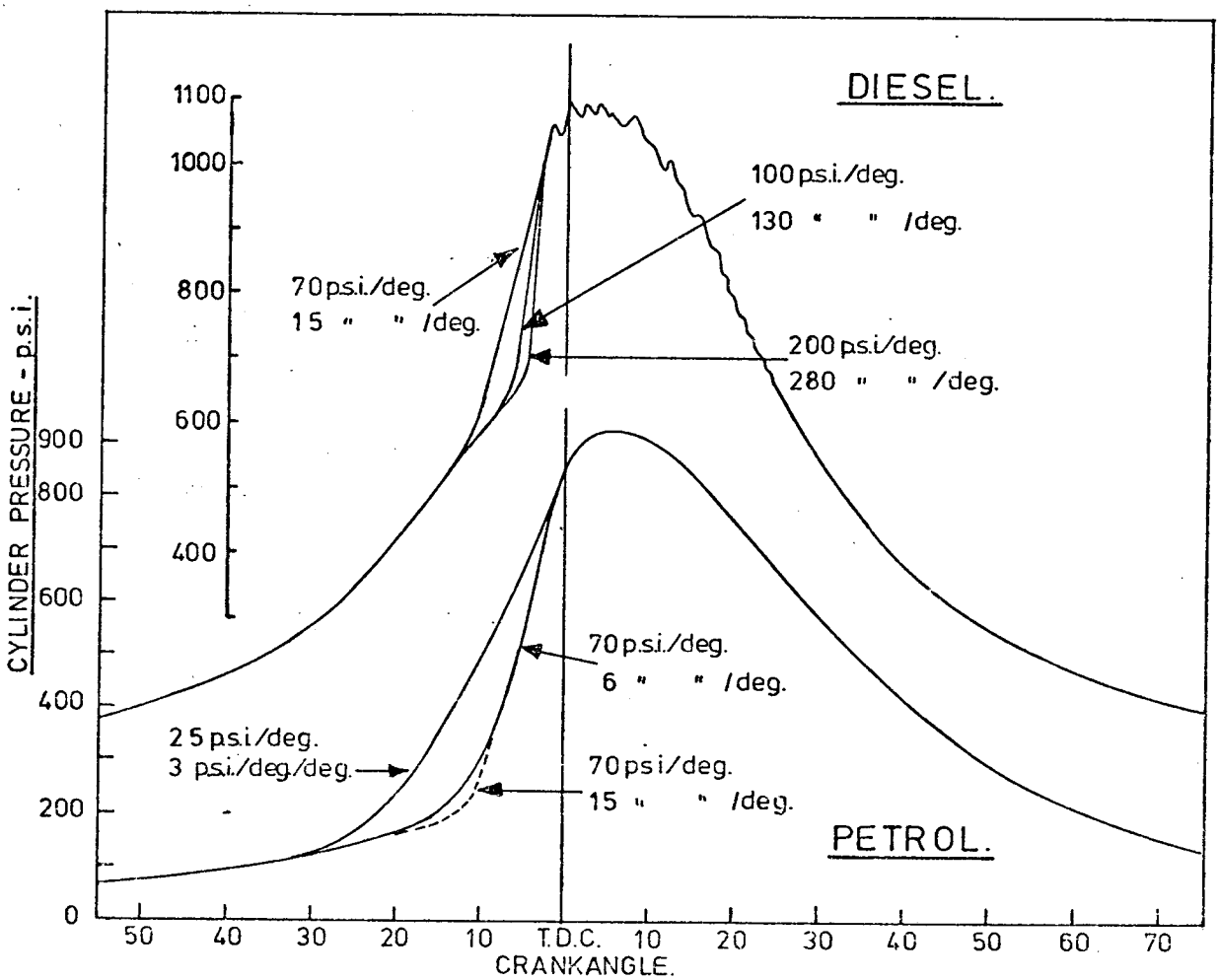

FIG. 8·8- DIESEL AND PETROL CYLINDER PRESSURE DEVELOPMENTS WITH SPECIFIC CHANGES.

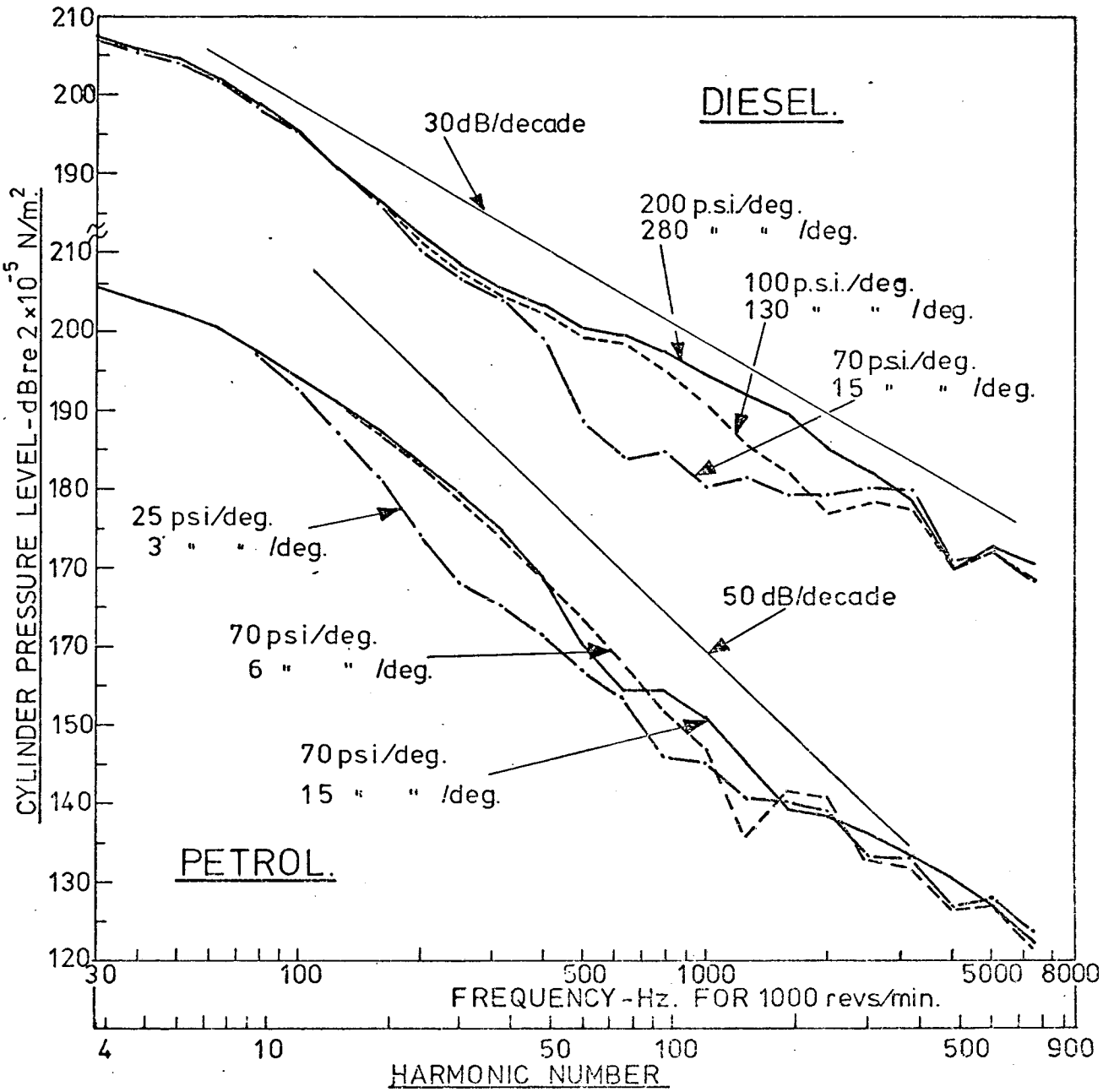

FIG. 8·9 - DIESEL AND PETROL COMPUTED CYLINDER PRESSURE SPECTRA FOR SPECIFIC CHANGES.

Thus it can be concluded that the effect of rate of pressure rise on the cylinder pressure exciting spectrum is not the same for typical diesel and petrol cycles. In the diesel the comparatively high rates of pressure rise affect mainly the harmonic range 40 to 200, whilst in the petrol engine this range is 9 to 120th harmonic. The effect of acceleration of pressure rise is generally in the range above the 70th harmonic for diesel and petrol cycles. The frequency range controlled by peak pressure, rate of pressure rise and acceleration of pressure rise depends greatly on engine speed. For the important frequency range 500-3000 Hz the excitation in an engine running at 1000 revs/min will mostly be controlled by acceleration of pressure rise whilst as the engine speed is increased the control will gradually pass to rate of pressure rise until at 5000 revs/min it is wholly controlled by rate of pressure rise. (Fig. 8.11).

Some general confirmation of these results, for a petrol engine, is shown in Fig. 8.10, reproduced from the discussion of Andon and Marks paper (ref. 2.6). The fast burn or surface ignition cycle has generally higher cylinder pressure spectrum levels up to 4000 Hz. Under knock conditions, with a small but abrupt change to the diagram (high acceleration and rate of pressure rise of small magnitude) then only frequencies above 1000 Hz are increased.

8.7 Cylinder Pressure Oscillations

In Fig. 8.10 the pronounced resonance in the cylinder pressure spectrum at 6500 Hz is due to natural oscillations of the combustion chamber space excited by the combustion pressure. This effect is important since it produces a subjectively harsh sound from an engine and can cause damage. It differs from the basic combustion excitation in that it is a response to the combustion which is superimposed on it to form the resulting cylinder pressure exciting spectrum.

If a simple vibratory system is loaded with an impulse it will respond to the impulse and this response will be greatest at the system natural frequency of vibration. In I.C. engines the cylinder volume will have acoustic

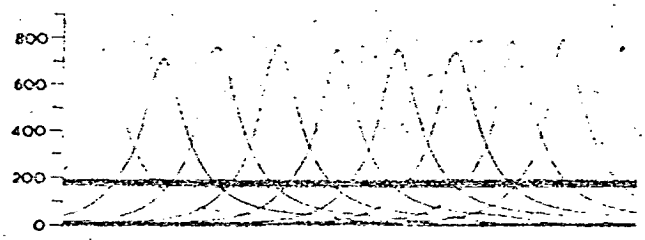

Fig. E1 – Normal combustion

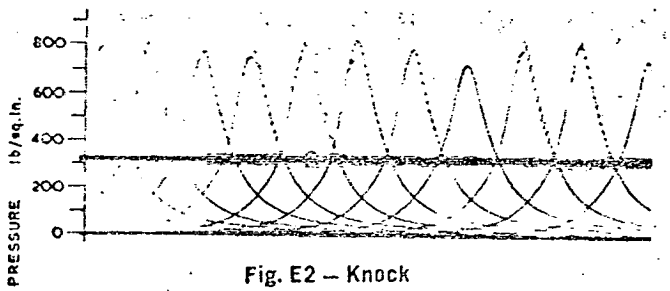

Fig. E2 – Knock

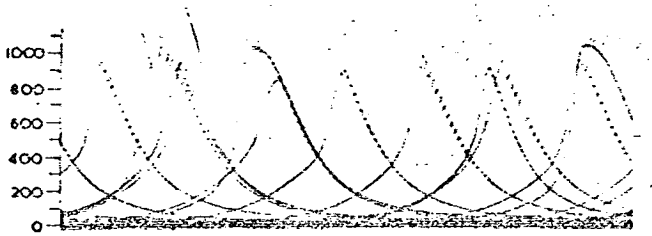

Fig. E3 – Surface ignition fast-burning

Fig. E – Cylinder pressure diagrams of 1.5 liter petrol engines at 2000 rpm, full load

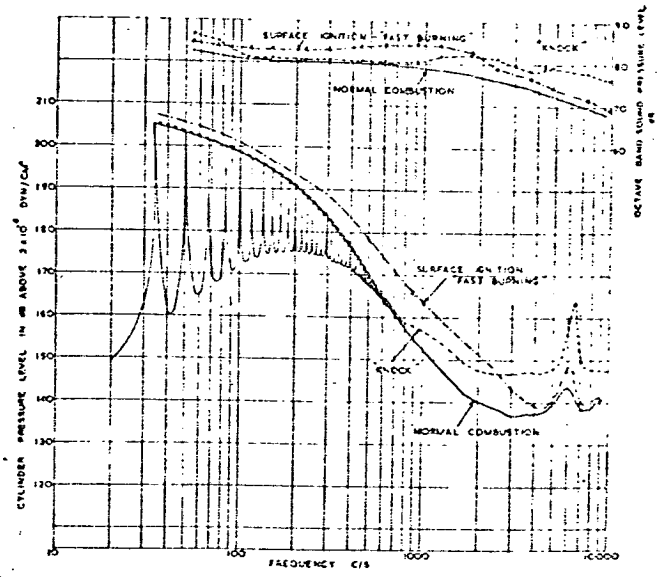

Fig. F – Cylinder pressure and corresponding noise spectra of 1.5 liter petrol engine at 2000 rpm, full load

FIG. 8·10 - FAST BURNING, KNOCK AND RUMBLE IN 1·5 LITRE PETROL ENGINE AT 2000 revs/min. FULL LOAD.

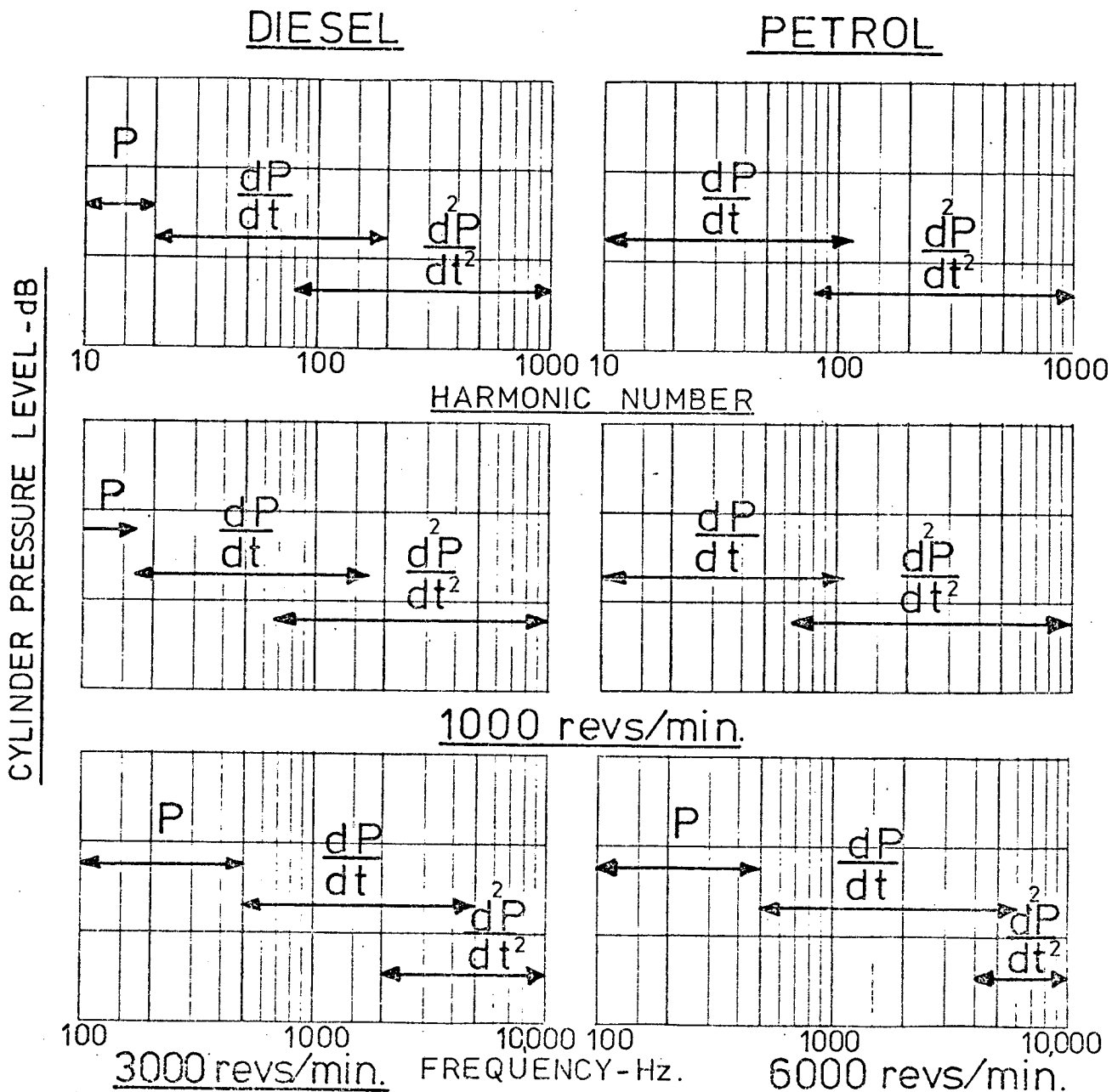

FIG. 8·11 - FREQUENCY RANGE OF P, $\frac{dP}{dt}$, $\frac{d^2P}{dt^2}$, EFFECT ON C.P. SPECTRA.

resonances just like a room. The impulsive load from the initial rapid pressure rise due to combustion excites these gas oscillations and, being a resonant condition, the response is then controlled by the amount of damping present. These oscillations are often termed "feathering" on cylinder pressure diagrams and where long passages are used to connect pressure transducer and cylinder, this is due to passage resonances. However, feathering is still observed (at a different frequency), when the transducer is flush mounted and when this is the case the effect is due to natural oscillations of the gas in the cylinder - cylinder pressure oscillations.

8.7.1 Frequencies and mode shapes

Originally the cylinder was treated like a closed pipe and therefore the lowest frequency would be associated with the largest dimension. Since the oscillations occur mainly at or near TDC, then this would be the cylinder bore. Thus the lowest frequency would be:

$$f = \frac{c}{2B} \text{ Hz} \qquad c = \text{velocity of sound; } B = \text{engine bore.}$$

Now the gas mixture is at a high temperature and so the velocity of sound is increased. Assuming that the sound waves are linear, then,

$$f = c_o \frac{\sqrt{T/273}}{2B} \text{ Hz} \qquad c_o = \text{velocity of sound at } 273^{\circ}\text{C}$$
$$T = \text{gas temperature in } {}^{\circ}\text{K}.$$

This was found to give good agreement with measured results over a range of engines.

A better model than this can be found in the theory for the natural frequencies of cylindrical rooms (ref. 8.8). Approximating the combustion space to a cylinder it is found that

$$f = c_o \sqrt{(T/273} \left| (\frac{n_z}{\ell})^2 + (\frac{2\alpha_{mn}}{B})^2 \right|^{\frac{1}{2}} \text{ Hz}$$

where ℓ = cylinder depth

B = cylinder bore

n_z = 0, 1, 2, ..., an integer

α_{mn} = values determined by a Bessel function

The values of α_{mn} are shown in Table I -

CHARACTERISTIC VALUES OF α_{mn} FOR THE CYLINDRICAL ROOM SOLUTIONS OF $DJ_m(a)/da = 0$

m \ n	0	1	2	3	4
0	0.0000	1.2197	2.2331	3.2383	4.2411
1	0.5861	1.6970	2.7140	3.7261	4.7312
2	0.9722	2.1346	3.1734	4.1923	5.2036
3	1.3373	2.5513	3.6115	4.6428	5.6624
4	1.6926	2.9547	4.0368	5.0815	6.1103
5	2.0421	3.3486	4.4323	5.5108	6.5494
6	2.3877	3.7353	4.8600	5.9325	6.9811
7	2.7304	4.1165	5.2615	6.3477	7.4065
8	3.0709	4.4931	5.6576	6.7574	7.8264

In general if $\ell << 0.85B$ (height of cylinder much less than bore) then the lowest frequency mode is that for which $n_z = 0$, $n = 0$, $m = 1$, then

$$f_1 = c_o\sqrt{T}/273\left(\frac{\alpha_{10}}{B}\right)$$

or

$$f_1 = c_o\sqrt{T}/273\ \left(\frac{0.5861}{B}\right)\text{Hz}$$

and the mode shape is a 'sloshing' of the gas from side to side as shown in Fig. 8.12. The next two higher frequencies are then the $n_z = 0$, $n = 0$, $m = 2$ mode, where

$$f_2 = c_o\sqrt{T}/273\left(\frac{0.9722}{B}\right)\ \text{Hz}$$

and the $n_z = 0$, $n = 1$, $m = 0$ mode, where

$$f_3 = c_o\sqrt{T}/273\left(\frac{1.2197}{B}\right)\ \text{Hz}.$$

The mode shapes are shown in Fig. 8.12.

8.7.2 Relation between frequency and gas temperature

Figure 9.18 shows the cylinder pressure spectra for full load conditions for a two stroke diesel. The cylinder pressure oscillations are marked and

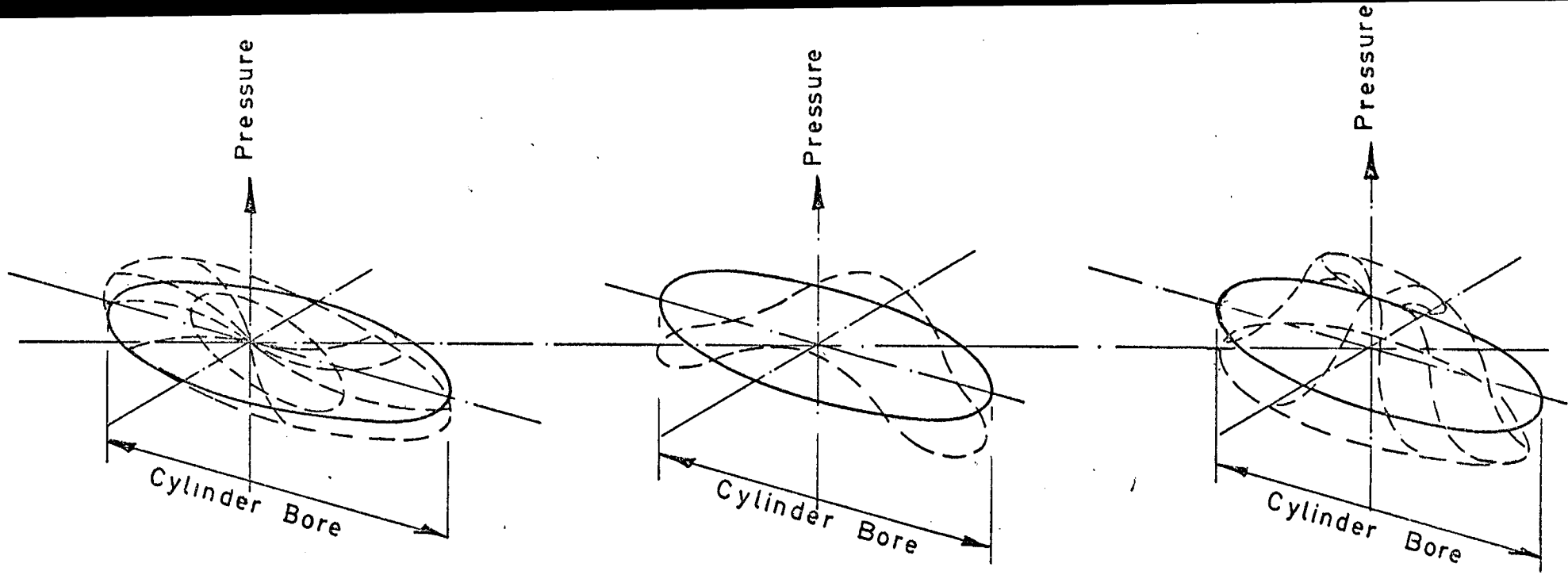

FIG. 8·12-MODAL PRESSURE DISTRIBUTION FOR THREE LOWEST FREQUENCY MODES OF A CYLINDRICAL SPACE IN WHICH $\ell < 0{\cdot}85\ B$.

have a frequency varying from 6000 Hz to 6500 Hz, depending on the engine speed. There is only one marked resonance and thus it can be assumed that this corresponds to the f_1, lowest frequency for cylindrical spaces.

Thus

$$6000 = 1130\sqrt{T}/273 \times \left(\frac{0.5861}{3.4375}\right) \times 12 \text{ Hz}.$$

And so the average temperature which must exist in the cylinder for this model to be true is 1815°K. Using this temperature the three lowest frequency gas oscillations will be:

f_1 = 6,000 Hz
f_2 = 9,950 Hz at 1815°K
f_3 = 12,460 Hz

and

f_1 = 6,500 Hz
f_2 = 10,500 Hz at 2125°K
f_3 = 13,500 Hz

The frequency of the oscillations at one engine condition also vary with time, since the cylinder gas temperature is changing. The temperature at which the frequency corresponds to that measured is 1885°. At a point 20° a.t.d.c. the oscillation frequency has increased and corresponds roughly to a doubling of cylinder gas temperature from that at t.d.c. This order of temperature change between t.d.c. and 15 to 20° a.t.d.c. is precisely that found by Lyn using colour Schlieren techniques.

Because of this change in frequency the cylinder pressure analysis will not show a discrete frequency but a general response centred on the frequency which exists for the longest time. Thus reliable values of damping are very difficult to measure.

8.7.3 Mode shapes

In many engines only the lowest frequency gas oscillation is observed and from the mode shapes given in Fig. 8.12 this will mean that there will be a rocking couple applied to the piston crown. The direction of the couple will be controlled by the spray characteristics and ignition centres as there are no valve cut-outs.

Because of the modal pressure distribution in this fundamental, the measured results will depend greatly on the position of the pressure transducer. In the case of the opposed piston two-stroke, for example, where the transducer is in the liner wall, either a maximum or minimum pressure will be measured, depending on the direction of the nodal line.

8.7.4 Damping of the oscillations

Since these oscillations are associated with the bore, if the bumper clearance is zero, then the lowest oscillation will be associated with the combustion chamber dimension and will probably be greater than 10,000 Hz. That the oscillations occur at lower frequency indicates that the 'sloshing' mode can exist in the very small depths of bumper clearances. It has been observed that if the bumper clearance is low, the amplitude of the oscillations is low, and this is thought to be due to viscous damping effects around the piston circumference. Now it can be shown (ref. 8.9) that the depth of viscous boundary layer that affects wave motion is given by $(2\eta/\omega)^{\frac{1}{2}}$, which for a frequency of 2 kHz, is equal to 0.020 inch, and at 6 kHz is equal to 0.012 inch. Comparison of data from several engines with oscillations in the range 5-6 kHz indicate that a bumper clearance less than 0.025 inch, i.e., twice viscous boundary layer for one surface, reduces the oscillation amplitude to a low level. Above about 0.035 inch bumper clearance oscillations become very marked. Thus, the maximum bumper clearance that can be used, so as to eliminate the oscillations, increases in proportion to the square root of the bore.

REFERENCES

8.1 W.T. Lyn. 'An experimental investigation into the effect of fuel addition to intake air on the performance of compression ignition engines'. Proc. Inst. I. Mech. E. 168, p.265. 1954.

8.2 J.S. Meurer. 'Evaluation of reaction kinematics eliminates diesel knock - the M combustion system of M.A.N.'. SAE paper 535. 1955.

8.3 Robinson, R.R., Mitchell, J.E. 'Development of a 300 lb/in^2 B.M.E.P. continuous duty diesel engine'. Paper A7 CIMAC 1965, ASME Paper 66-DGEP-9.

8.4 Paluska, R.T., Saletzki, J.S., Cheklich, C.E. 'Design and development of a very high-output VHO multifuel engine'. BICERA, Slough, England.

8.5 Mansfield, W.P., Tryhorn, D.W., Thorneycroft, C.H. 'Development of turbocharged diesel engine to high mean effective pressures without high mechanical and thermal loading'. CIMAC Paper A6, 1965.

8.6 Mansfield, W.P., May, W.S. Diesel combustion at high MEP with low compression ratio'. SAE paper 660343.

8.7 Basiletti and Blackburne. 'Recent developments in variable compression ratio engines'. SAE Paper 660344.

8.8 P.M. Morse. 'Vibration and Sound'. McGraw Hill Book Co.

8.9 J.A. Rogers. Undergraduate thesis, 1968/69. Southampton University.

9.0 ASSESSMENT OF GENERAL CHARACTERISTICS OF COMBUSTION EXCITATION IN INTERNAL COMBUSTION ENGINES

Since combustion is the primary source of noise excitation in the majority of present-day automotive Internal Combustion engines, then a knowledge of its variation with engine class will indicate the general combustion noise characteristics of that class. Combustion noise is again taken to be the noise radiated by the surface vibration of the engine and associated structures (gearbox, etc) due to cylinder pressure forces and excludes the noise due to the gas exchange process direct (open inlet and exhaust noise). For this purpose it is necessary to classify the Internal Combustion engines considered, and one classification can be:

Class 1 Four stroke direct injection diesel engines

Class 2 Four stroke indirect injection diesel engines

Class 3 Two stroke direct injection diesel engines

Class 4 Four stroke direct injection turbocharged diesel engines

Class 5 Two stroke direct injection turbocharged diesel engines

Class 6 Fuel injected petrol engines

Each of these six classes of engine possesses unique characteristics of their own which are discussed in this chapter. There are also general characteristics of fuel injection which affect all diesel engines and of carburation which affect all petrol engines. Despite these differences, however, there are some characteristics which are common to all classes of I.C. engine at rated speed and load, and these provide a general background for comparison of the individual classes.

9.1 General Characteristics of Combustion Noise in I.C. Engines, Based on Ideal Combustion

There are three fundamental variables which describe an engine. Firstly,

its physical size; secondly its speed of operation and thirdly the load at which it is operating. These three parameters are generally a sufficient basis on which to decide the suitability of an engine for a particular application, cost excepted. In general terms the choice of these parameters will specify not only the engine performance but also its associated noise level. The variation of noise with these three design parameters is shown in fig. 9.1 (reproduced from ref. 9.2), for the case where the cylinder pressure development, on a degree basis, does not change with speed.

The most influential parameter is that of speed. There is a rapid increase in noise with speed which depends on the type of combustion system employed. According to the speed and combustion system employed the overall noise level produced can vary by as much as 45 dBA. Noise intensity can be related to engine speed:

$$I \propto N^{2.5-5} \tag{9.1}$$

where the index depends on the combustion system.

The effect of size on noise is not so marked, and in the range 0.4 litres/cylinder to 30 litres per cylinder the variation in overall noise level is some 15 dBA.

Finally the effect of the loading (at reasonable power output) on the engine noise is found to be negligible. This is because the harmonics of cylinder pressure development which transfer power are not those which transfer noise excitation (see section 7.3).

The general observation which can be made from a consideration of these characteristics is that for low noise output, I.C. engines should be run at as low a speed and as high a load factor as is possible for the smallest engine size. In practice this generalisation is being achieved to a large extent by turbocharging.

SPEED

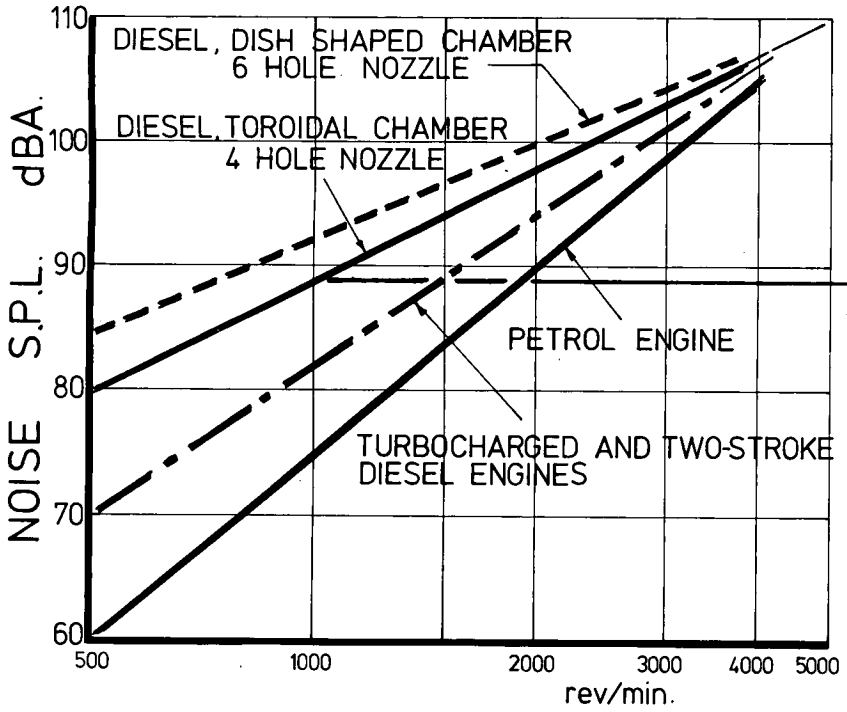

$$I \propto N^{2.5-5}_{\text{rev/min.}}$$

SIZE

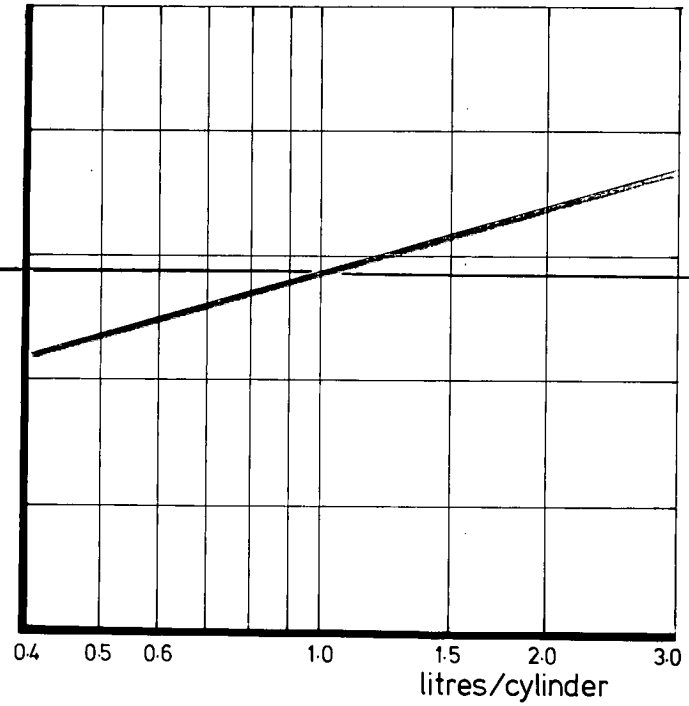

$$I \propto V^{1.75}_{\text{litres}}$$

LOAD

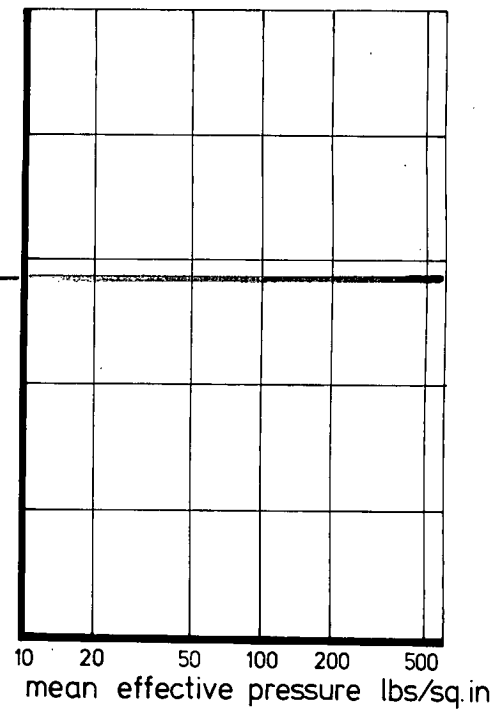

$$I \propto L^{0}$$

INTENSITY OF ENGINE NOISE $I = \text{CONST.} \times N^{2.5-5} \times V^{1.75}$

FIG 9·1

9.2 Assessment of Combustion Noise Level

The general method of assessing the contribution of combustion induced noise has been well established by Priede (9.1). His method defines a 'Critical Cylinder Pressure Level' at which mechanical noise and combustion noise are equal. The level of combustion noise is altered - usually by changing the injection or spark timing - and the effect on noise observed. In principle this is a simple process, but in practice it proves to be a very laborious one because the critical cylinder pressure level must be found throughout the audio frequency range, as well as at all operating speeds and load conditions. A typical set of results is shown in fig. 9.2 for a direct injection four stroke engine in normally aspirated and turbocharged forms. The use of a turbocharger for the purpose of Critical Cylinder Pressure Level analysis forms a valuable tool since a greater change in combustion excitation level can be obtained by this means as compared to a normally aspirated engine. By the analysis of curves relating cylinder pressure level and noise, such as shown in fig. 9.3, the critical cylinder pressure spectrum can be obtained. This enables an evaluation of the combustion noise controlled and mechanical noise controlled characteristics of an engine to be made. A typical result is shown in fig. 9.4. Depending on the injection timing and operation of the engine (turbocharged or not), then various frequency ranges change from combustion control to mechanical control as the fuel injection is retarded. It is found that in the majority of engines there are frequency ranges where the noise is controlled by mechanical sources. The decision as to whether or not an engine has combustion controlled or mechanically controlled noise will depend on the proportion of the Audio Frequency range occupied by one or the other.

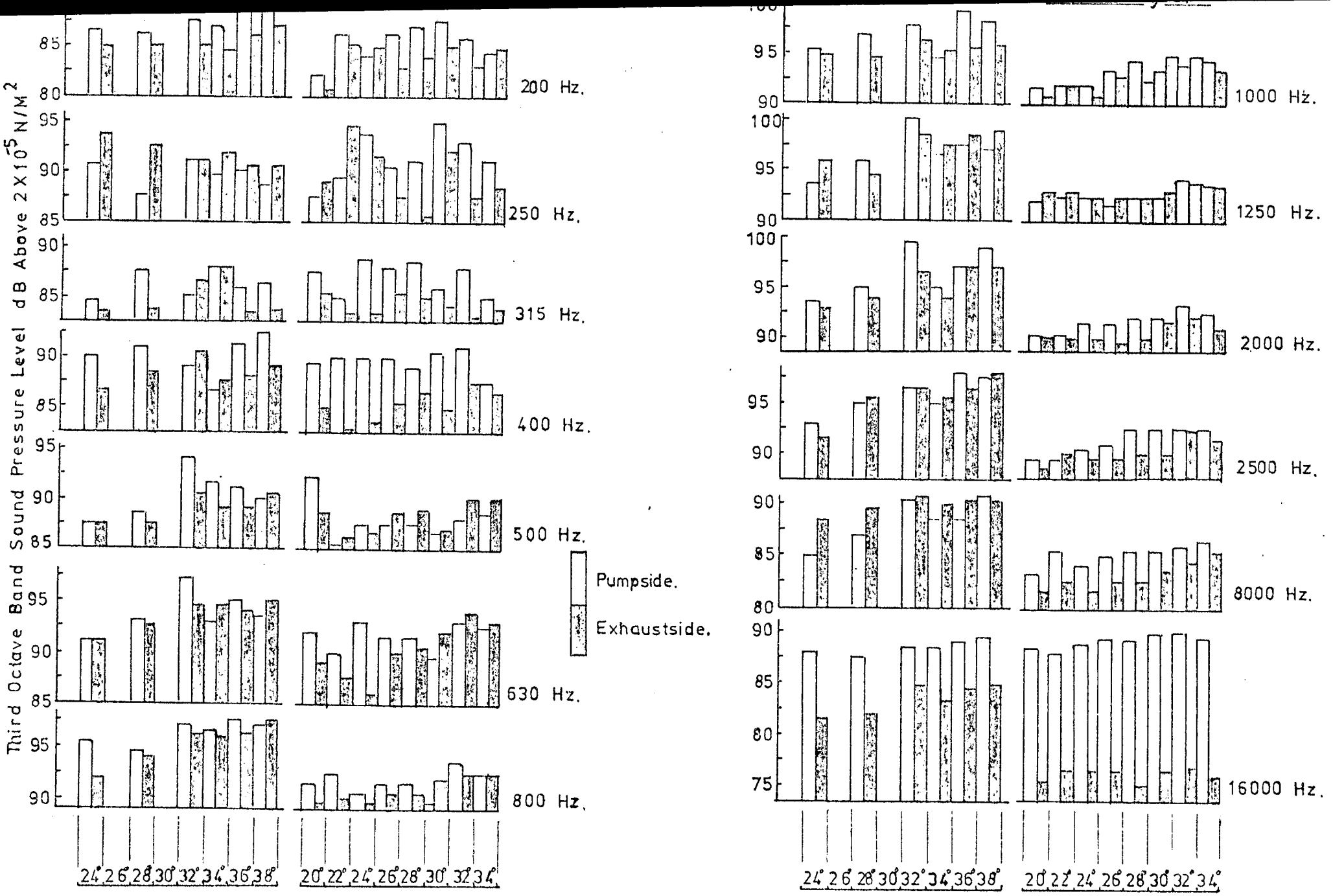

Fig. 9·2 - EFFECT OF INJECTION TIMING ON THIRD OCTAVE BAND NOISE. 2600 r.p.m. FULL LOAD.

Static Injection Timing	Naturally Aspirated. 2600 r.p.m.	Naturally Aspirated. 2000 r.p.m.	Turbo charged. 2600 r.p.m.	Turbo charged. 2000 r.p.m.
20° B.T.D.C.			m	u
22° ,,			n	v
24° ,,	a	g	o	w
26° ,,			p	x
28° ,,	b	h	q	y
30° ,,			r	z
32° ,,	c	i	s	+
34° ,,	d	j	t	⊙
36° ,,	e	k		
38° ,,	f	l		

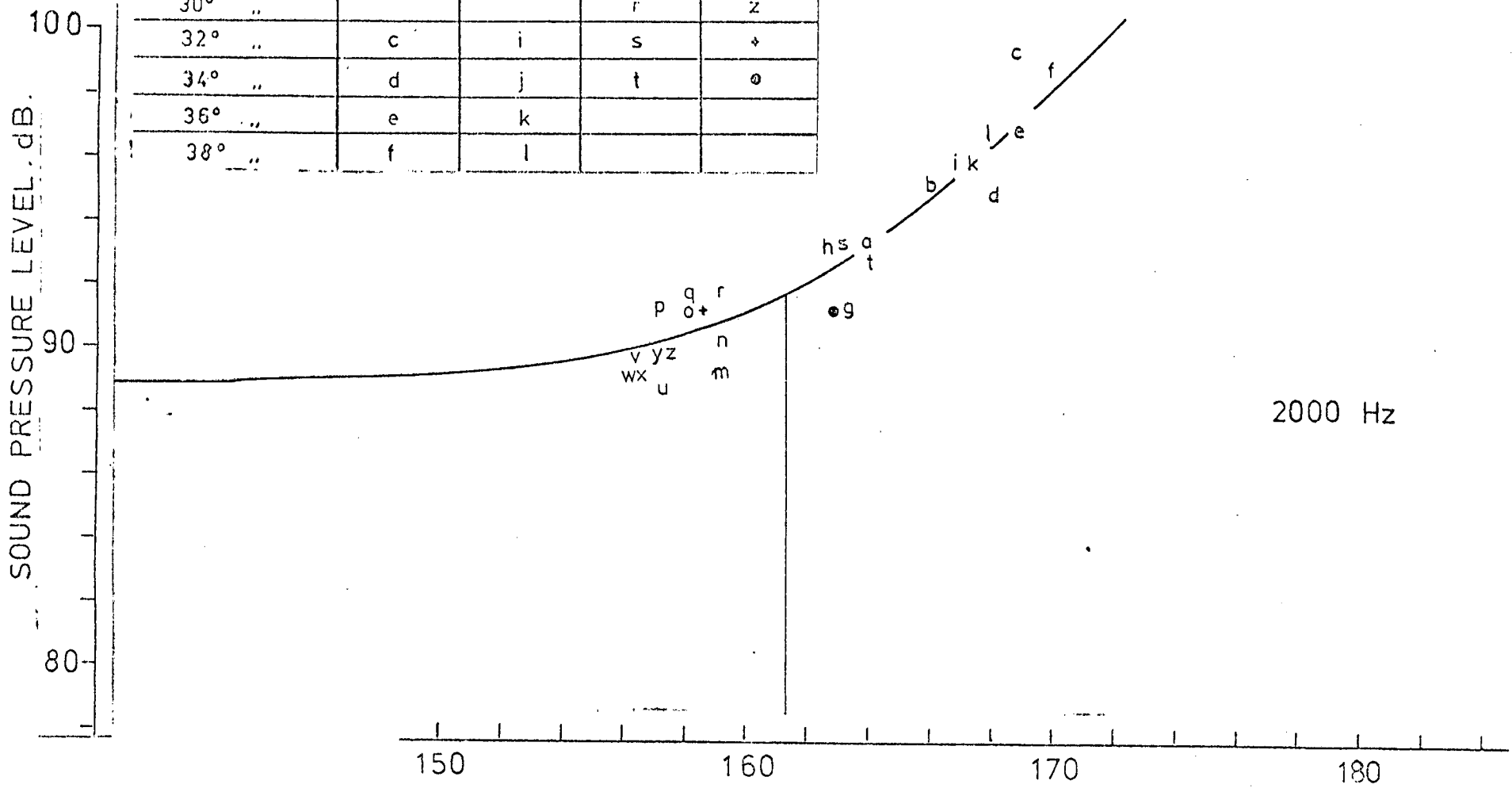

FIG. 9·3 - RELATION BETWEEN CYLINDER PRESSURE LEVEL AND NOISE. PUMPSIDE ENGINE.

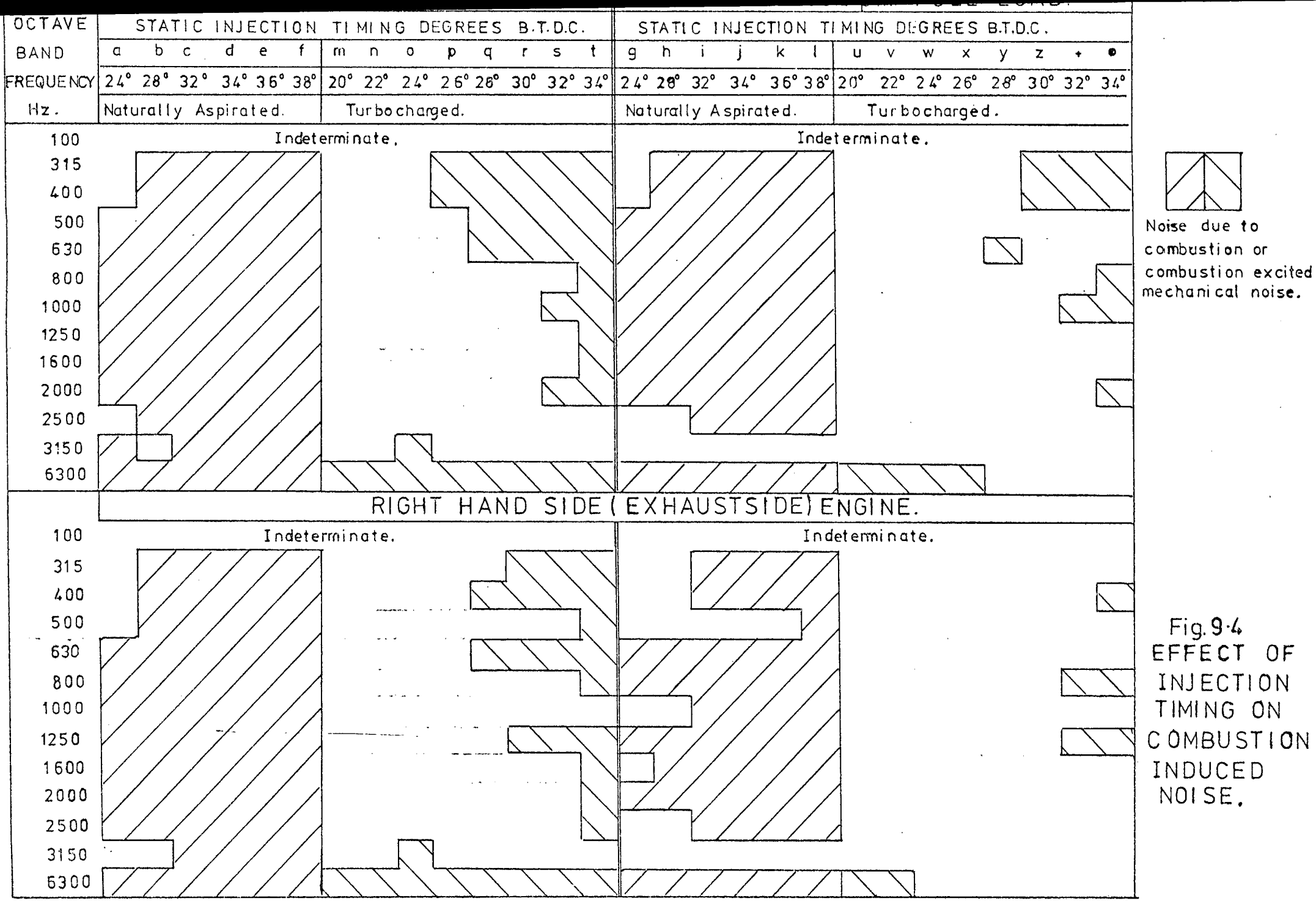

Fig. 9·4 EFFECT OF INJECTION TIMING ON COMBUSTION INDUCED NOISE.

9.3 Characteristics of Combustion and Noise in I.C. Engines

In the following sections measured cylinder pressure development and spectra together with measured noise spectra are presented as a function of speed and load for a selection of engines representative of their class.

9.3.1 Four stroke direct injection diesel engines

Figures 9.5, 9.6, 9.7 illustrate the combustion and noise characteristics of a 4.65" bore direct injection four stroke diesel engine with toroidal chamber, moderate swirl and five hole injector. The fuel pump used is an in-line pump with load advance.

At full load (fig. 9.5) the peak pressure gradually reduces from 1100 psi to 957 psi whilst the maximum rate of pressure rise also reduces from 70 to 60 psi/deg. However, the acceleration of pressure rise remains constant with speed. At no load the peak pressure is considerably reduced, the initiation of combustion retarded and rates of pressure rise reduced considerably at the higher speeds. The cylinder pressure spectra at full load (fig. 9.6) exhibit the same shape as the speed is increased, a general slope of 33 dB/decade being measured. At no load the low frequency cylinder pressure spectrum levels are lower due to the reduction in peak pressure and the general slope has increased to 45 dB/decade due to the lower rates and accelerations of pressure rise.

Figures 9.6 and 9.7 show that the engine noise increases with engine speed at the rate of 35 dBA/decade for both full load and no load, with the maximum noise being radiated in the 500 to 3000 Hz frequency range. From the combustion noise model it is expected that the slope of the cylinder pressure spectrum and the overall noise would be the same. This is so at full load, but at no load there is a considerable difference, 33 dB/decade as opposed to 45 dB/decade for noise.

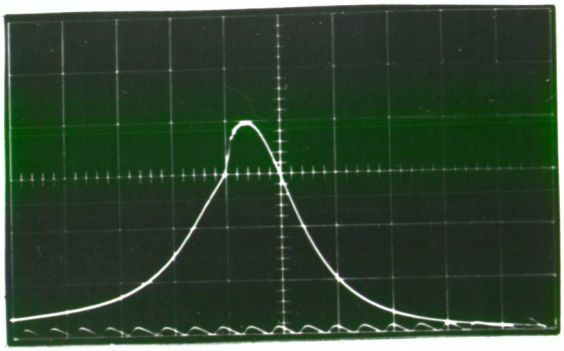

1000 r.p.m. NO LOAD

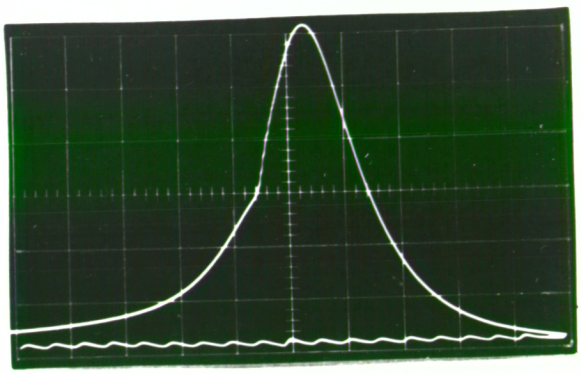

1000 r.p.m. FULL LOAD
(PEAK PRESSURE 1100 p.s.i.)

CYLINDER PRESSURE p.s.i. (175 p.s.i./division)

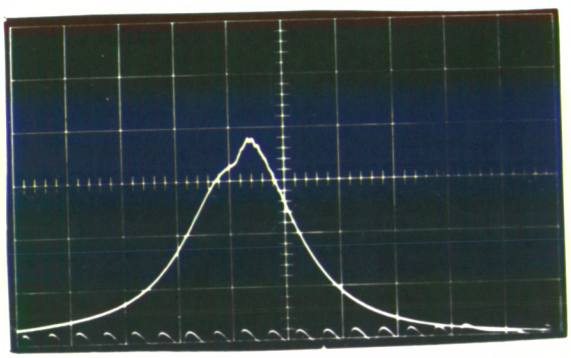

2000 r.p.m. NO LOAD

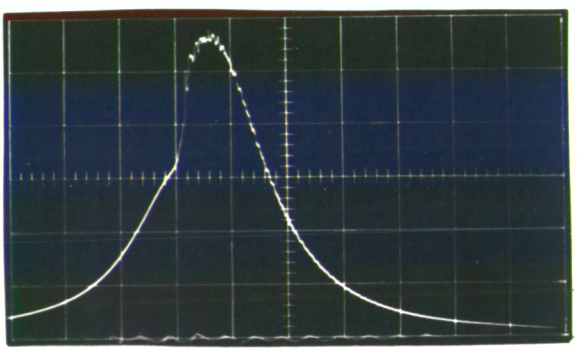

2000 r.p.m. FULL LOAD
(PEAK PRESSURE 1000 p.s.i.)

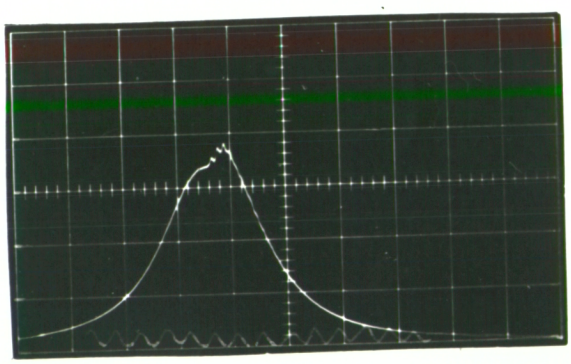

2600 r.p.m. NO LOAD

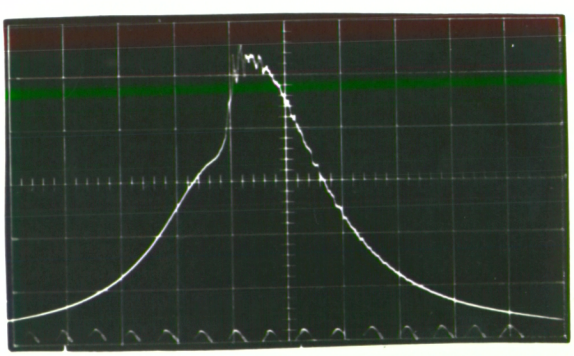

2600 r.p.m. FULL LOAD
(PEAK PRESSURE 957 p.s.i.)

FIG. 9.5 CYLINDER PRESSURE DEVELOPMENT FOR 4·65" BORE DIRECT INJECTION 4-STROKE DIESEL ENGINE.

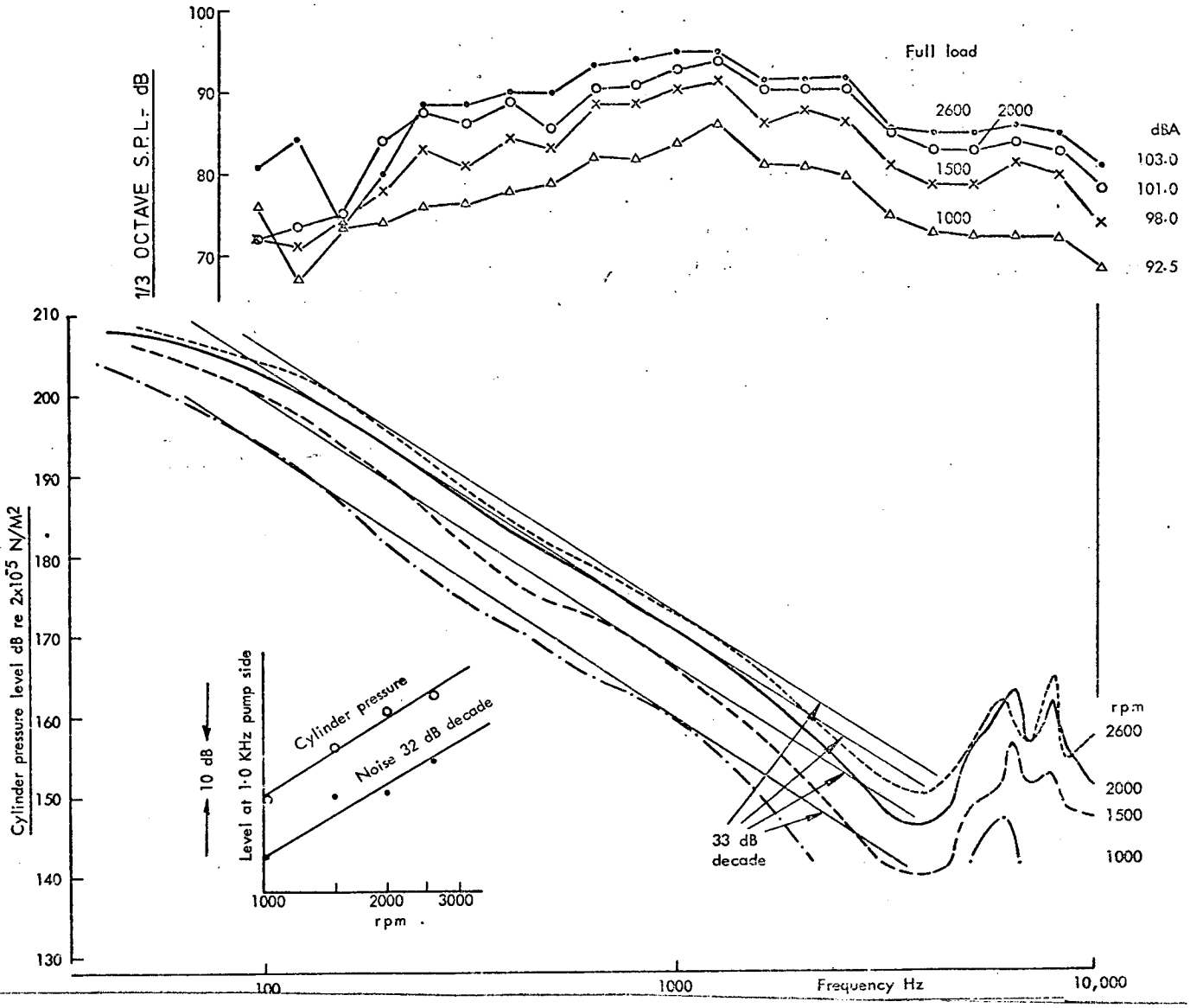

FIG. 9·6 - D.I. 4 STROKE FULL LOAD CHARACTERISTICS.

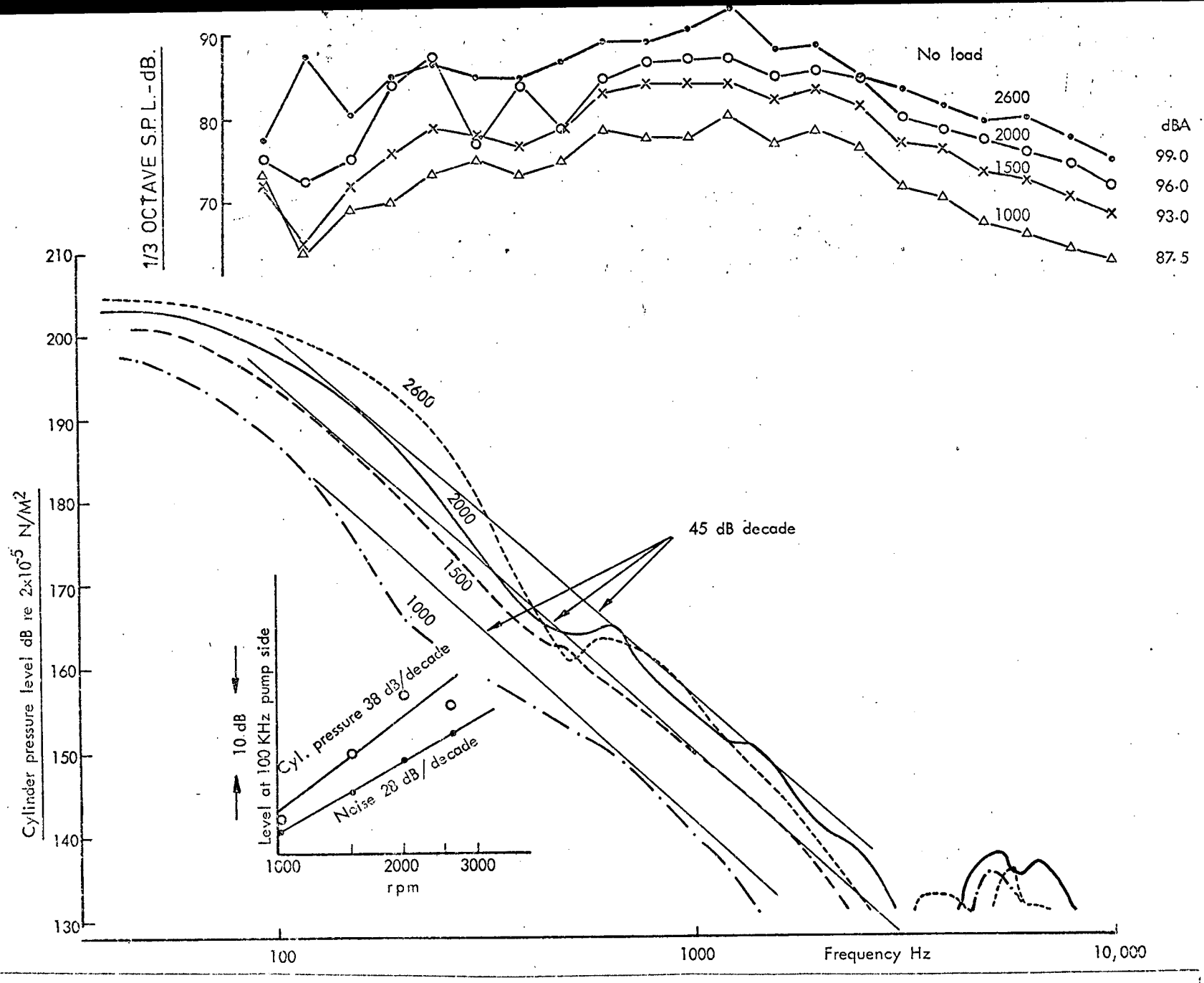

FIG. 9·7 - D.I. FOUR STROKE NO LOAD CHARACTERISTICS.

Since the combustion excitation is proportional to the overall level of the cylinder pressure spectrum over the most important frequency range, i.e., 500-3000 Hz, a comparison of the increase in noise which would be expected from a consideration of the cylinder pressure spectrum changes can be obtained from the overall level difference at two engine speeds. At full load the cylinder pressure spectrum differences are 6.5 (from 1000 revs/min to 1500 revs/min), 4.5 (from 1500 revs/min to 2000 revs/min) and 3 dBA (from 2000 revs/min to 2600 revs/min) and the corresponding measured increase in overall noise level is 5.5, 3 and 2 dBA, showing good correlation. At no load, however, the expected noise increases estimated from the cylinder pressure spectra are 8.0, 4.5 and 0.0 dBA. The corresponding measured increase in overall noise is 5.5, 3.0 and 3.0 dBA, indicating that at 2600 revs/min no load the noise is mechanically controlled.

From these results two important conclusions can be drawn. Firstly that although the full load cylinder pressure diagrams are not similar on a degree basis, the cylinder pressure spectrum shape is the same at all speeds. This is because the most prominent feature of the diagram - namely acceleration of pressure rise - remains the same. Secondly, that at no load conditions there is a sufficient change in the cylinder pressure diagram to produce a more steeply sloping spectrum at 2600 revs/min than at 2000 revs/min. The important finding here is that in this case the engine noise-speed relationship would not be expected to follow the general slope of the cylinder pressure diagram, but will follow the actual change in overall cylinder pressure spectrum level.

That this engine is representative of its class is illustrated in fig. 9.7a, where the cylinder pressure spectra for four normally aspirated direct injection diesel engines with various combustion chamber designs are shown. Only in the case of the M.A.N. design, where the fuel is sprayed directly

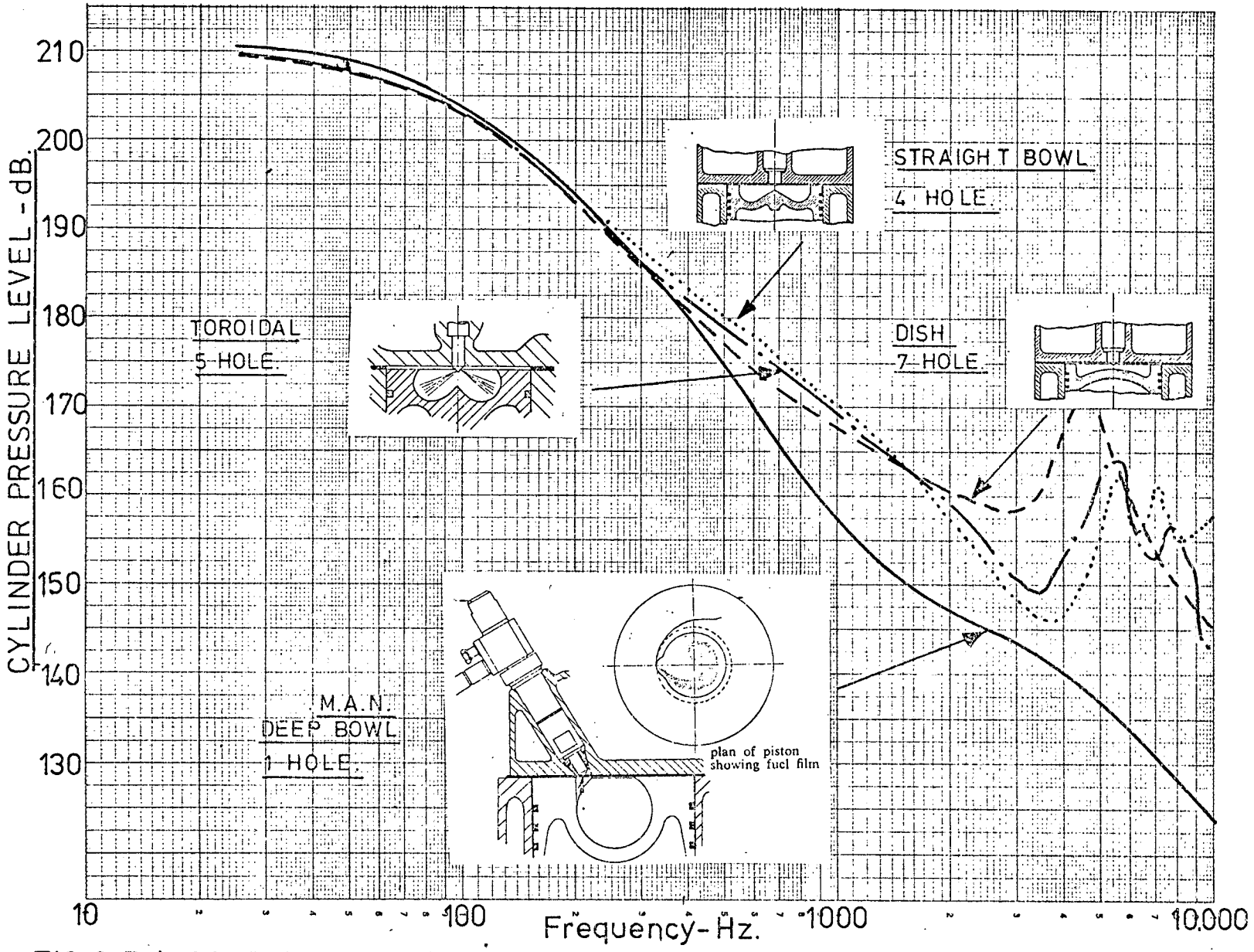

FIG. 9·7a) - COMPARISON OF VARIOUS D.I. COMBUSTION CHAMBERS.

onto the chamber wall is there a significant variation in excitation.

9.3.2 Four stroke indirect injection diesel engines

Figures 9.8, 9.9 and 9.10 show the combustion and noise characteristics of a 3.5" bore indirect injection diesel engine fitted with a Ricardo Mk. III combustion chamber and single hole nozzle. The fuel pump is a rotary pump.

There is very little difference in pressure between the no load and full load condition. All diagrams exhibit a marked retarding of initiation of combustion with increasing speed, this point being some 5^{o} after top dead centre at 3500 revs/min. The rate of pressure rise varies from 20 to 45 psi/deg and a generally smooth entry to combustion (low acceleration of pressure rise) is present.

The cylinder pressure spectra at full load (fig. 9.9) have a general slope of 45 dB/decade but the smoothing of the diagram from 3000 to 3500 revs/min by retarded injection appears as a slightly increased slope with combustion excitation being higher at the lower speed. A similar pattern emerges at no load again with a slope of 45 dB/decade.

The noise levels at full load and no load both increase at the rate of 36 dB/decade and again the predominant noise occurs in the frequency range 500-3000 Hz. The rate of increase of noise with speed and cylinder pressure spectrum slope are not the same. Comparison of the cylinder pressure spectrum overall level changes are 7.0, 5.0 and -2.0 dBA at full load; 17.0, 3.0, 0.0 dBA at no load. The corresponding measured noise level increases are 5.0, 6.5 and 3.0 dBA at full load and 12.5, 2.5 and 2.5 dBA at no load. The general trend is correct but some contribution from mechanical noise sources are present.

Thus the Indirect Injection diesel engine has a smoother cylinder pressure development as compared to the Direct Injection type and this results in a higher rate of increase in noise with speed of some 36 dB/decade

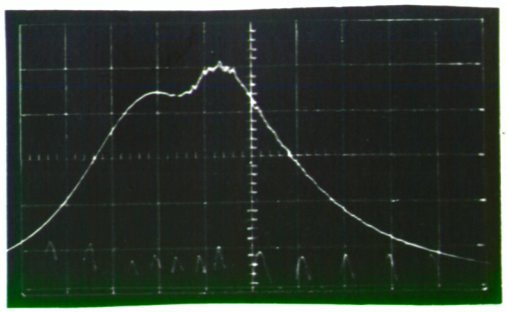

3500 rev./min. F.L.

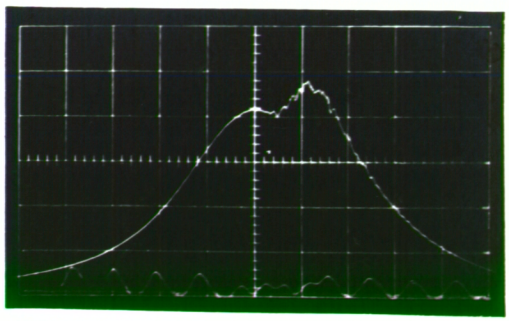

3500 rev./min. N.L.

(180 p.s.i./division)

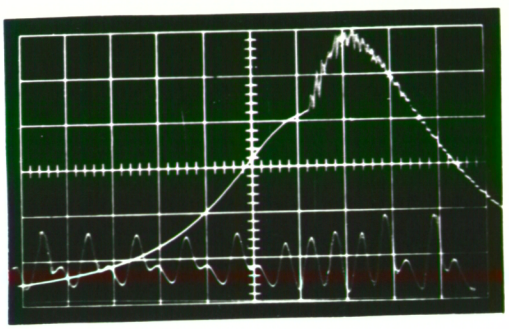

3000 rev./min. F.L.

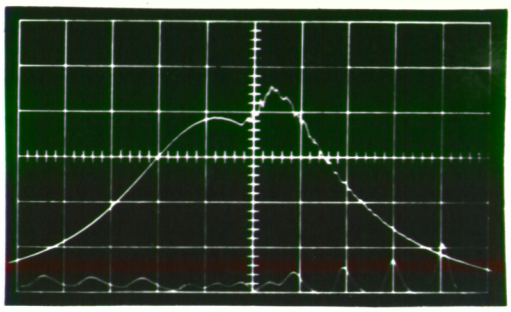

3000 rev./min. N.L.

CYLINDER PRESSURE p.s.i.

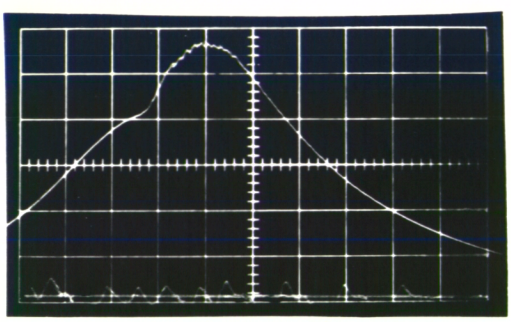

2000 rev./min. F.L.

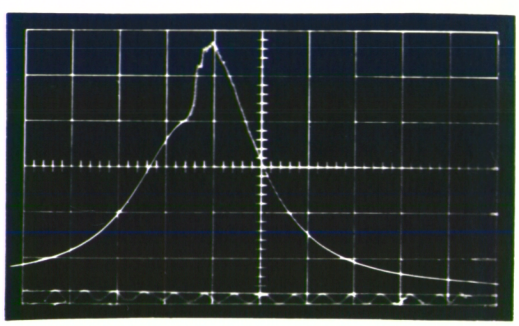

2000 rev./min. N.L.

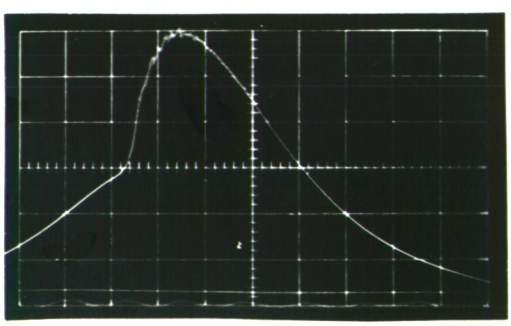

1000 rev./min. F.L.

(225 p.s.i./division)

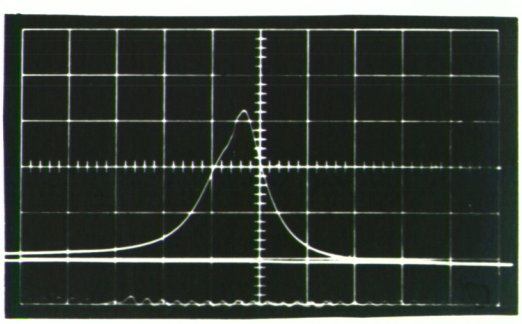

1000 rev./min. N.L.

FIG. 9.8 CYLINDER PRESSURE DEVELOPMENT FOR 3·5" BORE INDIRECT INJECTION 4-STROKE DIESEL ENGINE.

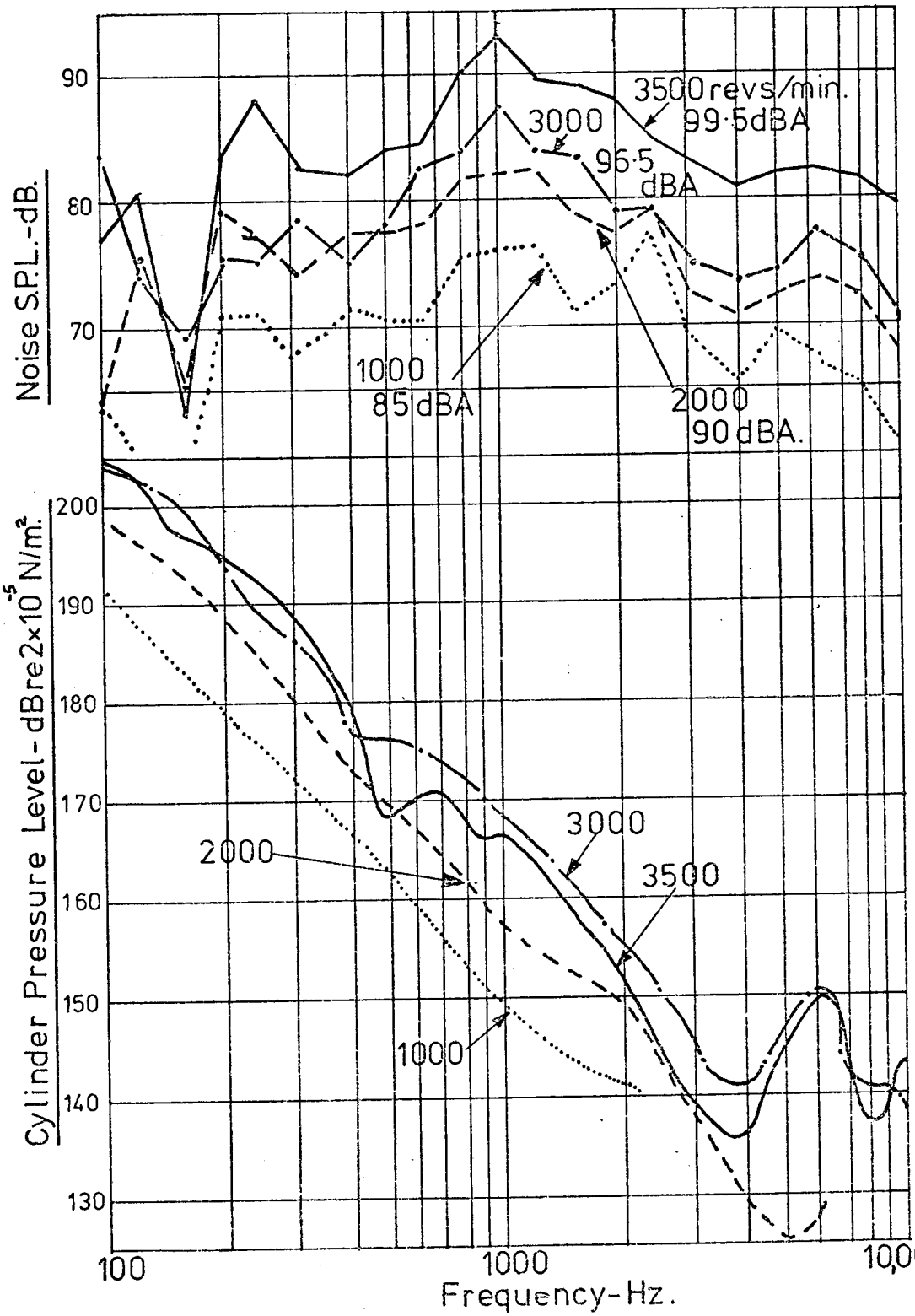

FIG.9·9 - I.D.I. FOUR STROKE FULL LOAD CHARACTERISTICS.

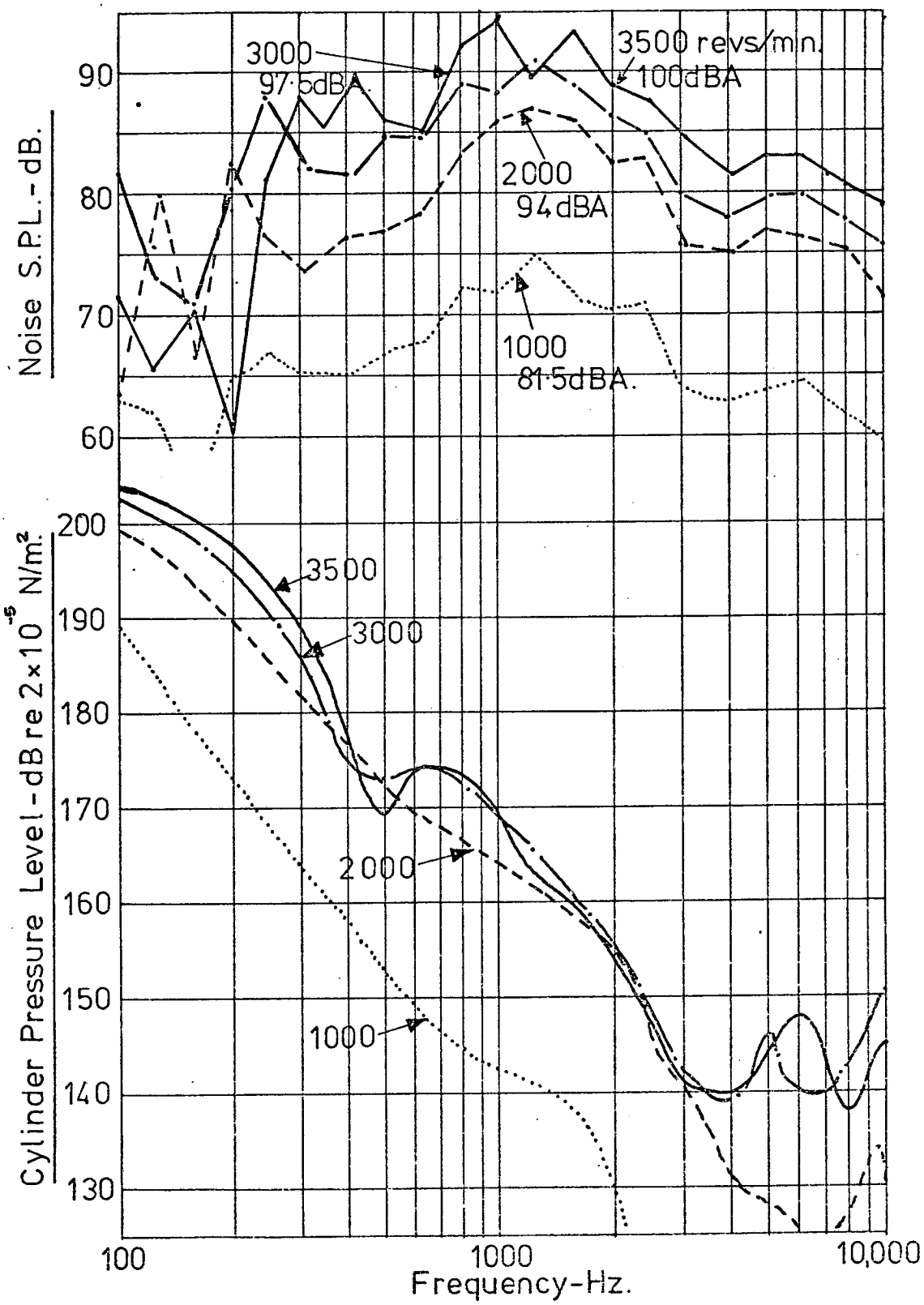

FIG. 9·10-I.D.I. FOUR STROKE NO LOAD CHARACTERISTICS.

as compared to 28 dB/decade.

In the indirect injection engine a comparison of the cylinder pressure spectrum for various engines does not show the same similarity as is the case with its direct injection counterpart. Fig. 9.10a shows a comparison between three 2.5 litre high speed indirect injection engines, all with Ricardo combustion chamber designs. For the 3.54 inch bore engine (Ricardo Mk V chamber) the timing is further retarded in production form as compared to the 3.688 inch bore engine (Ricardo Mk V chamber). This, and other detail differences, produces a marked reduction in the combustion excitation over the critical frequency range 500-3000 Hz which results in practice in a markedly quieter engine. A 3.5 inch bore engine (Ricardo Mk. III) with comparatively advanced timing is also shown for comparison.

For the indirect injection four stroke diesel considerable variation in combustion excitation may be expected from very similar combustion chamber designs. The choice of engine to represent the class is somewhat arbitrary but has been chosen as representing an engine with perhaps a slightly high combustion excitation, thus avoiding any possibility of exaggeration when general characteristics of the class are discussed (the I.D.I. is classed below the D.I.).

9.3.3 Two stroke direct injection diesel engine

Figures 9.11, 9.12 and 9.13 show the combustion and noise characteristics of a 3.62" bore valve in head two stroke diesel engine with deep bowl torroidal chamber utilising high swirl and a single hole nozzle.

The cylinder pressure development shows a fairly constant peak pressure with changing speed and reduces some 250 psi at no load conditions. The rate of pressure rise varies from 60 to 80 psi/degree with increasing speed but it can be seen that the diagram takes on a more smooth appearance with increasing speed. This is due to the increase in compression pressure with

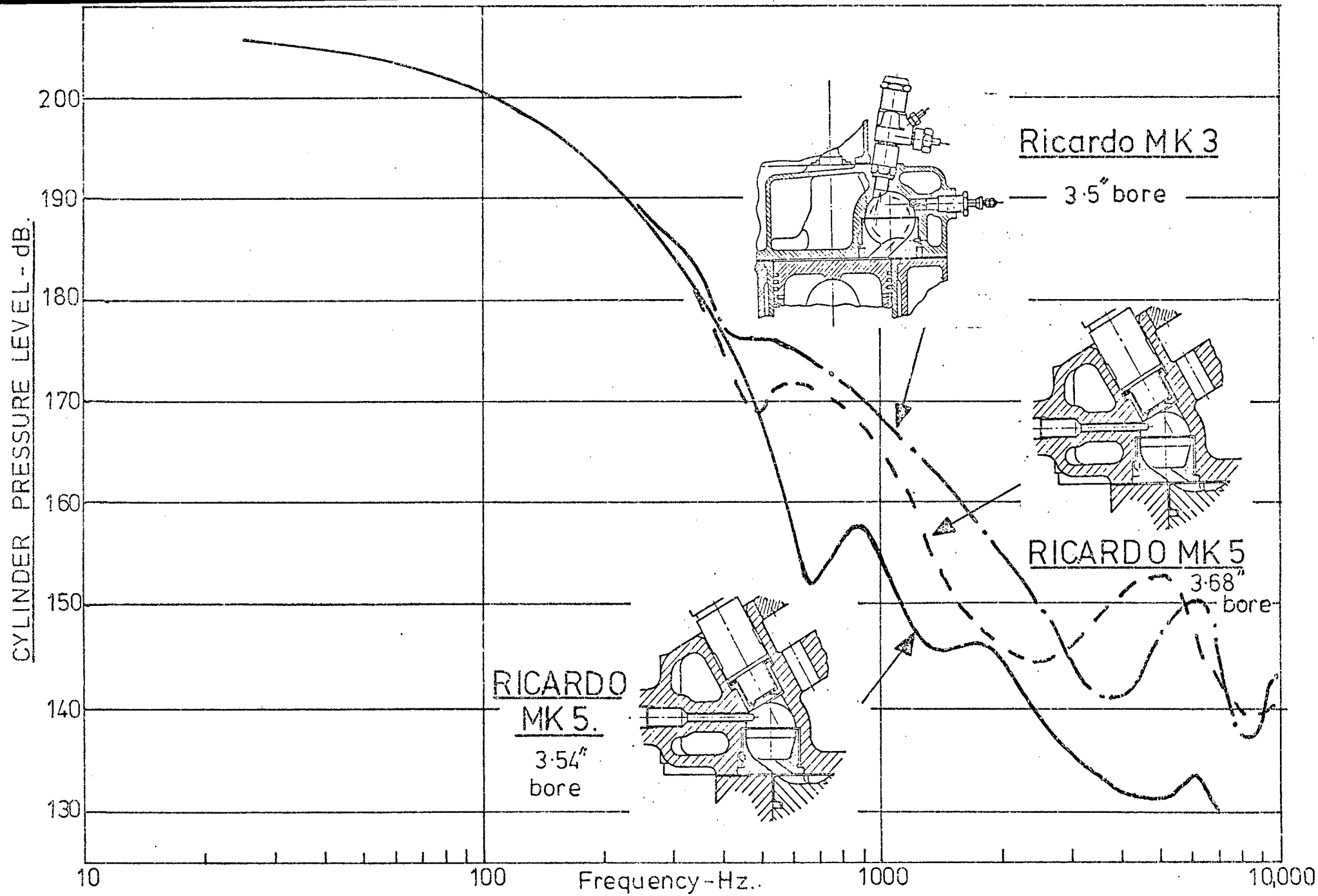

FIG. 9·10a COMPARISON OF I.D.I. COMBUSTION CHAMBERS - 3000 revs/min. F.L.

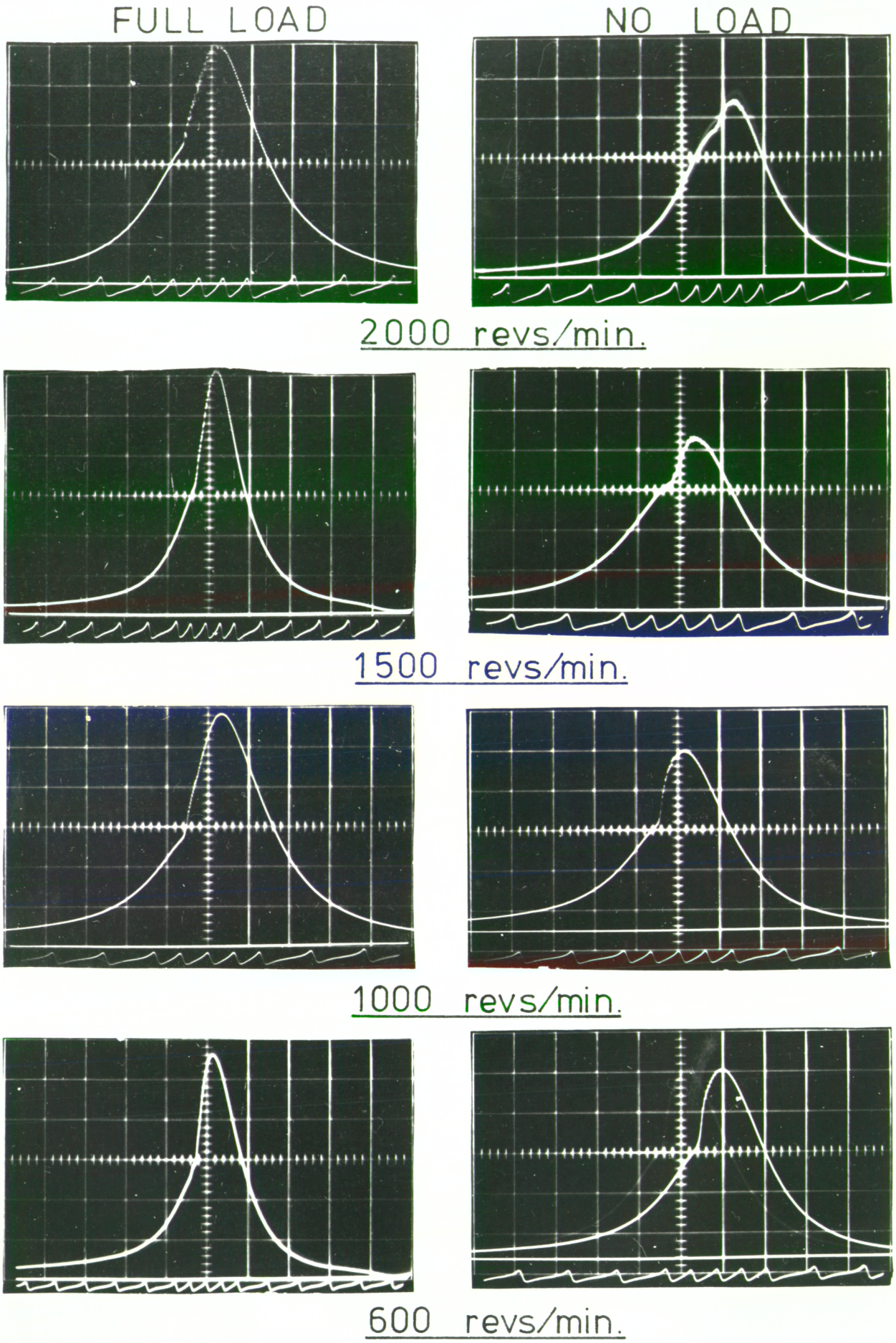

FIG. 9·11 - CYLINDER PRESSURE DEVELOPMENT FOR 3·62" BORE DIRECT INJECTION TWO STROKE DIESEL ENGINE.

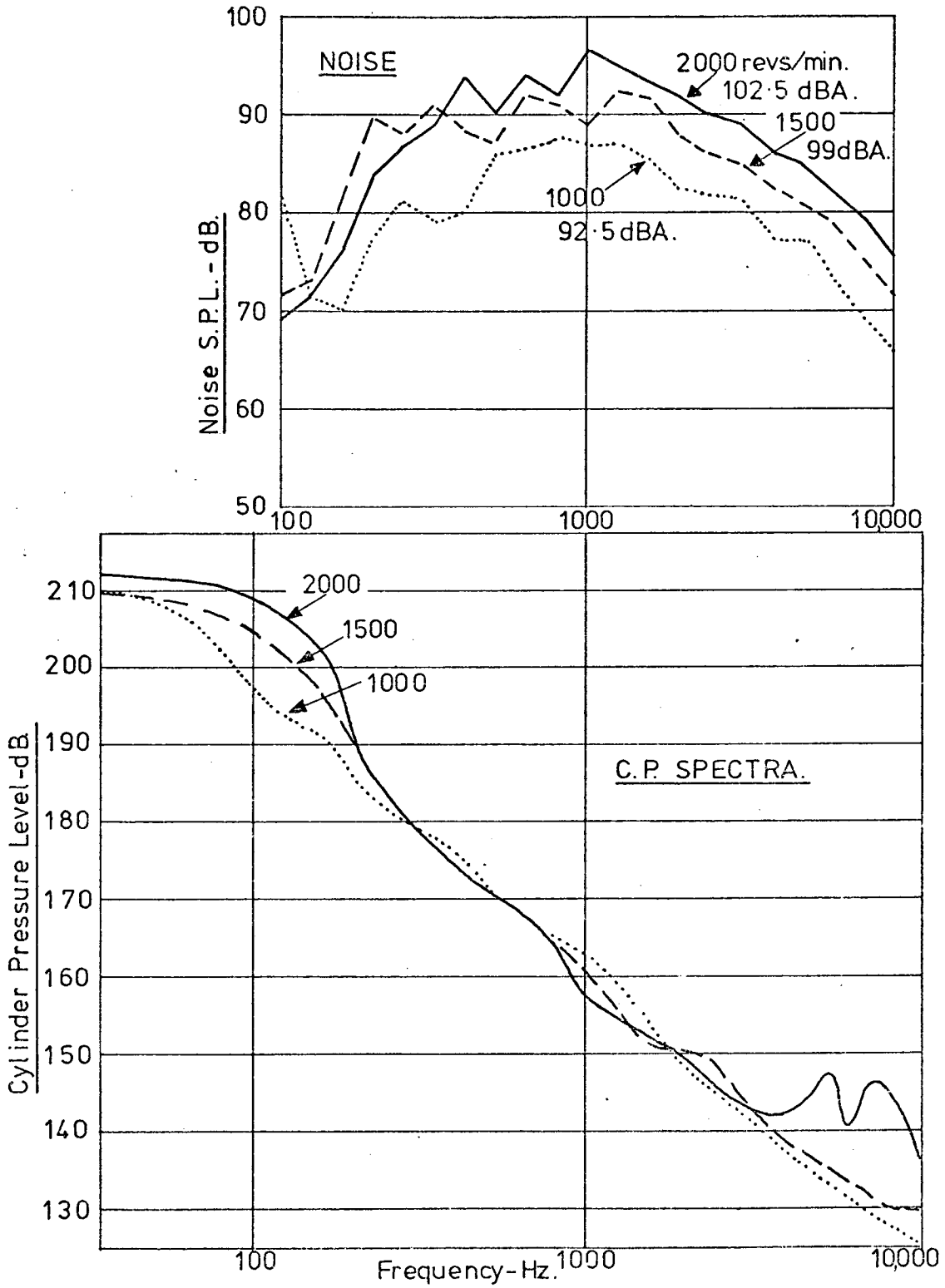

FIG.9·12 - D.I. TWO STROKE FULL LOAD CHARACTERISTICS.

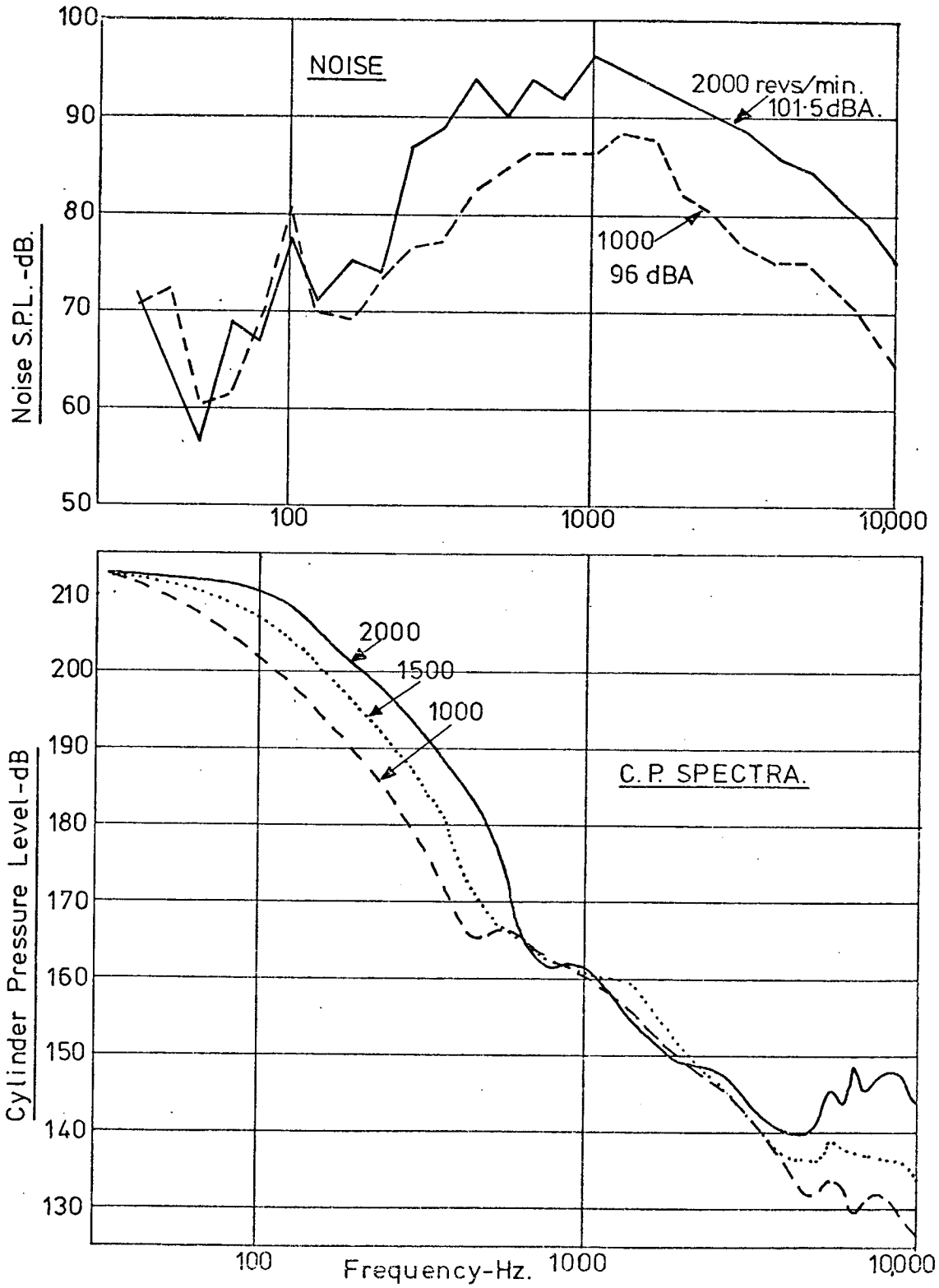

FIG.9·13 - D.I. TWO STROKE NO LOAD CHARACTERISTICS.

speed caused by the incorporation of a Roots blower. This is a feature of two stroke operation, and effectively reduces the acceleration of pressure rise as the speed is increased. Figure 9.14 shows a comparison between two stroke and four stroke compression pressures and speed. The increased compression pressure and temperature results in a reduction in delay period and consequent smoothing of the initiation of combustion.

The cylinder pressure spectra at full and no load are similar. The increased low frequency levels due to the two stroke cycle of operation are apparent and the general slope of 40 dB/decade indicates the smoothness of combustion. However, the effect of the gradual smoothing with speed is seen clearly in that there is virtually no difference in combustion excitation from 1000 to 2000 revs/min in the frequency range 600 to 3000 Hz. Hence no increase in combustion noise over this speed range would be expected.

Examination of the noise results, however, shows a general increase in noise with speed at the rate of 26 dB/decade. Again the predominant noise occurs in the 500 to 3000 Hz range. In this engine it was found that the noise radiated by the Roots blower casing became the predominant noise source at higher engine speeds.

ROOTS BLOWER NOISE - Figure 9.15 shows the effect of Roots blower noise on some two stroke diesel engines. The results were obtained by using a remote Lysholm blower (Fig. 9.16) to provide air to the engines so that they could be run without a Roots blower on the engine. The air was supplied via acoustically treated ducts with large volume settling tank so that noise was reduced in the incoming air. In this way the Roots blower casing noise could be investigated. A highly rated Roots blower (straight lobes) with 160 ft/sec tip speed provided the predominant noise source on an in-line opposed piston two stroke with noise levels some 6 dBA higher than that of the engine (fig. 9.15a). The noise was localised mainly to the blower side of the engine. Figure 9.15b shows the same type of measurement for a moderately rated Roots blower (helical lobes) with 100 ft/sec tip speed.

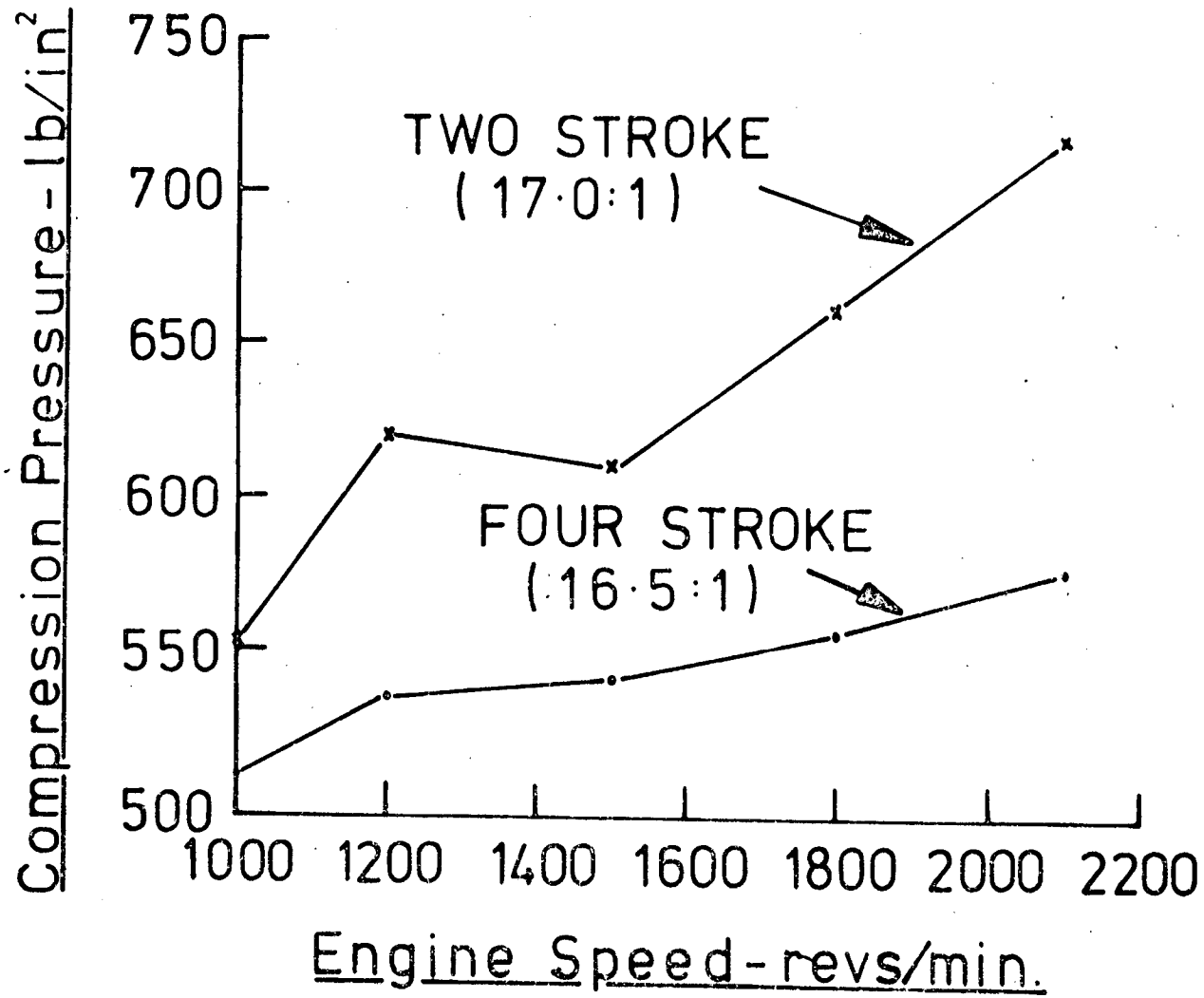

Fig. 9·14 - COMPARISON OF COMPRESSION PRESSURE IN TWO AND FOUR STROKE DIESELS.

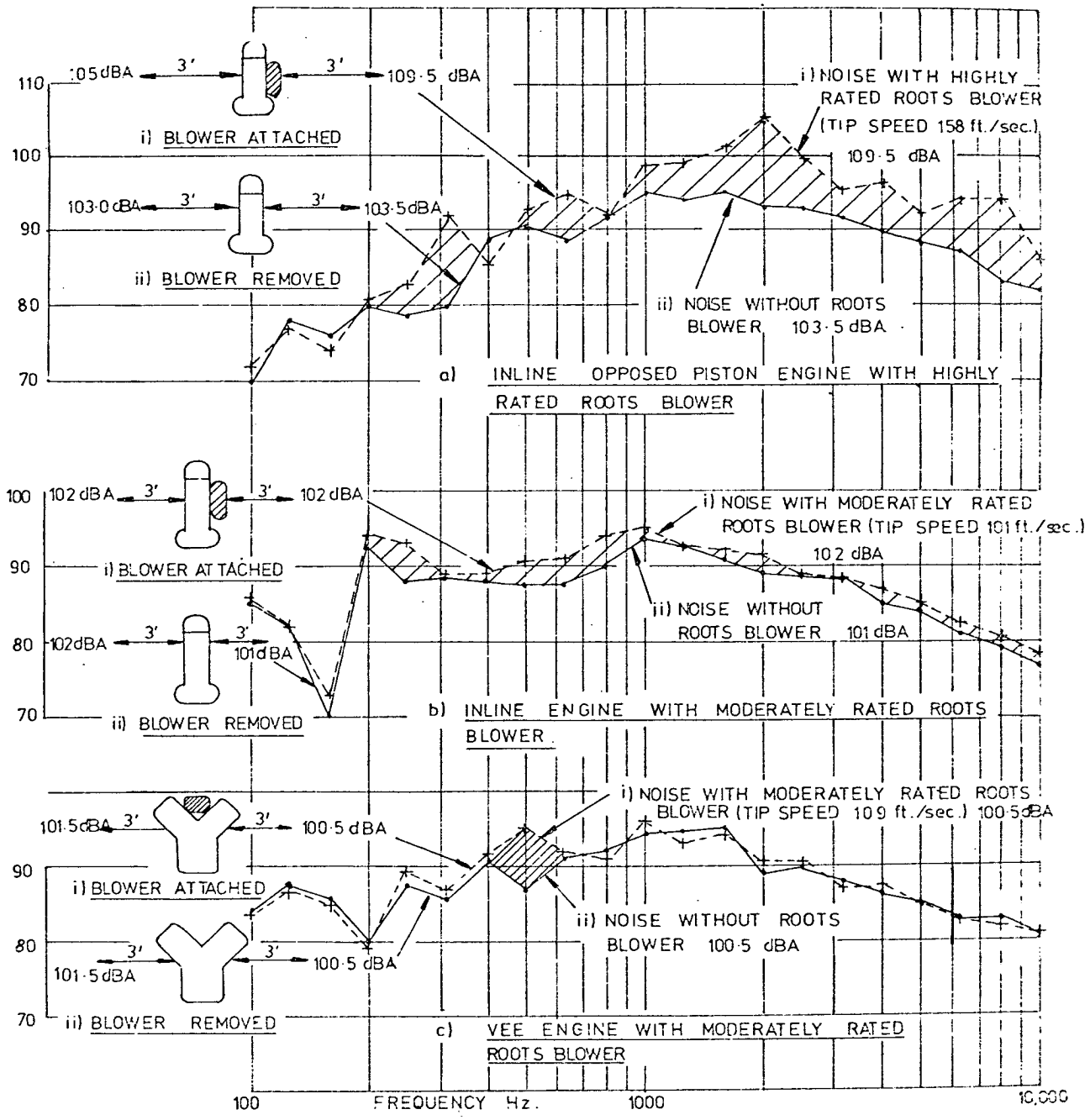

FIG. 9·15- EFFECT OF ROOTS BLOWER CASING NOISE AND LAYOUT ON TWO STROKE DIESEL ENGINE NOISE

Here the noise increase is only 1 dBA and again this is localised to the blower side of the engine. In figure 9.15c the effect of a moderately rated Roots blower (helical blades) on the noise of a Vee engine is shown. There is no noise increase on either side of the engine, the shielding effect of the cylinder banks being sufficient to counteract the blower casing noise. Thus with moderately rated Roots type blowers the casing noise can be reduced below that of the engine noise. Where blower noise is present the increased noise is of a localised nature.

The combustion and noise characteristics of a 3.4" bore opposed piston two stroke engine run without a Roots blower but supplying scavenge air with the Lysholm blower rig (fig. 9.16) are shown in figs. 9.17 and 9.18. The smoothing effect of the increasing compression pressure with speed is apparent in the cylinder pressure diagrams and shows more clearly on the cylinder pressure spectra where there is little increase in excitation above 1500 revs/min. The general slope is 35 dB/decade, indicating more abrupt combustion as compared to the valve in head engine. The noise does not increase greatly with speed in this case, the overall rate of increase in noise being some 20 dB/decade.

A comparison of the noise increases expected from changes in the cylinder pressure spectrum overall level with the measured overall noise increases are: 4.0, 2.0 and 1.5 dBA from combustion and 4.5, 1.5 and 1.0 dBA for measured noise showing that without the Roots blower casing noise the overall engine noise is directly controlled by combustion.

5.3.4 Four stroke turbocharged direct injection diesel engines

Figs. 9.19 and 9.20 show the combustion and noise characteristics of a 4.5" turbocharged direct injection four stroke diesel engine with shallow bowl combustion chamber utilising low swirl and five nozzle holes. A rotary injection pump is fitted. The cylinder pressure development at full

Fig. 9.16 Lysholm blower rig.

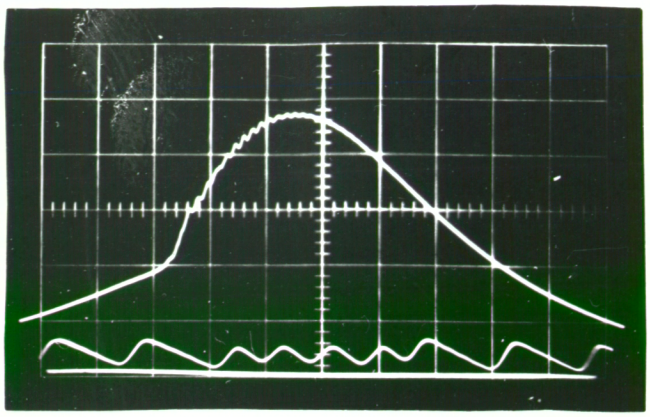

1000 r.p.m. FULL LOAD
NORMAL TIMING
(PEAK PRESSURE 1055 p.s.i.)

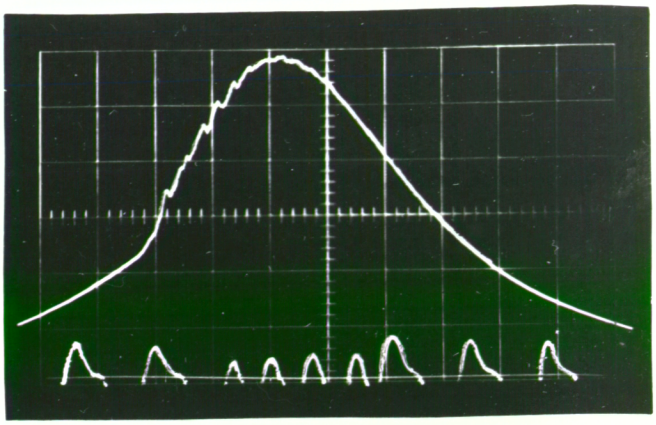

2400 r.p.m. FULL LOAD
NORMAL TIMING
(PEAK PRESSURE 1250 p.s.i.)

CYLINDER PRESSURE p.s.i. (225 p.s.i./ division)

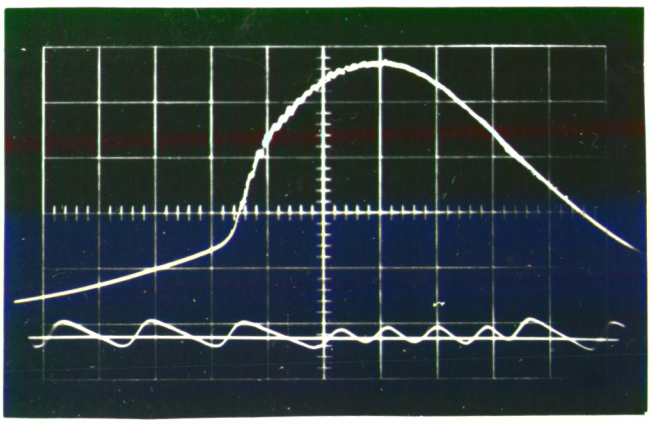

1000 r.p.m. FULL LOAD
5° ADVANCE
(PEAK PRESSURE 1115 p.s.i.)

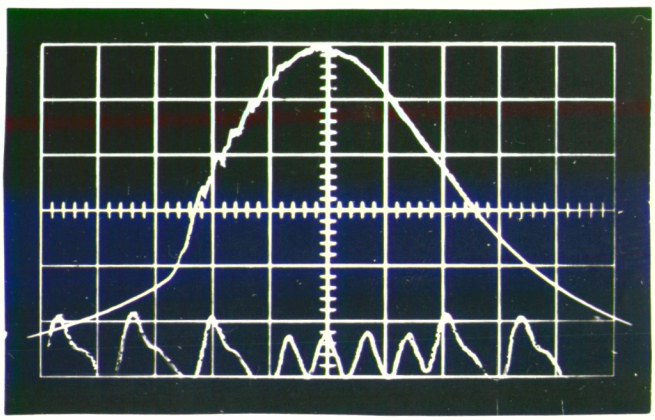

2400 r.p.m. FULL LOAD
5° ADVANCE
(PEAK PRESSURE 1340 p.s.i.)

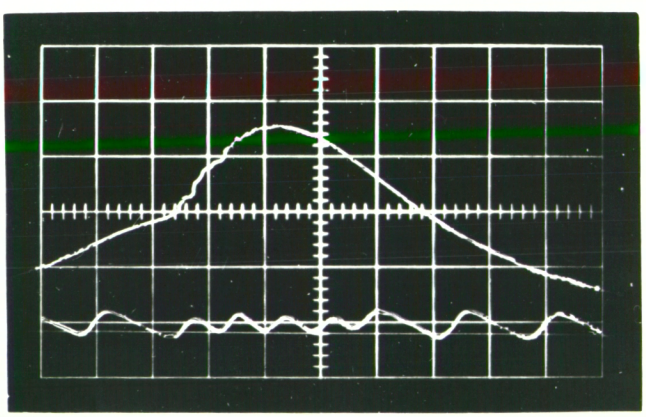

1000 r.p.m. FULL LOAD
5° RETARD
(PEAK PRESSURE 743 p.s.i.)

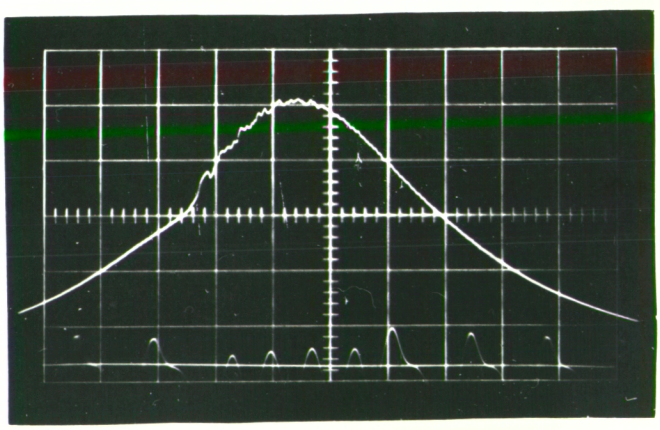

2400 r.p.m. FULL LOAD
5° RETARD
(PEAK PRESSURE 1080 p.s.i.)

FIG. 9·17 - CYLINDER PRESSURE DEVELOPMENT FOR 3·43" BORE OPPOSED PISTON TWO STROKE DIESEL ENGINE.

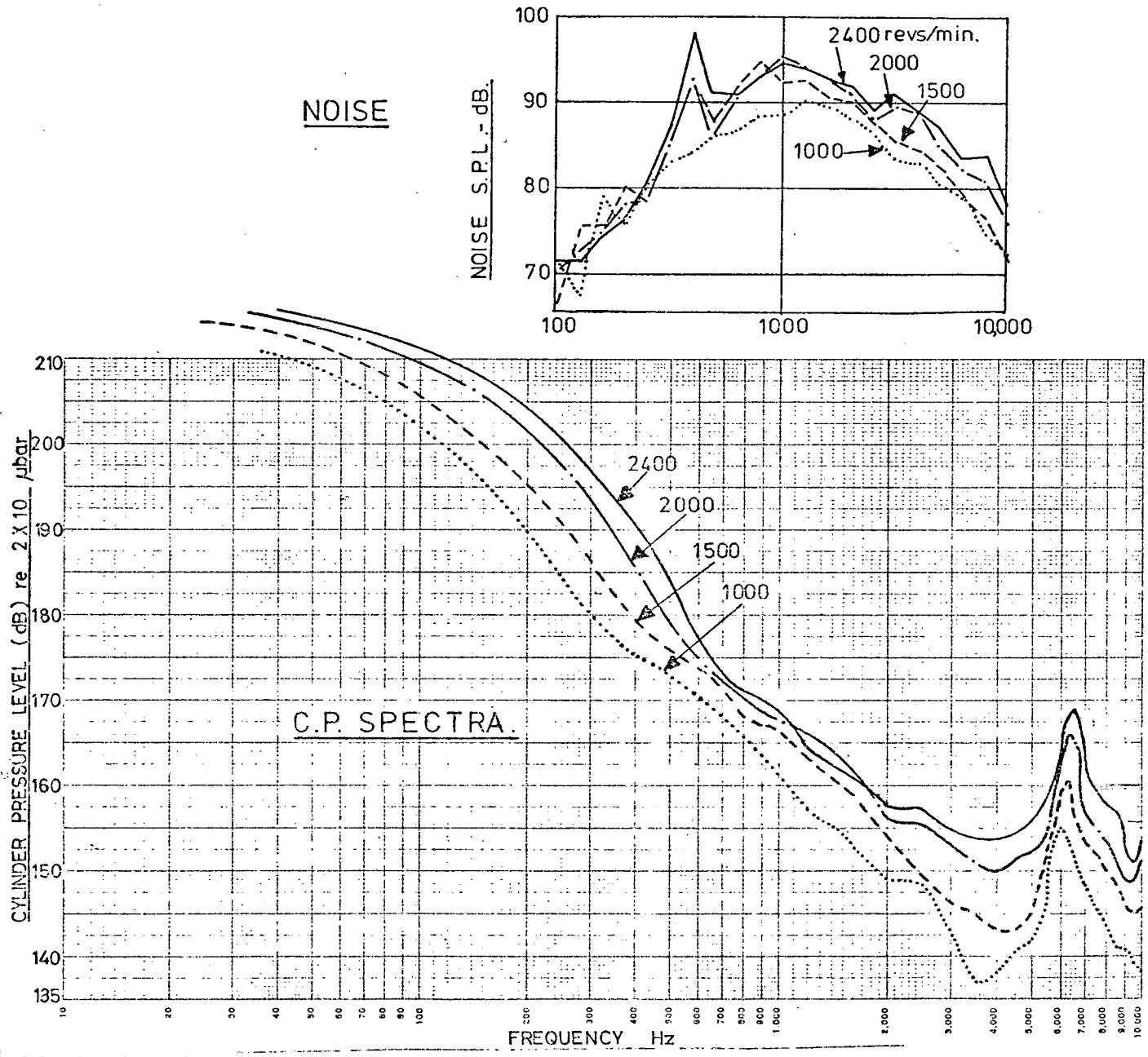

FIG. 9·18- OPPOSED PISTON 2 STROKE FULL LOAD CHARACTERISTICS - ROOTS BLOWER REMOVED.

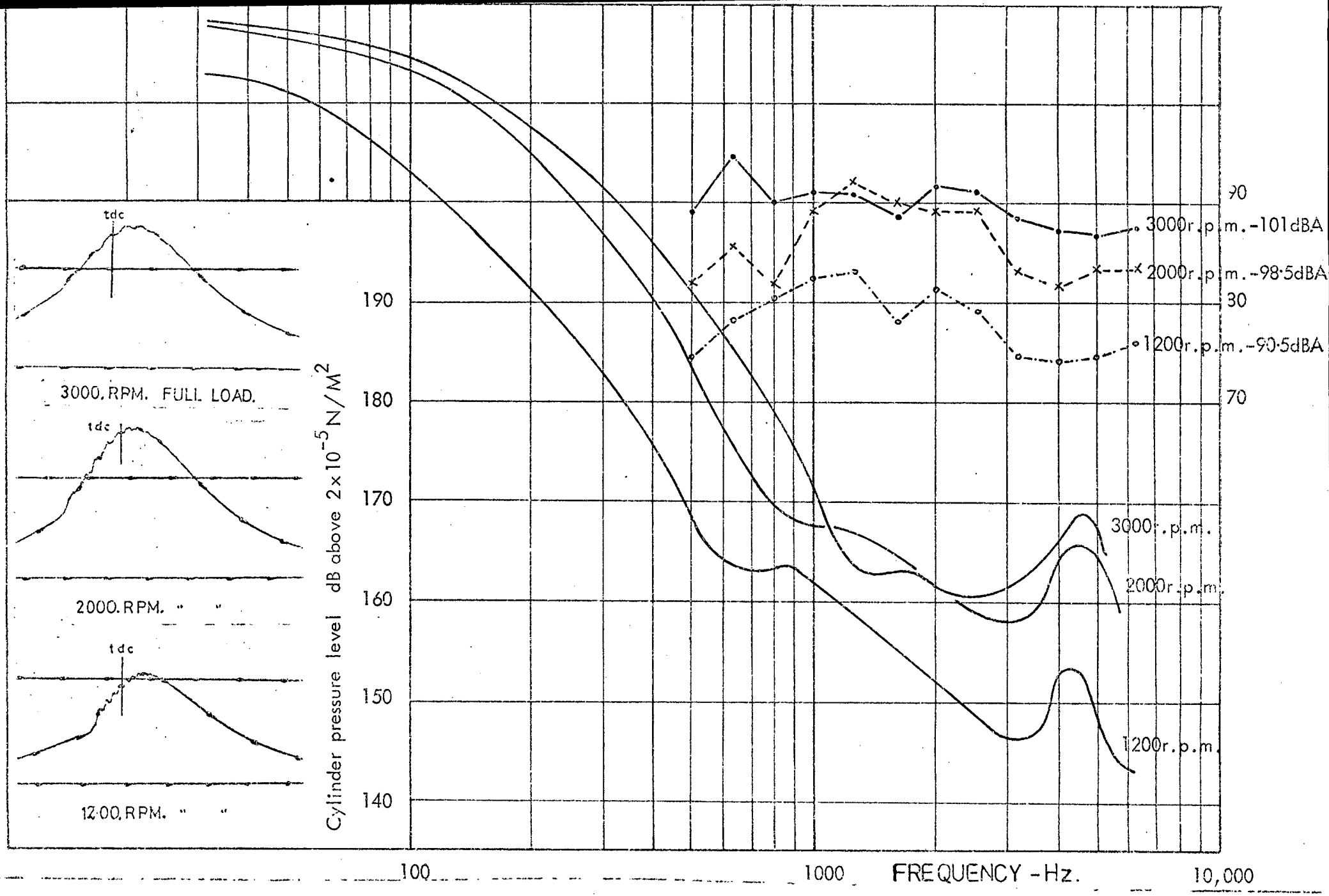

FIG.9·19 - TURBOCHARGED D.I. FOUR STROKE FULL LOAD CHARACTERISTICS.

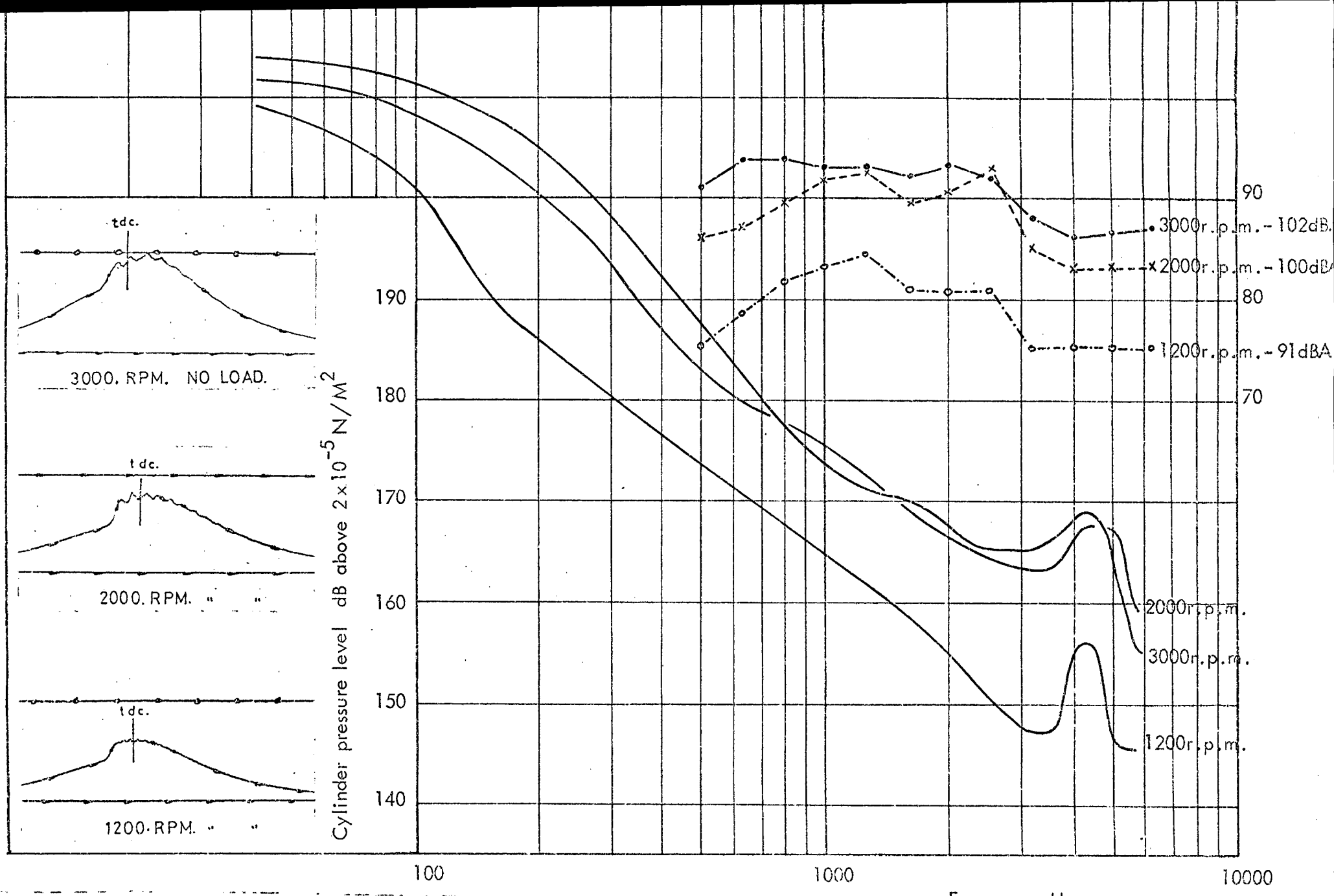

FIG. 9·20 - TURBOCHARGED D.I. FOUR STROKE NO LOAD CHARACTERISTICS.

load behaves rather like that of a two stroke, with the pressure diagram smoothing with increased engine speed. This is due to the turbocharger which effectively increases the pressure and temperature of compression and hence reduces the ignition delay. The cylinder pressure spectra are also similar in form to those of the two stroke, the combustion excitation at 2000 revs/min being only marginally changed at 3000 revs/min. The slope is some 45 dB/decade at full load. The measured overall noise level increases at 21 dB/decade, however, and again a direct comparison with the actual excitation level shows better correlation. The increases expected from the cylinder pressure spectra are 9.0 and 3.0 dBA, the measured values 8.0 and 2.5 dBA.

Under no load conditions, however, the turbocharger is not providing so much boost pressure and the cylinder pressure development and spectra are closer to the normally aspirated four stroke characteristic. Even so at higher engine speeds smoothing does occur. The general slope of cylinder pressure spectrum is 35 dB/decade and that of noise 23 dB/decade. Again the expected noise increase from the cylinder pressure excitation agrees closely with 10.0 and 1.5 dBA estimated and 9.0 and 2.0 dBA measured. The cylinder pressure excitation levels are higher at the no load condition as is also the measured noise.

9.3.5 Two stroke turbocharged direct injection diesel engine

Figures 9.21 and 9.22 show the combustion and noise characteristics of a turbocharged 3.62" bore valve in head two stroke diesel engine with deep bowl torroidal chamber utilising high swirl and a single hole nozzle.

The cylinder pressure development at both full load and no load are very smooth, but with similar rates of pressure rise as for the straight Roots scavenged engine because of the increased peak pressures. This

FULL LOAD

NO LOAD

CYLINDER PRESSURE - lb/in.^{2} (352 lb/in.^{2}/division.)

(220 lb/in/division.)

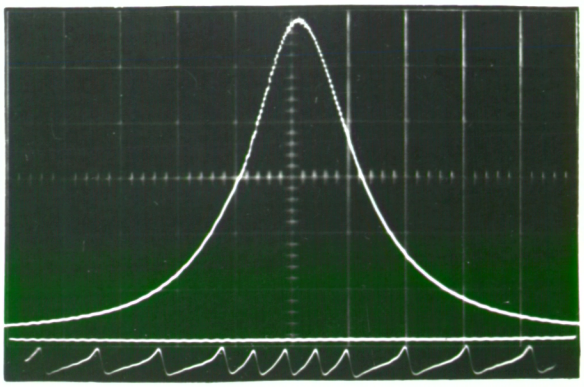

2000 revs/min.

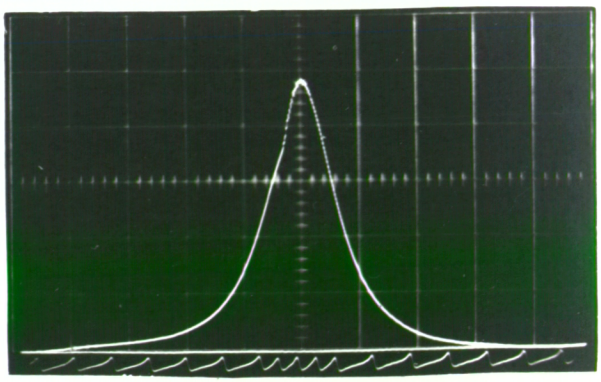

2000 revs/min.

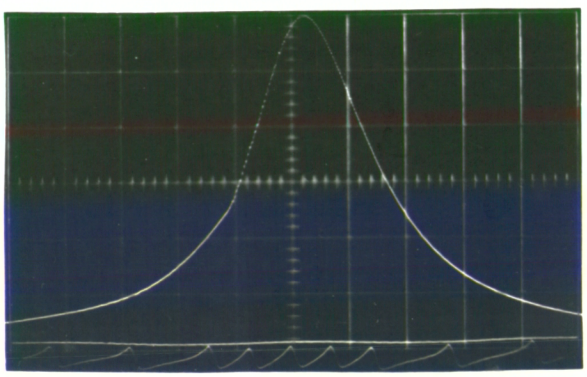

1500 revs/min.

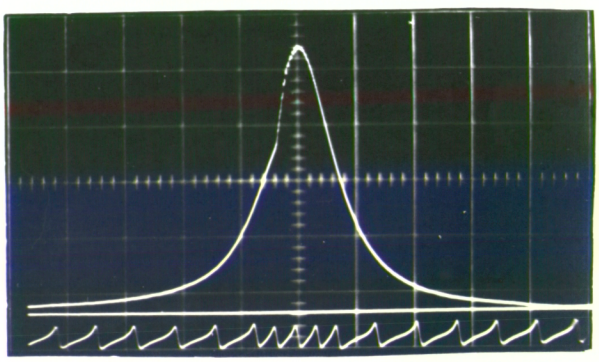

1500 revs/min.

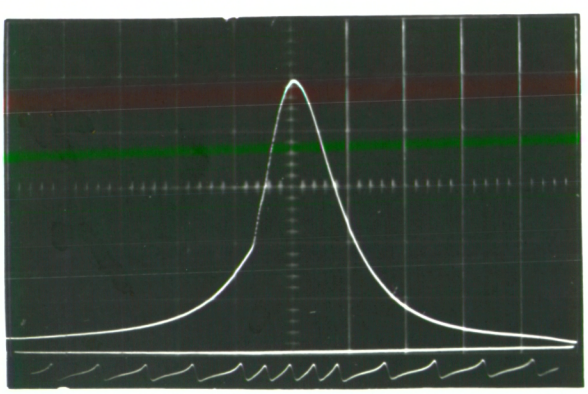

1000 revs/min.

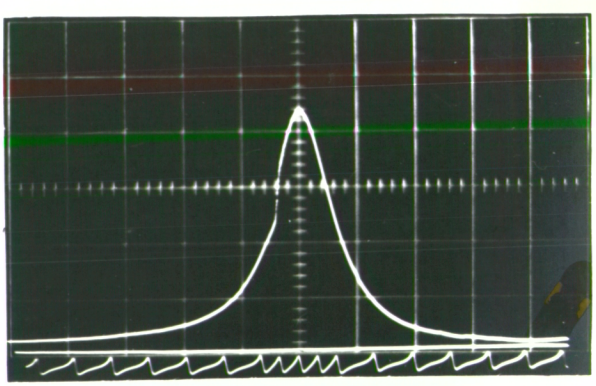

1000 revs/min.

FIG. 9·21 - CYLINDER PRESSURE DEVELOPMENT FOR 3·62" BORE TURBOCHARGED DIRECT INJECTION TWO STROKE DIESEL ENGINE.

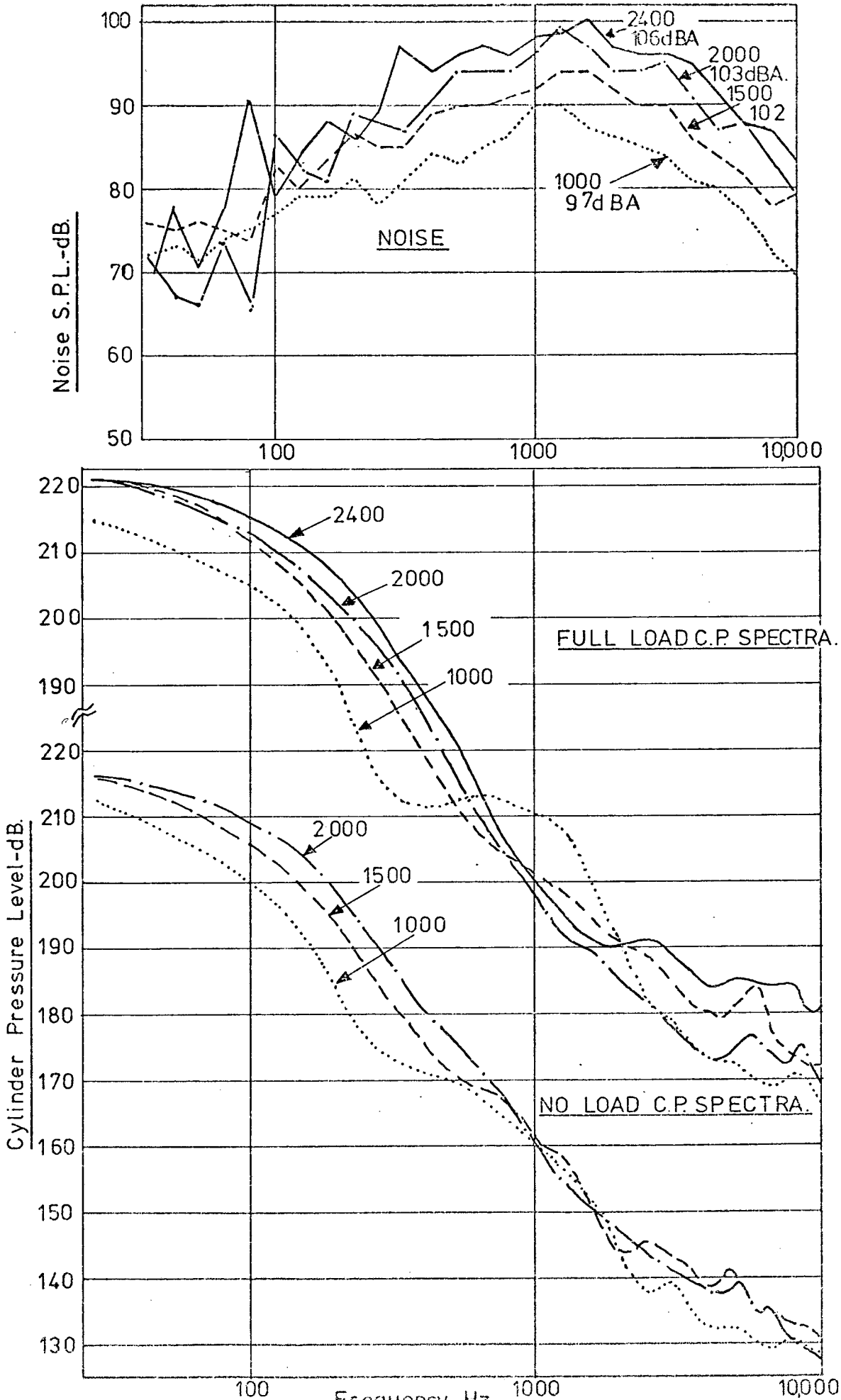

FIG.9·22 - TURBOCHARGED D.I. TWO STROKE FULL AND NO LOAD CHARACTERISTIC.

produces very smooth cylinder pressure spectra with very high values at low frequency and a general slope of 50 dB/decade (same as petrol engine). Again the smoothing effect is apparent, this time caused by a combination of Roots blower and turbocharger. Similar results are shown at no load.

The measured noise increases uniformly with engine speed and is again controlled by the radiation of noise from the Roots blower case and inlet trunking.

3.3.6 Fuel injected petrol engines

Figures 9.23 and 9.24 show the combustion and noise characteristics of a four stroke fuel injected 5.31" bore petrol engine.

The cylinder pressure development at full load has the appearance of a 'fast burn' cycle for a normally carburetted petrol engine and a high rate of pressure rise of some 60 psi/degree is present at all speeds. The general smoothness of the development in comparison to diesel operation is evident and examination of the cylinder pressure spectra show that the slope of the spectrum is some 55 dB/decade, the diagram remaining the same on a degree basis through the speed range (spark advance with speed).

Because an open air inlet was used, from a performance consideration, the air inlet noise is present in the measured noise level. The noise shows increasing levels with speed at the rate of 27 dB/decade. Comparison with the expected noise increase due to combustion excitation gives figures of 15.0, 6.0 and 6.0 dBA whilst the measured values are 8.0, 5.5 and 3.5 dBA, again indicating noise controlled by sources other than combustion.

9.3.7 Overall combustion excitation characteristics of six classes of I.C. engine

For the purposes of this comparison the combustion excitation characteristics (cylinder pressure spectrum level as a function of speed and load) are taken to be the reference characteristic.

FULL LOAD

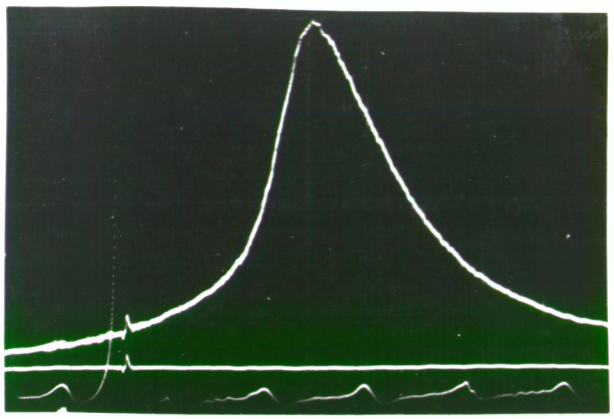

4000 revs/min.

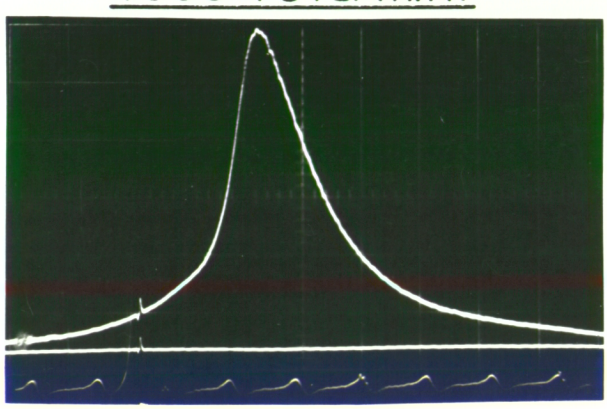

3000 revs/min.

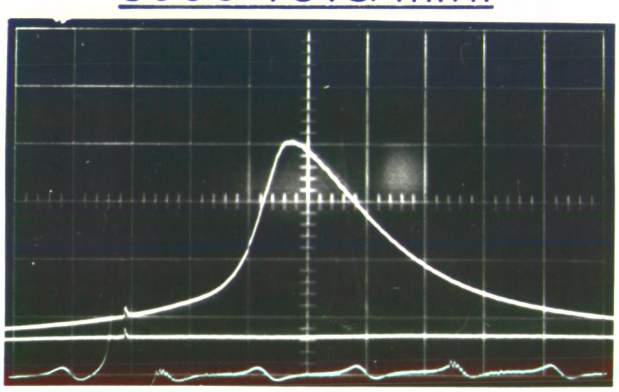

2000 revs/min.

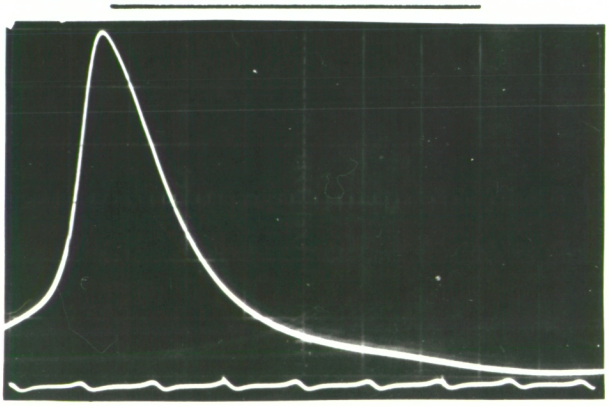

1000 revs/min.

CYLINDER PRESSURE - lb/in.^{2} (130 lb/in.^{2}/division.)

(260 lb/in/division.)

FIG. 9·23 - CYLINDER PRESSURE DEVELOPMENT FOR 5·31" BORE FUEL INJECTED FOUR STROKE PETROL ENGINE.

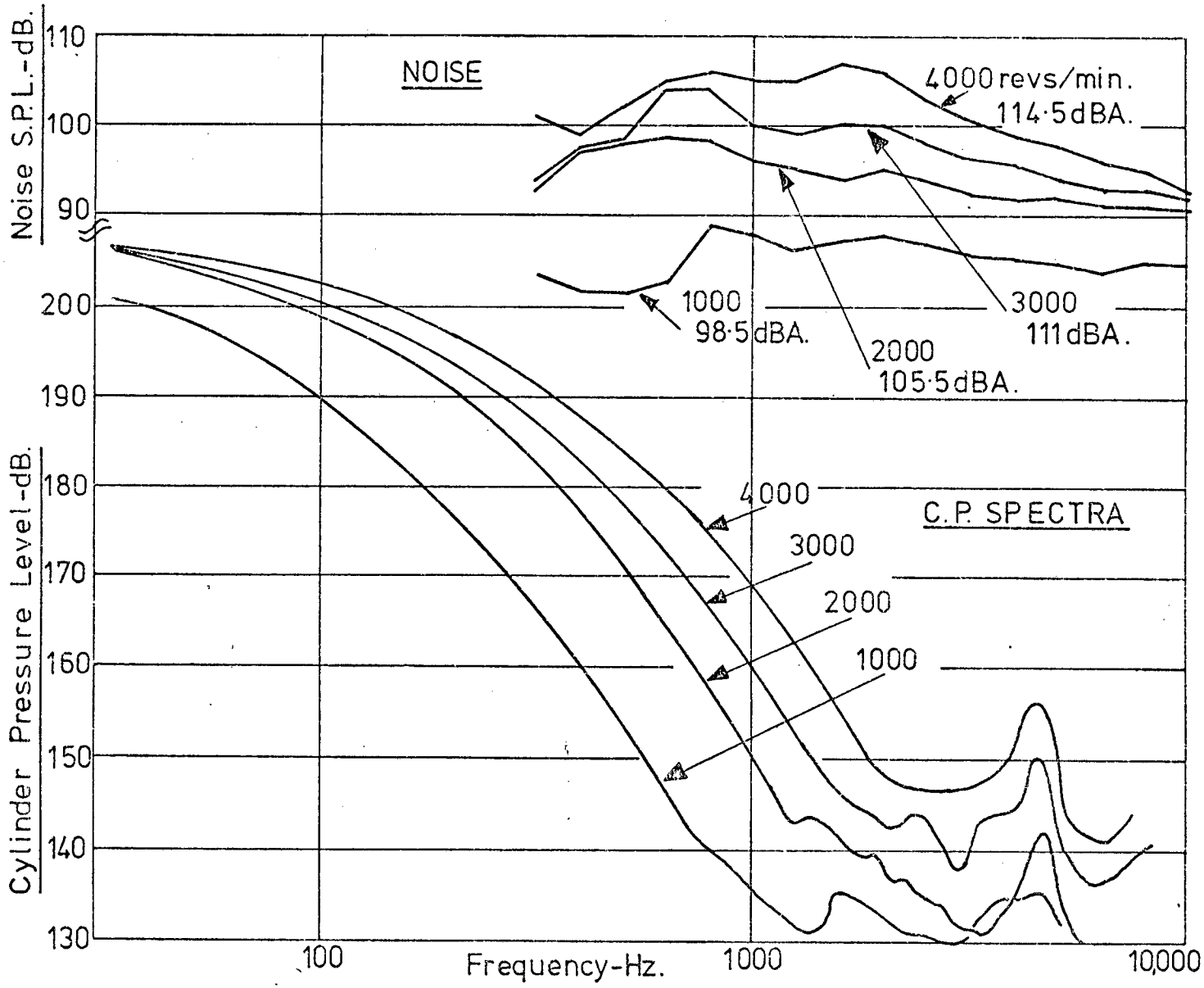

FIG. 9·24 - FUEL INJECTION PETROL ENGINE FULL LOAD CHARACTERISTICS.

The effect of turbocharging the four stroke cycle is shown in figure 9.25. The peak pressure and diagram width are increased which produces low frequency cylinder pressure spectrum levels approaching those of the two-stroke cycle engine. At the same time the increase in amount and temperature of the available air immediately prior to ignition tends to smooth the rates of pressure rise and rates of change of pressure rise and this produces a reduction in the combustion noise in the important frequency range above 500 Hz. The effect of turbocharging then is to provide lower combustion noise for increased power at the expense only of increased force inputs to the structure at low frequency.

Generally two stroke and four stroke engines tend to run at similar speeds for a given application. Figure 9.26 shows a comparison of two and four stroke cylinder pressure spectra at their rated speeds. It can be seen that over the important frequency range above 500 Hz, there is little difference in their noise exciting properties, even though peak pressures vary by a factor of nearly two. This is largely because the cylinder pressure levels over this frequency range are controlled by rates of pressure rise and rates of change of pressure rise (rate of injection, number of spray holes, swirl, etc.) rather than purely peak pressure.

It can therefore be concluded that the operating cycle has a profound effect on noise and that the two-stroke cycle principle can offer a substantial (6 dBA) advantage over the four-stroke for a given power output. This is so when both engines are run at the same bmep and have the same swept volume, but the two stroke operates at half the speed of the four stroke.

A comparison of the Direct Injection and Indirect Injection four stroke diesel engine at rated speed is shown in fig. 9.27. Because the I.D.I. can run with a more retarded injection timing, the cylinder pressure development is considerably smoother than for the D.I. engine. This causes the cylinder

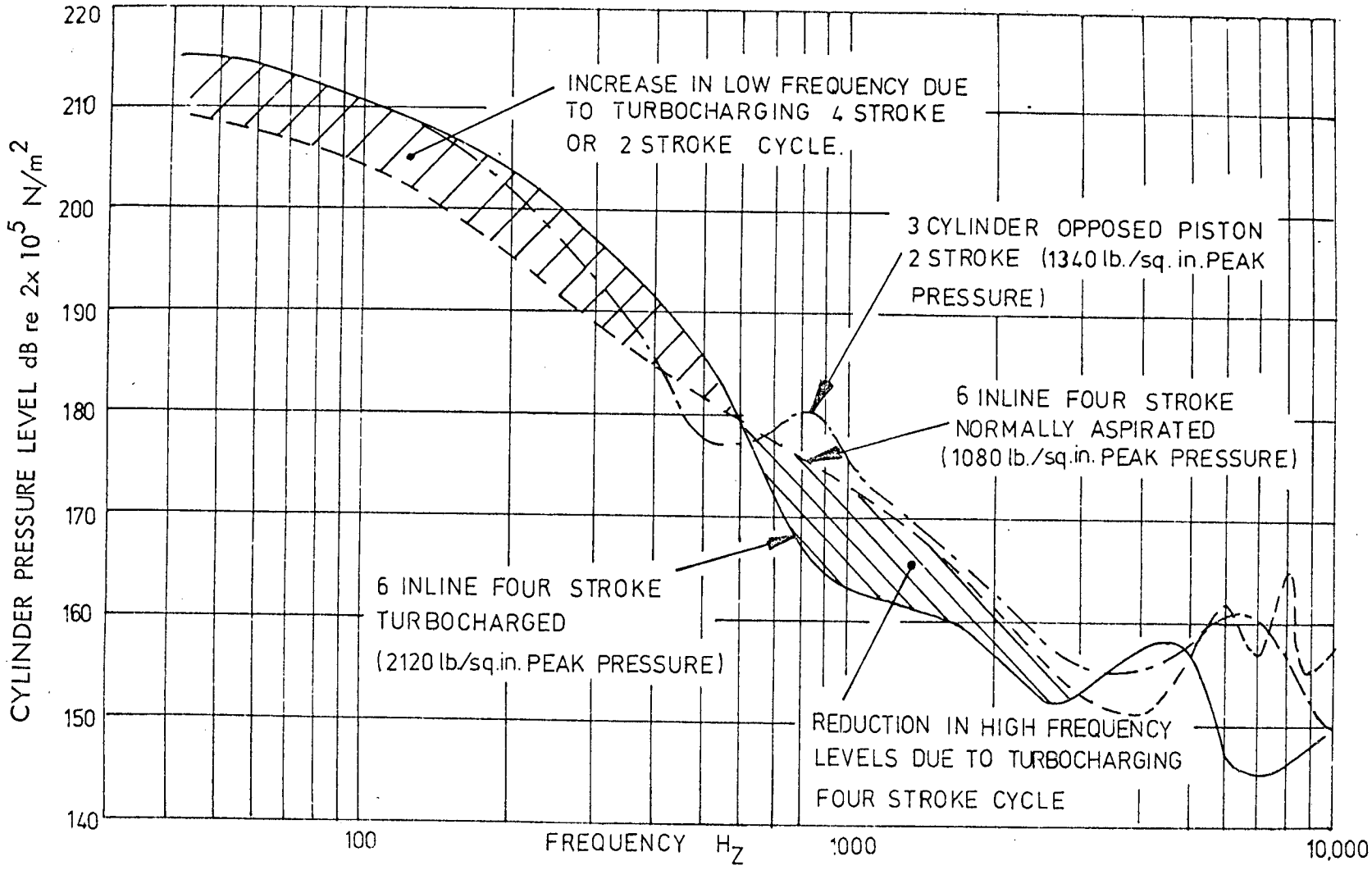

FIG. 9·25- EFFECT OF TURBOCHARGING ON CYLINDER PRESSURE SPECTRUM OF FOUR STROKE DIESELS AT RATED SPEED

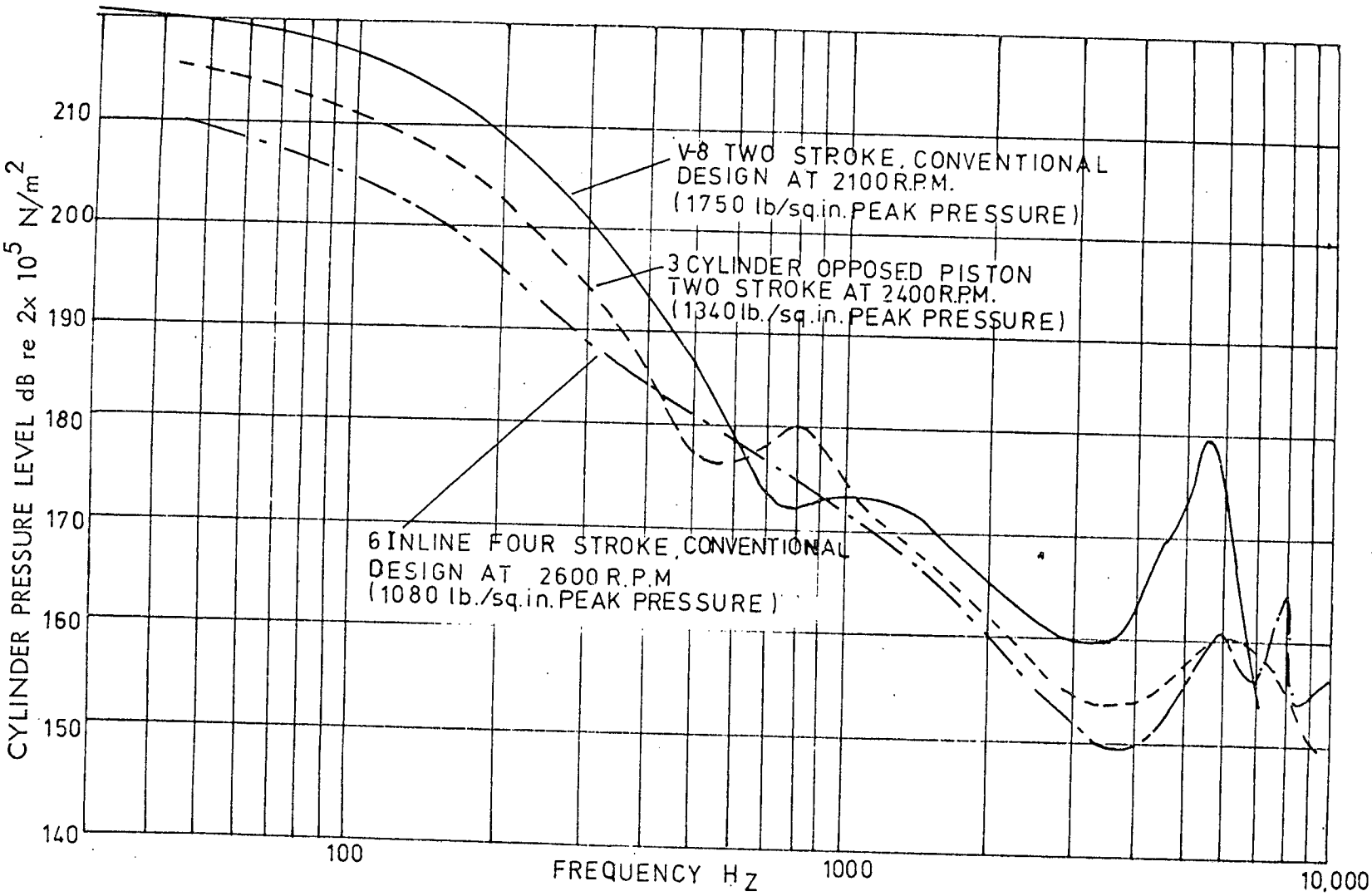

FIG. 9·26 COMPARISON OF FOUR AND TWO STROKE CYCLE DIESEL ENGINE CYLINDER PRESSURE SPECTRA AT RATED SPEED.

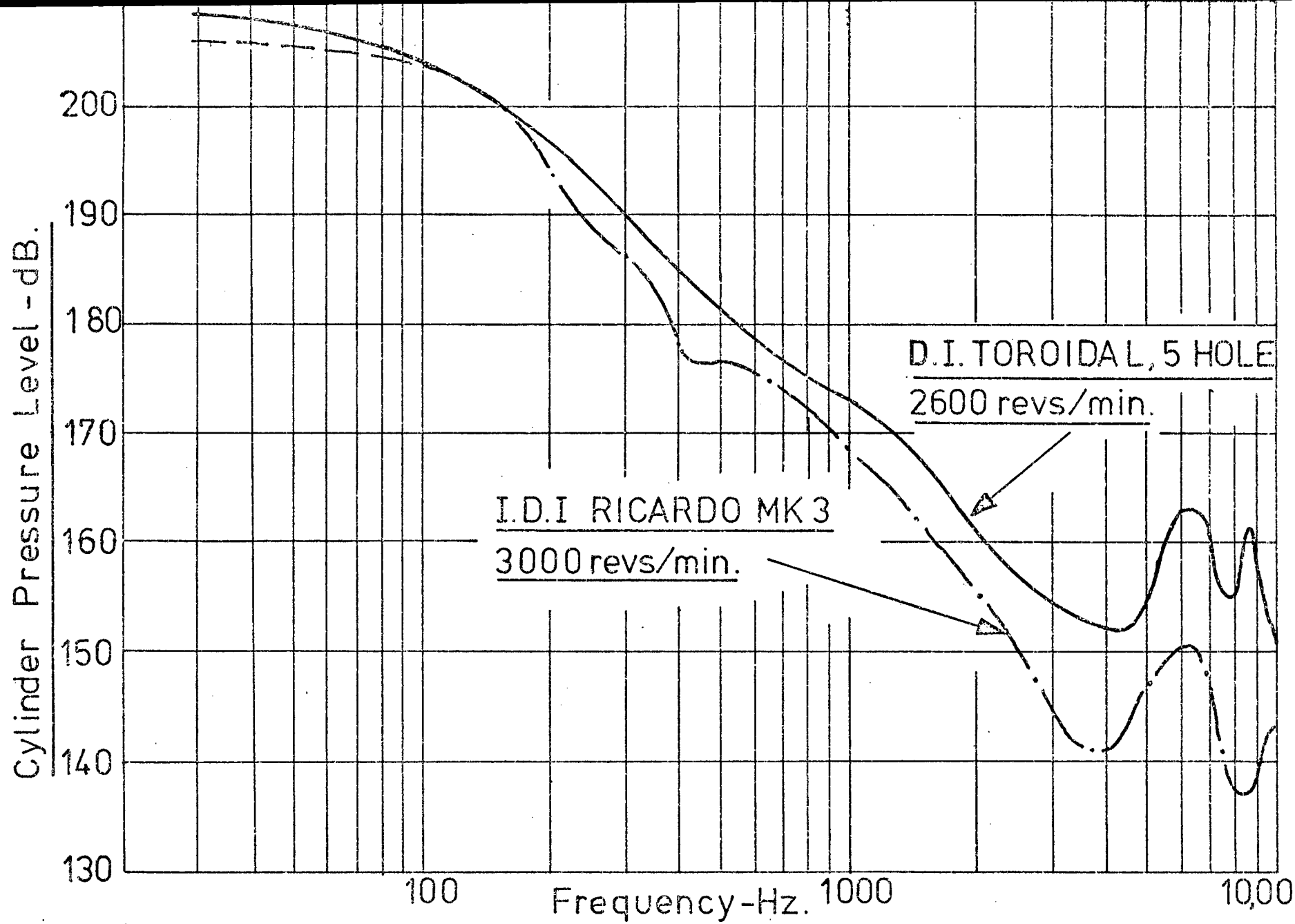

FIG. 9·27 - COMPARISO OF D.I. AND I.D.I. 4 STROKE DIESELS AT RATED SPEE

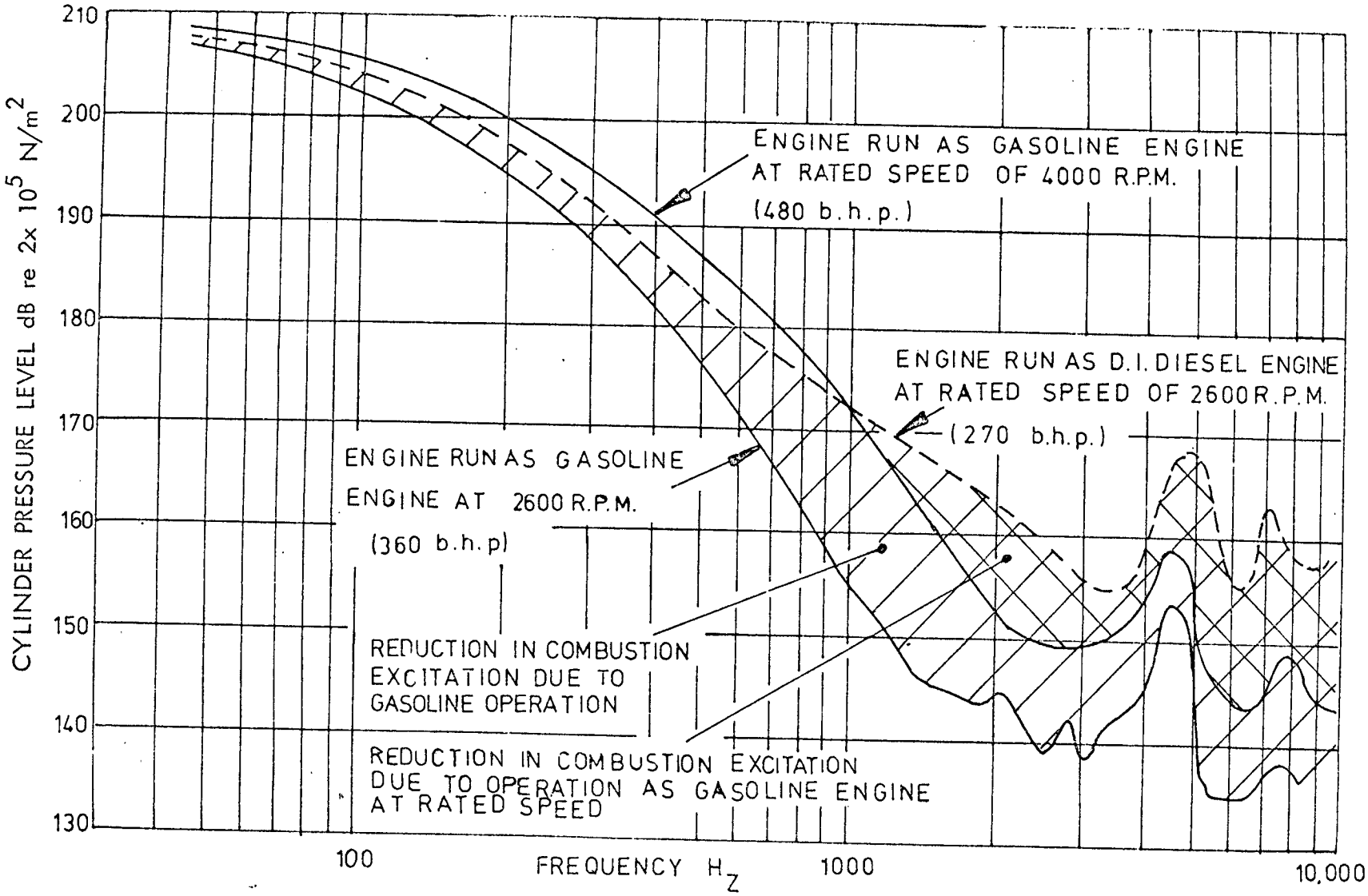

FIG. 9-28 - COMPARISON OF GASOLINE AND DIESEL COMBUSTION CYLINDER PRESSURE SPECTRA FOR SAME 800 cu.in.V-8 STRUCTURE.

pressure spectrum slope to be greater and consequently the combustion excitation to be lower in the critical 500-3000 Hz frequency range.

The effect of turbocharging the two stroke diesel engine is very similar to that of turbocharging the four stroke except that, because the combustion is smoother in the 'normally aspirated' form, the reduction in high frequency excitation is not so marked.

A number of engine structures are produced to run as either diesel or gasoline engines. A comparison of the cylinder pressure spectra for one such engine is shown in fig. 2.28. The spectrum for diesel operation is higher through the whole frequency range for the same engine speed. The reduction in excitation at high frequencies due to gasoline operation is very substantial, being some 10-20 dB. If the comparison is made at rated speed, however, then the difference is not so marked because of the higher operating speed allowed by gasoline operation. Even so, at frequencies above 1000 Hz the gasoline operation provides a substantial reduction in combustion induced noise.

9.4 Effect of Injection System Variables on Cylinder Pressure Diagram

In any combustion system considerable changes can be made by variations which can be provided by the injection system. This includes not only the geometry of injection, e.g., number of sprays, but also the injected fuel time history (rate of injection) and the injection timing. The injected fuel time history is purely a design feature of a particular injection system used, the cam design and injector design (open hole, pintle, pintle with delay, etc.).

In almost every case the fundamental aim is to reduce as far as possible the rapid pressure rise resulting from the inflammation of premixed fuel. In some combustion systems this is easier to achieve, while in others it is

more difficult. In all cases the fundamental factor is the amount of prepared fuel available, at the end of the ignition delay period, for spontaneous combustion.

One of the most important parameters influencing cylinder pressure development is the injection timing. An example from a direct injection engine is shown in fig. 9.29. With injection advance the ignition delay increases, causing the initial pressure rise to become greater, and the peak pressure higher. Levels of the cylinder pressure and noise spectra are higher, generally, over the whole frequency range.

The rate of injection too is significant. A gradual initial injection (delay nozzle) can produce pressure diagrams of extreme smoothness in comparison with the more rapid injection characteristics of pintle type nozzles.

Another important factor is the number of sprays used. This is logical, since the greater the number of sprays for a given combustion system, the larger is the volume of prepared fuel during the delay period and thus the pressure rise due to inflammation is more rapid. The final choice, however, is generally dictated by performance considerations. An example of the effect is shown in a comparison of a single hole nozzle high swirl, two stroke diesel and a seven hole quiescent chamber, two stroke diesel. This is shown in fig. 9.30. The slope of the cylinder pressure spectrum for the quiescent (seven hole) chamber is 30 dB/decade from 500 Hz upwards, as compared to 46 dB/decade for the single hole, high swirl engine. Consequently, the combustion excitation is significantly greater in the quiescent type of combustion chamber.

The general relationships between combustion and injection characteristics, and consequently noise, have been investigated by Ogegbo (9.3). His experimental investigation showed that a reduction of the ignition delay period does not necessarily lead to a reduction in combustion noise. It was

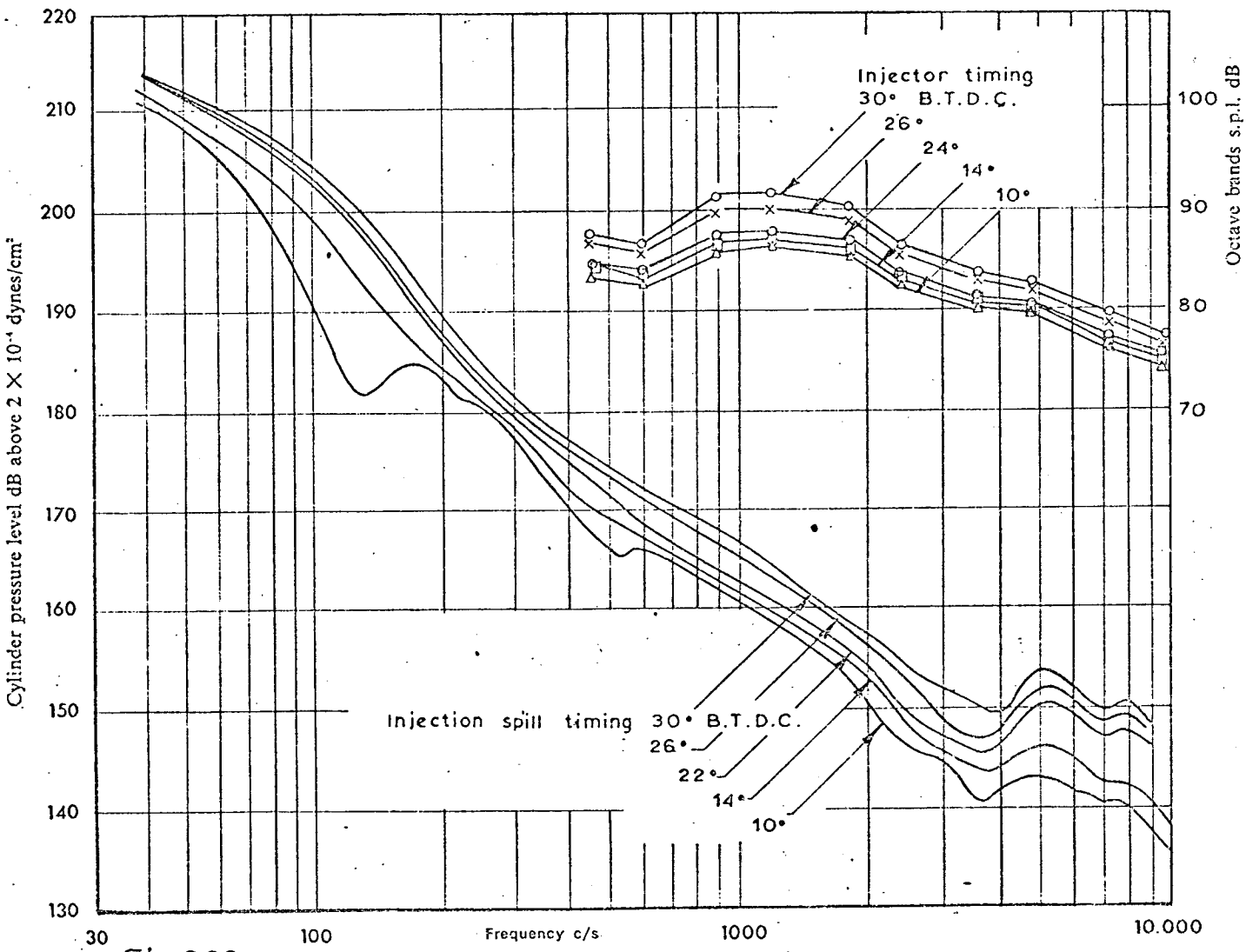

Fig.9-29—Noise and cylinder pressure spectra of 1·6 litre cylinder engine at various injection timings.

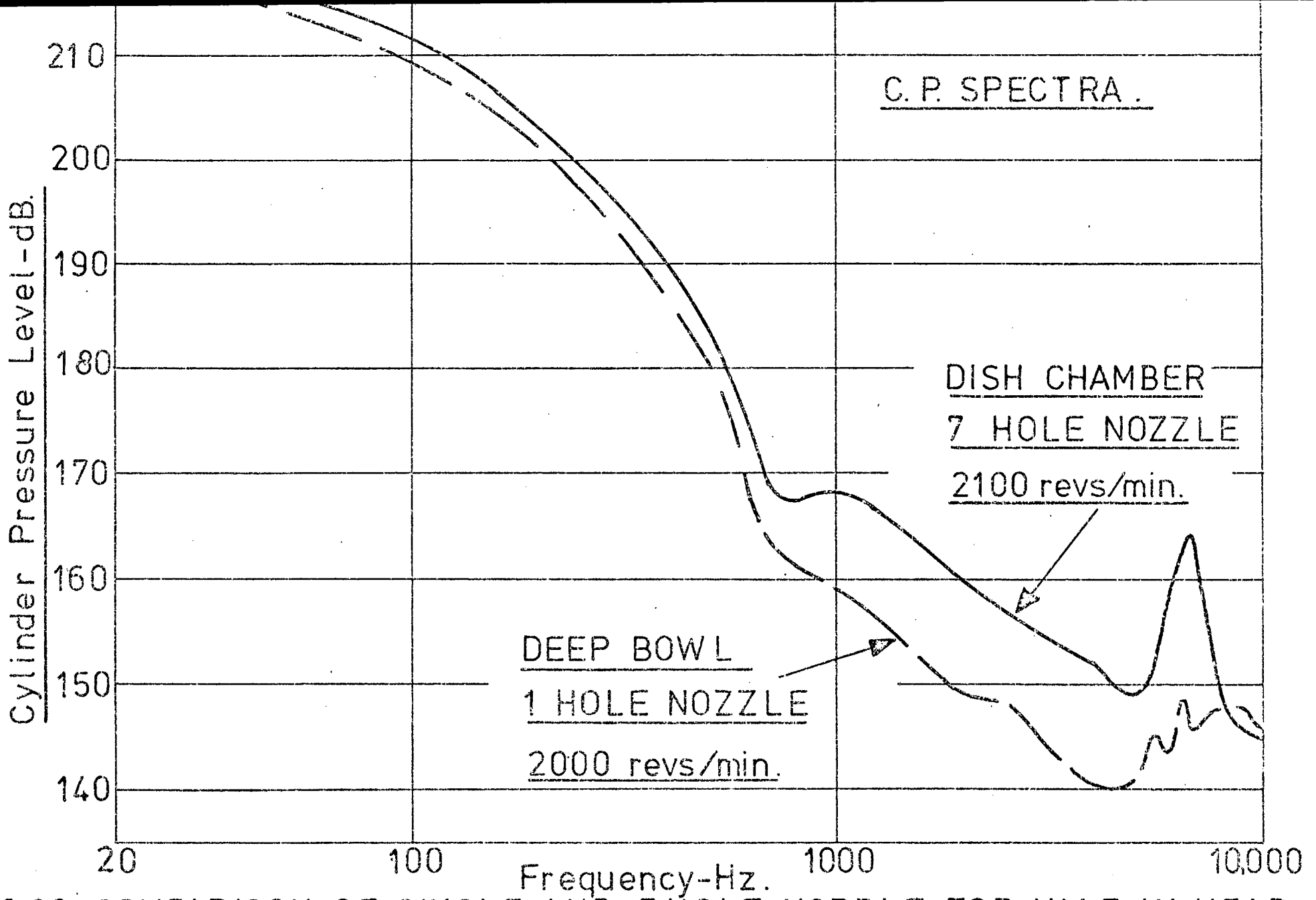

FIG. 9·30- COMPARISON OF SINGLE AND 7 HOLE NOZZLE FOR VALE-IN-HEAD 2 STROKE DIESELS.

found also that combustion noise is proportional to the initial heat release rate, which determined the rate of pressure rise. In the predominant frequency range from 500 to 3000 Hz a 2 dB increase in combustion noise was obtained per 10 Btu/lb air/^{o}CA increase in the initial peak heat release rate or 3 dB increase per 10 psi/^{o}CA increase in the rate of pressure rise.

A two-zone model of diesel combustion, based on modified single droplet and simplified jet theories was coupled to the fast Fourier analysis programme to allow direct computation of combustion noise excitation from a theoretically derived cylinder pressure diagram. The model assumed that the physical processes, such as atomisation, vapourisation and mixing rates control diesel combustion.

Results of the work indicate that combustion noise can be limited by controlling the preparation of combustible mixture prior to ignition by suitable selection of injection parameters. For example, increasing the Sauter Mean Diameter of the fuel droplets in the range 40-80 microns reduces combustion noise level by 4.5 dB per 10 microns throughout the 500-3000 Hz range. The level is also reduced in the range 500-3000 Hz by an increase in fuel cetane number at the rate of 4 dB per 10 cetane number.

9.5 General Characteristics of Combustion Noise in I.C. Engines, Taking Account of Changing Cylinder Pressure Diagram with Speed

In section 9.1 the three main parameters of speed, size and load and their effect on radiated noise, assuming that cylinder pressure development remained the same on a degree basis with increasing speed, were discussed and illustrated in section 9.1. The results given in section 9.3 show that this assumption is far from the truth in some classes of I.C. engine. Using this information, fig. 9.1 can be modified to show the measured characteristics of engines, as in fig. 9.31.

EFFECT OF ENGINE PARAMETERS ON EMITTED NOISE

SPEED

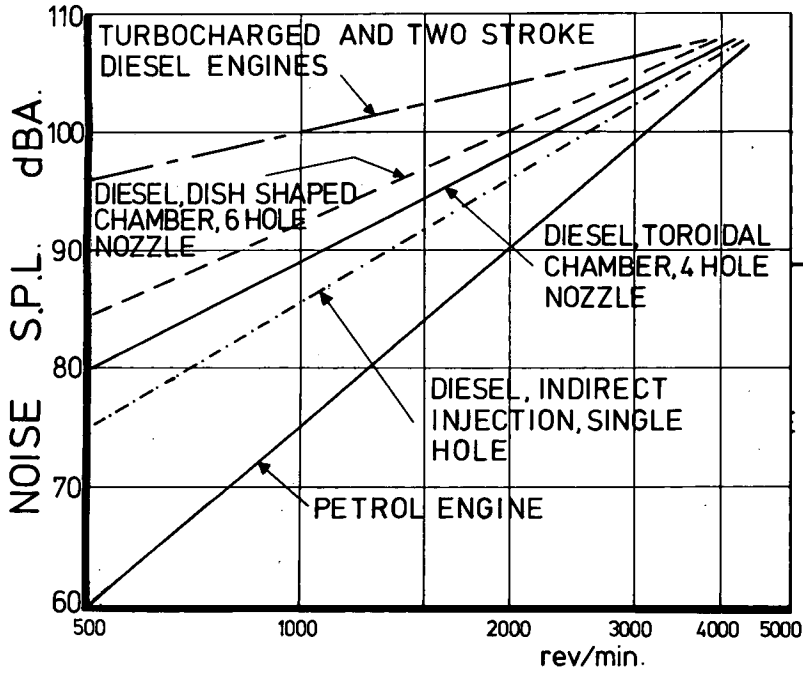

SIZE

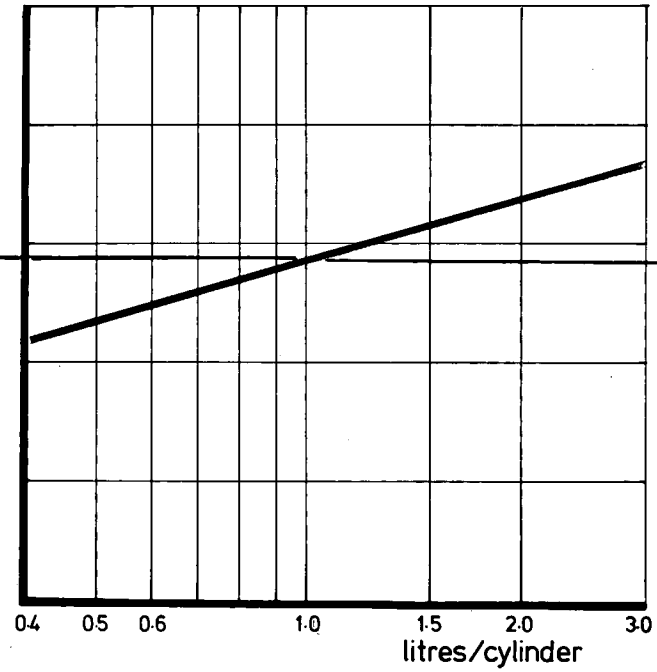

LOAD

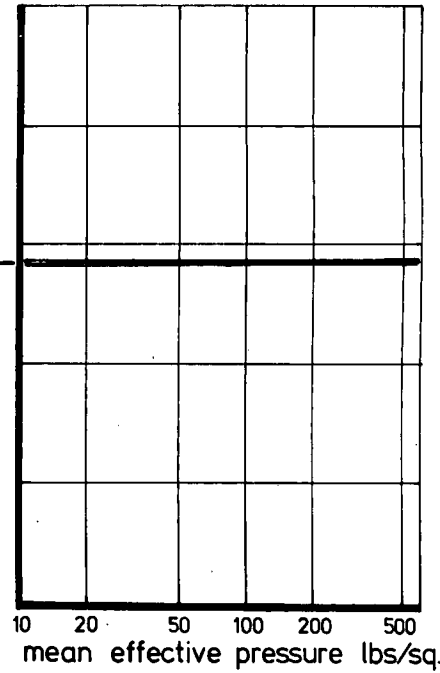

$$I \propto N^{2.0\text{-}5}_{\text{rev/min.}} \qquad I \propto V^{1.75}_{\text{litres}} \qquad I \propto L^{0}$$

INTENSITY OF ENGINE NOISE $I = \text{CONST.} \times N^{2.0\text{-}5} \times V^{1.75}$

FIG. 9·31

It is clear that only the effect of speed on noise is changed. The relationship between noise and speed is shown to have an even more marked effect than previously; the exact relation again depending upon the class of I.C. engine. The normally aspirated four stroke engine characteristic remains the same, but added to this is the four stroke I.D.I. engine which has a more rapid rate of increase of noise with speed. The two stroke cycle diesel and turbocharged four and two stroke diesels have, however, been shown to have a much lower rate of increase in noise with speed - 20 dB/decade as opposed to the 40 dB/decade when based on cylinder pressure spectrum slope. The petrol engine remains the same.

It can be concluded that from a consideration of the measured basic combustion excitation as expressed by cylinder pressure spectra, the general characteristics of overall engine noise can be predicted, provided that mechanical noise is not excessive. Even if this is so, the characteristics of engine noise due to combustion can still be predicted. Also the fact that such good agreement exists between combustion excitation characteristics and measured overall engine noise suggests that even now, and for most types of automotive engine, combustion excitation provides the over-riding factor in determining the general noise characteristics of Internal Combustion Engines.

REFERENCES

9.1 T. Priede. 'Relation between the form of cylinder pressure diagram and noise in diesel engines'. Proc. Instn. Mech. Engrs. (AD) No. 1, 1960-1961.

9.2 T. Priede. 'Explosion and combustion - the bases of road transportation'. Inaugural lecture, Southampton University, 1972.

9.3 A.M. Ogegbo. 'Automotive Diesel Combustion and Noise'. Ph.D. Thesis. Southampton University, 1973.

10.0 METHODS OF PREDICTION OF COMBUSTION INDUCED NOISE IN DIESEL ENGINES.

There are four different empirical relationships available in the literature for the prediction of diesel engine noise. Except for that due to Anderton, Grover, Lalor and Priede (2.10) they are all derived purely from a consideration of the statistical relations between measured parameters. Even that of reference (2.10) depends on an empirical constant derived from test results, although based on a consideration of the mechanism of combustion excitation.

The formulae for the sound intensity (proportional to sound pressure level generally) I in logarithmic quantity of dB are as follows:-

$$I = C_1 \log_{10} N + C_2 \log_{10} (\text{POWER}) + K_1 \qquad (10.1)$$

$$I = C_3 \log_{10} N + C_4 \log_{10} V_s + C_5 \log_{10} Z + K_2 \qquad (10.2)$$

$$I = C_6 \log_{10} C_p + C_7 \log_{10} L + C_8 \log_{10} Z + K_3 \qquad (10.3)$$

and $$I = C_9 \log_{10} N + C_{10} \log_{10} B + K_4 \qquad (10.4)$$

where N = engine revs/min

V_s = cylinder swept volume

Z = number of cylinders

C_P = mean piston speed

L = stroke

B = bore

C_n and K are constants

Equations of the type (10.1) were put forward by Slavin (2.12) and Pflaum and Hempel (2.13), the type (10.2) by Zinchenco (2.11) and of the type (10.3) by Cordier and Reyl (2.14) and of the type (10.4) by Anderton, Lalor, Grover and Priede (2.10).

By using the relationships which exist between the various parameters the formulae 10.1 to 10.4 can all be reduced to include engine speed and bore as the main variable.

Equation 10.1 reduces to

$$I = K_1 \log_{10} N + K_2 \log_{10} B + K_3 \log_{10} (\text{b.m.e.p.}) + K_3 \log_{10} S_R + A_1 \qquad (10.5)$$

where S_R = stroke to bore ratio

K_n and A_1 are constants

The terms involving stroke to bore ratio and engine load (which is known to have no direct effect on noise) can therefore be associated with the acoustic and structural characteristics of the engine, and the equation is therefore basically of the type (10.4).

Equation 10.2 reduces to

$$I = K_4 \log_{10} N + K_5 \log_{10} B + K_6 \log_{10} S_R + K_7 \log_{10} Z + A_2 \qquad (10.6)$$

where K_n and A_2 are constants

and the same comments can be made.

Equation 10.3 reduces to

$$I = K_8 \log_{10} N + K_9 \log_{10} B + K_{10} + S_R + K_{11} \log_{10} Z + A_3 \qquad (10.7)$$

where K_n and A_3 are constants

and again the same comments apply.

It is clear that all the formulae for predicting diesel engine noise ultimately depend on the same main parameters of bore and speed, with some variations to take account of the acoustic and structural characteristics.

The interesting conclusion that can be drawn is that since the dependance of engine speed and bore is derived from considerations of combustion excitation, then there is strong evidence here to support the thesis that even in large marine diesel engines the basic control of noise is dependent upon the combustion characteristics. This suggestion of dependence of marine diesel engine noise on combustion is very much against the generally held belief in the Industry that large marine diesel engine noise is mechanically controlled, usually by piston slap.

10.1 Prediction of Automotive Diesel Engine Noise, Based on Combustion Noise Model.

It was shown in Chapter 6 that the intensity of noise in Internal Combustion Engines, due to combustion excitation, was given by

$$I_o = K N^n B^6 S_{ASO} \qquad (10.8)$$

The overall acoustic and structural factor cannot at present be assessed and therefore a set of prediction formulae can only be obtained by an empirical method and will apply at rated speed only. From tests on many engines in the various classes of I.C. engine the following relations have to be obtained. They predict the overall engine noise at rated speed and load measured in dBA and at 1 metre distance from the engine surface: (N = revs/min, B = bore in inches)

Class 1 - Normally Aspirated four stroke direct injection diesel engines

Overall Noise = $30 \log_{10} N + 60 \log_{10} B - 38.0$ dBA

Class 2 - Indirect injection four stroke diesel engines

Overall Noise = $36 \log_{10} N + 60 \log_{10} B - 60.0$ dBA

Class 3 - Two stroke normally aspirated direct injection diesel engines (10.9)

Overall Noise = $20 \log_{10} N + 60 \log_{10} B + 18.0$ dBA

where for opposed piston engines the equivalent bore $B_{eq} = B\sqrt{2}$ is used.

Class 4 - Turbocharged four stroke direct injection diesel engines

Overall Noise = $20 \log_{10} N + 60 \log_{10} B + 13.0$ dBA

Insufficient data was available on which to base an empirical value for the constant in the case of Class 5 (Turbocharged two stroke) and Class 6 (petrol) engines.

Table 10.1 shows a comparison between measured and predicted noise levels using equations.

TABLE 10.1

COMPARISON OF MEASURED AND PREDICTED NOISE LEVELS AT 1 METRE FOR VARIOUS DIESEL ENGINES USING RELATIONS (10.9)

ENGINE TYPE	INDUCTION	BORE INCHES	RATED SPEED REV/MIN	OVERALL NOISE LEVEL AT 1 METRE	
				CALCULATED	MEASURED
V Form 8 Cyl.	Direct Injection Four Stroke Normally Aspirated	4.625	3300	107.4	108
"	"	4.625	3300	107.4	109
"	"	4.5	3000	107.7	106.5
"	"	4.25	2800	103.2	103.5
"	"	5.31	2600	107.9	109.0
In Line 6 Cyl.	"	5.5	2100	106.2	106.0
"	"	4.65	2600	104.4	102.0
"	"	4.56	2800	105.0	105.0
"	"	4.125	2800	102.4	102.5
"	"	3.875	2800	100.8	103.0
"	"	3.81	2800	100.4	102.0
In Line 4 Cyl.	"	3.875	2800	100.8	103.0
In Line 4 Cyl.	Indirect Injection Normally Aspirated Four Stroke	3.688	4000	103.8	107.0
"	"	3.125	4000	99.5	101.5
"	"	3.50	3500	100.4	101.5
"	"	3.543	4500	104.5	100.0
V Form 8 Cyl.	Turbocharged Direct Injection Four Stroke	5.5	2600	105.6	107.0
In Line 6 Cyl.	"	5.5	2100	103.9	102.0
"	"	4.75	2200	101.5	100.0
"	"	4.30	3000	100.5	101.0
Opposed Piston In Line 6 Cyl.	Two Stroke Diesels with Low Roots Blower Noise	3.44	2400	106.8	103.0
In Line 6 Cyl.	"	4.25	2100	102.2	102.0
V Form 8 Cyl.	"	4.25	2100	102.2	103.5
V Form 6 Cyl.	"	3.875	2800	102.2	103.5

The correlation is good the mean error being some ±2 dBA.

A useful comparison can be made to Table 6.2 in Chapter 6 where measured and predicted noise levels, based on a combustion model but not including the effect of engine radiating area, are shown for a range of engines. The accuracy of prediction is slightly better in the case of equations 10.9.

In the case of the Indirect Injection normally aspirated diesel engines there is a greater difference between measured and calculated results - for instance between the 3.688 inch bore engine and the 3.543 inch bore engine which both have Ricardo pre-combustion chamber designs (MK V).

10.2 Variation of Combustion Excitation from Engines of Similar Design.

A comparison of the reduced cylinder pressure spectra for these two indirect injection engines is shown in Fig 10.1. There is some change in spectrum shape with speed and two straight line representations are presented in each case, one for rated speed and another representing the average of all speeds. These lines can be defined by two parameters:

1) The slope in dB/decade

2) The reduced cylinder pressure level at f/N = 1.0

These parameters were developed in Chapter 6 for use with the combustion noise prediction formulae given in equations 6.41.

For cylinder pressure spectrum

$$\text{Overall noise dBA} = \text{C.P.L.}_{(1000)} + 60 \log_{10} B - X \text{ dB}$$

For reduced cylinder spectrum (6.41)

$$\text{Overall noise dBA} = \text{C.P.L.}_{R}(1.0) + 60 \log_{10} B + 10_n \log_{10} \frac{N}{1000} - X \text{ dB}$$

The slope of the spectrum will determine the value of the

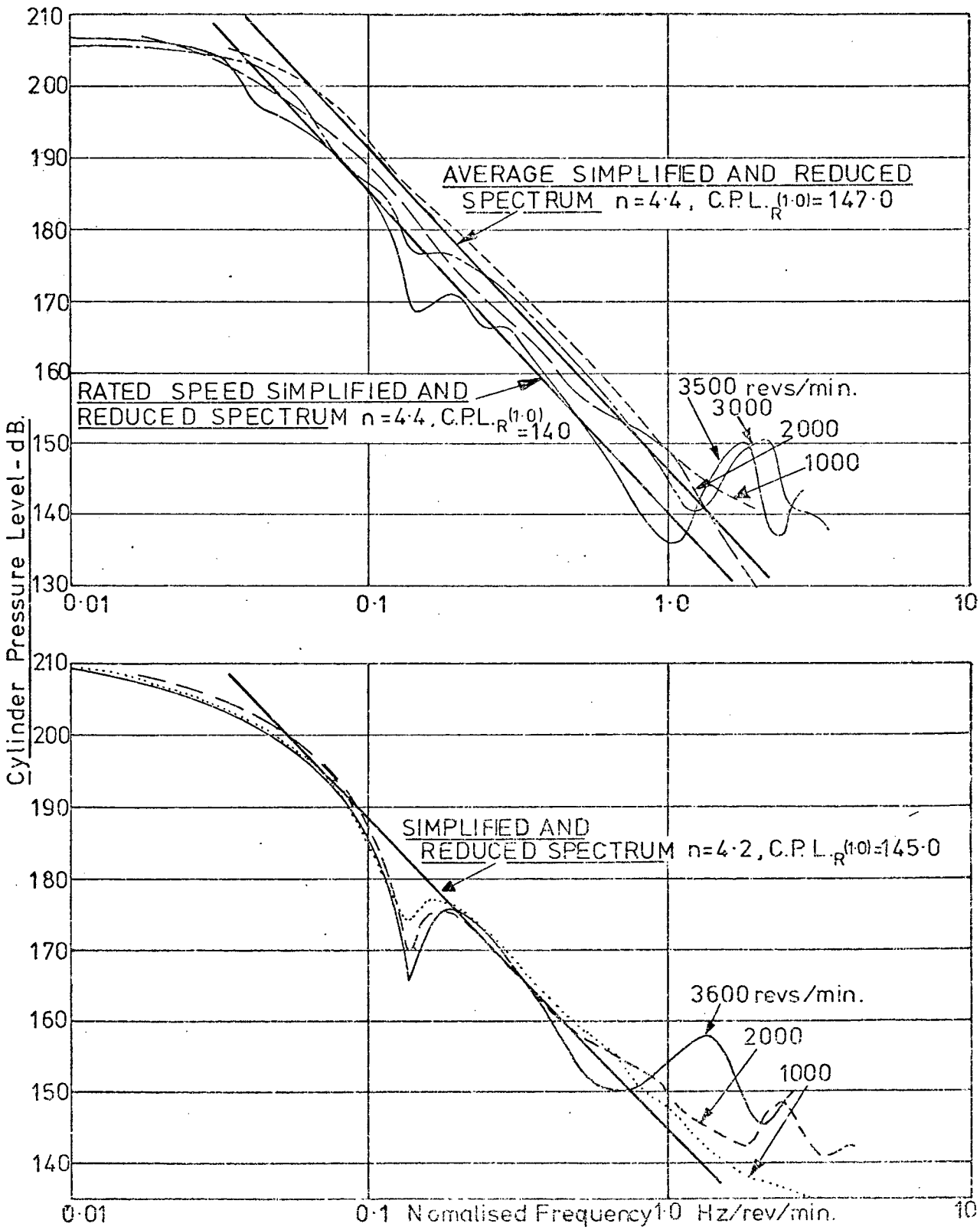

FIG. 10·1 - REDUCED CYLINDER PRESSURE SPECTRA FOR I.D.I. DIESELS. AT FULL LOAD.

Spectrum Shape Factor X, whilst the reduced cylinder pressure at f/N = 1.0 will determine the level of the exciting spectrum and hence is the major determining factor for combustion noise. The values for the Indirect Injection engines considered (at rated speed) are:

Slope 43 dB/decade $C.P.L._R(1.0) = 144.5$ dB

for the 3.688" engine and:

Slope = 57.5 dB/decade $C.P.L._R(1.0) = 133.5$ dB

for the 3.543" engine.

Thus the combustion excitation level is some 11 dB overall higher in the 3.688" engine and consequently a much higher noise level, as is in fact measured, would be expected from this engine.

This then is the major weakness of all the diesel engine noise prediction formulae so far produced. It is inherently assumed that when using any type of equation 10.1 to 10.4 and also 10.9 that the overall level of combustion excitation, in terms of cylinder pressure, does not vary. This assumption is reasonable for normally aspirated direct injection diesel engines with in line pumps but is certainly not true for indirect injection engines.

For the level of combustion excitation to be included in the calculation of noise levels the excitation values must be measured.

In the following sections typical measured combustion excitation results are presented and used to calculate

1) The combustion noise level for a range of engines
2) The general characteristics of the first four classes of Internal Combustion Engine.

10.3 Prediction of Combustion Induced Noise from Measured Cylinder Pressure Spectra.

Figs 10.1, 10.2, 10.3, and 10.4 show typical reduced cylinder

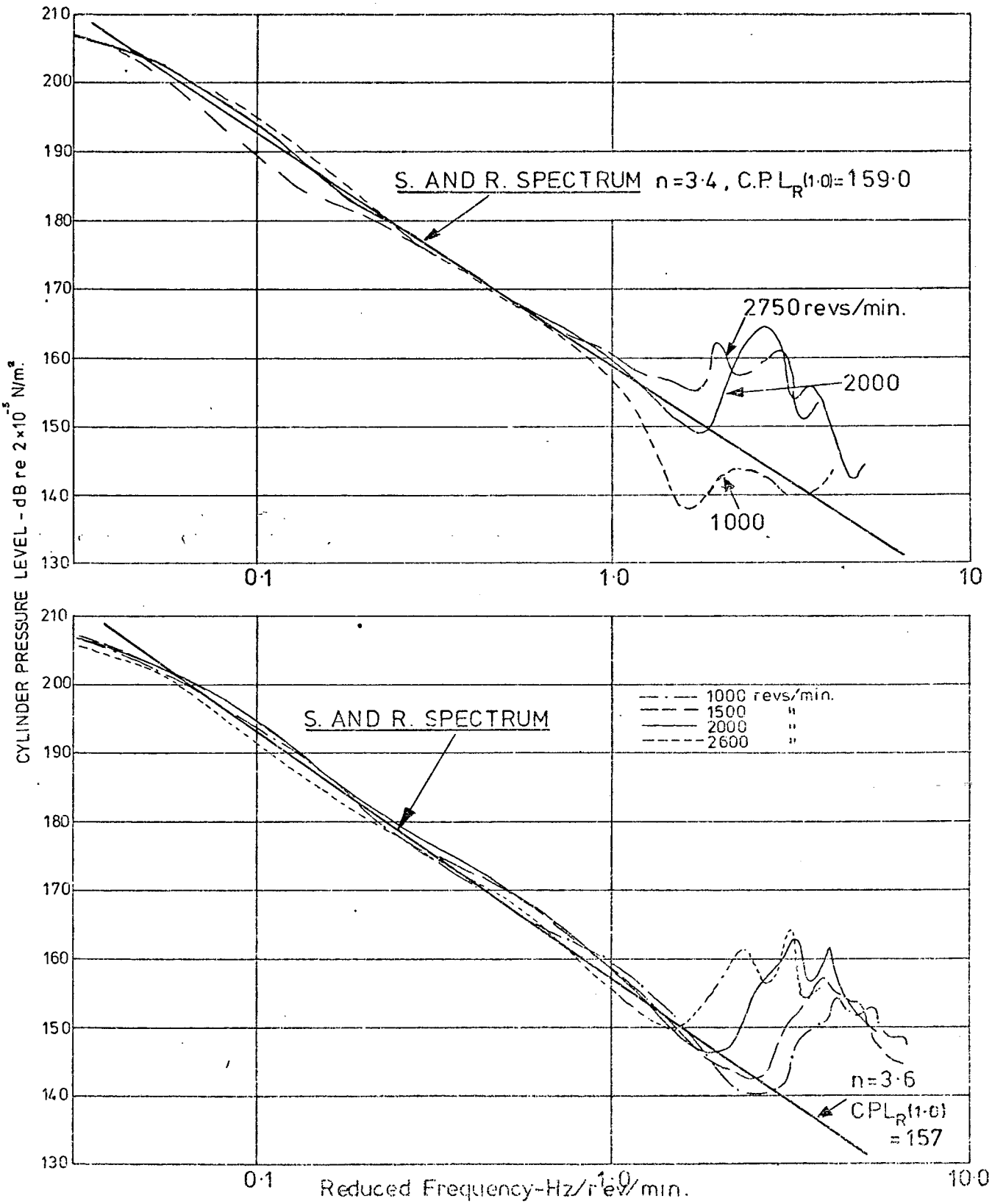

FIG.10·2 - REDUCED CYLINDER PRESSURE SPECTRA FOR D.I. DIESELS AT FULL LOAD.

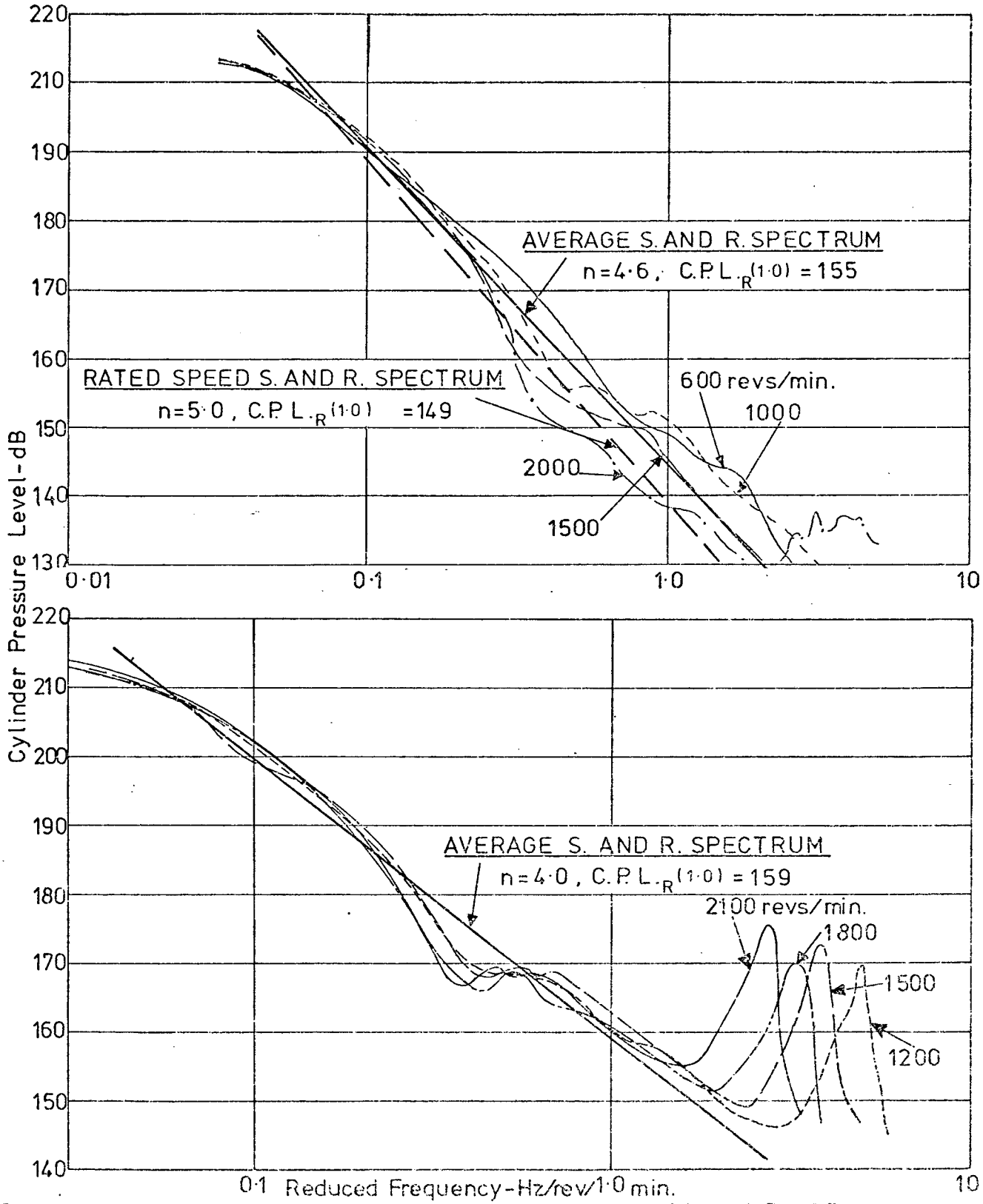

FIG. 10·3 - REDUCED CYLINDER PRESSURE FOR TWO STROKE DIESELS AT FULL LOAD.

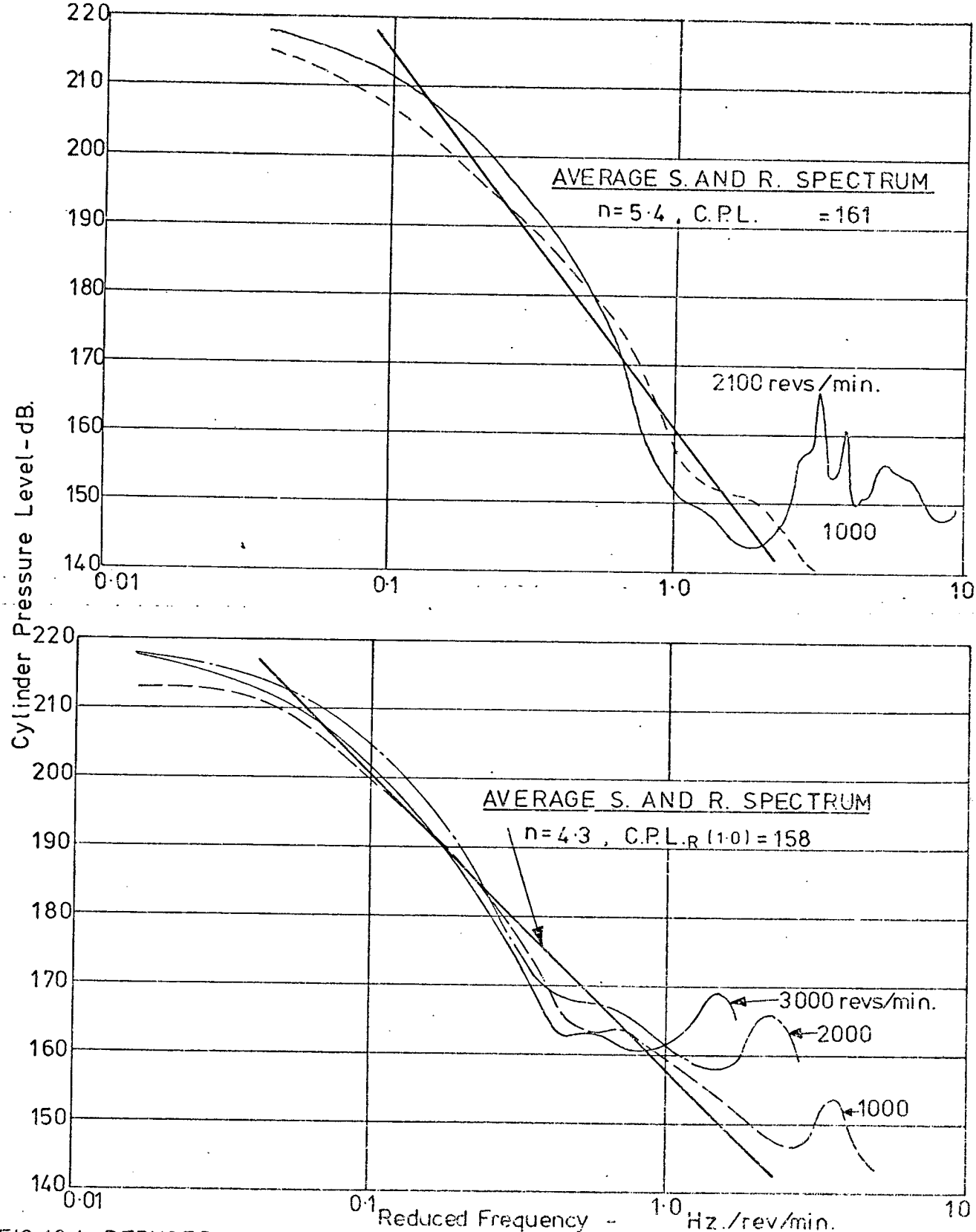

FIG.10·4 - REDUCED CYLINDER PRESSURE FOR TURBOCHARGED 4 STROKE DIESEL AT FULL LOAD.

pressure spectra for the first four classes of I.C. engine considered, namely direct, indirect, turbocharged four stroke cycle and direct injection two stroke cycle. The variations in spectrum shape at different engine speeds become apparent with this type of presentation, being mainly due to changes in injection timing, fuel quantity and the cylinder gas condition immediately before closing of the inlet valves (Roots Blower, Turbocharger).

A set of Simplified Reduced spectra, in the form of straight line representations of the actual spectra, in which the level of combustion excitation as a function of engine speed and frequency is represented by the slope and the value of $C.P.L._R(1.0)$ and also shown in Figure 10.1 to 10.4. In some cases, for instance for I.D.I. engines, both an average slope and a slope for rated speed are presented.

The values of the Reduced and Simplified spectra for a range of engines can now be used in two ways. Firstly by using the reduced spectrum values for rated speed condition, the overall combustion noise which would be radiated by a 'standard' engine (i.e. one with a Standard Structure Attenuation Factor) can be calculated from equations 6.41. Secondly the reduced spectrum values can be arranged to find the general comparative combustion excitation characteristics of the first four classes of I.C. engines.

10.3.1 Combustion Noise at Rated Speed

From the measured cylinder pressure spectra for a range of engines the overall noise radiated due to combustion excitation has been calculated according to the relations (equations 6.41).

$$\text{Overall Noise due to Combustion} = C.P.L._{(1000)} + 60 \log_{10} B - X \text{ dBA}$$

where $C.P.L._{(1000)}$ = level of cylinder pressure spectrum at 1000 Hz

B = engine bore in inches

X = Spectrum Shape Factor (Fig 6.13)

for a range of engines in the first four classes of I.C. engine. A comparison of these values is given in Table 10.2, and a surprisingly good agreement with the measured overall noise obtained.

In some engines the predicted combustion noise level is so much below that of the measured engine that it is safe to conclude that mechanical noise sources are controlling noise.

This simplified approach indicates the general trends in an engine. However, by utilising the computed cylinder pressure spectrum values, the exact combustion noise, for a 'standard engine structure', can be calculated using the precise cylinder pressure spectrum shape.

10.3.2 General Prediction of Combustion Noise Characteristics in I.C. Engines.

The overall combustion excitation characteristics of engines can be represented by their Reduced and Simplified cylinder pressure spectra. Fig 10.5 shows the full load reduced and simplified cylinder pressure spectra for a range of engines. The level of excitation varies by some 20 to 25 dB indicating the great variation obtained from engine to engine and depending primarily on form of combustion and injection characteristics.

Fig 10.6 shows the range of values associated with the form of combustion, as represented by the engine class. There are four distinct groupings for normally aspirated diesel injection, four stroke normally aspirated indirect injection four stroke, two stroke Roots scavenged and turbocharged direct injection four stroke diesels.

The average full load reduced and simplified cylinder pressure spectrum for each class of engine is shown in Fig 10.7, and forms a convenient basis on which to compare the present day levels of combustion excitation. In general it will be seen that the two stroke

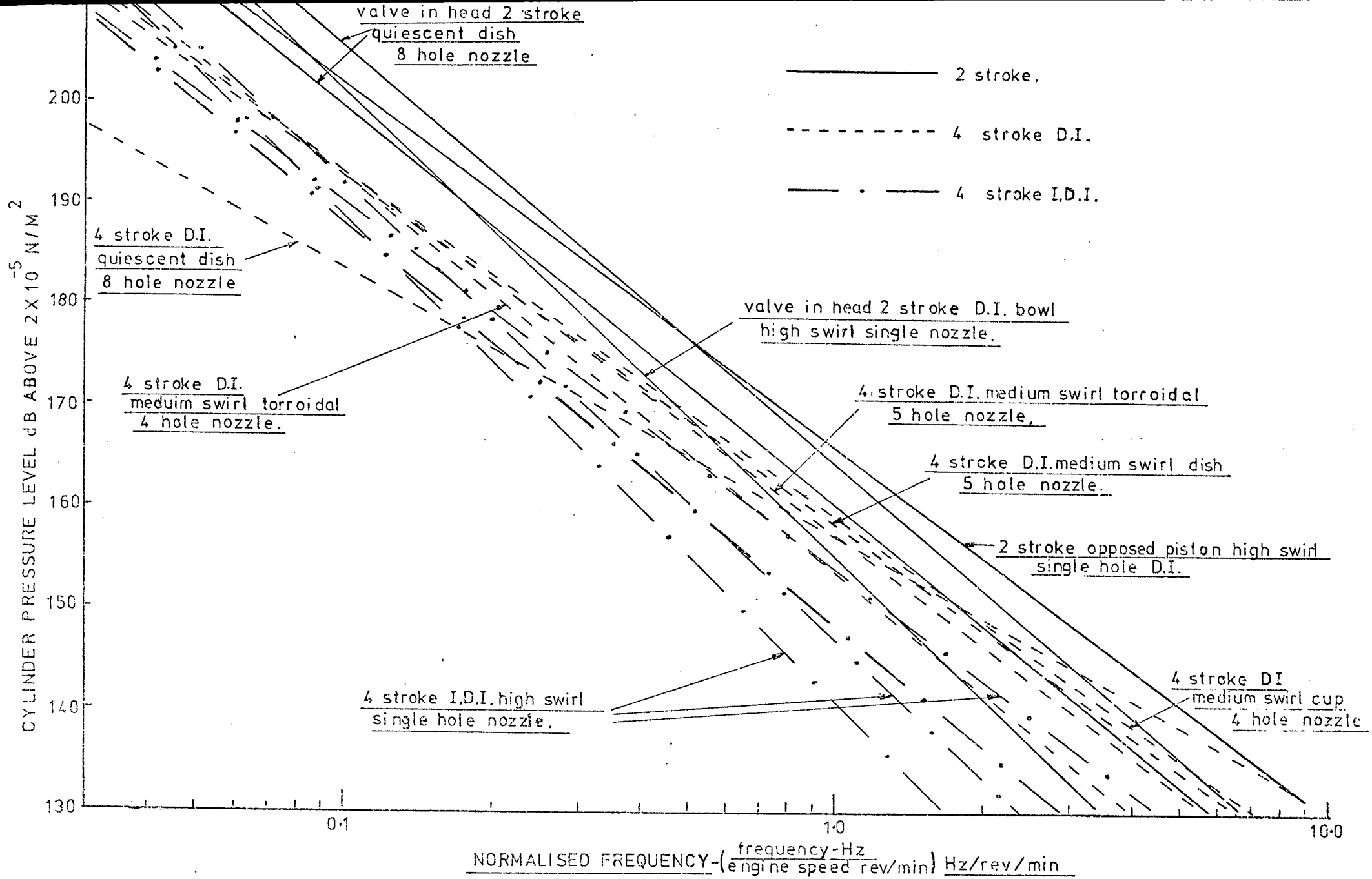

FULL LOAD REDUCED AND SIMPLIFIED CYLINDER PRESSURE SPECTRA FOR A RANGE OF ENGINES.

Fig 10·5

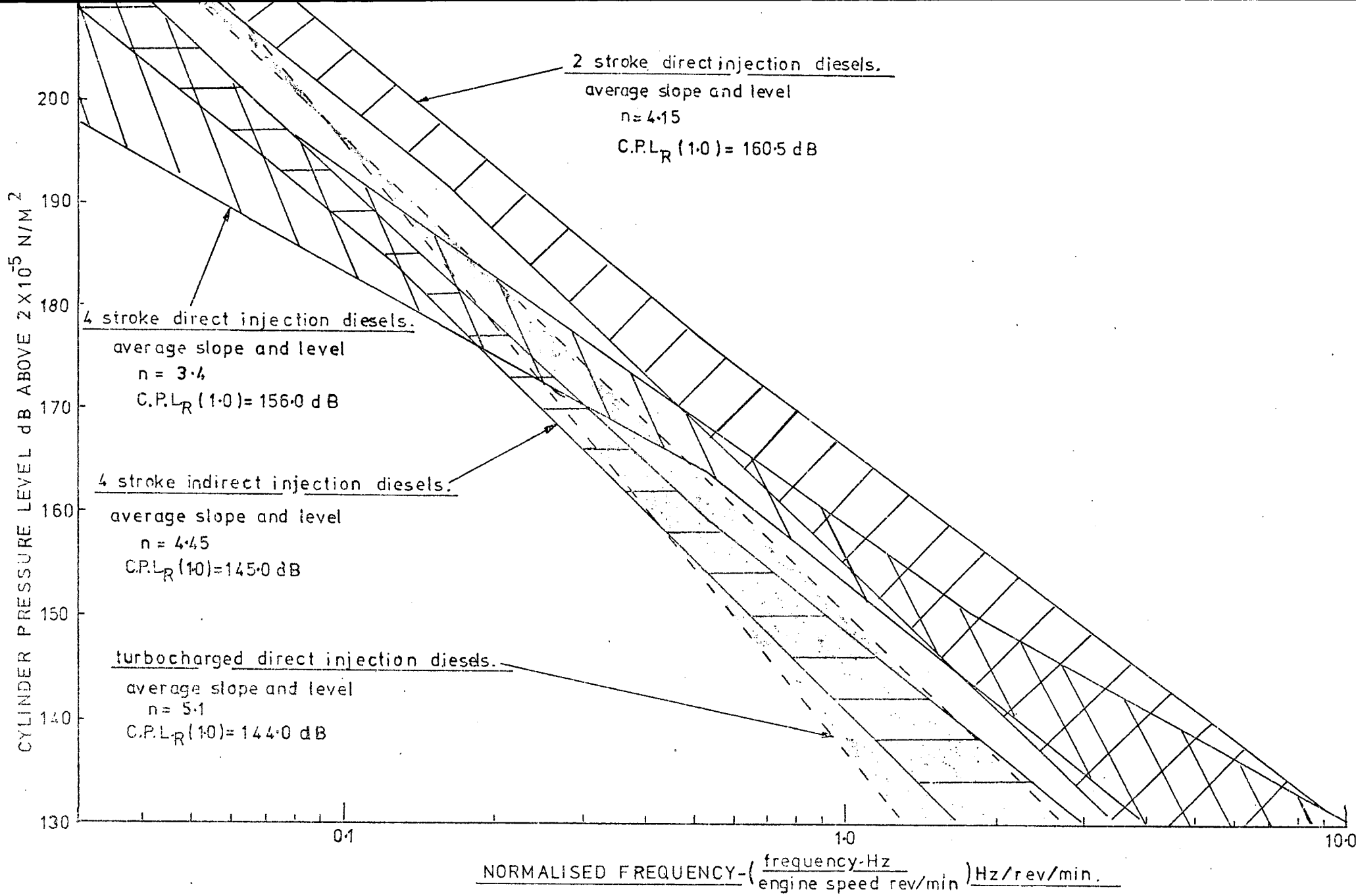

Fig 10·6 FULL LOAD REDUCED AND SIMPLIFIED CYLINDER PRESSURE SPECTRA GROUPED ACCORDING TO FORM OF COMBUSTION.

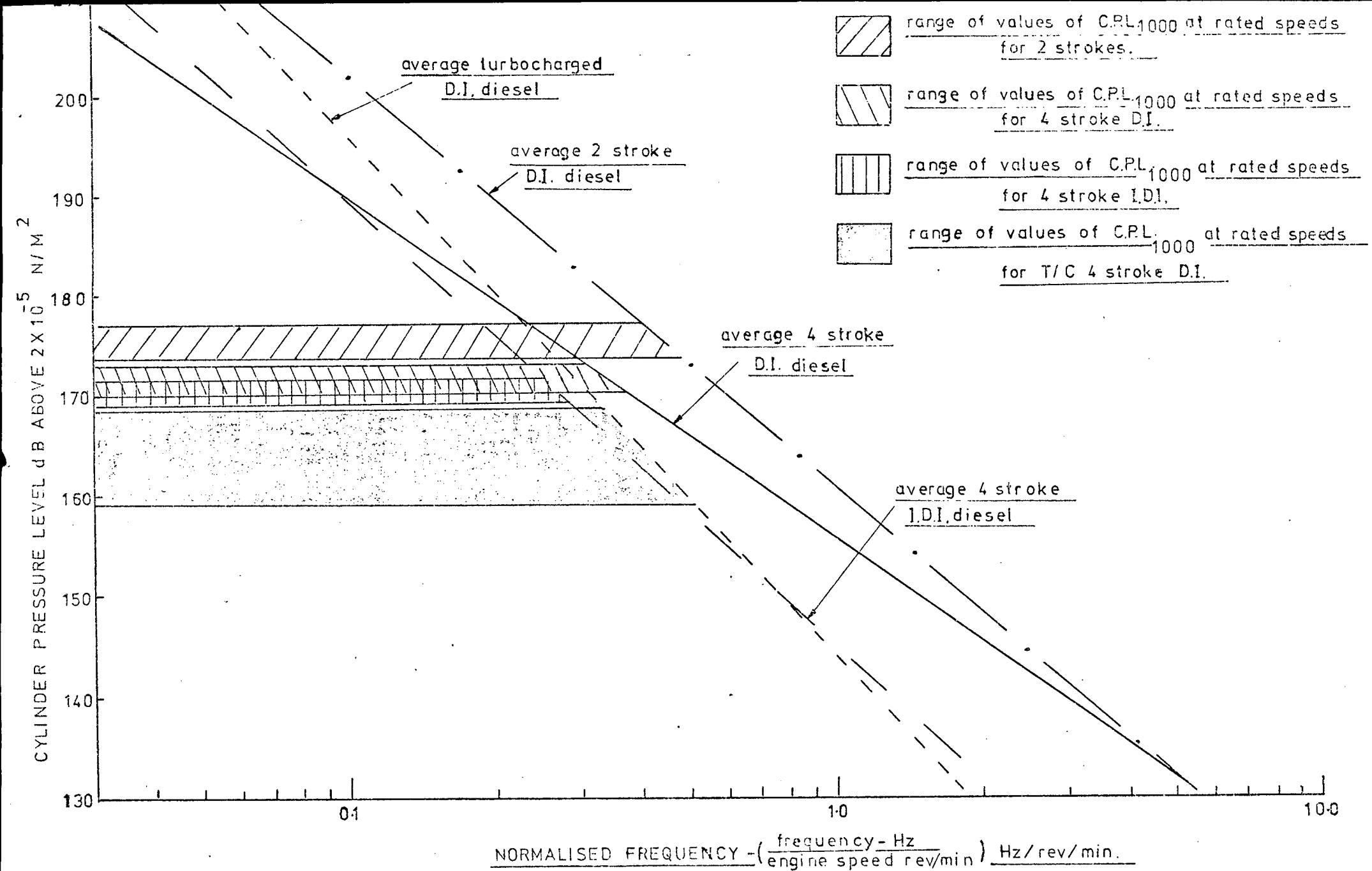

Fig 10·7 AVERAGE FULL LOAD REDUCED AND SIMPLIFIED CYLINDER PRESSURE SPECTRA GROUPED ACCORDING TO FORM OF COMBUSTION.

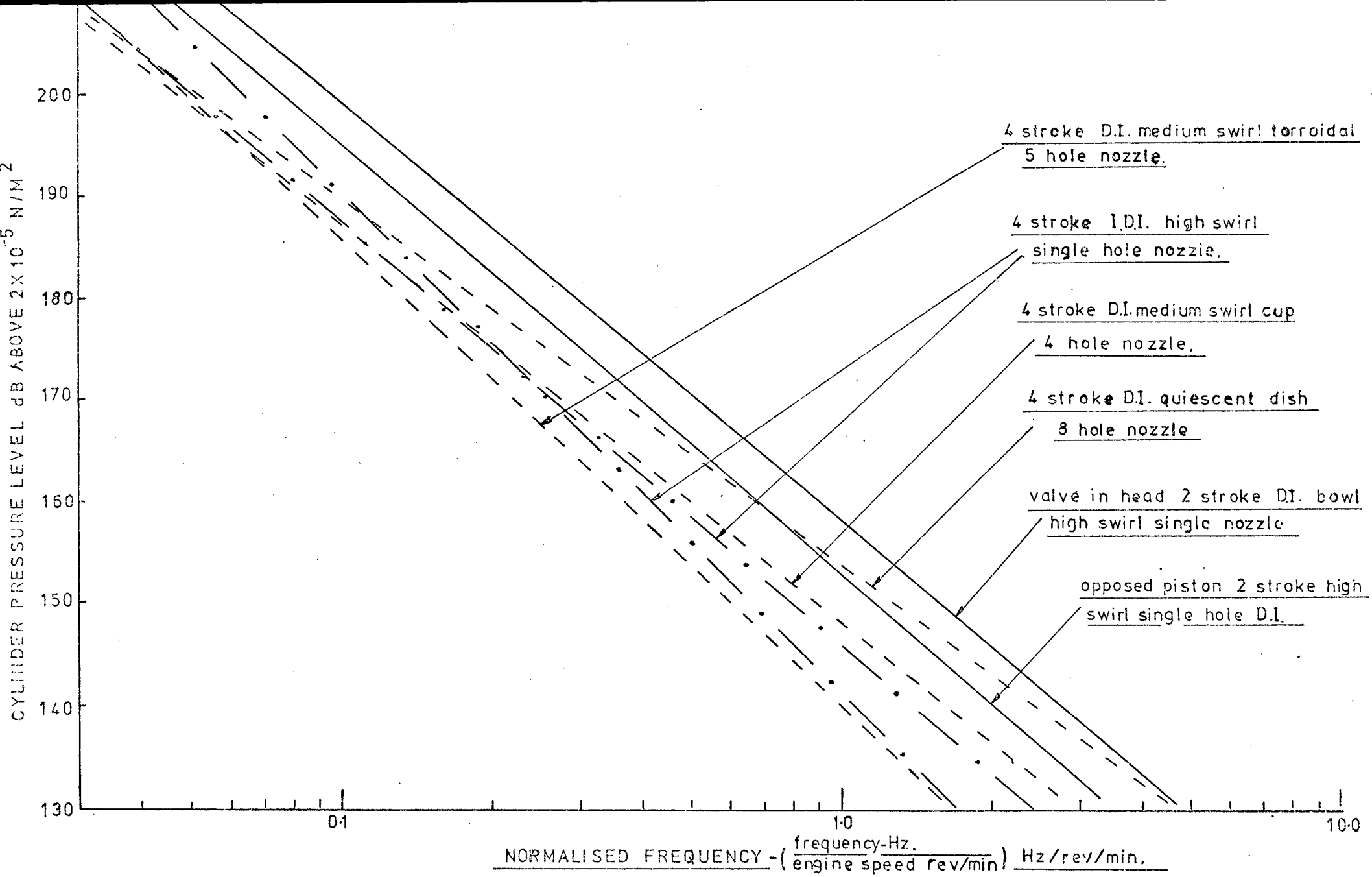

Fig10·8 NO LOAD REDUCED AND SIMPLIFIED CYLINDER PRESSURE SPECTRA. FOR A RANGE OF ENGINES.

TABLE 10.2

COMPARISON OF PREDICTED COMBUSTION INDUCED NOISE LEVELS AND MEASURED NOISE LEVELS FOR A RANGE OF ENGINES

ENGINE TYPE	INDUCTION	BORE	SPEED	CYLINDER PRESSURE SPECTRUM SLOPE	LEVEL OF CYLINDER PRESSURE SPECTRUM AT 1000 Hz C.P.L.(1000)	SPECTRUM SHAPE FACTOR X -dB	MEASURED OVERALL NOISE LEVEL	CALCULATED COMBUSTION INDUCED OVERALL NOISE LEVEL	COMMENTS
		ins	revs/min	dB/Decade	dB re 2×10^{-5} N/m^2	re 2×10^{-5} N/m^2	- dBA	- dBA	
V Form 8 Cyl.	Normally Aspirated Direct Injection Four Stroke	5.31	2600	34.0	172.5	-107.4	109	108.6	Combustion Control
"	"	4.625	3300	27.5	172.0	-106.0	108.5	105.9	Noise reduced 3 dBA by elimination of piston slap.
In Line 6 Cyl	"	4.65	2600	36.0	172.0	-107.8	103.0	104.2	Combustion Control
"	"	4.125	2800	34.0	174.0	-107.4	102.5	101.5	Combustion Control
"	"	3.81	2800	38.0	171.0	-108.2	102.0	98.7	Mechanical Control
In Line 4 Cyl.	Normally Aspirated Indirect Injection Four Stroke	3.50	3000	44.0	171.5	-109.5	96.5	94.4	Combustion Control
"	"	3.688	3600	42.0	171.0	-109.0	98.0	96.0	Joint Control
"	"	3.543	4000	57.5	168.0	-105.1	95.5	95.9	Combustion Control
In Line 6 Cyl.	Turbocharged Direct Injection Four Stroke	4.3	3000	43.0	173.0	-109.3	101.0	101.7	Combustion Control
"	"	5.13	2100	62.5	157.5	-101.5	106.0	98.6	Mechanical Control
V Form 8 Cyl.	Two Stroke Diesels with Low Roots Blower Noise	4.25	2100	39.5	172.5	-108.2	103.5	102.0	Combustion Control
Opposed Piston In Line 6 Cyl.	"	3.44	2400	37.5	170.5	-108.1	103.0	94.6	Mechanical Control
In Line 6 Cyl.	"	4.25	2100	39.0	173.0	-108.4	103.0	102.3	Combustion Control
"	"	3.875	2200	42.5	165.0	-109.2	102.0	91.0	Roots Blower Control

cycle provides the highest excitation, with the four stroke direct injection engine next and both indirect injection and turbocharged four stroke providing the lowest excitation. The relative level differences depend greatly on speed of operation, but as a general trend it can be seen that the differences become smaller at higher engine speeds, except in the case of the two stroke. The comparative levels of the 1000 Hz cylinder pressure level ($C.P.L._{(1000)}$) over typical operating speeds for each class of engine are also shown in Fig 10.7. A comparison of direct injection engine and indirect injection four stroke levels shows that the basic advantage of low combustion noise in the indirect engine is offset in practice by using a higher operating speed (for more power) and consequently the resultant noise levels of the two types are virtually the same in practice. It is clear that operation of an indirect injection engine at lower speeds would provide a very substantial reduction in combustion induced noise.

A similar comparison of the engine classes at no load shows a markedly different picture. Fig 10.8 shows the Reduced and Simplified cylinder pressure spectra for a range of engines. At no load there is no clear distinction in characteristics between engine classes and it must be concluded that at no load the effect of injection characteristics is more important than the form of combustion.

11.0 CONCLUSIONS

Many detailed conclusions have been drawn from the information presented in the foregoing chapters and these appear in the relevant sections. Even so, it is useful to summarise briefly the more important among them.

1. As regards the assessment of the exciting propensities of cylinder pressure development it has been found that small piezo-electric pressure transducers give accurate results. It is shown that engines of any size can be satisfactorily instrumented for cylinder pressure by novel installation techniques. The accuracy of results could be improved for heat release measurements by attention to

(a) Increased pressure transducer linearity

(b) Reduction in flame sensitivity.

A Fast Fourier Analysis computational method has been developed for use in the frequency analysis of pressure developments. Two novel features are involved. Firstly the speed of computation has been increased over straightforward methods by a factor of 20 by employing a computational algorithm to reduce the number of sine and cosine calculations. Secondly the assumption of a linear variation between input data points has allowed the computation of any number of harmonics from a given number of these data points. Accurate results with reasonable times of computation have been obtained up to 2000 harmonics.

2. The developed computer programme has enabled the assessment of the basic characteristics of combustion excitation offered by the various operating cycles. It has been shown that:

(a) A fundamental difference exists between the combustion excitation of four and two stroke and turbocharged four stroke operating cycles. At

equal firing frequency the excitation of the two stroke cycle, above 200 Hz, is 6 dB lower than for the four stroke. As a consequence a two cycle engine can always be designed with a 6 dBA overall noise level lower than a four cycle engine, for a given power output. The turbocharged four stroke is shown to approach nearer to the two stroke characteristics as the degree of turbocharging is increased.

(b) That the harmonics of cylinder pressure development responsible for transmission of engine power are the first two in the two stroke cycle and the 2nd and 4th in the four stroke cycle.

(c) Increasing the diagram width in relation to the repetition length has the effect of increasing the level of the first few harmonics of the cylinder pressure spectrum substantially. In the case of the two cycle and four cycle engines the level of the fundamental is doubled in two stroke operation.

3. It was found that the complete form of the cylinder pressure development is required to specify the full cylinder pressure spectrum. However, three parameters can be taken as representing the major influencing factors. These are:

(a) Peak pressure

(b) Rate of pressure rise

(c) Acceleration of pressure rise.

The effect of these parameters was found to vary between diesel and petrol operation and also to vary with engine speed.

For the two types of diagram the following harmonic ranges were found to be affected:

Diagram	Peak Pressure P	Rate of Pressure Rise - dp/dt	Acceleration of Pressure Rise - d^2p/dt^2
Diesel	1 - 20	20 - 120	100 and above
Petrol	1 - 10	10 - 90	80 and above

Thus for a typical diesel at rated speed of 2500 revs/min the following frequency ranges will be affected:

Four strcke Diesel at 2500 revs/min	P	dp/dt	d^2p/dt^2
	21 - 420 Hz	400-2520 Hz	2100 Hz and above

and at idling (600 revs/min)

Four stroke Diesel at 600 revs/min	P	dp/dt	d^2p/dt^2
	5-100 Hz	100-600 Hz	500 Hz and above

For a typical petrol engine at rated speed of 5000 revs/min the following frequency ranges will be affected:

Four strcke Petrol at 5000 revs/min	P	dp/dt	d^2p/dt^2
	42-420 Hz	420-3780 Hz	3360 Hz and above

and at idling (600 revs/min)

Four strcke Petrol at 600 revs/min	P	dp/dt	d^2p/dt^2
	5-50 Hz	50-450 Hz	400 Hz and above

4. Two methods of obtaining high power outputs are the variable compression ratio piston, where peak pressures are limited, and a fixed compression ratio employing a very strong structure to withstand the very high peak pressures.

A comparison of the combustion exciting propensities of these two types at 350 b.m.e.p. shows that by using the variable compression ratio piston lower cylinder pressure spectrum levels result throughout the whole audio frequency range. However, at normal engine speeds and rates of pressure rise, it is found that the acceleration of pressure rise at the discontinuity around initiation of combustion still controls the spectrum levels above about 1000 Hz, even with peak pressures of 3,300 psi.

5. In considering the characteristics of six classes of I.C. engine:

(i) normally aspirated four stroke direct injection diesel

(ii) " " " " indirect injection diesel

(iii) turbocharged four stroke direct injection diesel

(iv) two stroke direct injection diesel

(v) turbocharged two stroke diesel

(vi) fuel injected petrol engines

an assessment of the general characteristics of combustion excitation and overall noise shows that at full load conditions the combustion characteristics, as expressed by cylinder pressure spectra, are the major single controlling factor determining the engine overall noise characteristics. Use of the concept of reduced cylinder pressure spectra has enabled the relative combustion excitation levels of the six classes of engine to be assessed. In descending order of excitation,

(a) two stroke N.A.

(b) four stroke D.I., N.A.

(c) four stroke I.D.I., N.A.

(d) turbocharged four and two stroke D.I. equally

(e) petrol.

6. The investigations reveal that the pressure diagram can only be assumed to remain the same on a degree basis for normally aspirated direct injection diesels employing an in-line pump with no speed or load advance and run at moderate speed. With the introduction of more varied control for injection characteristics, turbocharging and two stroke operation this assumption is no more valid. As a result of this finding, the mechanism causing increase in noise with speed, based on the slope of the cylinder pressure spectrum, has been modified.

7. The combustion noise model shows that the combustion noise radiated is dependent on:

(a) the level of cylinder pressure exciting spectrum

(b) the surface area of the engine

(c) the acoustic radiation ratio of the engine

(d) the structural impedance linking force input with engine surface vibration.

The ratio of overall acoustic radiation to overall structural impedance is found to be nearly constant for current production diesel engines.

Three different methods for predicting the level of combustion noise in diesel engines have resulted from the combustion noise model.

(a) In conjunction with empirically found constants, prediction formulae based on bore and speed only have been formulated for rated speed conditions. Very good agreement between predicted and measured levels is obtained.

(b) The use of a standard structural attenuation factor and the combustion noise model provides a method of calculating combustion induced

noise levels at any speed or load condition. A simplified form is presented which enables the combustion noise to be predicted simply from the average level and slope of the cylinder pressure spectrum and the engine bore size.

APPENDIX I - THE FAST FOURIER ANALYSIS COMPUTER PROGRAMME

The general method used for the calculation of a large number of Fourier coefficients has been described in Chapter 5. During the period of the work reported in this thesis a considerable number of computer programmes were developed as requirements for certain items, such as indicated power calculations, etc., became obvious. In this Appendix the initial simple straight line assumption programme (V17E) is described and presented in full. Also two later programmes are listed. Firstly, programme V17J, which was a complex programme in which the straight line or polynomial approximation could be called, a constant percentage analysis of any bandwidth, the computation of Fourier transform values and also the indicated power could be calculated. The third programme is a modification of the original V17E programme, and is the simplest programme used in which only the straight line approximation appears, a 1/3 octave fixed frequency analysis is carried out and the input data, calculated input data and resultant spectrum is displayed graphically. A job statistics card for the computation of two Fourier analyses up to 1200 harmonics from two sets of 350 input data points is also shown, giving the computer store requirement and typical running times and costs.

A1.1 The Programme V17E

A block diagram of the programme is given in Fig. 1. Data is fed into block 1. In block 2 the input data points required for a Simpson's rule integration are calculated. In block 3 this data is used to calculate the harmonic values. In block 4 these values are printed out. Block 5 tests the data and if more harmonics are required then more calculated input data points can be computed and the programme is then run through again. If the correct number of harmonics have been computed, then the programme either

ends or returns to block 1 to accept a new data set, depending on the value of an integer fed in as part of the original data set.

A1.2 Programme Results

Each input value is discussed below in the order in which they are fed into the computer.

i) L

Tells computer whether to expect more data. If L > 5 computer expects more data cases.

ii) IX

This is the number of equally spaced Y ordinates used in the numerical integration (in this case Simpson's Rule). The value of IX must satisfy two conditions:-

(a) IX $\geq$ (IB) $\times$ (5). This ensures that the highest harmonic needed can be specified adequately.

(b) /D(IXX) - D(1)//IX must be smaller than the minimum value of /D(J) - D(J - 1)/ present in the input data in order to utilise fully the input data.

iii) IY

If IY = 1 harmonics 1, 2, 3, ..., IB calculated

If IY = 2 harmonics 1, 3, 5, 7 ..., IB calculated

iv) IXX

Number of input data cards. (One set of D(J) and E(J) to a card).

v) I CASE

Data case number for identification.

vi) IYA, IYB, IYC

Used as for IY when more input coordinates have been calculated.

vii) AFAC and AFAG are Scaling Factors

AFAC

Input data E(J) peak value (for pressure diagrams p.s.i.).

AFAG

Equivalent number for peak value of E(J) in arbitrary units.

If AFAC = AFAG then value of E(J) is assumed to be in lb/in^2 for calculation of harmonics re 2×10^{-4} μbar.

viii) AL the Repetition Length

AL = (IX - 1), written as a variable.

ix) X and Y Coordinates of Input Data

D(J) and E(J) are input coordinates of repetitive pulse to be analysed. For computation E(J) is multiplied by ten and then harmonic values corrected for this before being printed out. There is no limitation on the number or spacing of these input coordinates as the equi-spaced data is computed from this input by the programme.

A1.3 Programme Output

The outputs from the programme are:

On Line Printers

i) A(K)

This is the value of the cosine component of the Fourier series.

ii) B(K)

This is the value of the sine component of the Fourier series.

iii) R(K)

$R(K) = ((A(K))^2 + (B(K))^2)^{\frac{1}{2}}$ and is therefore the modulus of the harmonic amplitudes.

iv) DB(K)

$$DB(K) = 20 \log_{10} \frac{R(K)}{2.94 \times 10^{-9}} \quad \text{if } R(K) \text{ is in } lb/in^2$$

DB(K) is expressed in dB relative to 2×10^{-4} μbar and is therefore the cylinder pressure spectrum level at the K^{th} harmonic.

v) K

This is the harmonic number.

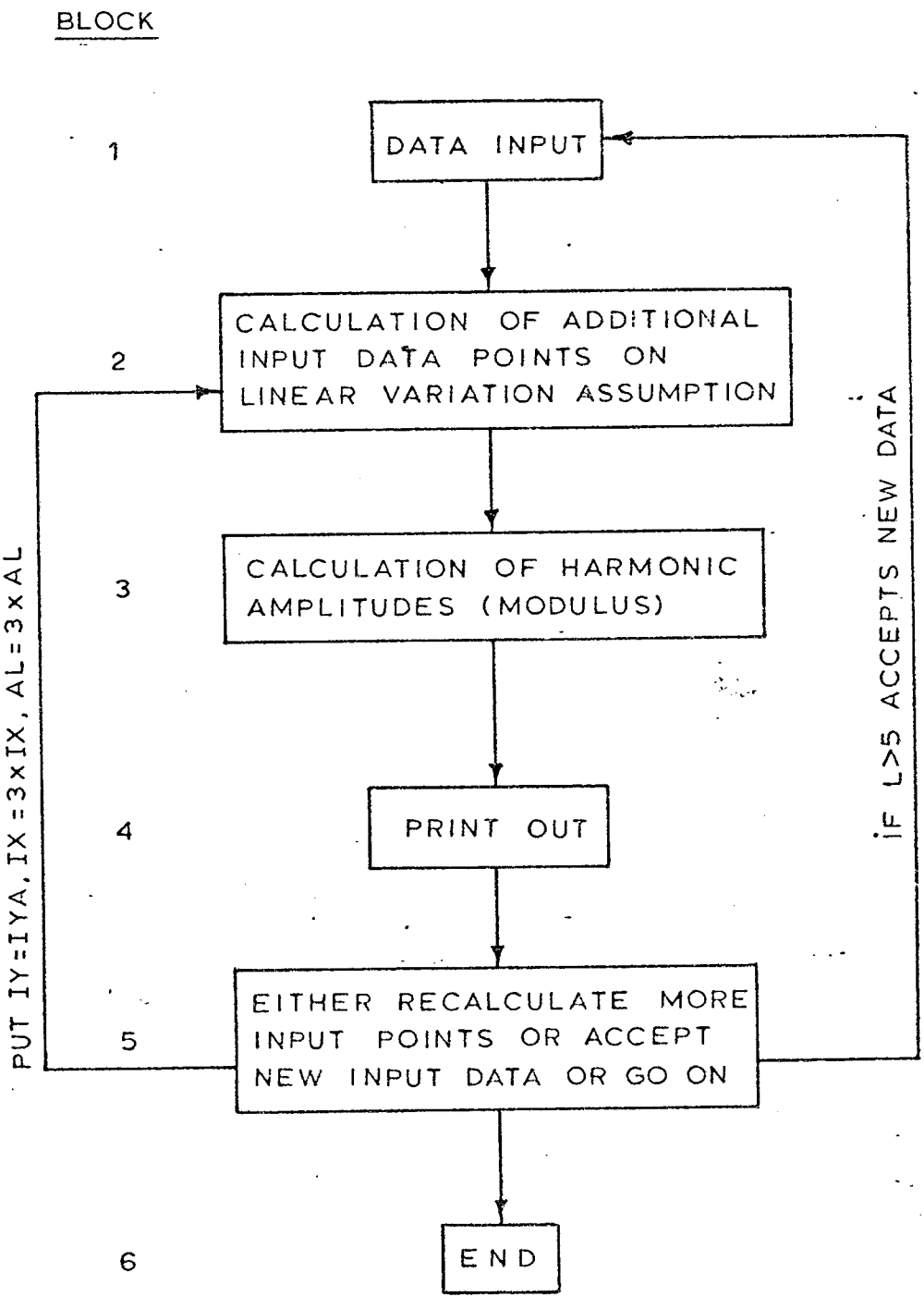

Fig. 1 Block diagram of Fourier Analysis Program

```
      MASTER FOURIER ANALYSIS PA
      DIMENSION C(4500),D(900),E(900),A(900),R(900),CN(900),AIAN(900),AK
     1(900),S(900)
   11 CALL TIME (T)
      WRITE(6,16)T
   16 FORMAT(//16H THE TIME IS NOW,A8)
      READ(5,99)L,IX,IY,IB,IXX,ICASE,IYA,IYB,IYC
   99 FORMAT(I5)
      READ(5,299)AFAC,AFAG ,AL
  299 FORMAT(F12.8)
      READ(5,219)(D(J),E(J),J=1,IXX)
  219 FORMAT(F6.1,1X,F6.1)
      IPA=1
      AM=1.0
  902 FORMAT(1X,25HX AND Y INPUT COORDINATES)
      WRITE(7,902)
      WRITE(7,901)(D(J),E(J),J=1,IXX)
      CALL RUNOUT (7)
      KTD=0
      FL=D(IXX)-D(1)
      CAFA=AFAC/AFAG
   58 KTD=KTD+2
      ITCH=(IX-1)/(5)
      DIV=1.0/(AL)
      IXT=(IX+1)
      C(1)=E(1)
      DO 89 IT=2,(IX+1)
      AIT=FLOAT(IT)
      X(IT)=(AIT-1.0)*DIV*FL
      DO 88 J=2,IXX
      IF(D(J).LT.X(IT))GO TO 88
      IF(D(J).EQ.X(IT))C(IT)=E(J)
      IS=J-1
      IF(D(J).GT.X(IT))C(IT)=E(IS)+(E(J)-E(IS))*(X(IT)-D(IS))/(D(J)-D(IS
     1))
      GO TO 89
   88 CONTINUE
   89 CONTINUE
   91 DO 92 LA=1,(IX-1)/(2)
      JOT=LA*2
      C(JOT)=C(JOT)*2.0
   92 CONTINUE
      C(1)=C(1)/(2.0)
      C(IX)=C(IX)/(2.0)
      IF(KTD.GT.3) GO TO 4
      CALL TIME (T)
      WRITE(6,16) T
    4 DO 15 K=IPA,IX,IY
      IF(K.GT.IB)GO TO 401
      AK(K)=FLOAT(K)
      IF(K.GT.((IX-1)/(5))) GO TO 401
      P1=0.0
      P2=0.0
      DARK=(6.283185*AK(K)*AM)/(AL)
      COSK=COS(DARK)
      SINK=1.0-COSK
      SIN(K)=SIN(DARK)
      DO 10 IZ=1,IX
      IM=K*IT-IZ
      PO=C(IM)*P1*ACOC-P2
      P2=P1
      P1=PO
```

```
   19 CONTINUE
      A(K)=(FC-F2*COSX)*(0.05333*AH)/(AL)
      B(K)=(F2*SINX*0.05333*AH)/(AL)
      R(K)=SQRT(A(K)*A(K)+B(K)*B(K))*CAFA
      DB(K)=R(K)/(0.00000000296)
      DB(K)=20.0*ALOG10(DB(K))
      AIAN(K)=50.0*ALOG10(AK(K))
   15 CONTINUE
  401 IX=IX
      CALL TIME (T)
      WRITE(6,16) T
      IF(KTD.GT.3) GO TO 75
      WRITE(6,400)
  400 FORMAT(33H PROGRAM V17F D.ANDERTON I,S,V,R,)
   17 FORMAT(12H CASE NUMBER,I5)
      WRITE(6,17)ICASE
  505 FORMAT(50X,4H IX ,7X,4H IY ,10X,4H IB ,7X,5H IXX )
      WRITE(6,505)
  555 FORMAT(48X,I5,7X,I5,9X,I5,7X,I5)
      WRITE(6,555)IX,IY,IB,IXX
  606 FORMAT(20X,3HAH ,23X,4H AL ,23X,4HAFAC,23X,4HAFAG)
      WRITE(6,606)
  666 FORMAT(15X,4F20.5)
      WRITE(6,666)AH,AL,AFAC,AFAG
  626 FORMAT(50X,5H IYA ,7X,5H IYB ,10X,5H IYC )
      WRITE(6,626)
  633 FORMAT(50X,I5,7X,I5,10X,I5)
      WRITE(6,633)IYA,IYB,IYC
  699 FORMAT(52X,24HHARMONIC AMPLITUDE IN DB)
      WRITE (6,699)
  700 FORMAT(10X,4HA(K),20X,4HB(K),16X,4HR(K),13X,5HDB(K),18X,3H K )
      WRITE(6,700)
      WRITE(7,400)
      WRITE(7,17)ICASE
      WRITE(7,699)
      CALL RUNOUT (7)
   73 IF(IB.GT.ITCH) GO TO 78
      ITCH=IB
   78 WRITE(6,800)(A(K),B(K),R(K),DB(K),AK(K),K=IPA,ITCH,IY)
  800 FORMAT(1X,5F20.5)
  901 FORMAT(2F12.1,2X)
      WRITE(7,901)(AIAN(K),DB(K),K=IPA,ITCH,IY)
      IF(ITCH-IB)63,13,13
   63 IY=((IX-1)*5)+1
      AL=AL*5.0
      IY=IYA
      IPA=ITCH
      IF(KTD.GT.3) GO TO 66
      GO TO 58
   66 IY=IYB
      IF(KTD-5) 58,58,67
   67 IY=IYC
      GO TO 5
   13 ENDFILE 7
      CALL TIME(T)
      WRITE(6,16)  T
      IF(I .GT.5) GO TO 11
      STOP
      END
```

```
      MASTER FOURIER ANALYSIS DA
      DIMENSION FR(28)
      DIMENSION C(4100),D(1001),E(1001),DB(1001),AIAN(1001),R(1001),
     1FREQ(1001),AB(200),AC(200),CD(200),A(1001),B(1001),PHI(1001)
      DATAFR(1),FR(2),FR(3),FR(4),FR(5),FR(6),FR(7),FR(8),FR(9),FR(10),
     1     FR(11),FR(12),FR(13),FR(14),FR(15),FR(16),FR(17),FR(18),
     2     FR(19),FR(20),FR(21),FR(22),FR(23),FR(24),FR(25),FR(26),
     3     FR(27),FR(28)/20.0,25.0,31.5,40.0,50.0,63.0,80.0,100.0,
     4     125.0,160.0,200.0,250.0,315.0,400.0,500.0,630.0,800.0,1000.0,
     5     1250.0,1600.0,2000.0,2500.0,3150.0,4000.0,5000.0,6300.0,
     6     8000.0,10000.0/
      EQUIVALENCE (D(1),DB(1)),(E(1),AIAN(1))
      X(IT)=(AIT-1.0)*DIV*FL
      SUMP=0
   11 CALL TIME (T)
      WRITE(6,16)T
   16 FORMAT(///16H THE TIME IS NOW,A8)
      READ(5,99)ICASE,L,IX,IY,IB,IXX,NEB,LAMB,JAP,MAN,ICOT,I3OCT
   99 FORMAT(I5)
C     IF I3OCT=1 PROGRAM GIVES 1/3 OCT BAND ANALYSIS
C     IF L>5 EXPECTS MORE DATA.IX=NO. ORDINATE POINTS CHOSEN.IY=HARMONIC
C     C SEPERATION.IB=HIGHEST HARMONIC TO BE CALCULATED.IXX=NUMBER INPUT
C     DATA CARDS.ICASE=CASE NUMBER.IYA,IYB,IYC ARE HARMONIC NUMBER
C     SEPERATIONS ON RECALCULATING MORE ORDINATE POINTS(3*IX IN EACH
C     CASE).
C     THIS PROGRAM REVISED SO THAT NON-INTEGER VALUES OF K CAN BE USED
C     NEB=RATIO OF PULSE LENGTH TO HARMONIC REPETITION LENGTH.
C     D(1) MUST ALWAYS BE ZERO
      READ (5,299) AFAC,AFAG,AL,FUND,TWOF,POJ,RO,XLCR,XXX,APER,AREAP
      ARE=ABS(AREAP)
  299 FORMAT(F12.8)
C     IF AREAP>0 INDICATED POWER IS CALCULATED
C     INDICATED POWER IS CALCULATED USING THE PREVIOUS CASE AND THE
C     CURRENT PISTON MOTION CASE
C     AFAC=PEAK PRESSURE IN P.S.I. AFAG=PEAK PRESSURE IN DIGITS(FROM
C     OSCAR READER).AL=REPETITION LENGTH(IX=1).FUND=ENGINE R.P.M.
C     TWOF=1.0 FOR TWO STROKE AND =0.5 FOR FOUR STROKE ENGINE
C     NEB; IF NEB=1 FOURIER ANALYSIS COMPLETED;IF NEB>1 FOURIER TRANSFOR
C     M COMPLETED WITH EVERY T/NEB VALUE CALCULATED.WHERE T=TOTAL TIME
C     OF TRANSIENT
C     LAMB; IF LAMB<5 FOURIER COEFFICIENTS CALCULATED WITH STRAIGHT LINE
C     APPROXIMATION BEYWEEN INPUT DATA POINTS;IF5<LAMB<10 THIRD ORDER
C     POLYNOMIAL ASSUMED BETWEEN INPUT DATA POINTS;IF LAMB>10 PROGRAM
C     CALCULATES AND ANALYSES PISTON MOTION.
C     JAP;  EASYREAD PRINTOUT OF CALCULATED INPUT DATA AT 1 DEGREE
C     INTERVALS.IF JAP=361 FOR TWO STROKE CYCLE.JAP=721 FOR FOUR STROKE
C     CYCLE
C     MAN;  IFMAN=0 PAPER TAPE OUTPUT OF; AIAN(K),PHI(K),A(K),B(K),IF
C     MAN>0 PAPER TAPE OUTPUT OF; AIAN(K),ANDDB(K) ONLY.
C     POJ;  PHASE OF INPUT DATA IN THE SAME UNITS AS X COORDINATE OF THE
C     DATA.
C     RO;  CRANK RADIUS IN INCHES.
C     XLCR;  CONNECTING ROD LENGTH IN INCHES.
C     XXX;  PHASE ANGLE OF PISYON MOTION RELATIVE TO B.D.C. IN DEGREES.
C     APER;  HALF PERCENTAGE BANDWIDTH OF ANALYSIS.
      IF (LAMB.GT.10) GO TO 669
      IF(ICOT.EQ.1) GO TO 3
C     IF ICOT=1 PROGRAM READS INPUT DATA FROM PAPER TAPE.IF ICOT>1 READS
C     INPUT DATA FROM CARDS.
      READ(5,219)(D(J),E(J),J=1,IXX)
  219 FORMAT(F6.1,1X,F7.2)
C     D(J)=X COORDINATE OF INPUT DATA. E(J)=Y COORDINATE OF INPUT DATA.
      GO TO 669
```

```
220 FORMAT (F5.0)
  3 READ (4,220) (E(J),J=1,IXX)
    IF(E(IXX).NE.E(1)) E(IXX)=E(1)
    DO 1 J=1,IXX
  1 D(J)=J-1
669 CONTINUE
    AMULT=FUND*TWOF/(60.0)
    WRITE(6,400)
400 FORMAT(77H PROGRAM V17J FOURIERANALYSIS OF REPEATING WAVEFORMS AND
   1 TRANSIENT WAVEFORMS )
    WRITE(6,422)
422 FORMAT(20H D.ANDERTON I.S.V.R.)
 17 FORMAT(12H CASE NUMBER,I5)
    WRITE(6,17)ICASE
410 FORMAT(50X,25H TABULATION OF INPUT DATA)
    WRITE(6,410)
505 FORMAT(45X,3H L ,7X,4H IX ,8X,4H IY ,10X,4H IB ,7X,5H IXX )
    WRITE(6,505)
555 FORMAT(40X,I5,7X,I5,7X,I5,9X,I5,7X,I5)
    WRITE(6,555) L,IX,IY,IB,IXX
606 FORMAT(28X,5H FUND,15X,4H AL ,16X,4HAFAC,16X,4HAFAG,16X,5HAMULT)
    WRITE(6,606)
666 FORMAT(15X,5F20.5)
    WRITE(6,666) FUND,AL,AFAC,AFAG,AMULT
626 FORMAT(45X,3HNEB,7X,4HLAMB,8X,4H JAP,10X,4H MAN,7X,4H NAB)
    WRITE(6,626)
633 FORMAT(40X,I5,7X,I5,7X,I5,9X,I5,7X,I5)
    WRITE(6,633)NEB,LAMB,JAP,MAN,NAB
    WRITE(6,607)
607 FORMAT(60X,4H POJ,10X,2HR0,18X,3HLCR)
608 FORMAT(10X,5F20.5)
    WRITE (6,608) APER,XXX,POJ,R0,XLCR
    KMAX=0
    IJK=1
    IND=0
    IPA=1
    IF (LAMB.GT.10) GO TO 444
238 FORMAT(///50X,30H X AND Y COORDINATE INPUT DATA)
    WRITE(6,238)
    WRITE(6,204)(D(J),E(J),J=1,IXX)
902 FORMAT(1X,25HX AND Y INPUT COORDINATES)
    IF (ABS(POJ).LT..1E-7) GO TO 223
    DO 3002 I=1,IXX
    C(I)=B(I)
3002 C(IXX+I)=E(I)
    D(1)=0.0
    DO 3003 I=1,IXX
    IF (ABS(C(I)-POJ).LT..1E-7) GO TO 3004
    IF (C(I).GT.POJ) GO TO 3005
3003 CONTINUE
3004 IA=I+1
    E(1)=E(I)
    IMP=0
    IA1=IA-2
    GO TO 3006
3005 IA=I
    IMP=1
    IA1=IA-1
    E(1)=E(IA1)+(E(IA)-E(IA1))*(POJ-D(IA1))/(D(IA)-D(IA1))
3006 J=2
    DO 3007 I=IA,IXX
     D(J)=C(I)-POJ
    E(J)=C(I+IXX)
```

```
 3007 J=J+1
      JXX=J-1
      IF (IA1.LT.2) GO TO 3010
      DO 3008 I=2,IA1
      D(J)=D(JXX)+C(I)
      E(J)=C(I+IXX)
 3008 J=J+1
 3010 F(J)=F(1)
      D(J)=C(IXX)
      IXX=IXX+JMP
      PHASE=POJ*360.0/(TWOF*D(IXX))
      WRITE (6,3009) PHASE,(D(J),E(J),J=1,IXX)
 3009 FORMAT (///30X,37HX AND Y INPUT DATA PHASE CORRECTED TO,
     1F12.4//(40X,2F20.5))
  223 WRITE (7,902)
  910 FORMAT(/)
      WRITE(7,910)
      WRITE(7,901)(D(J),E(J),J=1,IXX)
      CALL PUNOUT (7)
      ENDFILE 7
      WRITE(6,2600)
 2600 FORMAT(///60X,16H INPUT DATA TEST)
      ICT=1
      EVAD=EL/(AL)
      IF(ABS(E(1)-E(IXX)).LT..1E-7) GO TO 2002
      WRITE(6,2008)
 2008 FORMAT(43H Y COORDINATES E(1) AND E(IXX) DO NOT MATCH)
 2002 IF (ICOT.EQ.1) GO TO 75
      DO 2007 J=2,IXX
      IF((D(J)-D(J-1)).GT.3.0) GO TO 2003
      WRITE(6,2004) J,D(J-1),D(J)
 2004 FORMAT(55H FIRST DATA CHECK-D(J)IS AT <3.0 UNITS SEPARATION
     115,2X,2(E14.6,5X))
      DAVE=D(J)-D(J-1)
      IF(DAVE.LT.EVAD) WRITE(6,2500)
 2003 IF((D(J)-D(J-1)).GT.2.0) GO TO 2005
      WRITE(6,2006) J,D(J-1),D(J)
 2006 FORMAT(55H SECOND DATA CHECK-D(J)IS AT <2.0 UNITS SEPARATION
     115,2X,2(E14.6,5X))
   75 CONTINUE
      DAVE=D(J)-D(J-1)
      IF(DAVE.LT.EVAD) WRITE(6,2500)
 2500 FORMAT(60X,21H ERROR IN CHOOSING IX)
 2005 IF((D(J)-D(J-1)).GT..1E-7) GO TO 2007
      WRITE(6,2001) J,D(J-1),D(J)
 2001 FORMAT(11H DATA ERROR,I5,2X,2(E14.6,5X))
      ICT=10
 2007 CONTINUE
      CALL TIME (T)
      WRITE(6,16) T
      IF(ICT.GT.5) WRITE(6,2015)
 2015 FORMAT(60X,22H DATA ERROR **********)
      IF(ICT.GT.5) GO TO 18
      IF(ICT.LT.2) WRITE(6,2010)
 2010 FORMAT(60X,16H INPUT DATA O.K.)
  444 CONTINUE
      KTD=0
      IPT=0
      FL=D(IXX)-D(1)
      CAFA=AFAC/AFAG
      FACA=CAFA/(0.00000000294)
   58 CONTINUE
      ISOX=0
```

```
 23 CONTINUE
    IF(ISOX.GT.5) GO TO 22
    ISAG=IX
    IX=JAP
    ALSA=AL
    AL=JAP+1
 22 CONTINUE
    ITCH=(IX-1)/(5)
    DIV=1.0/(AL)
    BEER=0.13333*DIV
    IXT=(IX+1)
    C(1)=F(1)
    CALL TIME (T)
    WRITE(6,16) T
    IF (LAMB.GT.10) GO TO 667
    IF(LAMB.GT.5) GO TO 21
    KYD=0
    FL=D(IXX)-D(1)
    CAFA=AFAC/AFAG
    ITCH=(IX-1)/(5)
    DIV=1.0/(AL)
    IXT=(IX+1)
    C(1)=F(1)
    DO 3000 IT=2,(IX+1)
    AIT=FLOAT(IT)
    DO 3001 J=2,IXX
    IF(D(J).LT.X(IT)) GO TO 3001
    IF(D(J).EQ.X(IT))C(IT)=E(J)
    IS=J-1
    IF(D(J).GT.X(IT))C(IT)=E(IS)+(E(J)-E(IS))*(X(IT)-D(IS))/(D(J)-D(IS
   1))
    GO TO 3000
3001 CONTINUE
3000 CONTINUE
    GO TO 89
 21 KYD=0
    DO 5 LB=2,(IXX-2)
    LT=LB-1
    EAT=D(LB+1)-D(LB)
    EBT=D(LB+2)-D(LB)
    ECT=D(LB+2)-D(LB+1)
    AAT=D(LB)-D(LT)
    ABT=D(LB+1)-D(LT)
    ACT=D(LB+2)-D(LT)
    EET=D(LB+2)+D(LB)-2.0*D(LT)
    CD(LB)=((E(LB)-E(LT))/(AAT*EAT*EBT))-((E(LB+1)-E(LT))/(ABT*EAT*ECT
   1))+((E(LB+2)-E(LT))/(ACT*EBT*ECT))
    BC(LB)=((E(LB+2)-E(LT))/(ACT*EBT))-((E(LB)-E(LT))/(AAT*EBT))-(CD(L
   1B)*EET)
    AB(LB)=((E(LB)-E(LT))-(BC(LB)*AAT*AAT)-(CD(LB)*AAT*AAT*AAT))/(AAT)
  5 CONTINUE
    EAT=D(2)
    EBT=D(3)
    ECT=D(3)-D(2)
    DELT=D(IXX)-D(IXX-1)
    AAT=DELT
    ABT=D(2)+DELT
    ACT=D(3)+DELT
    EET=D(3)+2.0*DELT
    CD(1)=((E(1)-E(IXX-1))/(AAT*EAT*EBT))-((E(2)-E(IXX-1))/(ABT*EAT*EC
   1T))+((E(3)-E(IXX-1))/(ACT*EBT*ECT))
    BC(1)=((E(3)-E(IXX-1))/(ACT*EBT))-((E(1)-E(IXX-1))/(AAT*EBT))-CD(1
   1)*EET
```

```
      AB(1)=((F(1)-E(IXX-1))-(BC(1)*AAT*AAT)-(CD(1)*AAT*AAT*AAT))/(AAT)
      FAT=DELT
      FBT=D(2)+DELT
      FCT=D(2)
      AAT=D(IXX-1)-D(IXX-2)
      ABT=D(IXX)-D(IXX-2)
      ACT=D(2)+D(IXX)-D(IXX-2)
      FET=D(2)+D(IXX)-D(IXX-2)+D(IXX-1)-D(IXX-2)
      CD(IXX-1)=((E(IXX-1)-E(IXX-2))/(AAT*FAT*FBT))-((E(IXX)-E(IXX-2))/(
     1ABT*FAT*FCT))+((E(2)-E(IXX-2))/(ACT*FBT*FCT))
      BC(IXX-1)=((E(2)-E(IXX-2))/(ACT*FBT))-((E(IXX-1)-E(IXX-2))/(AAT*FB
     1T))-(CD(IXX-1)*FET)
      AB(IXX-1)=((E(IXX-1)-E(IXX-2))-(BC(IXX-1)*AAT*AAT)- (CD(IXX-1)*AAT
     1*AAT*AAT))/(AAT)
  909 FORMAT(1X,2I5)
      CALL TIME (T)
      WRITE(6,16) T
      IT=1
   13 IT=IT+1
      AIT=FLOAT(IT)
      XIT=(AIT-1.0)*DIV*FL
  908 FORMAT(1X,F20.5)
      J=1
      IS=0
   12 J=J+1+IS
      IF(D(J).LT.XIT)GO TO 88
      IF(D(J).EQ.XIT)C(IT)=E(J)
      IF(D(J).EQ.XIT)GO TO 90
      IF(J.EQ.2) GO TO 35
      IS=J-1
      ISS=IS-1
      XITT=XIT-D(ISS)
      GO TO 34
   35 IS=1
      ISS=(IXX-1)
      XITT=XIT+DELT
   34 C(IT)=E(ISS)+(AB(IS)*XITT)+(BC(IS)*XITT*XITT)+(CD(IS)*XITT*XITT*XI
     1TT)
      GO TO 90
   88 IF(J-IXX)12,12,89
   90 IF(IT-IXT)13,13,89
  667 DELTPHI=360.0/(IX-1)
  670 FORMAT(35X,33H CALCULATED PISTON MOTION CASE NO,I5)
      WRITE(6,670)ICASE
      HIP=XXX
      XLCR1=XLCR/R0
      XLCR12=XLCR1*XLCR1
      DO 668 I=1,IX
      HI=HIP*3.1415926536/180.0
      SINP=SIN(HI)
      C(I)=R0*(1-COS(HI )+XLCR1*(1-SQRT(1-SINP*SINP/XLCR12)))
      COSP=COS(HI)
  831 FORMAT(1X,7E16.5)
      C(I)=10000*C(I)
      IF (ABS(HIP-360.0).LT..1E-7) HIP=0.0
      HIP=HIP+DELTPHI
  668 CONTINUE
   89 CONTINUE
      CALL TIME (T)
      WRITE(6,16) T
      IF(ISOX.GT.5) GO TO 24
  903 FORMAT(F12.1,2X)
  411 FORMAT(50X,58H TABULATION OF CALCULATED,'EQUI-SPACED' INPUT COORDI
```

```
     1NATES )
      WRITE(6,411)
      WRITE(6,237)
  204 FORMAT(40X,2E20.5)
      DO 25 J=1,JAP
      OOJ=J-1
      WRITE(6,204) OOJ,C(J)
   25 CONTINUE
      WRITE(7,237)
      WRITE(7,910)
      WRITE(7,906)(C(J),J=1,JAP)
  906 FORMAT(E16.5,2X)
      CALL RUNOUT (7)
      ENDFILE 7
   24 ISOX=ISOX+10
      IX=ISAG
      AL=ALSA
      IF(ISOX.LT.15) GO TO 23
C     POLYNOMIAL VARIATION BETWEEN POINTS ASSUMED.
C     C(IT)=AB(IS)*X(ITT)+BC(IS)*X(ITT)*X(ITT)+CD(IS)*X(ITT)*X(ITT)*X(IT
C     T),WHERE AB(IS),BC(IS),CD(IS) ARE CONSTANTS.
C     CD(IS)=Y1/X1(X2-X1)(X3-X1)-Y2/X2(X2-X1)(X3-X2)+Y3/X3(X3-X1)(X3-X2
C     )
C     BC(IS)=Y3/X3(X3-X1)-Y1/X1(X3-X1)-CD(IS)(X3-X1).
C     AC(IS)=X1/(Y1-BC(IS)X1X1-CD(IS),X1,X1,X1)
   91 DO 92 LA=1,(IX-1)/(2)
      JOT=LA*2
      C(JOT)=C(JOT)*2.0
   92 CONTINUE
      C(1)=C(1)/(2.0)
      C(IX)=C(IX)/(2.0)
      IF(KTD.GT.3) GO TO 4
      CALL TIME (T)
      WRITE(6,16) T
  320 FORMAT(35X,3H AB,25X,3H BC,25X,3H CD)
  237 FORMAT(///50X,34HCALCULATED Y COORDINATE INPUT DATA)
  310 FORMAT(20X,3E20.5)
    4 BEN=FLOAT(NEB)
      M=0
      KTD=KTD+2
      IPA=KMAX+IY
      DO 15 K=IPA,IX,IY
      AMPK=FLOAT(K)
      AK=AMPK/(BEN)
      IF (K.GT.18) GO TO 401
      IF(K.GT.((IX-1)/(5))) GO TO 401
      F1=0.0
      F2=0.0
      DARK=(6.28318512*AK)/(AL)
      COOK=COS(DARK)
      ACOC=2.0*COOK
      SOOD=SIN(DARK)
      DO 19 IZ=1,IX
      IM=IXT+IZ
      F0=C(IM)+F1*ACOC-F2
      F2=F1
      F1=F0
   19 CONTINUE
      M=M+1
      IF (ARF.LT..1E-7) GO TO 461
  460 IF (ABS(TWOF-1.0).LT..1E-7) GO TO 462
      M2=2*M
      AS=S(M2)
```

```
      BS=B(M2)
      GO TO 461
  462 AS=A(M)
      BS=B(M)
      M2=M
  461 CONTINUE
      A(M)=(F0-(F2*COOK))*CAFA*BEER
      B(M)=F2*SOOD*CAFA*BEER
      PHI(M)=ATAN(A(M)/B(M))*180.0/3.14159256
      R(M)=SQRT(A(M)*A(M)+B(M)*B(M))
      DB(M)=R(M)/(0.000000002%4)
      IF(DB(M).LT.1.0) DB(M)=1.0
      DB(M)=20.0*ALOG10(DB(M))-3.0
      AIAN(M)=50.0*ALOG10(AK)
      FREQ(M)=AK*AMULT
      IF (ARE.GT..1E-7) SUMP=SUMP+M2*(B(M)*AS-A(M)*BS)
      IF (ARE.GT..1E-7) WRITE (6,466) SUMP
  466 FORMAT(6H SUMP=,E12.6)
   15 CONTINUE
C     CALCULATION OF DB(K) SIMPLIFIED AND OUTPUT MODIFIED TO SUIT.
  401 IX=IX
      SUMP=SUMP*3.1415926535*AREAP*FUND/396000000.0
      KMAX=K
      MMAX=M
      CALL TIME (T)
      WRITE(6,16) T
      IF(NEB.GT.1) GO TO 77
 2610 FORMAT(35X,54HFOURIER COEFFICIENTS (MODULUS) FOR REPEATING WAVEFOR
     1MS)
      WRITE(6,2610)
      IF(NEB.EQ.1) GO TO 79
   74 FORMAT(35X,54H FOURIER COEFICIENTS (MODULUS) FOR TRANSIENT WAVEFOR
     1MS)
   77 WRITE(6,74)
   79 CONTINUE
  499 FORMAT(///4X,15HR.M.S. HARMONIC,6X,9HFREQUENCY,5X,15HHARMONIC NUMB
     1ER,2X,14HPEAK HARMONIC,7X,5HPHASE,13X,6HCOSINE,12X,4HSINE)
      WRITE (6,499)
  491 FORMAT(4X,15HAMPLITUDE IN DB,8X,3HC/S,24X,18HAMPLITUDE LB/SQ.IN,
     124X,9HCOMPONENT,9X,9HCOMPONENT)
      WRITE(6,491)
  700 FORMAT(7X,5HDB(K),13X,7HFREQ(K),11X,1HK,14X,4HR(K),16X,3HPHI,8X,4H
     1A(K),15X,4HB(K))
      WRITE(6,700)
      WRITE(7,400)
      WRITE(7,17)ICASE
      WRITE(7,499)
      CALL RUNOUT (7)
   73 CONTINUE
      DO 43 K=1,MMAX
      GAG=((K-1)*IY+IPA)
   78 WRITE (6,800) DB(K),FREQ(K),GAG,R(K),PHI(K),A(K),B(K)
   43 CONTINUE
  800 FORMAT(1X,7F17.7)
  901 FORMAT(2F12.1,2X)
      IF (ABS(SUMP).LT..1E-7) GO TO 464
      WRITE (6,463) SUMP
  463 FORMAT(17HOINDICATED POWER=,F12.6)
      SUMP=0.0
  464 CONTINUE
      CALL TIME (T)
      WRITE(6,16) T
      IF (ISOCT.EQ.1) GO TO 7
```

```
      IJK=IJK+1
      K=1
  113 II=1
      FRACTM=(100.0-APER)/(100.0)
      FRACTP=(100.0+APER)/(100.0)
      ICOUNT=1
      TOUNT=FLOAT(ICOUNT)
      SUM=R(1)*R(1)
      I=2
  105 PER1=FREQ(II)*FRACTP
  100 IF(FREQ(I).GE.PER1) GO TO 101
      ICOUNT=ICOUNT+1
      TOUNT=FLOAT(ICOUNT)
      SUM=SUM+R(I)*R(I)
      I=I+1
      IJK=IJK+1
      IF(IJK.GT.IB) GO TO 107
      GO TO 100
  101 DBC=SQRT(SUM/TOUNT)
      DBC=DBC/(0.000000000294)
      IF(DBC.LT.1.0) DBC=1.0
      DB(K)=20.0*ALOG10(DBC) -3.0
      AIAN(K)=FREQ(II)
      ILAST=II
      SUM=0
      ICOUNT=0
      TOUNT=FLOAT(ICOUNT)
  103 PER2=FREQ(I)*FRACTM
      IF(PER2.GT.PER1) GO TO 104
      SUM=SUM+R(I)*R(I)
      ICOUNT=ICOUNT+1
      TOUNT=FLOAT(ICOUNT)
      I=I+1
      IJK=IJK+1
      IF(IJK.GT.IB) GO TO 108
      GO TO 103
  104 II=I-1
      K=K+1
      IF(II.NE.ILAST) GO TO 105
      I=I+1
      IJK=IJK+1
      II=II+1
      SUM=R(II)*R(II)
      ICOUNT=ICOUNT+1
      TOUNT=FLOAT(ICOUNT)
      GO TO 105
  200 FORMAT(10X,39H CONSTANT PERCENTAGE BANDWIDTH ANALYSIS)
  107 AIAN(K)=FREQ(II)
      GO TO 109
  108 K=K+1
      AIAN(K)=FREQ(IB)
  109 DBC=SQRT(SUM/TOUNT)
      DBC=DBC/0.000000000294
      IF (DBC.LT.1.0) DBC=1.0
      DB(K)=20.0*ALOG10(DBC)-3.0
      MAXK=K
      IF (K.EQ.0) GO TO 6002
  820 FORMAT(1X,2F22.7)
      WRITE(6,200)
      WRITE(6,820)(DB(K),AIAN(K),K=1,MAXK)
 6002 CALL TIME(T)
      WRITE(6,16) T
   18 ENDFILE 7
```

```
      GO TO 221
    7 CONTINUE
      INK=1
      DO 14 I=1,28
      ICOUNT=0
      SUM=0.0
      HAT=FR(I)*.115
      PER1=FR(I)-HAT
      PER2=FR(I)+HAT
      DO 6 J=INK,18
      IF (FREQ(J).LT.PER1) GO TO 6
      IF (FREQ(J).GT.PER2) GO TO 8
      SUM=SUM+R(J)*R(J)
      ICOUNT=ICOUNT+1
    6 CONTINUE
      INK=18
      GO TO 9
    8 INK=J
    9 IF (ICOUNT.EQ.0) GO TO 10
      DBC=SQRT(SUM/ICOUNT)
      DBC=DBC/0.00000000294
      IF (DBC.LT.1.0) DBC=1.0
      DB(I)=20.0*ALOG10(DBC)-3.0
      GO TO 14
   10 DB(I)=0.0
   14 CONTINUE
      WRITE (6,222)
  222 FORMAT (//10X,24H1/3 OCT BAND CENTRE FREQ,10X,10HBAND LEVEL/18X,
     16HIN C/S,20X,21HDB RE 2*E-4 MICRO BAR//)
      WRITE (6,20) (FR(I),DB(I),I=1,28)
   20 FORMAT (15X,F12.6,12X,F12.6)
  221 CONTINUE
      CALL TIME(T)
      WRITE(6,16) T
      IF(L.GT.5) GO TO 11
      STOP
      END

END OF SEGMENT, LENGTH  3737, NAME  FOURIERANALYSISDA
```

```
COURSE JOB REQUEST 13176 WORDS
COURSE JOB REQUEST 10176 WORDS

FORTRAN COMPILATION BY #XFAT MK 6C     DATE 20/04/76  TIME 02/25/22

            LIST(LP)
            PROGRAM(U1MOU14)
            INPUT 5=CR0
            OUTPUT 6=LP0
            OUTPUT 7=TP0
            CREATE 8=MT0/(GRAPHPLOTTER)
            TRACE 0
            END
```

MODIFIED V17E

```
      MASTER FOURIER ANALYSIS DA
      DIMENSION FR(28)
      DIMENSION C(6050),D(400),E(400),A(1200),B(1200),DB(1200),AIAN(12
     100),AK(1200),F(1200),X(6050),TXT(7),FREQ(1200),DC(310),EC(310)
      DIMENSION  AIANT(1200),DBT(1200)
      DATAFR(1),FR(2),FR(3),FR(4),FR(5),FR(6),FR(7),FR(8),FR(9),FR(10),
     1     FR(11),FR(12),FR(13),FR(14),FR(15),FR(16),FR(17),FR(18),
     2     FR(19),FR(20),FR(21),FR(22),FR(23),FR(24),FR(25),FR(26),
     3     FR(27),FR(28)/20,0,25,0,31,5,40,0,50,0,63,0,80,0,100,0,
     4     125,0,160,0,200,0,250,0,315,0,400,0,500,0,630,0,800,0,1000,0,
     5     1250,0,1600,0,2000,0,2500,0,3150,0,4000,0,5000,0,6300,0,
     6     8000,0,10000,0/
   11 CALL TIME (T)
      WRITE(6,16)T
   16 FORMAT(//16H THE TIME IS NOW,A8)
      READ(5,99)L,IX,IY,IB,IXX,ICASE
   99 FORMAT(I5)
      READ(5,299)AFAC,AFAG,AL,ENB,RPM
  299 FORMAT(F12,8)
      READ(5,219)(D(J),E(J),J=1,IXX)
  219 FORMAT(F5,0,1X,F4,0)
C     Y COORDINATE INPUT FORMAT CHANGED TO ACCOMODATE 6 FIGURE INPUT
C     DATA,
      IPA=1
      AN=1,0
  902 FORMAT(1X,25HX AND Y INPUT COORDINATES)
      WRITE(6,902)
      WRITE(6,901)(D(J),E(J),J=1,IXX)
      CAFA=AFAC/AFAG
      DO 90 J=1,IXX
      E(J)=E(J)*CAFA
   90 CONTINUE
      DO 93 J=1,IXX
      D(J)=D(J)*360,0*ENB/(D(IXX))
   93 CONTINUE
      IN=7
      WRITE(8) D,E,IXX,IN
      KTD=0
      FL=D(IXX)-D(1)
   55 KTD=KTD+2
      ITCH=(IX-1)/(5)
      DIV=1,0/(AL)
      IXT=(IX+1)
      C(1)=E(1)
      X(1)=D(1)
      DO 89 IT=2,(IX+1)
      AIT=FLOAT(IT)
```

```
0056                A(IT)=A(IT-1,0)*.01**2
0057                DO 25 J=2,IX
0058                IF(A(J),LT,A(IT))GO TO 88
0059                IF(A(J),EQ,A(IT))C(IT)=E(J)
0060                IS=J-1
0061                IF(A(J),GT,A(IT))C(IT)=E(IS)+(E(J)-E(IS))*(A(IT)-D(IS))/(D(J)-D(IS
0062               1))
0063                GOTO 25
0064              88 CONTINUE
0065              25 CONTINUE
0066                A(IT)=IT-1
0067                A(IT)=A(IT)*500,0*ENB/(AL)
0068              89 CONTINUE
0069                N=IX-1
0070                DC(1)=D(1)
0071                EC(1)=E(1)
0072                IMAS=IX/20
0073                DO 5 J=2,IMAS,1
0074                I=J*20
0075                DC(J)=A(I)
0076                EC(J)=C(I)
0077              5 CONTINUE
0078                WRITE (6)  DC,EC,IMAS
0079              91 DO 92 L=1,((IX-1)/(2)
0080                JOT=L+1
0081                C(JOT)=C(JOT)*2,0
0082              92 CONTINUE
0083                C(1)=C(1)/(2,0)
0084                C(IX)=C(IX)/(2,0)
0085                IF(KTD,GT,3) GO TO 4
0086                CALL TIME (T)
0087                WRITE(6,18) T
0088              4 CONTINUE
0089                DO 15 K=IPA,IX,IY
0090                IF(K,GT,13)GO TO 401
0091                AK(K)=FLOAT(K)
0092                IF(K,GT,((IX-1)/(5))) GO TO 401
0093                F1=0,0
0094                F2=0,0
0095                DAK=6,283185307*AK(K)/(AL)
0096      C         VALUE OF PYE TO 11 SIG, FIG, INSTEAD OF 8 SIG, FIG,
0097                COCK=COS(DARK)
0098                ACOC=2,0*COCK
0099                SOCD=SIN(DARK)
0100                DO 19 IZ=1,IX
0101                IM=IAT+12
0102                F0=C(IM)+F1*ACOC-F2

0103                F2=F1
0104                F1=F0
0105              19 CONTINUE
0106                A(K)=(F0-F2*COCK)*1,5555554/(AL)
0107                B(K)=(F2*SOCD*1,5555554)/(AL)
0108                R(K)=SQRT(A(K)**2(K)+B(K)*B(K))
0109                DB(K)=R(K)/(0,0000000416)
0110                IF (DB(K) ,LT, 0,0000001) GOTO 10
0111                DB(K)=20,0*ALOG10(DB(K))
0112                IF (DB(K) ,LT, 0,0000001 ) GOTO 10
0113                GOTO 9
0114              10 DB(K)=0,0
0115              9  CONTINUE
0116                FREQ(K)=AK(K)*RPM/(60,0*ENB)
0117                AIAN(K)=ALOG10(FREQ(K))
0118              15 CONTINUE
0119             401 IX=IA
0120                 CALL TIME (T)
0121                 WRITE(6,18) T
0122                 IF(KTD,GT,3) GO TO 73
0123                 WRITE(6,600)
0124             600 FORMAT(33H PROGRAM V17E D,ANDERTON I,S,V,R,)
0125              17 FORMAT(12H CASE NUMBER,I5)
0126                 WRITE(6,17)ICASE
0127             505 FORMAT(5UX,4H IX ,7X,4H IY ,10X,4H IB ,7X,5H IXX )
0128                 WRITE(6,505)
0129             555 FORMAT(46X,I5,7X,I5,9X,I5,7X,I5)
0130                 WRITE(6,555)IX,IY,IB,IXX
0131             606 FORMAT(20X,3HAM ,23X,4H AL ,23X,6HAFAC,23X,6HAFAG)
0132                 WRITE(6,606)
0133             665 FORMAT(15X,4F20,5)
0134                 WRITE(6,666)AM,AL,AFAC,AFAG
0135             699 FORMAT(62X,26HMAXIMUM MUSIC AMPLITUDE IN DB)
0136                 WRITE (6,699)
0137             700 FORMAT(1UX,6HA(K),20X,6HB(K),16X,6HR(K),13X,5HDB(K),16X,3H K )
0138                 WRITE(6,700)
0139              73 IF(IB,GT,ITCH) GO TO 78
0140                 ITCH=IB
0141              78 WRITE(6,600)(A(I),B(I),R(K),DB(K),AK(K),K=IPA,ITCH,IY)
0142             600 FORMAT(1X,5F20,5)
0143             601 FORMAT(2F16,1,2X)
0144                 M=IE/IY
0145                 IF (IY,EQ,1)  GO TO 32
0146                 J=0
0147                 DO 30 I=1,IB,IY
0148                 J=J+1
0149                 AIAN1(J)=AIAN(I)
```

```
0150                  DBT(J)=DB(I)
0151               30 CONTINUE
0152               32 CONTINUE
0153                  IF (IY.GT.1) GO TO 33
0154                  GO 35 I=1,IB,IY
0155                  AIAN(I)=AIAN(I)
0156                  DBT(I)=DB(I)
0157               35 CONTINUE
0158                  WRITE (2)  AIANT,DBT,N
0159                  IF(ITCH-18)65,10,18
0160               65 IX=((IX-1)*3)+1
0161               18 CONTINUE
0162                  INK=1
0163                  DO 14 I=1,28
0164                  ICOUNT=0
0165                  SUM=0.0
0166                  MAT=FR(I)*.115
0167                  PER1=FR(I)*MAT
0168                  PER2=FR(I)+MAT
0169                  DO 6 J=INK,18
0170                  IF (FREQ(J).LT.PER1) GO TO 6
0171                  IF (FREQ(J).GT.PER2) GO TO 8
0172                  SUM=SUM+R(J)*R(J)
0173                  ICOUNT=ICOUNT+1
0174               6  CONTINUE
0175                  INK=IB
0176                  GO TO 29
0177               8  INK=J
0178               29 IF (ICOUNT.EQ.0) GO TO 26
0179                  DB(I)=SQRT(SUM/ICOUNT)
0180                  DBC=DB(I)/0.0000000296
0181                  IF (DBC.LT.1.0) DBC=1.0
0182                  DB(I)=20.0*ALOG10(DBC)+3.0
0183                  GO TO 14
0184               26 DB(I)=0.0
0185               14 CONTINUE
0186                  WRITE (6,222)
0187               222 FORMAT (//10X,24H1/3 OCT BAND CENTRE FREQ,10X,10HBAND LEVEL/18X,
0188                  16HIN C/S,20X,21HDB RE 2*E-4 MICRO BAR//)
0189                  WRITE (6,20) (FR(I),DB(I),I=1,28)
0190               20 FORMAT (15X,F12.0,14X,F12.0)
0191                  CALL TIME(T)
0192                  WRITE(6,16)  T
0193                  IF(L.GT.5) GO TO 11
0194                  REWIND 8
0195                  STOP
0196                  END


END OF SEGMENT, LENGTH   965, NAME  FOURIERANALYSISDA
```

TYPICAL JOB STATISTICS

```
COOPS| $01MU,DEL 1=00
COOPS|
COOPS|
COOPS| STATISTICS OF JOB
COOPS| --------|-------|-------|-------|-------|-------|-------|-------|-------|-------|-------|-------|-------|-------
COOPS| GRAND TOTAL INPUT RECORDS SUBMITTED     900  ON 20/06/74 AT 02/00/41
COOPS| --------|-------|-------|-------|-------|-------|-------|-------|-------|-------|-------|-------|-------|-------
COOPS|         |NOTIONAL |CPU|  CR|  LP|  TR|  TP|  CP|MIDECKS|MIPERIS|EDS MAX|EDS#  |EDPERIS|  CST
COOPS|         |  SECS|  SECS|  PERIS|  PERIS|  PERIS|  CHANS|  PERIS|       |& OPENS|EDUNITS|  K(M)|& OPENS|  & ST
COOPS| --------|-------|-------|-------|-------|-------|-------|-------|-------|-------|-------|-------|-------|-------
COOPS| REQUEST |  3000|       |       |  10000|       |   0|   0|   1|       |(M)   1|   0|       |  38178
COOPS|         |      |       |       |       |       |    |    |    |       |(U)   0|   0|       |  56016
COOPS| --------|-------|-------|-------|-------|-------|-------|-------|-------|-------|-------|-------|-------|-------
COOPS| COMPILE |   27|   13|  197|   256|   0|   0|   0|   0|       0|(M)   3|   2|   244|  18176
COOPS|         |      |       |       |       |       |    |    |    |       0|(U)   |  100|     4|
COOPS| --------|-------|-------|-------|-------|-------|-------|-------|-------|-------|-------|-------|-------|-------
COOPS| RUN     |    33|    7.4|   697|  2590|   0|   0|   0|   1|     135|(M)   0|   0|   0|
COOPS|         |      |       |       |       |       |    |    |    |       1|(U)   |   0|   0|  55504
COOPS| --------|-------|-------|-------|-------|-------|-------|-------|-------|-------|-------|-------|-------|-------
COOPS|  £   37.73 = COMPUTING VALUE
COOPS| A/C CODE| OF /C00674/02
COOPS| 7516 WAS PROCESSED ON  20/06/74  FROM  02/25/16 TO 02/42/11
COOPS| CHAIN JOB  1

        P1 NOW  *£      .00    P2 NOW  *£  420.80    P1 DEPT *£      .00    P2 DEPT *£ 8420.80    FUNDS   *£      .00
```